

Lawrence Berkeley National Laboratory

Recent Work

Title

Recovery of Carboxylic Acid at pH Greater than pK_{a}

Permalink

<https://escholarship.org/uc/item/7xv1x0m2>

Author

Tung, L.A.

Publication Date

1993-08-01



Lawrence Berkeley Laboratory

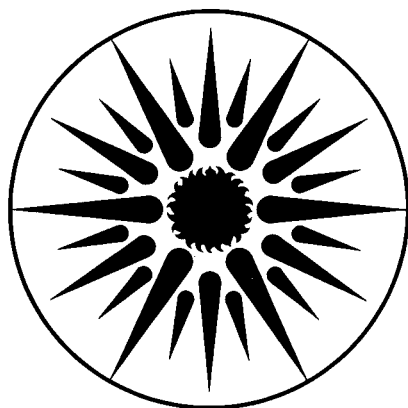
UNIVERSITY OF CALIFORNIA

ENERGY & ENVIRONMENT DIVISION

Recovery of Carboxylic Acids at pH Greater than pK_a

L.A. Tung
(Ph.D. Thesis)

August 1993



ENERGY & ENVIRONMENT
DIVISION

REFERENCE COPY	_____
Does Not Circulate	_____
Bldg. 50 Library.	_____
Copy 1	_____
LBL-34669	_____

DISCLAIMER

This document was prepared as an account of work sponsored by the United States Government. While this document is believed to contain correct information, neither the United States Government nor any agency thereof, nor the Regents of the University of California, nor any of their employees, makes any warranty, express or implied, or assumes any legal responsibility for the accuracy, completeness, or usefulness of any information, apparatus, product, or process disclosed, or represents that its use would not infringe privately owned rights. Reference herein to any specific commercial product, process, or service by its trade name, trademark, manufacturer, or otherwise, does not necessarily constitute or imply its endorsement, recommendation, or favoring by the United States Government or any agency thereof, or the Regents of the University of California. The views and opinions of authors expressed herein do not necessarily state or reflect those of the United States Government or any agency thereof or the Regents of the University of California.

Recovery of Carboxylic Acids at pH Greater than pK_a

Lisa A. Tung
(Ph.D. Thesis)

Department of Chemical Engineering
University of California

and

Energy and Environment Division
Lawrence Berkeley Laboratory
University of California
Berkeley, CA 94720

August 1993

This work was funded by the Biological and Chemical Technology Research (BCTR) Program, Advanced Industrial Concepts Division, Office of Industrial Technologies, U. S. Department of Energy under Contract No. DE-AC03-76SF00098, and by a National Science Foundation Graduate Fellowship.

Abstract

Recovery of Carboxylic Acids at pH Greater than pK_a

by

Lisa Ann Tung

Doctor of Philosophy in Chemical Engineering

University of California at Berkeley

Professor C. Judson King, Chair

Many fermentations to produce carboxylic acids operate most effectively at pH above the pK_a of the acid. One approach to acid recovery is to use strongly basic sorbents and extractants, which show substantial capacities even at moderately high values of pH. These extractants and sorbents can be regenerated by back-extraction of the acid into an aqueous trimethylamine solution, followed by thermal decomposition of the resulting complex.

Experiments were performed to measure the uptakes of lactic and succinic acids, as functions of pH, by several basic polymeric sorbents. The regenerabilities of the sorbents were also tested. Both performance at $pH > pK_a$ and regenerability are functions of sorbent basicity. Apparent pK_a and monomer pK_a can be used to predict sorbent performance.

Two basic amine extractants, Alamine 336 and Amberlite LA-2, in various diluents, were also studied. The extractants are able to sustain capacity to higher pH in diluents that stabilize the acid-amine complex through hydrogen bonding. Secondary amines perform better than tertiary amines in diluents that solvate the additional proton. All of the extractants are regenerable by leaching with aqueous trimethylamine.

Competitive uptake of sulfate and phosphate is an interference in actual fermentation systems. Experiments show that these species are taken up by sorbents more strongly than by extractants.

The third step in the proposed process, the cracking of the trimethylammonium carboxylate, was also examined experimentally. Previous research demonstrated that with low-solubility acids, like succinic, the trimethylammonium salt can be cracked thermally, yielding acid crystals and trimethylamine vapor. Because lactic acid is more soluble and tends to self-esterify, simple thermal cracking does not completely remove all of the trimethylamine. Cracking with addition of a solvent, such as methylisobutyl ketone or butyl acetate, was examined experimentally in this work. Additional trimethylamine was removed, but the final distillation to remove solvent from the product is problematic. A more promising approach is to esterify the trimethylammonium lactate by reaction with an alcohol. The feasibility of this approach was demonstrated through laboratory-scale experiments with 1-butanol. Other studies are needed to determine the viability of the esterification approach.

ACKNOWLEDGMENTS

I would like to thank my research advisor, Professor C. Judson King, for his guidance and encouragement. It has been a pleasure working with him. I would also like to thank Professors Scott Lynn and Ken Raymond for reading this dissertation and giving helpful commentary. Special thanks go to Professor Lynn and to Professor John Prausnitz for their help and encouragement during my stay here.

I would like to express my appreciation to Judie Powers, for all of her administrative help, and for making my stay a more enjoyable one with her friendliness and her wonderful sense of humor.

I am grateful to Jack Starr for helping me get started on this project, and to Lucy Randel and Paul Verderber for their companionship during those initial years. More recently, I have had the pleasure of working with Jorge Sunkel, Scott Moor, Jane Lee and Rob Broekhuis. Special thanks go to Scott for always encouraging me, to Rob for allowing me to bounce ideas off him, and to Jane for injecting fun into the lab.

I would also like to express my appreciation to Susan Kegley, for so graciously allowing me to use her ion chromatograph.

The years I have spent here have been enriched by my involvement in Loaves and Fishes. To all the special people I have met through this group, thank you.

Finally, I would like to thank my family, for their constant support, and especially my husband, Gene, who has been such an important part of my life during our years in graduate school.

This research has been supported by the Biological and Chemical Technology Research (BCTR) Program, Advanced Industrial Concepts Division, Office of Industrial Technologies, U.S. Department of Energy, and by a National Science Foundation Graduate Fellowship.

TABLE OF CONTENTS

	page
Abstract	
Acknowledgments	iii
Table of Contents	iv
List of Tables	xi
List of Figures	xiii
 CHAPTER 1. INTRODUCTION	
1.1 The Separation Problem	1
1.2 Possible Approaches	2
1.2.1 Precipitation of the Calcium Salt	
1.2.2 Water-Splitting Electrodialysis	
1.2.3 Ion Exchange	
1.2.4 Ligand Exchange	
1.2.5 Adsorption/Extraction with Addition of Acid	
1.3 Recovery Using Strongly Basic Sorbents and Extractants	7
1.3.1 Effect of Basicity on Uptake	
1.3.2 Regeneration of Sorbent/Extractant	
1.3.3 Proposed Process	
1.4 Project Goals	10
1.4.1 Identification of Promising Sorbents and Extractants	
1.4.2 Improved Process for Cracking Trimethylammonium Lactate	
1.5 Acids of Interest	13
1.5.1 Lactic Acid	
1.5.2 Succinic Acid	
1.6 Overview of Dissertation	15

TABLE OF CONTENTS (continued)

	page
CHAPTER 2. EXPERIMENTAL PROCEDURES AND EQUIPMENT	
2.1	16
2.1.1	16
2.1.2	16
2.1.3	16
2.2	22
2.2.1	22
2.2.2	22
2.2.3	22
2.2.4	22
2.2.5	22
2.2.6	22
2.3	23
2.3.1	23
2.3.2	23
2.3.3	23
2.3.4	23
2.3.5	23
2.3.6	23
2.3.7	23
2.4	29
2.4.1	29
2.4.2	29
2.4.3	29
2.5	30
2.5.1	30
2.5.2	30
2.6	33
2.6.1	33
2.6.1.1	33
2.6.1.2	33
2.6.2	38

TABLE OF CONTENTS (continued)

	page
CHAPTER 3. RECOVERY USING BASIC POLYMERIC SORBENTS	
3.1 Overview	39
3.2 Sorbent Characterization	39
3.2.1 Macroporosity	39
3.2.2 Chemical Structures	40
3.2.3 Measured Capacities	45
3.2.4 Sorbent Basicities	49
3.2.4.1 Apparent pK_a Values	
3.2.4.2 Monomer pK_a Values	
3.3 Sorption Isotherms	57
3.3.1 Composite and Individual Isotherms	57
3.3.2 Isotherm Models	58
3.3.2.1 The Langmuir Isotherm	
3.3.2.2 Other Models	
3.3.3 Fitting of Isotherms to Experimental Data	62
3.3.4 Results and Discussion	63
3.3.4.1 Lactic Acid	
3.3.4.2 Succinic Acid	
3.3.4.3 Comparison of Results for Lactic and Succinic Acids	
3.3.5 Summary	87
3.4 Uptake-pH Curves	87
3.4.1 Modelling of Uptake-pH Curves	88
3.4.1.1 Monocarboxylic Acids	
3.4.1.2 Dicarboxylic Acids	
3.4.2 Results and Discussion	92
3.4.2.1 Lactic Acid	
3.4.2.2 Succinic Acid	
3.4.3 Summary	115

TABLE OF CONTENTS (continued)

	page
CHAPTER 3. (continued)	
3.5 TMA Leaching Curves	115
3.5.1 Modeling of the Leaching Curve	115
3.5.2 Results and Discussion	118
3.5.2.1 Lactic Acid	
3.5.2.2 Succinic Acid	
3.5.3 Summary	133
3.6 Discussion of Sorbents Not Studied	133
3.7 Fixed-Bed Experiments	138
3.7.2 Breakthrough Curves	138
3.7.2.1 Background	
3.7.2.2 Modelling of Breakthrough Curves	
3.7.2.3 Results and Discussion	
3.7.3 Leaching Curves	156
3.7.4 Summary and Conclusions	161
CHAPTER 4. RECOVERY USING LIQUID AMINE EXTRACTANTS	
4.1 Previous Studies	162
4.2 Law-of-Mass Action Modeling of Extraction Systems	163
4.3 Importance of Complexation Constants to Performance at $\text{pH} > \text{pK}_a$	165
4.4 Factors Affecting Amine Extractant Basicities	167
4.4.1 Diluent Effects	
4.4.2 Effects of Amine Type	
4.5 Choice of Extraction Systems for Study	172
4.6 Previous Results for Alamine 336	173

TABLE OF CONTENTS (continued)

	page
CHAPTER 4. (continued)	
4.7 Loading of Amine Extractants as a Function of pH	175
4.7.1 Results and Discussion	175
4.7.1.1 Lactic Acid	
4.7.1.2 Succinic Acid	
4.7.2 Modeling of Loading-pH Curves	184
4.8 Regenerability of Extracts	196
4.8.1 Results and Discussion	
4.8.2 Modeling of Back-Extraction	
4.9 Process Issues	201
4.10 Summary	201
 CHAPTER 5. ACTUAL FERMENTATION SYSTEMS	
5.1 Implementation of Sorption/Extraction Process	203
5.2 Nature of the Fermentation Broth	208
5.3 Competitive Uptake of Other Species	208
5.3.1 Broth Compositions	208
5.3.2 Expected Interferences	211
5.3.3 Experiments with an Actual Fermentation Broth	211
5.3.4 Phosphate/Sulfate Uptake Experiments	214
5.3.4.1 Phosphate/Sulfate Uptake by Dowex MWA-1	
5.3.4.2 Separation Factors	
5.3.5 Summary and Conclusions	225
5.4 Temperature Effects	226
5.4.1 Effects of Temperature on Sorption/Extraction Equilibria	
5.4.2 Thermal Stabilities of Sorbents and Extractants	
5.4.3 Process Considerations	
5.5 Toxicity to the Microorganism	231
5.6 Summary	235

TABLE OF CONTENTS (continued)

page

CHAPTER 6. CRACKING OF THE TRIMETHYLAMMONIUM CARBOXYLATE

6.1	Simple Thermal Cracking	236
	6.1.1 Background	
	6.1.2 Experimental Results and Discussion	
	6.1.3 Summary and Conclusions	
6.2	Thermal Cracking with Solvent Addition	240
	6.2.1 Background	
	6.2.2 Experimental Results	
	6.2.3 Discussion and Conclusions	
6.3	Esterification	246
	6.3.1 Background	247
	6.3.1.1 Simple Esterification	
	6.3.1.2 Esterification of Ammonium Lactates	
	6.3.2 Esterification Step	249
	6.3.2.1 Conversion Experiments	250
	6.3.2.1.1 Results	
	6.3.2.1.2 Discussion	
	6.3.2.2 Reaction Rate Experiments	255
	6.3.2.3 Summary and Conclusions	268
	6.3.3 Hydrolysis Step	268
	6.3.4 Distillation Steps	269
	6.3.4.1 Distillation of Esterification Mixture	
	6.3.4.2 Distillation of Hydrolysis Mixture	
	6.3.4.3 Summary	
	6.3.5 Process Considerations	273
	6.3.5.1 Choice of Alcohol	
	6.3.5.2 Process Implementation	
6.4	Conclusions	277

TABLE OF CONTENTS (continued)

	page
CHAPTER 7. CONCLUSIONS	279
REFERENCES	284
APPENDICES	
A. Experimental Data	291
A.1 Sorption Isotherms	
A.2 Sorbent pH Experiments	
A.3 TMA Leaching Experiments	
A.4 Fixed-Bed Experiments	
A.5 Back-Extraction of Lactic Acid from Aliquat 336 in Toluene	
A.6 Extractant pH Experiments	
A.7 Back-Extraction of Lactic Acid from Amberlite LA-2 in 1-Octanol	
A.8 Uptakes of Sulfuric and Phosphoric Acids by Dowex MWA-1	
A.9 Breakthrough Curves for Lactic Acid on Dowex MWA-1 in Presence of Sulfate and Phosphate	
A.10 Leaching of Sulfate and Phosphate from Dowex MWA-1	
A.11 Selectivity Experiments	
A.12 Dowex MWA-1 Isotherm at 37 °C	
A.13 Thermal Cracking of Trimethylammonium Lactate	
A.14 Esterification of Trimethylammonium Lactate	
B. Fitting of Sorption Isotherms	344
B.1 Langmuir Isotherms	
B.2 Model Choices for Succinic Acid Isotherms	
B.3 Use of Competitive Langmuir Model with Low-pH Isotherms	
C. Nomenclature	361

LIST OF TABLES

Table	page
2-1 Sources and Descriptions of Chemicals Used	16
2-2 Composition of Alamine 336	17
2-3 Basic Sorbents Used	20
2-4 Maximum Sorbent Operating Temperatures	21
3-1 Sorbent Capacities	50
3-2 Apparent pK Values (Gustafson et al. [60])	52
3-3 Apparent pK _a Values (Garcia and King [22], Clifford and Weber [56])	53
3-4 Calculated Monomer pK _a Values	55
3-5 K Values for Lactic Acid Isotherms	70
3-6 Comparison Between q _m for Lactic Acid and Capacity Measurements	73
3-7 K Values for Succinic Acid Isotherms	83
3-8 Comparison Between q _m for Succinic Acid and Capacity Measurements	85
3-9 Comparison of K Values for Lactic and Succinic Acids	86
3-10 Results of Leaching Succinic Acid from Reillex 425 with Methanol	132
3-11 Breakthrough Curve Results	155
4-1 log(K _{pg}) Values for Extraction of Lactic and Succinic Acids by Alamine 336 in Various Diluents	174
4-2 Partition Coefficients	175
5-1 Compositions of Representative Fermentation Media for <i>L. delbreuckii</i>	210
5-2 Initial Composition of Fermentation Broth Used in Experiments	212
5-3 Results of Sorption Experiments with Actual Fermentation Broth	213

LIST OF TABLES (continued)

Table	page
5-4 α Values for Sulfate/Lactic Acid	224
5-5 α Values for Phosphate/Lactic Acid	225
6-1 Distillation of Esterification Mixture	271
6-2 Distillation of Hydrolysis Mixture	272
A-1 Experimental Data for Sorption Isotherms	291
A-2 Data from Sorbent Uptake-pH Experiments	297
A-3 Data from TMA Leaching Experiments	300
A-4 Data from Fixed-Bed Experiments	304
A-5 Results of Back-Extracting Lactic Acid from 0.3 M Aliquat 336 in Toluene	314
A-6 Data from Extraction Experiments	315
A-7 Data from Back-Extraction of Lactic Acid from Amberlite LA-2 in 1-Octanol	319
A-8 Uptake Data for Sulfuric and Phosphoric Acids on Dowex MWA-1	320
A-9 Breakthrough Data for Lactic Acid on Dowex MWA-1 in the Presence of Sulfate and Phosphate	321
A-10 Data from Leaching of Sulfate and Phosphate from Dowex MWA-1	326
A-11 Data from Selectivity Experiments	327
A-12 Uptake Data for Lactic Acid on Dowex MWA-1 at 37 °C	329
A-13 Rate Data for Thermal Cracking of Trimethylammonium Lactate	330
A-14 Rate Data for Esterification of Trimethylammonium Lactate	333

LIST OF FIGURES

Figure	page
1-1 Effect of Sorbent Basicity on (a) Sorption Isotherm (b) Uptake-pH Curve	8
1-2 Carboxylic Acid Recovery Process	11
1-3 Driving Forces for Sorption/Extraction and Regeneration Processes	12
2-1 Equilibrium Composition of Aqueous Lactic Acid	18
2-2 Apparatus for Fixed-Bed Experiments	27
2-3 Apparatus for Cracking Experiments	31
2-4 Apparatus for Cracking with Solvent Addition	34
2-5 Apparatus for Esterification Experiments	36
3-1 (a) Chemical Structure of Reillex 425 (b) Quaternized Group on Reillex HPQ	41
3-2 Formation of Intermediate in Ring-Opening of Reillex HPQ	42
3-3 Chemical Structure of Duolite A7	43
3-4 Chemical Structure of Dowex MWA-1 and Dowex 66	43
3-5 Chemical Structure of Bio-Rad AG3-X4	46
3-6 Chemical Structure of Amberlite IRA-35	46
3-7 Chemical Structures of Strong-Base Ion Exchangers	47
(a) Type I	
(b) Type II	
3-8 Effect of Sorbent K Value on	60
(a) Sorption Isotherm	
(b) Uptake-pH Curve	
3-9 Sorption Isotherms for Lactic Acid on Reillex 425	64
3-10 Sorption Isotherms for Lactic Acid on Duolite A7	65
3-11 Sorption Isotherms for Lactic Acid on Dowex MWA-1	66
3-12 Sorption Isotherms for Lactic Acid on Amberlite IRA-35	67

LIST OF FIGURES (continued)

Figure	page
3-13 Sorption Isotherms for Lactic Acid on Amberlite IRA-910	68
3-14 Comparison Between the Experimental K Values for Lactic Acid and Various Measures of Sorbent pK_a	71
3-15 Sorption Isotherms for Succinic Acid on Reillex 425	74
3-16 Sorption Isotherms for Succinic Acid on Reillex HPQ	75
3-17 Sorption Isotherms for Succinic Acid on Duolite A7	76
3-18 Sorption Isotherms for Succinic Acid on Bio-Rad AG3-X4	77
3-19 Sorption Isotherms for Succinic Acid on Dowex MWA-1	78
3-20 Sorption Isotherms for Succinic Acid on Dowex 66	79
3-21 Sorption Isotherms for Succinic Acid on Amberlite IRA-35	80
3-22 Sorption Isotherms for Succinic Acid on Amberlite IRA-910	81
3-23 Comparison Between Experimental K Values for Succinic Acid and Various Measures of Sorbent pK_a	84
3-24 Conversion of Strong-Base Site from Carboxylate to Bicarboxylate Form	91
3-25 Effect of pH on Uptake of Lactic Acid by Reillex 425	93
3-26 Effect of pH on Uptake of Lactic Acid by Duolite A7	94
3-27 Effect of pH on Uptake of Lactic Acid by Dowex MWA-1	95
3-28 Effect of pH on Uptake of Lactic Acid by Amberlite IRA-35	96
3-29 Effect of pH on Uptake of Lactic Acid by Amberlite IRA-910	97
3-30 Effect of pH on Normalized Uptakes of Lactic Acid	98
3-31 Effect of pH on Uptakes of Lactic Acid at an Equilibrium Solution Concentration of 1.0 wt.%	100
3-32 Effect of pH on Uptake of Succinic Acid by Reillex HPQ	101
3-33 Effect of pH on Uptake of Succinic Acid by Reillex 425	102
3-34 Effect of pH on Uptake of Succinic Acid by Duolite A7	103

LIST OF FIGURES (continued)

Figure	page
3-35 Effect of pH on Uptake of Succinic Acid by Bio-Rad AG3-X4 (Freundlich Isotherm)	104
3-36 Effect of pH on Uptake of Succinic Acid by Dowex MWA-1 (Freundlich Isotherm)	105
3-37 Effect of pH on Uptake of Succinic Acid by Amberlite IRA-35 (Freundlich Isotherm)	106
3-38 Effect of pH on Uptake of Succinic Acid by Bio-Rad AG3-X4 (Competitive Langmuir Isotherm)	107
3-39 Effect of pH on Uptake of Succinic Acid by Dowex MWA-1 (Competitive Langmuir Isotherm)	108
3-40 Effect of pH on Uptake of Succinic Acid by Amberlite IRA-35 (Competitive Langmuir Isotherm)	109
3-41 Effect of pH on Uptake of Succinic Acid by Amberlite IRA-910	110
3-42 Effect of pH on Normalized Uptakes of Succinic Acid	113
3-43 Effect of pH on Uptakes of Succinic Acid at an Equilibrium Solution Concentration of 1.0 wt.%	114
3-44 Leaching of Lactic Acid from Reillex 425 into Aqueous Solutions of Varying TMA Concentration	119
3-45 Leaching of Lactic Acid from Duolite A7 into Aqueous Solutions of Varying TMA Concentration	120
3-46 Leaching of Lactic Acid from Dowex MWA-1 into Aqueous Solutions of Varying TMA Concentration	121
3-47 Leaching of Lactic Acid from Amberlite IRA-35 into Aqueous Solutions of Varying TMA Concentration	122
3-48 Leaching of Lactic Acid from Amberlite IRA-910 into Aqueous Solutions of Varying TMA Concentration	123
3-49 Leaching of Succinic Acid from Reillex 425 into Aqueous Solutions of Varying TMA Concentration	125
3-50 Leaching of Succinic Acid from Duolite A7 into Aqueous Solutions of Varying TMA Concentration	126
3-51 Leaching of Succinic Acid from Dowex MWA-1 into Aqueous Solutions of Varying TMA Concentration	127

LIST OF FIGURES (continued)

Figure	page
3-52 Leaching of Succinic Acid from Amberlite IRA-35 into Aqueous Solutions of Varying TMA Concentration	128
3-53 Leaching of Succinic Acid from Bio-Rad AG3-X4 into Aqueous Solutions of Varying TMA Concentration	129
3-54 Leaching of Succinic Acid from Reillex HPQ into Aqueous Solutions of Varying TMA Concentration	130
3-55 Leaching of Succinic Acid from Amberlite IRA-910 into Aqueous Solutions of Varying TMA Concentration	131
3-56 Chemical Structure of Poly(benzimidazole) Resin	135
3-57 Chemical Structure of Poly[N,N-bis(2-aminoethyl)-vinylbenzylamine] Resin	135
3-58 Chemical Structures of Novel Sorbents	137
(a) DAMP Resin	
(b) DAP Resin	
3-59 Effect of Column Length on Breakthrough of Succinic Acid on Dowex MWA-1	144
3-60 Breakthrough of Succinic Acid on Dowex MWA-1, F = 1.2 ml/min, L = 24.5 cm, C _{ao} = 5.25 wt.% (Linear-Driving-Force Model)	145
3-61 Breakthrough of Succinic Acid on Dowex MWA-1, F = 3.1 ml/min, L = 24.5 cm, C _{ao} = 5.25 wt.% (Linear-Driving-Force Model)	146
3-62 Breakthrough of Succinic Acid on Dowex MWA-1, F = 1.54 ml/min, L = 29.2 cm, C _{ao} = 5.25 wt.% (Linear-Driving-Force Model)	146
3-63 Breakthrough of Succinic Acid on Dowex MWA-1, F = 1.4 ml/min, L = 24.5 cm, C _{ao} = 2.53 wt.% (Linear-Driving-Force Model)	148
3-64 Breakthrough of Lactic Acid on Dowex MWA-1, F = 1.5 ml/min, L = 24.5 cm, C _{ao} = 4.0 wt.% (Linear-Driving-Force Model)	149
3-65 Breakthrough of Succinic Acid on Dowex MWA-1, F = 1.2 ml/min, L = 24.5 cm, C _{ao} = 5.25 wt.% (Pore Diffusion Model)	150

LIST OF FIGURES (continued)

Figure	page
3-66 Breakthrough of Succinic Acid on Dowex MWA-1, F = 3.1 ml/min, L = 24.5 cm, C _{ao} = 5.25 wt.% (Pore Diffusion Model)	151
3-67 Breakthrough of Succinic Acid on Dowex MWA-1, F = 1.54 ml/min, L = 29.2 cm, C _{ao} = 5.25 wt.% (Pore Diffusion Model)	152
3-68 Breakthrough of Succinic Acid on Dowex MWA-1, F = 1.4 ml/min, L = 24.5 cm, C _{ao} = 2.53 wt.% (Pore Diffusion Model)	153
3-69 Breakthrough of Lactic Acid on Dowex MWA-1, F = 1.5 ml/min, L = 24.5 cm, C _{ao} = 4.0 wt.% (Pore Diffusion Model)	154
3-70 Breakthrough and Leaching Curves for Succinic Acid on Dowex MWA-1 (F = 1.5 ml/min, L = 18 cm, 5.25 wt.% Acid Feed, 5.25 wt.% TMA Feed)	157
3-71 Breakthrough and Leaching Curves for Succinic Acid on Dowex MWA-1 (F = 3.1 ml/min, L = 24.5 cm, 5.25 wt.% Acid Feed, 5.25 wt.% TMA Feed)	159
3-72 Leaching Curve for Succinic Acid on Dowex MWA-1 (F = 1.4 ml/min, L = 24.5 cm, 10.2 wt.% TMA Feed)	160
4-1 Proposed Structure for (2, 1) Acid-Amine Complex	166
4-2 Effect of Complexation Constants on Loading	168
(a) Effect of K ₁₁	
(b) Effect of K ₂₁	
4-3 Stabilization of Amine-Carboxylic Acid Complexes Through Hydrogen-Bonding with an Alcohol	171
4-4 Stabilization by Oxygenated Diluents	171
(a) Secondary Amine	
(b) Tertiary Amine	
4-5 Effect of pH on the Extraction of Lactic Acid by Alamine 336 in Various Diluents	176
4-6 Effect of pH on the Extraction of Lactic Acid by Amberlite LA-2 in Various Diluents	178
4-7 Effect of Amine Type on Uptake of Lactic Acid Using a Chloroform Diluent	179

LIST OF FIGURES (continued)

Figure	page
4-8 Effect of Amine Type on Uptake of Lactic Acid Using an MiBK Diluent	180
4-9 Effect of Amine Type on Uptake of Lactic Acid Using a 1-Octanol Diluent	181
4-10 Effect of pH on the Extraction of Succinic Acid by Alamine 336 in Various Diluents	183
4-11 Effect of pH on the Extraction of Succinic Acid by Amberlite LA-2 in Various Diluents	185
4-12 Effect of Amine Type on Uptake of Succinic Acid Using a Chloroform Diluent	186
4-13 Effect of Amine Type on Uptake of Succinic Acid Using an MiBK Diluent	187
4-14 Effect of Amine Type on Uptake of Succinic Acid Using a 1-Octanol Diluent	188
4-15 Modeling of the Effect of pH on the Extraction of Lactic Acid by Alamine 336 in MiBK	191
4-16 Modeling of the Effect of pH on the Extraction of Lactic Acid by Alamine 336 in Chloroform	192
4-17 Modeling of the Effect of pH on the Extraction of Succinic Acid by Alamine 336 in MiBK	193
4-18 Modeling of the Effect of pH on the Extraction of Succinic Acid by Alamine 336 in Chloroform	194
4-19 Modeling of the Effect of pH on the Extraction of Succinic Acid by Alamine 336 in 1-Octanol	195
4-20 Effect of pH on the Loading of 0.3 M Alamine 336 in Various Diluents by Lactic Acid at an Equilibrium solution Concentration of 0.10 M	197
4-21 Effect of pH on the Loading of 0.3 M Alamine 336 in Various Diluents by Succinic Acid at an Equilibrium solution Concentration of 0.10 M	198
4-22 Back-Extraction of Lactic Acid from Loaded Amberlite LA-2 in 1-Octanol ($Z = 1.04$) with Aqueous TMA Solutions	199

LIST OF FIGURES (continued)

Figure	page
5-1 Methods of Incorporating Solvent Extraction Process	204
(a) In-Situ Extraction	
(b) External Recycle Loop	
5-2 Biparticle Fluidized-Bed Bioreactor	207
5-3 Uptake of Sulfuric Acid by Dowex MWA-1	215
5-4 Uptake of Phosphoric Acid by Dowex MWA-1	216
5-5 Effect of Sulfate on Breakthrough of 4.00 wt.% Lactic Acid on Dowex MWA-1	218
5-6 Effect of Phosphate on Breakthrough of 4.00 wt.% Lactic Acid on Dowex MWA-1	219
5-7 Breakthrough and Leaching Curves for Lactic Acid and Sulfate on Dowex MWA-1	220
5-8 Breakthrough and Leaching Curves for Lactic Acid and Phosphate on Dowex MWA-1	221
5-9 Effect of Temperature on the Loading of 0.3 M Alamine 336 in Chloroform with Succinic Acid at an Aqueous Phase Concentration of 0.1 M	227
5-10 Effect of Temperature on the Loading of 0.3 M Alamine 336 in Chloroform with Lactic Acid at an Aqueous Phase Concentration of 0.1 M	228
5-11 Effect of Temperature on Uptake of Lactic Acid by Dowex MWA-1	230
6-1 Simple Thermal Cracking of Trimethylammonium Lactate	238
6-2 Cracking with MiBK Addition	242
6-3 Cracking with Butyl Acetate Addition	244
6-4 Chromatographs of Final Solutions	254
(a) Esterification of Lactic Acid	
(b) Esterification of Trimethylammonium Lactate	
6-5 Results of Esterification Rate Experiment, 0.21 mol lactic acid, 0.13 mol TMA, 0.53 mol butanol and 0.1 mol water initially present	256

LIST OF FIGURES (continued)

Figure	page
6-6	Results of Esterification Rate Experiment, 0.20 mol lactic acid, 0.17 mol TMA, 0.50 mol butanol and 0.7 mol water initially present 257
6-7	Results of Esterification Rate Experiment, 0.20 mol lactic acid, 0.20 mol TMA, 0.50 mol butanol and 5.7 mol water initially present 258
6-8	Effect of Degree of Preconcentration on Reaction Rate 259
6-9	Cracking of Trimethylammonium Lactate (0.2 mol lactic acid, 0.14 mol TMA, 0.65 mol water initially present) 262
6-10	Results of Rate Experiment, Esterification of Lactic Acid 263
6-11	Effect of Sulfuric Acid Catalyst on Esterification Rate 265
6-12	Effects of Amberlyst 15 and Silica Gel on Esterification Rate 266
6-13	Effect of Butanol: Lactic Acid Ration on Esterification Rate 267
6-14	Esterification and Hydrolysis with Continuous Recycle 275
6-15	Esterification and Hydrolysis of Ester Using Two Simultaneous Reaction-Distillation Columns 276
B-1	Uptake of Lactic Acid by Duolite A7 Fitted with Langmuir Isotherm 345
B-2	Uptake of Succinic Acid by Duolite A7 Fitted with Langmuir Isotherm 346
B-3	Uptake of Succinic Acid by Bio-Rad AG3-X4 Fitted with Langmuir Isotherm 347
B-4	Uptake of Succinic Acid by Dowex MWA-1 Fitted with Langmuir Isotherm 348
B-5	Uptake of Succinic Acid by Amberlite IRA-35 Fitted with Langmuir Isotherm 349
B-6	Uptake of Succinic Acid by Amberlite IRA-910 Fitted with Langmuir Isotherm 350

LIST OF FIGURES (continued)

Figure		page
B-7	Uptake of Succinic Acid by Reillex HPQ Fitted with Langmuir Isotherm	351
B-8	Residuals from Fit of Langmuir Isotherm to succinic Acid/Amberlite IRA-35 Data	353
B-9	Residuals from Fit of Freundlich Isotherm to Succinic Acid/Amberlite IRA-35 Data	354
B-10	Uptake of Succinic Acid by Amberlite IRA-35 Fitted with Dual-Site Langmuir Isotherm	355
B-11	Residuals from Fit of Dual-Site Langmuir Isotherm to Succinic Acid/Amberlite IRA-35 Data	356
B-12	Uptake of Succinic Acid by Bio-Rad AG3-X4 Fitted with Competitive Langmuir Model	358
B-13	Uptake of Succinic Acid by Dowex MWA-1 Fitted with Competitive Langmuir Model	359
B-14	Uptake of Succinic Acid by Amberlite IRA-35 Fitted with Competitive Langmuir Model	360

Chapter 1. INTRODUCTION

There exists a large market for carboxylic acids in the food, pharmaceutical and other industries (1). With the exception of citric, gluconic, lactic and itaconic acids, which are made through fermentation, most carboxylic acids are currently produced synthetically from petroleum-based feedstocks. If dependence on fossil fuel sources is to be avoided, research and development efforts must be directed toward developing processes for producing these acids from alternate sources, such as biomass (e.g., corn starch, cane and beet sugar, whey, etc.). Advances in fermentation technology have made it possible to produce a variety of carboxylic acids, including acetic, propionic, butyric, fumaric, succinic, maleic and lactic acids, from biomass sources (1).

The economics of producing carboxylic acids by fermentation is often dominated, not by the cost of the fermentation itself, but by the cost of recovering and purifying the acids from dilute, complex aqueous solutions. Powerful and efficient recovery methods are therefore needed to make commercialization of these fermentations possible.

1.1 The Separation Problem

The recovery of carboxylic acids from fermentation broths presents a challenging separation problem. The broths are dilute and quite complex, and the acids of interest are hydrophilic and often have low volatilities. Thus, a highly selective recovery method, which is capable of preferentially pulling the carboxylic acid out of solution, is needed.

An important aspect of this problem concerns the pH of the fermentation broth. Many fermentations operate best at pH greater than pK_{a1} of the acid being produced. For example, lactic acid, which has pK_a equal to 3.86 (2), is typically produced at pH 5 to 6 (1, 3). Succinic acid, a di-acid with pK_{a1} equal to 4.2 and pK_{a2} equal to 5.6 (2), is produced at pH 5 to 7 (4, 5, 6). (Citric acid, a notable exception, is produced at low pH, typically less than 3.5 [7].) For most acids, then, if the recovery method is to be used *in-situ* in the

fermenter, or in an external loop without pH change, the method must function well at $\text{pH} > \text{pK}_a$. The ability to recover the carboxylic acid as it is formed is important, since higher overall yields can be achieved when product inhibition normally occurs (8, 9). Integrating the separation step and the fermentation step is also important in moving from batch to continuous processes.

1.2 Possible Approaches

There are a number of options for recovering carboxylic acids at $\text{pH} > \text{pK}_a$, each with its own advantages and disadvantages.

1.2.1 Precipitation of the Calcium Salt

The conventional method for recovering low-volatility carboxylic acids from fermentation broths is through formation of the calcium carboxylate. Lactic and citric acids have been recovered this way industrially (3, 7). In the lactic acid process, the broth is heated and the lactic acid is neutralized with calcium hydroxide or lime. After a series of filtration and carbon adsorption steps, the solution is concentrated through evaporation and acidified with sulfuric acid, which protonates the lactate and causes calcium sulfate to precipitate from solution. The mixture is filtered and the aqueous lactic acid is decolorized, de-ionized and then concentrated to its final form (3). Citric acid is produced in a similar manner (7).

For batch fermentations the calcium salt process functions well at $\text{pH} > \text{pK}_a$ since calcium hydroxide can be used to control pH as the fermentation progresses. Additional calcium hydroxide is then added at the end of the fermentation to complete the neutralization. pH must be carefully controlled to avoid precipitating product before separating the broth from the cells and solid debris. Otherwise, a solids separation problem will be created. Furthermore, precipitation of vital nutrients must be avoided. For lactic acid production, these issues have apparently not been problematic. For citric acid, the performance at $\text{pH} >$

pK_a is not an issue, since the acid is produced at low pH. Calcium hydroxide therefore is not added to a batch citric acid fermentation until acid production is complete.

For continuous fermentations, implementation of the calcium salt method may be more difficult. The series of filtration, precipitation and concentration steps performed on the broth would most likely preclude its recycle to the fermenter. Fresh medium would therefore have to be continually resupplied to the fermenter.

The major disadvantage of the calcium salt process, however, is that for every mole of carboxylic acid produced, one mole each of acid and base are consumed, and one mole of waste calcium sulfate is created. This calcium sulfate poses a real disposal problem, especially as environmental controls tighten. A more efficient process would avoid the consumption of chemicals and the production of high-volume waste streams.

1.2.2 Water-Splitting Electrodialysis

A second approach to recovering carboxylic acids from fermentation broths at $pH > pK_a$ is water-splitting electrodialysis. This process utilizes bipolar, or water-splitting, membranes, each of which is manufactured by laminating together a cation- and an anion-selective membrane. In the water-splitting electrodialysis process, pH control is maintained in the fermenter through addition of a base, such as sodium hydroxide. The solution of carboxylic acid/sodium carboxylate is fed continuously to an electrodialysis unit, comprising a series of cell units stacked between two electrodes. Each cell unit consists of a series of compartments separated by a cation-selective membrane, an anion-selective membrane, and a bipolar membrane. As the solution passes into the electrodialysis unit, an applied electric field pulls carboxylate ions toward the anode and sodium ions toward the cathode. Water dissociates at the bipolar membrane, forming hydroxyl ions and protons, which are then transported through the membrane toward the anode and cathode, respectively. The net result is that lactic acid product and sodium hydroxide, available for recycle to the fermenter, are

produced in alternating compartments of the electro dialysis unit. Several sources discuss this process in more detail (10, 11, 12).

Problems encountered in water-splitting electro dialysis include membrane instability at elevated pH, fouling of membranes, loss of product through diffusion and oxidation, and loss of ionic nutrients (4, 10, 13, 14). Research in the area of membrane development has led to significant advances (10). Glassner and Datta (4) used water-splitting electro dialysis in a continuous fermentation to produce a succinic acid product. They were able to electro dialyze whole broth without experiencing fouling problems. Ion-exchange polishing steps were needed to remove anionic and cationic impurities from the product.

1.2.3 Ion Exchange

Carboxylate anions can be recovered by exchange with counter-ions (e.g. chloride) associated with polymeric ion-exchange resins or liquid ion exchangers. The effectiveness of the recovery depends on the relative affinities of the carboxylate and the counter-ion for the ion exchange site. Reschke and Schügerl (15), for example, discuss the recovery of penicillin G from aqueous solutions at pH 7 using Adogen 464 (trioctylmethylammonium chloride) in xylene. Drawbacks of the ion exchange approach include contamination of the broth by the counter-ion and a problematic regeneration step. Regeneration generally involves contacting the ion exchanger with a concentrated salt solution containing the initial counter-ion. This method consumes chemicals and recovers the carboxylate salt, rather than the acid.

1.2.4 Ligand Exchange

Zhu and Sengupta (16, 17) have recovered carboxylic acids from dilute aqueous solutions at $\text{pH} > \text{pK}_a$ using polymeric ligand exchangers. These exchangers are chelating polymers with closely spaced nitrogen donor atoms that are capable of chelating metal ions such as Cu^{2+} . In the Cu^{2+} form, the ligand exchangers formed coordination compounds with

carboxylic acid anions at moderate to high values of pH. Furthermore, carboxylate was taken up preferentially to other anions, such as chloride and sulfate, which can be found in fermentation broths.

There are, however, several disadvantages to using ligand exchangers. Because Cu^{2+} must always have an associated counter-ion, the carboxylate merely exchanges with some other anion, such as nitrate or chloride, which then contaminates the broth. A gradual loss of Cu^{2+} from the ligand exchange column is also a problem, although Zhu and Sengupta overcame this by using a layer of virgin chelating polymer at the bottom of the column to capture leaking Cu^{2+} ions. A more serious shortcoming of the ligand exchange approach is that regeneration of the exchanger is problematic. The carboxylate can be removed by leaching with a salt solution (16, 17), in which case the carboxylate salt, and not the acid, is formed. An alternative is to leach with aqueous ammonia (16), but this approach also removes Cu^{2+} ions. A process for separating and recovering Cu^{2+} from the acid product then becomes necessary.

1.2.5 Adsorption/Extraction with Addition of Acid

Yet another method for recovering carboxylic acids at $\text{pH} > \text{pK}_a$ is adsorption or extraction with addition of acid. In processes of this type, a stream is withdrawn from the fermenter, filtered, acidified, and sent to an external extractor or adsorption column, where the carboxylic acid is recovered from the broth. The pH of the treated broth must be adjusted with base if it is to be returned to the fermenter.

The process can utilize several types of sorbents and extractants. Extractants may be simple organic solvents or solvents with added chemical extractants, such as long-chain amines or organo-phosphorus-based compounds (e.g., trioctylphosphine oxide, or TOPO). Potential sorbents include activated carbons, non-functionalized polymeric resins, and weak or strong base anion exchangers. In general, the choice of sorbent/extractant is influenced by the need to balance extractant capacity and selectivity with ease of regenerability.

There have been several examples in the literature of sorption/extraction with concomitant acidification. Seevaratnam et al. (18) recovered lactic acid from fermentation broths via extraction with HCl addition. They used a paraffin oil extractant with and without the addition of Bonopore, a non-functionalized polymeric resin. The broth was treated with NaOH before it was returned to the fermenter. Kulprathipanja et al. (19, 20, 21) recovered lactic and citric acids at low pH using non-functionalized polystyrene-divinylbenzene resins or weak-base anion exchange resins with amine or pyridine functional groups. Sulfuric acid was used to reduce the pH before extraction.

There are several different approaches to regenerating the sorbents/extractants used in the recovery process. For non-functionalized resins and physical solvents, regeneration is relatively straightforward. Non-functionalized sorbents, and sorbents which complex only weakly with the carboxylic acid, have been regenerated by leaching with a volatile solvent (8, 22) or with hot water (23, 24). Physical solvents can be regenerated by precipitation of the acid through removal of solvent or of small amounts of coextracted water (25). Functionalized sorbents or chemical extractants that complex more strongly with the carboxylic acid are somewhat more difficult to regenerate. Temperature- and diluent-swing processes have been investigated for organic amine extractant systems (26). A temperature-swing process using amines is currently used to recover citric acid industrially at low pH (27). In general, though, satisfactory regeneration, resulting in a highly concentrated product, requires more powerful methods, such as pH-swing processes.

The major disadvantage of recovering the carboxylic acid by extraction/sorption with acid addition is that acid and base are consumed, and salts build up in the fermentation broth. A related approach (28, 29) uses extraction coupled with acidification by carbon dioxide under pressure. This approach is promising in that it does not involve consumption of an acid and a base. However, only moderate pH changes can be achieved.

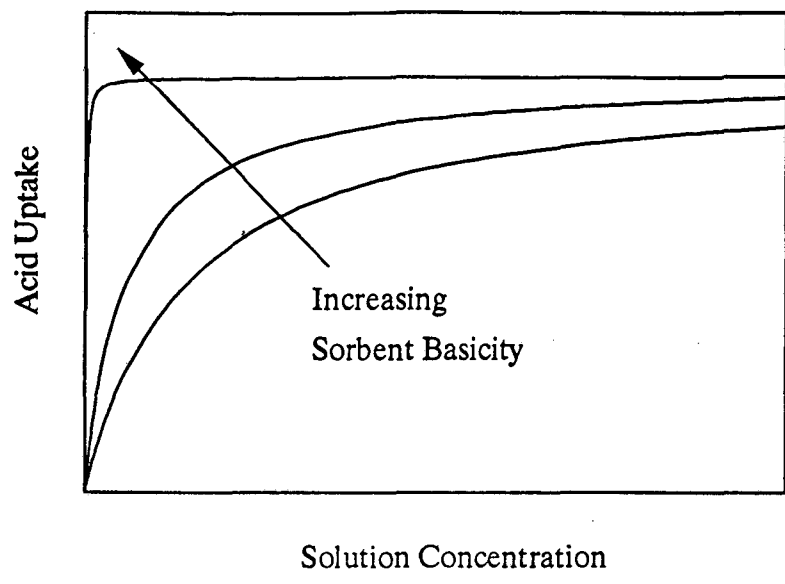
1.3 Recovery Using Strongly Basic Sorbents and Extractants

1.3.1 Effect of Basicity on Uptake

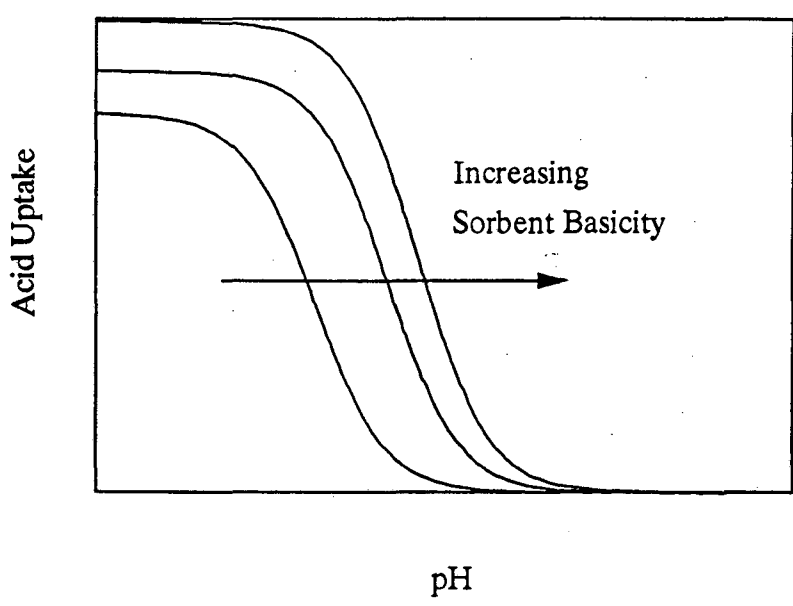
The recovery method investigated in this research focusses on the use of strongly basic sorbents and extractants, which can sustain capacity to several pH units above the pK_a of the carboxylic acid. Figure 1-1 schematically compares sorption isotherms and uptake-pH curves for sorbents of different basicities. Analogous curves could be drawn for extraction systems. For more strongly basic sorbents, the initial slope of the sorption isotherm (Figure 1-1(a)) is steeper, and the amount of acid sorbed reaches its maximum value at a very low solution concentration.

Increased basicity also results in a shift in the uptake-pH curve (Figure 1-1(b)) toward higher pH values. The reason for this shift can be understood by looking at the isotherms. At low values of pH, the concentration of un-ionized acid is high, and all of the sorbents have high uptakes of acid. However, at higher values of pH, the concentration of un-ionized acid decreases, and the uptake of acid by the more weakly basic sorbents begins to decrease. The stronger the sorbent, the higher the pH value at which this drop begins to occur. Thus, strongly basic sorbents are desirable for sustaining capacity at high pH.

The major advantage of using strongly basic sorbents and extractants is that recovery occurs at the pH of the fermentation broth. Thus, the recovery process can be carried out directly in the fermenter, or it can occur in an external loop without consumption of chemicals for pH adjustment. The choice of implementation is related to other issues, including toxicity concerns. The toxicity of sorbents or extractants is a subject of current research and can be overcome by use of sequential processing, a membrane, or other means. Toxicity issues will be discussed in greater detail in Section 5.3.



(a)



(b)

Figure 1-1. Effect of Sorbent Basicity on
(a) Sorption Isotherm (b) Uptake-pH Curve

1.3.2 Regeneration of Sorbent/Extractant

Strongly basic extractants and sorbents require correspondingly powerful regeneration methods. Many of the approaches that are effective with the physical solvents or non-functionalized resins used in the low-pH processes described above are much less effective with strongly basic sorbents/extractants. One method which is sufficiently powerful is back-extraction into an aqueous solution at higher pH, or "pH-swing." The aqueous base can effectively compete with the basic sites on the sorbent/extractant for the acid, pulling the acid into the aqueous phase and regenerating the sorbent/extractant.

If an ordinary base (e.g., NaOH or $\text{Ca}(\text{OH})_2$) is used, an acid (e.g., H_2SO_4) must be added in order to form the carboxylic acid product. This approach will consume chemicals and generate a waste salt stream, as in the conventional calcium precipitation process or a process using extraction/sorption with acid addition.

An alternative method involves leaching with an aqueous solution of trimethylamine (TMA). Poole and King (30), extending a related concept of Urbas (31), have shown that amine-carboxylic acid extracts can be regenerated by leaching with aqueous TMA. The resulting trimethylammonium carboxylate can be decomposed thermally, yielding acid product and TMA and water vapor, available for recycle. It is also possible to leach with aqueous ammonia or a primary or secondary amine, but some irreversible amide formation may occur during the thermal decomposition.

For slightly soluble acids, such as succinic and fumaric acids, partial evaporation of the aqueous trimethylammonium carboxylate results in crystal formation. After washing and/or recrystallization steps, product recoveries of 67 to 81 % were achieved in a single stage, with 0.004 to 0.05 mols TMA/mol acid remaining in the acid crystals (30). Higher yields and purity levels should be attainable through further refinement of the cracking and washing processes.

Because lactic acid is much more water-soluble than succinic or fumaric acids and tends to form intermolecular esters in concentrated solution, trimethylammonium lactate is

much more difficult to crack (30). As the aqueous lactate solution was heated, the viscosity of the solution increased steadily. Only 62% of the TMA present in the initial solution was driven off, and a viscous solution of water, TMA, lactic acid and lactate polymers was left behind. Further studies of the trimethylammonium lactate system were left to future work.

1.3.3 Proposed Process

In this study, a three-step process for recovering carboxylic acids at $\text{pH} > \text{pK}_a$ is investigated. This process has been granted U.S. Patent 5,132,456 (32). As shown in Figure 1-2, the acid is extracted (or adsorbed) from the fermentation broth by a strongly basic sorbent or extractant that is capable of sustaining capacity at $\text{pH} > \text{pK}_a$. The acid is then back-extracted from the organic phase into an aqueous trimethylamine solution. The resulting trimethylammonium carboxylate is heated to drive off water and TMA, which are recycled to the process. Acid product is then sent to further purification steps.

1.4 Project Goals

The primary goals of the current research are: (1) to identify extractants and adsorbents that sustain capacity to two pH units or more above pK_{a1} and are regenerable by leaching with aqueous TMA, and (2) to understand the equilibria involved. A secondary goal is to improve the cracking process for lactic acid.

1.4.1 Identification of Promising Sorbents and Extractants

The choice of sorbent/extractant involves balancing the performance at $\text{pH} > \text{pK}_a$ with the regenerability. The sorption/extraction and regeneration processes can be viewed in terms of the driving forces involved, as shown in Figure 1-3. Lactic acid, for example, has a pK_a of 3.86, and TMA has a pK_a of 9.8. Thus, approximately six pH units are available as a driving force for the sorption/extraction and regeneration processes. The goal is to choose a sorbent or extractant with an equivalent pK_a such that the driving force for

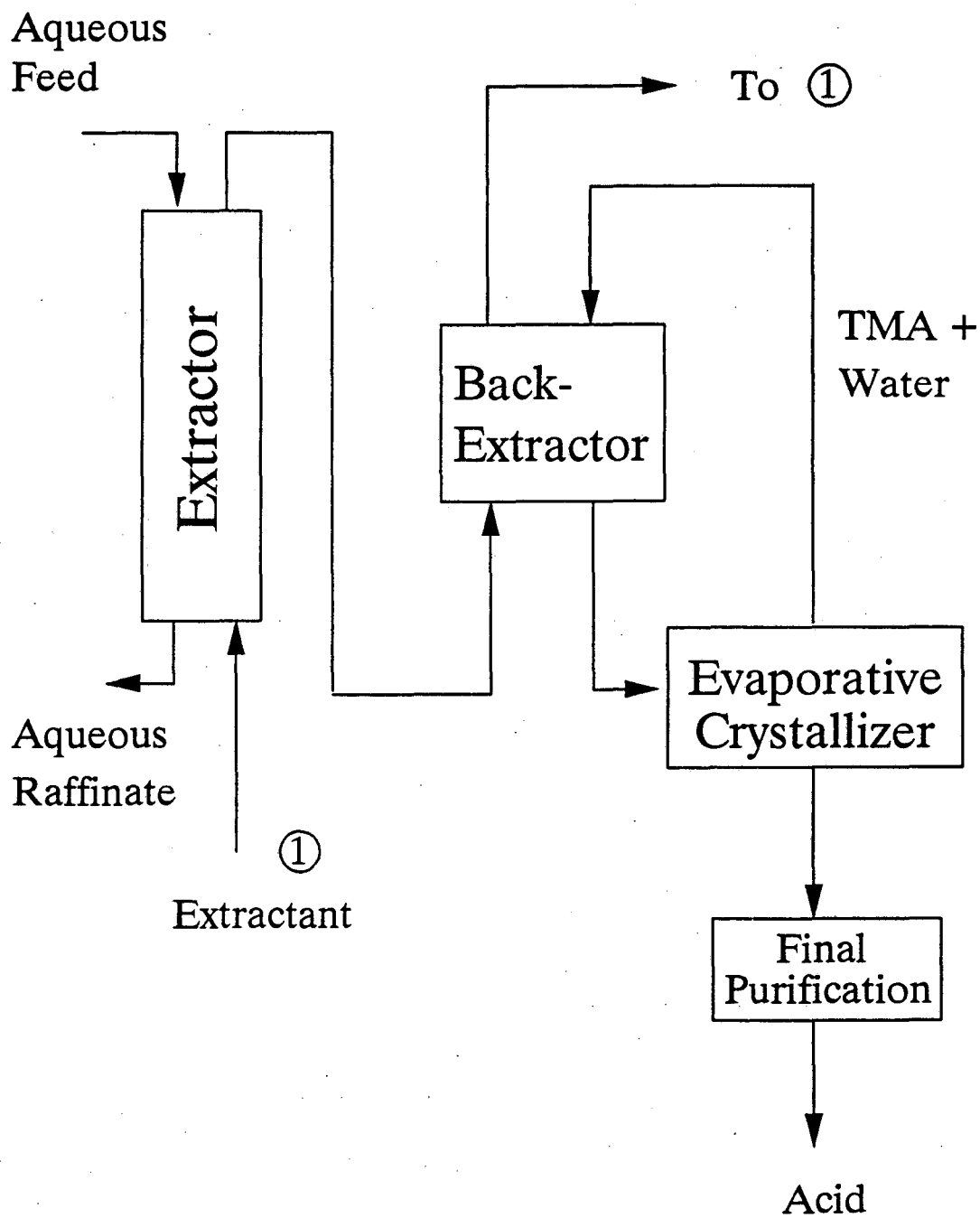


Figure 1-2. Carboxylic Acid Recovery Process

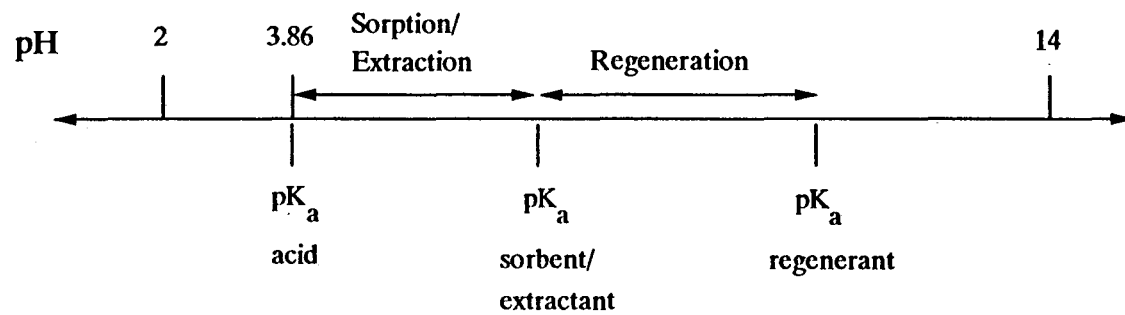


Figure 1-3. Driving Forces for Sorption/
Extraction and Regeneration Processes

sorption/extraction is high enough to sustain capacity well about the pK_a of the acid and also such that the driving force for regeneration is sufficiently high that complete regeneration is possible.

The process of choosing a sorbent/extractant which performs well at $pH > pK_a$ and is completely regenerable would be greatly facilitated by an understanding of the various equilibria involved. This work attempts to provide that understanding by looking at a range of sorbents and extractants and relating structural differences to differences in basicity. These differences in basicity are in turn related to differences in performance at $pH > pK_a$ and differences in regenerability.

1.4.2 Improved Process for Cracking Trimethylammonium Lactate

The other goal of this work is to improve the process for cracking trimethylammonium carboxylate. Two different approaches are studied: (1) cracking in the presence of an organic solvent, and (2) direct esterification of the trimethylammonium lactate. Processing considerations are also discussed.

1.5 Acids of Interest

The acids of interest in this work generally have low volatilities and are produced by fermentations that operate at $pH > pK_a$. While other acids may be recovered by the techniques outlined here, other methods, such as distillation, may be more appropriate. Non-volatile carboxylic acids with large potential markets include lactic acid and the C_4 dicarboxylic acids. The acids investigated in this work are lactic and succinic.

1.5.1 Lactic Acid

Lactic acid is a specialty chemical with current markets in the food, pharmaceutical, cosmetics, leather, textile, and other industries (1). Its current price is \$1.03 to 1.06 per pound for 88 percent food or technical grade acid (33). In 1982 more than 50% of all lactic acid was

used as a food acidulent and preservative, and 20% was used to produce stearyl-2-lactylates, which are used in baking (3). Lactic acid can also be used to form biodegradable polymers for use as packaging or in medical applications, such as resorbable sutures or prosthetic devices (34). Cargill, Inc. recently announced plans to build a plant that could produce 250 million pounds per year of biodegradable plastic from lactic acid (35). Although the annual U.S. market was just under 50 million pounds in 1986 (34), the potential market is much greater both because of the interest in biodegradable polymers and because several large-volume chemicals can be produced from lactic acid. For example, it is possible to produce polyesters, acrylics, and propylene glycol from lactic acid feedstocks (1, 34).

There is also a smaller market for lactate esters in the food, pharmaceutical and other industries. Butyl and ethyl lactates are used as flavorings and solvents. Ethyl lactate is used as a lubricant, in cryogenic greases, and in some anti-inflammatory drugs. Ethyl and isopropyl lactate are used in the manufacture of certain pesticides and herbicides. There are markets for other alkyl lactates as stripping lacquers, inks and flavorings (3).

Lactic acid is currently produced both synthetically and by fermentation, with production split almost equally between the two in 1985 (3). The synthetic route involves the hydrolysis of lactonitrile, which can be made from hydrogen cyanide and acetaldehyde. The acid is purified through formation of the methyl ester. Industrial fermentations use several homofermentative bacteria of the *Lactobacillus*, *Streptococcus*, and *Pediococcus* genera. Typical feedstocks are sucrose from cane and beet sugar; whey containing lactose; and maltose and dextrose from hydrolyzed starch. The fermentation generally operates at pH 5 to 7 (5 to 6.5 for *L. delbreuckii*) and temperatures above 40 °C. Vickroy (3) discusses the production of lactic acid by fermentation in greater detail.

1.5.2 Succinic Acid

Succinic acid has applications in agriculture, food, pharmaceuticals, plastics, textiles, plating and waste-gas scrubbing (7). It has a market on the order of a million pounds per year

(36), at a price of \$4.35 per pound for purified crystals (33). The acid has applications as a food acidulant, as an additive in bread doughs, or for producing edible, thermally stable synthetic fats. It also has a large potential market as an intermediate in the production of 1,4-butanediol, tetrahydrofuran, γ -butyrolactone and other C_4 chemicals, which have a worldwide market of 600 million pounds annually (1).

Succinic acid is produced industrially by the catalytic hydrogenation of maleic acid, maleic anhydride or fumaric acid (1, 7). It is also a major byproduct of the production of adipic acid for use in nylon. Fermentation is not currently used to produce succinic acid, although fermentation systems have been studied in Japan and appear to be economically competitive. Problems faced by researchers include low productivities and multiple product formation (1). The acid can be produced by several strains of bacteria, using feedstocks such as sucrose, acetone, and isopropyl alcohol (7). Recently, *Anaerobiospirillum succiniciproducens* has been shown to produce succinic acid at high yield and rate from glucose syrup or whey lactose (1). The preferred pH range for this fermentation is 5.8 to 6.6 (4). Succinic acid has also been produced from citric and other acids by *Lactobacillus* at pH 6.5 to 6.8 (5). Fermentations producing succinic acid from n-paraffins typically have final pH values in the range of 4.9 to 6.3 (6).

1.6 Overview of Dissertation

After a brief description of the experimental procedures and analytical methods used (Chapter 2), the first two steps of the proposed process are examined. In Chapter 3, the effectiveness and regenerability of several polymeric sorbents are discussed. Analogous material for extraction systems is presented in Chapter 4. The use of sorption and extraction in real fermentation systems is discussed in Chapter 5. In Chapter 6 the focus shifts to the third step of the proposed process, the cracking of the trimethylammonium carboxylate. Finally, in Chapter 7, issues related to process implementation are discussed.

CHAPTER 2. EXPERIMENTAL PROCEDURES AND EQUIPMENT

2.1 Materials

2.1.1 Laboratory Chemicals

The chemicals used and their sources are shown in Table 2-1.

Table 2-1. Sources and Descriptions of Chemicals Used

Chemical	Source	Description
Lactic acid	Aldrich	85+% in water, A.C.S. reagent grade
Succinic acid	Fluka	> 99.5%
Trimethylamine	Aldrich	25 wt% in water, > 99.5% purity
Methylisobutyl ketone	Mallinckrodt	Analytical reagent grade
Chloroform	Fisher Scientific	99.9%
1-Octanol	Fisher Scientific	Certified A.C.S. grade
Toluene	Mallinckrodt	Analytical reagent grade
1-Butanol	Fisher Scientific	99.8%
Butyl lactate	Aldrich	99%
Aluminum oxide	ICN Pharmaceuticals	99.9%
Silica gel	Davidson Co.	-
Amberlyst 15 strongly acidic, macroreticular ion exchange resin	Aldrich	-
Alamine 336	Henkel Corp.	-
Amberlite LA-2	Fluka	-
Aliquat 336	Aldrich	-

Distilled water which had been passed through a Milli-Q water purification system (Millipore Corp.) was used in the preparation of all solutions.

Lactic acid forms intermolecular esters in concentrated solutions. The degree of polymer formation varies with concentration as shown in Figure 2-1. The 85% commercial syrup contains a significant percentage of polylactic acids, but below 20 wt.%, the lactic acid monomer is virtually the only species present. Given enough time, the 85% solution can be diluted to produce an aqueous solution of the monomer. However, because the hydrolysis kinetics are slow, the solution should be boiled for 12 hours to increase the rate of hydrolysis (37). In this work, the 85% syrup was diluted with water and boiled under total reflux for at least 12 hours. The final solution concentration was typically 20 wt.%. Complete hydrolysis of the esters was confirmed by HPLC analysis.

2.1.2 Extractants

The liquid extractant Alamine 336 (Henkel Corp.) was used as received. The manufacturer describes it as a straight-chain tertiary amine having a mixture of about 67% C₈ and 33% C₁₀ side chains. Small amounts of primary and secondary amine impurities are also reported, as shown in Table 2-2 (38). These results were confirmed by Ricker (39), who performed a gas chromatographic analysis of Alamine 336.

Table 2-2. Composition of Alamine 336 (38)

Component	%
3° Amine	95-97
2° Amine	1
1° Amine	0.2
Water	0.2

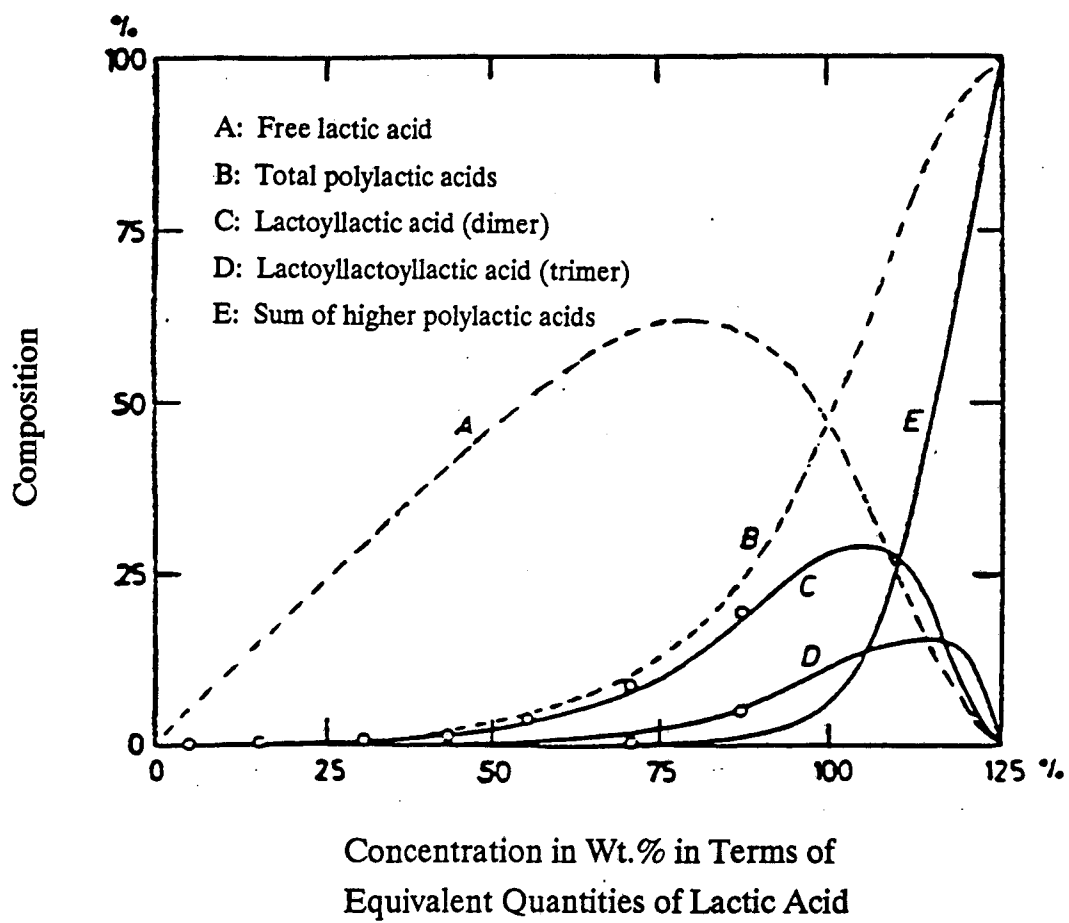


Figure 2-1. Equilibrium Composition of Aqueous Lactic Acid (from Holten [37])

The manufacturer reports an average molecular weight of 392 g/mol for Alamine 336, but Tamada et al. (40) determined an effective molecular weight of 406 g/mol. Because the Alamine 336 used in this work was from the same batch as that used by Tamada et al., a molecular weight of 406 g/mol was used in all calculations.

Amberlite LA-2 (Rohm and Haas Co.) was also used as received. It is described as an asymmetric alkyl amine with one straight C₁₂ chain and one highly-branched chain with 12-15 carbons (41). Low-molecular-weight amine impurities have also been reported for this extractant (42). The manufacturer's stated capacity is 2.2 - 2.3 mmol amine/ml (43); an average value of 2.25 mmol/ml was used in all calculations.

Aliquat 336 (Henkel Corp.) is a quaternary alkylammonium chloride with an average molecular weight of 442 g/mol, produced by methylating Alamine 336 (44). In some experiments it was used as received, in Cl⁻ form. In other experiments an attempt was made to convert the Aliquat 336 to OH⁻ form. A 0.3 M solution of Aliquat 336 in the appropriate diluent was contacted with an equal volume of 2 N NaOH in a separatory funnel. The two phases were mixed for several minutes and then allowed to settle. The phases were separated, and the aqueous phase was acidified and analyzed for Cl⁻. The process was then repeated with fresh NaOH. The Cl⁻ analysis indicated that even after 8 successive contacts with NaOH, the Aliquat 336 was not completely converted to OH⁻ form. The Aliquat 336 solution was therefore contacted with an equal volume of concentrated (near saturation) NaOH. The organic phase turned from amber to dark brown. The final conversion of this brown Aliquat 336 solution to OH⁻ form was slightly less than 50%.

2.1.3 Sorbents

Several different sorbents were used in this work. Their manufacturers and stated structures are given in Table 2-3. The manufacturers' suggested maximum operating temperatures are listed in Table 2-4.

Bio-Rad AG3-X4 was used without further purification. The unquaternized, or free base, resins (Dowex MWA-1, Dowex 66, Reillex 425, Duolite A7, and Amberlite IRA-35) were washed repeatedly with water, methanol, sodium hydroxide (0.05 to 0.2 N), and

Table 2-3. Basic Sorbents Used (45, 46, 47, 48)

Sorbent	Manufacturer	Matrix	Functional Groups	Mesh Size *
Bio-Rad AG3-X4 (Dowex XUS40091)	Dow Chemical Company	Polystyrene-divinylbenzene	90% 3° Amine/ 10% 4° Ammonium	20 - 50
Dowex MWA-1	Dow Chemical Company	Polystyrene-divinylbenzene	3° Amine	20-50
Dowex 66	Dow Chemical Company	Polystyrene-divinylbenzene	3° Amine	20-50
Reillex 425	Reilly Industries, Inc.	Poly(4-vinyl pyridine)	Pyridine	18-50
Reillex HPQ	Reilly Industries, Inc.	Poly(4-vinyl pyridine)	37% pyridine 63% 4° pyridine salt	30-60
Duolite A7	Rohm & Haas Corporation	Phenol-formaldehyde-polyamine	Polyamine	16-50
Amberlite IRA-910	Rohm & Haas Corporation	Polystyrene-divinylbenzene	4° Ammonium (Type II)	16-50
Amberlite IRA-35	Rohm & Haas Corporation	Acrylic	3° Amine	16-50

* Manufacturer's stated value

hydrochloric acid (0.05 to 0.1 N), then further purified by Soxhlet extraction with methanol for 24 hours. The quaternized resins were treated somewhat differently. Reillex HPQ was washed repeatedly with methanol and water. Amberlite IRA-910 was washed repeatedly with water, methanol, sodium hydroxide (0.05 to 0.2 N), and hydrochloric acid (0.05 to 0.1 N).

Both resins were converted to hydroxide form by contacting with 1 N sodium hydroxide in a column until no chloride was detected in the effluent, then rinsed with water until the pH of the effluent was less than 9.

Table 2-4. Maximum Sorbent Operating Temperatures (45, 46, 47, 48)

Sorbent	Maximum Operating Temperature (° C)
Bio-Rad AG3-X4 (Dowex XUS40091)	93
Dowex MWA-1	100
Dowex 66	100
Reillex 425	260
Reillex HPQ	~200
Duolite A7	40
Amberlite IRA-910	77 (Cl ⁻) 41 (OH ⁻)
Amberlite IRA-35	60

Bio-Rad AG3-X4 and the free base resins were dried to constant weight in a vacuum oven at 60°C and 50-60 kPa. For Duolite A7, this temperature is somewhat higher than the manufacturer's stated maximum operating temperature, which is 40 °C, but tests confirmed that drying of the resin did not affect the adsorption isotherm, nor was there any discoloration. With the exception of Reillex 425, the free base resins were used in the dry form. Reillex 425 proved difficult to wet with water, and was therefore pre-wet by stirring in methanol under vacuum and then displacing the methanol with water. The two quaternized resins were also used in the water-wet form. The wet resins were centrifuged before use to remove interstitial water. A small sample was dried to obtain the moisture content gravimetrically.

2.2 Analytical Methods

2.2.1 Titrations

Titration of acid or base solutions were performed with standardized sodium hydroxide or hydrochloric acid (0.01 or 0.10 N). The endpoint was determined either potentiometrically or by using an appropriate indicator (phenolphthalein for titrations of acids, methyl red for titrations of trimethylamine). pH was measured using an Orion 601A pH meter equipped with an Orion Ross combination pH electrode.

2.2.2 Chloride Analysis

For the sorbent capacity determinations, chloride concentration was measured by titration with silver nitrate in the presence of potassium chromate (47, 49). Other chloride measurements were performed with an Orion 601A meter equipped with an Orion Model 96178 chloride electrode.

2.2.3 High-Performance Liquid Chromatography

High performance liquid chromatography (HPLC) analyses for organic acids were performed with a Perkin-Elmer Series 10 liquid chromatograph and a differential refractometer detector (Waters, Model R401). Initial analyses used a Waters Resolve C18 Column contained in a radial compression module (Waters, RCM) and a 0.01 N H_2SO_4 mobile phase. A Shodex DE-613 polymethacrylate column, which was found to be more stable at low pH, was used in later analyses. For samples containing TMA, a Bio-Rad HPX-87H Micro-Guard cartridge, positioned between the chromatograph and the analytical column, served to replace trimethylammonium cations with hydrogen ions, thereby facilitating the analysis.

2.2.4 Ion Chromatography

Ion chromatography was performed using a Dionex DX 300 Gradient Chromatography System equipped with an AS4A Column (hydrophobic core resin agglomerated with aminated latex particles). The mobile phase was 0.045 mM sodium carbonate/0.0425 mM sodium bicarbonate at a flow rate of 2 ml/minute. Samples were typically diluted 100- to 1000-fold.

2.2.5 Gas Chromatography

Gas chromatography was performed with a Varian Model 3700 gas chromatograph equipped with a flame-ionization detector and a 5-6 ft Porapak PS column (Waters). In the analysis of aqueous samples containing TMA and/or carboxylic acid, the chromatograph was operated isothermally at 160 °C. For the esterification experiments the chromatograph was operated with temperature programming as follows: (1) 3 minutes at 110 °C; (2) 30 °C/min to 200 °C; and (3) 7 minutes at 200 °C.

2.2.6 Elemental Analysis

All elemental analyses were performed by the Microanalytical Laboratory, College of Chemistry, at the University of California at Berkeley using a Perkin Elmer Model 2400 Elemental Analyzer.

2.3 Sorbent Experiments

2.3.1 Sorbent Capacities

Resin capacity measurements were performed using the ammonia-nitrate method (47, 49). A known weight (about 5 g) of wet resin was slurry-packed into a glass column. The resin was converted to chloride form by passing 1 liter of 4% HCl through the column in approximately 30 to 45 minutes, followed by a 1-liter absolute ethanol rinse. The weak-base capacity was then measured by passing through 1 liter of 0.15 M aqueous ammonia and

measuring the total chloride in the effluent by titration with silver nitrate. The strong-base capacity was then determined by passing through 1 liter of 4% sodium nitrate and again titrating for chloride in the effluent. The moisture content of the wet resin, needed to calculate the capacities on a dry-weight basis, was determined gravimetrically by drying a second sample of wet resin.

Nace (49) points out that the ammonia-nitrate technique may result in artificially high weak-base capacity measurements and low strong-base capacities due to hydrolysis of strong base sites by ammonia and interference by ammonia in the titration procedure. Nace recommends a more complicated procedure wherein total anion exchange capacity and strong base capacity are measured separately, with weak base capacity calculated by difference. This alternate procedure was tested on Reillex HPQ, and the results were not significantly different than those obtained with the ammonia-nitrate procedure. Nace does state that the error in the ammonia-nitrate technique is greatest with Type II strong base anion exchangers and with acrylic resins.

2.3.2 Sorption Isotherms

Sorption isotherms were generated by contacting known weights of sorbent (typically 1 g) and acid solution (typically 10 g) in a 20-ml scintillation vial sealed with a foil-lined cap. The pH of the solution was not adjusted, and buffering agents were not used. The vial was placed on a shaker bath (Fisher Scientific Versa-Bath S) at 25°C and 80 rpm for approximately 48 hours. Previous studies (22) have shown that under these conditions equilibrium is achieved in less than 20 hours. Additional studies with lactic acid and Dowex MWA-1 showed that equilibrium was reached within the experimental error within 1 hour.

Aqueous-phase acid concentrations were determined by potentiometric titration. The wet sorbent was centrifuged in a 15-ml, coarse grade, fritted glass filter placed in a plastic centrifuge tube. The centrifuge (Damon/IEC Model HN-SII) was operated for 8 minutes at 2000 rpm. These conditions are sufficient to remove nearly all of the interstitial and adhering

bulk liquid (50). The weight of the centrifuged sorbent was used to calculate the total solution uptake.

2.3.3 Uptake-pH Curves

Aqueous solutions of 0.45 M lactic or succinic acid (corresponding to 4.0 % (w/w) lactic acid or 5.3 % (w/w) succinic acid) were adjusted to a range of pH values using sodium hydroxide. 11.0 g of each solution was contacted with 1.0 g dry sorbent in a sealed vial which was placed on a shaker bath at 25°C for 48 hours. After equilibration, the pH of the solution was measured. The pH of the sample was adjusted to 2.0, and the aqueous phase acid concentration was determined by HPLC. The wet sorbent was also centrifuged as before and weighed to provide information on total solution uptake.

2.3.4 Leaching Experiments

Leaching experiments were performed by contacting acid-laden sorbent with aqueous trimethylamine solutions (0.1 to 0.9 M) in sealed vials placed on the shaker bath at 25°C for 48 hours. The initial TMA concentration was determined by titration with sodium hydroxide. The concentration of acid in the final aqueous phase was determined by HPLC. The final leached sorbent was centrifuged as before and weighed, and the weight of the wet sorbent was used to calculate the total solution remaining in the pore volume.

2.3.5 Experiments with Actual Fermentation Broth

Experiments with actual fermentation broths were conducted in a manner similar to the sorption isotherm experiments. The concentrations of lactic and acetic acids and ethanol in the initial and final solutions were determined via HPLC. Initially, growth of mold spores in the samples was a problem. Therefore, two precautions were taken to prevent the growth of molds and other organisms. Before solution and sorbent were added to the scintillation vials, the vials were rinsed with a solution of 70% ethanol in water and drained face down on

clean paper towels. In addition, the samples were placed on the shaker bath at 25 °C for only 5 to 6 hours, rather than 48 hours. This length of time was long enough for the system to come to equilibrium but short enough that growth of molds was not a problem.

2.3.6 Sulfate and Phosphate Uptake Experiments

Aqueous solutions containing lactic acid and sodium sulfate or sodium phosphate were contacted with sorbent in sealed vials, as in the sorption isotherm experiments. Initial and final concentrations of lactic acid were determined via HPLC, and concentrations of sulfate and phosphate were determined by ion chromatography. Sorbents were also leached with TMA solutions as in the leaching experiments, and the concentrations of lactic acid and sulfate/phosphate in the leachate were measured. For some samples, the change in solution concentration was so small that the uptakes of lactic acid and/or sulfate/phosphate were more precisely determined from the leachate analysis.

2.3.7 Fixed-Bed Sorption Studies

Fixed-bed studies were performed using the apparatus shown in Figure 2-2. The apparatus consists of a 10 mm inner diameter X 30 cm length glass column with a 20 μm polyethylene bed support (Rainin Economy Column) and a needle valve at the outlet. An adjustable Delrin plunger (Rainin) with a Viton O-ring was used to provide a leak-free seal. The hollow plunger was inserted into the column, and the O-ring was expanded against the column by turning a compression screw at the top of the plunger. This action locked the plunger into position and formed a leak-free seal. Solution was then fed into the column via PTFE tubing extending into the hollow plunger. Solutions were delivered to the column at a constant flow rate with a Masterflex (Cole-Parmer Co.) pump. Samples were collected from the outlet of the column over 5-minute periods in glass scintillation vials using a fraction collector (LBK-Produkter AB).

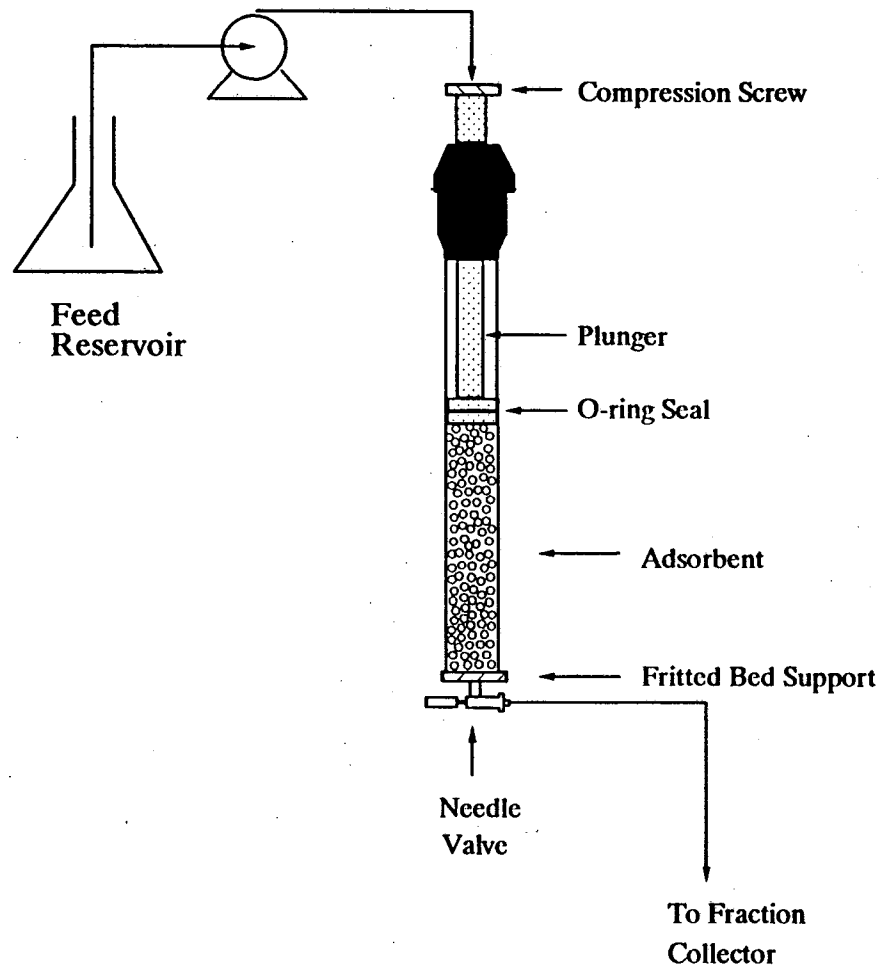


Figure 2-2. Apparatus for Fixed-Bed Experiments

The procedure for generating a breakthrough curve was designed to minimize any mixing volume above the packed bed. The cleaned, dried resin was pre-wet with methanol and then water, and slurry-packed into the column, which had been filled one-third of the way with water. The bed was topped off with approximately 1 cm of fine glass beads, and the water level was then drained to the top of these beads. The pump and the inlet lines to the column were filled with solution. The following steps were then performed in quick succession: Several milliliters of solution were added to the top of the column; the plunger assembly was screwed onto the top of the column; the bottom valve was opened; and the fraction collector was started.

Leaching curves were generated in a similar manner, after the column was drained and the lines flushed with aqueous TMA. The solution reservoir was kept tightly sealed to avoid loss of TMA, and the outlet samples were capped as soon as they were complete. The volume and pH of each outlet sample was then measured, and the concentrations of acid or other species were determined as in previous experiments. In certain experiments, TMA concentrations were measured using gas chromatography.

Minor losses of TMA from the outlet samples may have occurred, since the vials were open to the atmosphere for 2-5 minutes before being capped. However, for much of the leaching process the concentration of carboxylic acid present in the samples was sufficient to prevent significant volatilization. For samples taken at later stages of the leaching process, the carboxylic acid concentrations were low, and a more significant loss of TMA was observed. Whereas final outlet TMA concentrations should have leveled off at the feed value, measured concentrations were only 93-97% of the feed value. Overall, the concentrations of carboxylic acid in the outlet samples appeared to be unaffected by minor TMA losses, as confirmed by mass balances for the acid, which closed within 5%.

An overall void volume was also necessary for breakthrough curve calculations. The interstitial void fraction for the packed bed (defined as the volume of liquid between the sorbent particles divided by the total volume of the bed) was determined as follows. The

column was weighed, filled with water and water-wetted resin of a known dry weight, and weighed a second time. The interstitial void fraction was then calculated from the difference between the two column weights, the weight of the dry resin, and an independently determined value of the moisture content of the wetted resin. The bulk (packing) density of the resin was calculated from the known cross-sectional area of the column and a measured value of the height of a known weight of sorbent in the column. The amounts of liquid holdup in the bottom tubing and valve were also measured by filling these pieces with water and weighing. From the interstitial void fraction, the bulk density, and the tubing/valve void volume, an overall void volume could be calculated for any given run.

2.4 Extraction Experiments

2.4.1 Uptake - pH Curves

Aqueous solutions of 0.45 M lactic or succinic acid were adjusted to various pH values using sodium hydroxide. The solutions were then contacted with equal volumes of 0.3 M extractant in the appropriate diluent in 40-ml vials equipped with Teflon-lined caps. The vials were placed on a shaker bath (Fisher Scientific Versa-Bath S) at 25°C and 80 rpm for approximately 48 hours. Previous experiments showed that this amount of time was more than sufficient to achieve equilibrium. After equilibration, the phases were separated by centrifugation for 8 minutes at 2000 rpm. There was no detectable change in the volume of either phase. Aqueous phase acid concentrations were determined by HPLC. Organic phase acid concentrations were determined by two-phase titration with aqueous sodium hydroxide. Mass balances on the system closed within 1 to 5%.

2.4.2 Back-Extraction Experiments

Back-extraction experiments were performed by contacting samples of acid-laden organic phase with a known volume of 0.1 to 0.9 M aqueous trimethylamine. The samples

were equilibrated in sealed vials as in the pH experiments. After equilibration, the two phases were separated by centrifugation for 8 minutes at 2000 rpm. There was no detectable change in the volume of either phase. The concentration of acid in the final aqueous phase was determined by HPLC.

2.4.3 Sulfate and Phosphate Uptake Experiments

Sulfate and phosphate uptake experiments for extraction systems were entirely analogous to those for adsorption systems.

2.5 Trimethylammonium Lactate Cracking Experiments

2.5.1 Simple Thermal Cracking

The apparatus for the trimethylammonium lactate cracking experiments is depicted in Figure 2-3. An aqueous solution (typically 75 ml) of 1.0 M trimethylammonium lactate was placed in a 3-neck, 100-ml, round-bottom flask and heated with a heating mantle (Glas-Col Apparatus Co.) attached to a voltage regulator (The Superior Electric Co., Powerstat). The solution was stirred with a magnetic stirbar.

The experiments were performed at 460-480 mm Hg abs., which was maintained with a vacuum pump (Marvac Scientific Manufacturing Co., Model 2AAR2) attached to a regulator. Nitrogen from a cylinder was sparged into the trimethylammonium carboxylate solution at a flow rate of approximately 75 ml/min to prevent possible oxidation of TMA. The flow rate was monitored with a shielded rotameter (Omega Engineering, Model FL-111). The pressure at the rotameter, which was necessary to calculate the nitrogen flow rate, was measured with a manometer.

Water was driven from the solution, condensed, and collected in a graduated water collection cylinder. The rate of water accumulation was monitored. TMA was absorbed by a solution of dilute sulfuric acid in an absorber flask. Initially, the absorber was filled with

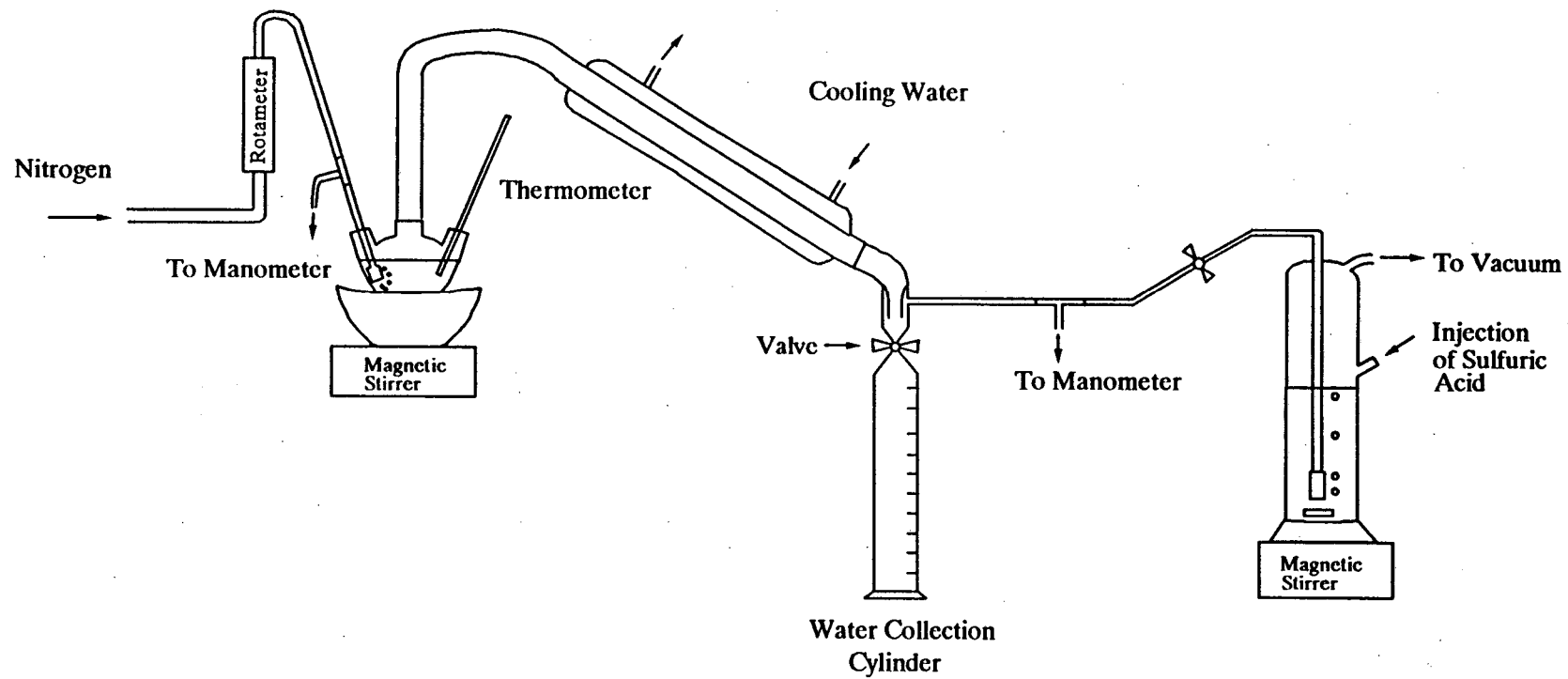


Figure 2-3. Apparatus for Cracking Experiments

400 - 500 ml of H_2SO_4 at a concentration sufficient to neutralize approximately 10% of the TMA present in the initial trimethylammonium lactate solution. Methyl red was added to the absorber solution as an indicator. When 10% of the TMA was absorbed, the solution changed in color from red to yellow. At this point, the time was noted and 5 ml of a concentrated H_2SO_4 solution, enough to neutralize another 10% of the TMA present in the system, was injected into the absorber through a septum, causing the absorber solution to become red again. This procedure was repeated throughout the course of the experiment, yielding a history of TMA evolution with time.

The temperature of the trimethylammonium lactate solution was monitored throughout each experimental run. As TMA and water vapor were driven off, the temperature of the solution was allowed to increase gradually with the boiling point. Late in the run, when most of the TMA and water vapor had been driven off, there was generally a very sharp rise in temperature. During initial runs, the solution was allowed to reach very high temperatures, at one point up to 200 °C. Since this caused severe discoloration of the solution and even some charring at the highest temperatures, in later runs the voltage regulator was adjusted to keep the temperature below 120 °C.

At the end of a run, the absorber solution was titrated with sodium hydroxide to determine the amount of unneutralized sulfuric acid. The water in the water collection cylinder was titrated with hydrochloric acid to determine the amount of TMA that had been absorbed by the water. When the system was under vacuum, this amount was typically less than 2.5% of the TMA present in the system. The amount of TMA remaining in the concentrated trimethylammonium lactate was determined by elemental analysis of the nitrogen present. Mass balances for TMA generally closed within 5%.

2.5.2 Cracking with Solvent Addition

Cracking experiments were also performed with the addition of solvent. The first part of the procedure was a simple thermal cracking, as described above. When the evolution of

TMA ceased, the voltage regulator was turned off and the system cooled. The condenser was then moved to a vertical position, as shown in Figure 2-4, and 30 or 40 ml solvent were added to the reaction flask. The solution was boiled under total reflux, at 470 mm Hg abs. and under a nitrogen environment. The evolution of TMA was monitored as usual. When TMA evolution again ceased, the condenser was switched back to the original position and the solvent boiled off. The final absorber solution was titrated with sodium hydroxide, and the flask contents were analyzed by elemental analysis. A mass balance on the TMA closed within 2%.

In an initial experiment, using MiBK, a slightly different procedure was followed. After the solution from the simple thermal cracking was cooled, 30 or 40 ml solvent were added to the solution and evaporated by heating at 445 mm Hg abs. under a nitrogen atmosphere. The evolution of TMA was monitored as usual. After three cycles of solvent addition and evaporation, 60 ml MiBK were added, the condenser was moved to the vertical position, and the solution was heated under total reflux conditions. When the evolution of TMA ceased, the solvent was boiled off. A mass balance on the TMA for this experiment closed within 11%.

2.6 Esterification Experiments

2.6.1 Esterification

2.6.1.2 Conversion Experiments

A concentrated trimethylammonium lactate solution was prepared by combining equimolar amounts of lactic acid (as the 21 wt.% solution) and TMA (as the 25 wt.% solution), and concentrating the resulting solution at 420 mm Hg abs. to 3.6 to 8.0 M. The TMA driven off during this step was absorbed by a sulfuric acid solution. The amount of TMA driven off

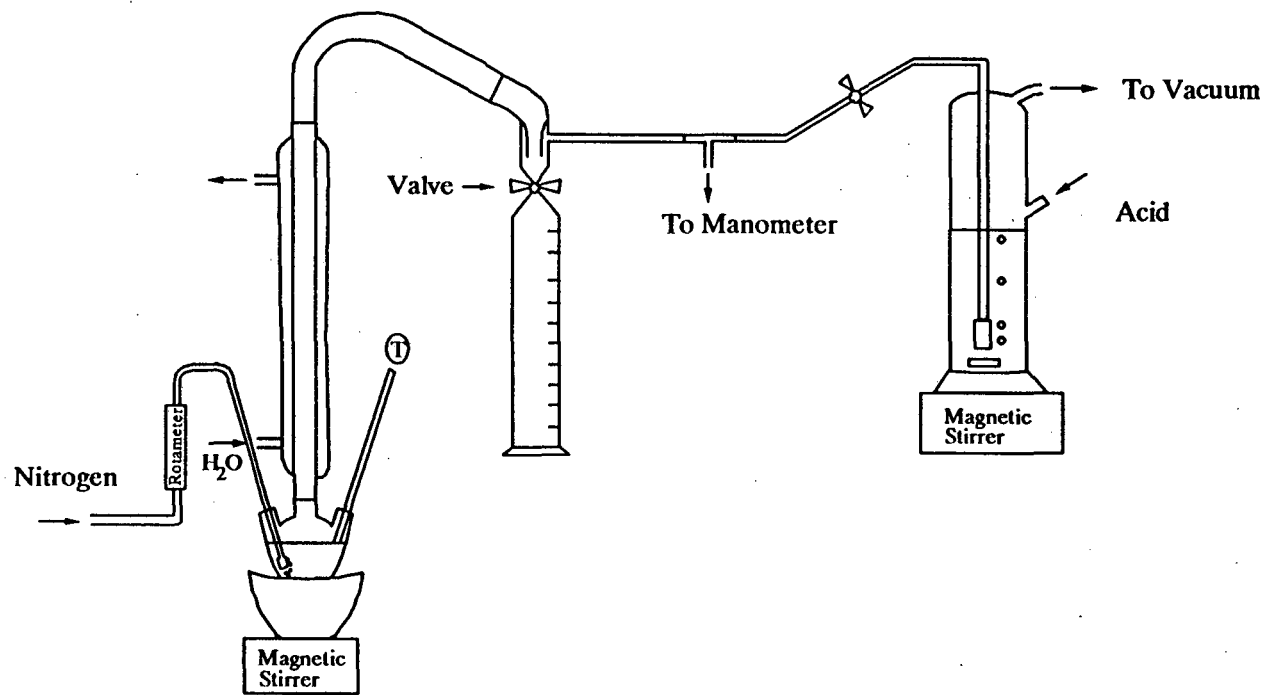


Figure 2-4. Apparatus for Cracking with Solvent Addition

varied with the amount of water removed and was typically between 15 and 30% of the total TMA present.

The concentrated trimethylammonium lactate solution was reacted with 1-butanol in the apparatus shown in Figure 2-5. The reaction mixture was heated in a 3-neck, 500-ml, round-bottom flask by a heating mantle attached to a voltage regulator, as in the cracking experiments. Nitrogen was sparged into the mixture through one side neck of the flask, and a thermometer was inserted into the second side neck through an adapter or rubber septum. The reaction mixture was stirred with a magnetic stirrer.

Vapor from the reacting mixture passed through a silver-jacketed column (11 in long X 1 in inner diameter) packed with glass helices and was condensed over a modified Dean-Stark water trap. The condensate consisted of two phases: the top, butanol-rich phase was automatically returned to the reaction flask through the column; the bottom, aqueous phase was periodically withdrawn from the trap using the stopcock. The level of water in the trap and the cumulative amount of water driven off were monitored as a function of time. Trimethylamine was also driven off and sent to an absorber flask. As in the cracking experiments, the rate of evolution of TMA was monitored over time.

The temperature in the reaction flask, monitored with a thermometer, was allowed to increase with the boiling point of the mixture. Typically, all reaction had ceased (as indicated by a zero rate of production of water and TMA) by the time the reaction mixture reached 142°C.

The amounts of 1-butanol and butyl lactate in the final reaction mixture were determined using gas chromatography. In some cases, the nitrogen content was determined via elemental analysis. The overall mass balance closed within 5-10 %, but the amount of 1-butanol present in the final solution was, on average, only about 78 % of the amount expected based on the percent conversion to butyl lactate.

Some of the reaction mixtures were distilled at 420 mm Hg abs. using the silver-jacketed column packed with glass helices. A fine capillary tube was inserted into the flask

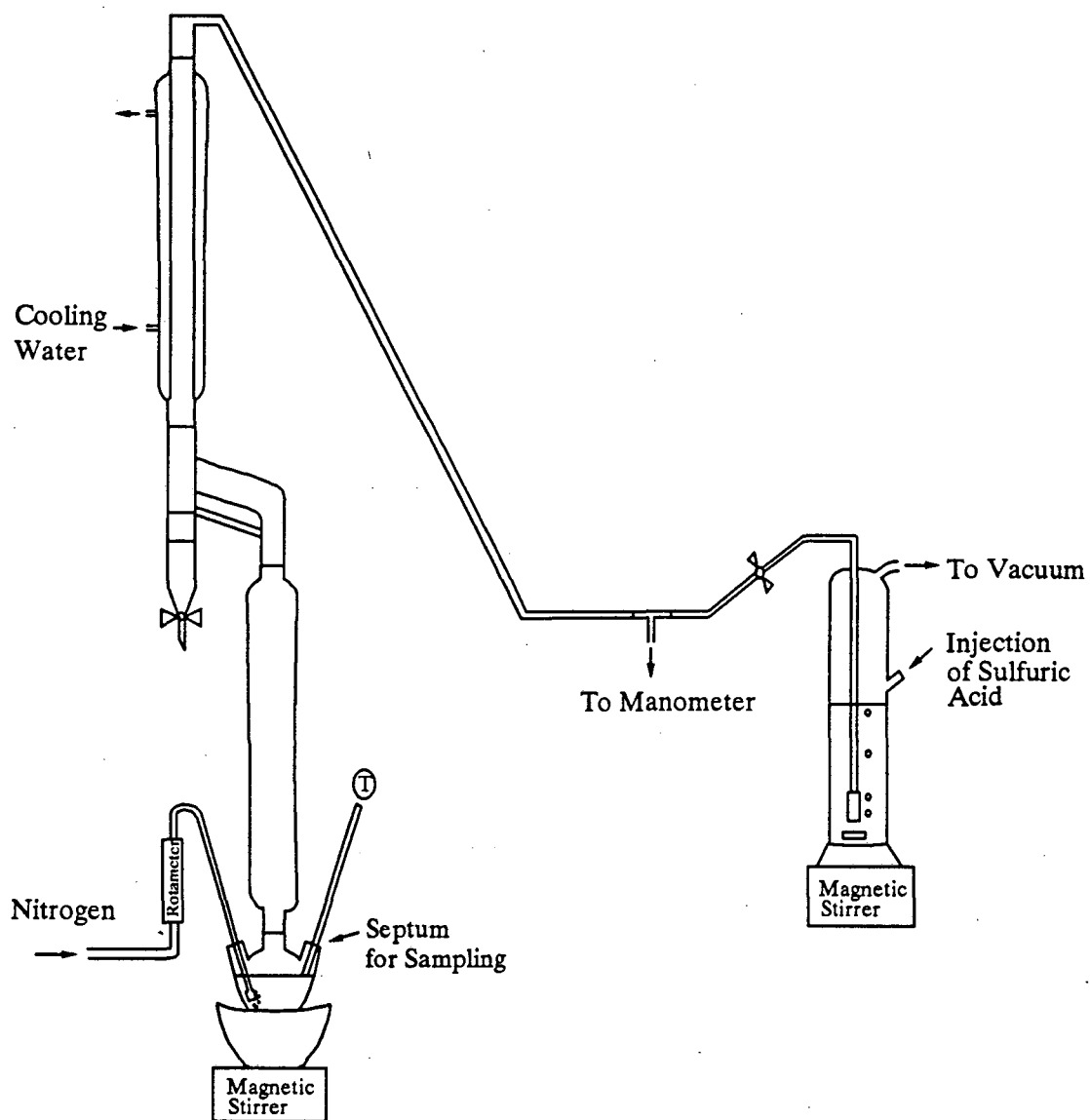


Figure 2-5. Apparatus for Esterification Experiments

to provide ebullition. A Perkin triangle was used to maintain the vacuum while the distillate receiving flask was changed.

2.6.1.2 Reaction Rate Experiments

The reaction rate experiments were also carried out at the boiling point of the mixture, and the heating rate was kept approximately constant from one run to the next by maintaining a constant setting on the voltage regulator. The procedure was then same as that given in the previous section, with a few modifications. The thermometer was inserted into the vial through a small hole drilled in a rubber septum. Small (circa 0.1-0.2 ml) samples were withdrawn periodically through this septum and analyzed by gas chromatography to monitor the rate of butyl lactate production. Whenever a sample was withdrawn, the amount of holdup in the Dean-Stark trap and the total amount of water collected up to that time were noted. From these two measurements and the final volume of the system, an estimate could be made of the total volume in the reaction flask at the time the sample was withdrawn.

The experiments involving catalysts (concentrated sulfuric acid, Amberlyst 15 cation exchange resin, silica gel, or alumina powder) were identical except that the catalyst was added to the reaction flask at the beginning of the experiment. For experiments with sulfuric acid, the catalyst made up 0.3 wt.% of the reaction mixture. Other catalysts were present at 2 to 7 wt. %.

The rate of esterification of a lactic acid solution, not containing TMA, was also studied. The procedure was entirely analogous to that described for trimethylammonium lactate solutions, except that TMA was not evolved.

In a final experiment, the rate of cracking of trimethylammonium lactate was examined. The experimental procedure was identical to that followed in the simple thermal cracking experiments (Section 2.5.1). However, the trimethylammonium lactate solution was heated in a constant-temperature oil bath set at approximately 140 °C, rather than with a

heating mantle, to allow for better temperature control. The temperature of the solution and the rate of evolution of TMA were monitored over time as in the cracking experiments.

2.6.2 Hydrolysis

In the hydrolysis experiments, 1 mol butyl lactate was combined with 3 mol water and 1 ml concentrated sulfuric acid catalyst in a 3-neck, 500-ml, round-bottom flask. The solution was heated under total reflux at atmospheric pressure, and samples were periodically withdrawn through a septum seal placed in one of the flask necks. The reaction flask held a cloudy, two-phase mixture until reaction was essentially complete, at which point enough 1-butanol had been produced that the solution became one clear phase. The resulting reaction mixture was neutralized with sodium hydroxide and distilled under 420 mm Hg abs. as in the esterification experiments. When most of the 1-butanol had been removed, the pressure was lowered to 90 mm Hg abs., and the distillation was completed at this pressure.

Chapter 3. RECOVERY USING BASIC POLYMERIC SORBENTS

3.1 Overview

A variety of basic polymeric sorbents were tested for their abilities to recover carboxylic acids at $\text{pH} > \text{pK}_a$. Sorbent basicities were compared using two different measures of pK_a . The effects of basicity on the sorption isotherms, the uptakes at $\text{pH} > \text{pK}_a$, and the regenerabilities were measured experimentally and the results modelled. Finally, the kinetics of the sorption and regeneration processes were examined via fixed-bed studies.

3.2 Sorbent Characterization

3.2.1 Macroporosity

The sorbents studied are all commercially available, macroporous (macroreticular) resins. Unlike gel resins, which are poreless polymer networks that take in solution via swelling, macroporous resins have fixed networks of pores and high internal surface areas. Solution uptake is by pore filling, with smaller degrees of swelling. Phenol-formaldehyde-amine and epoxy-amine resins are naturally macroporous. Other resins can be produced in macroporous form in the presence of higher amounts of crosslinking agent and a suitable solvent, called a porogen (51). The advantages of macroporosity include high osmotic shock resistance, less dramatic swelling, and higher oxidation resistance (51, 52). Macroporous resins may also demonstrate improved kinetics over gel-type resins (45, 51). However, because macroporous resins generally have lower capacities, gel resins are often preferred. Although macroporous resins were used exclusively in this work, the major conclusions presented here are expected to apply to gel-type resins as well.

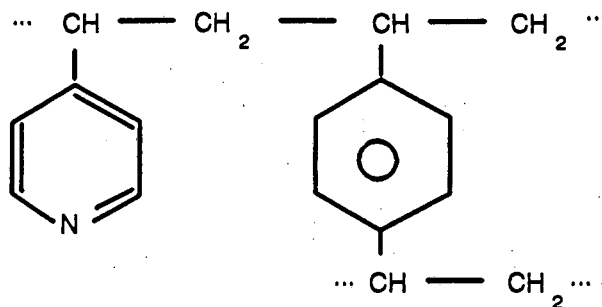
3.2.2 Chemical Structures

The resins studied contain a range of functional groups typically seen in commercially available basic sorbents -- pyridine, phenol-formaldehyde-amine, epoxy-amine, polystyrene-based tertiary amine, acrylic-based tertiary amine, N-methyl pyridinium and quaternary ammonium. Other commercially available basic resins contain amide, N-oxide, and benzimidazole functionalities. These resins, and the reasons for their exclusion from this study, will be discussed in a later section.

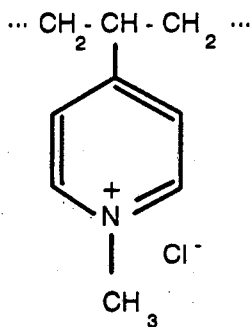
The quaternary ammonium and N-methyl pyridinium functionalities are fixed cationic groups, or strong-base anion exchange sites. Anion exchangers were mentioned in Section 1.2.3 in conjunction with ion exchange processes. In a true ion exchange process, the carboxylate anion exchanges with a counter-ion such as Cl^- or NO_3^- . Contamination of the aqueous phase by counter-ions and production of the carboxylate salt make this approach difficult to justify economically. In this work, however, the ion exchanger is converted to hydroxide form, and, as such, functions as a very strong base.

Two different poly(vinylpyridine) resins were studied. Reillex 425, depicted in Figure 3-1(a), is a monofunctional resin of crosslinked poly(4-vinylpyridine) (46). Reillex HPQ is similar, but 63% of the pyridine rings are quaternized by reaction with methyl chloride to form the N-methyl pyridinium chloride (45), as in Figure 3-1 (b). The resin was converted to the hydroxide form for these studies. It was later discovered that, under basic conditions, the quaternized rings can undergo a ring-opening reaction (53). This reaction may follow a mechanism discussed by Perrin et al. (54), in which the species shown in Figure 3-2 is first formed.

Duolite A7 is formed from the condensation polymerization of phenol, formaldehyde, and a polyalkyleneamine (43). Resins of this kind typically have the strongest osmotic shock resistances (51). For most phenol-formaldehyde-amine resins, the added amine is either diethylenetriamine or triethylenetetramine. Hodgkin and Eibl (55) show the structure presented in Figure 3-3 for Duolite A7, suggesting that the added amine is



(a)



(b)

Figure 3-1. (a) Chemical Structure of Reillex 425
(b) Quaternized Group on Reillex HPQ

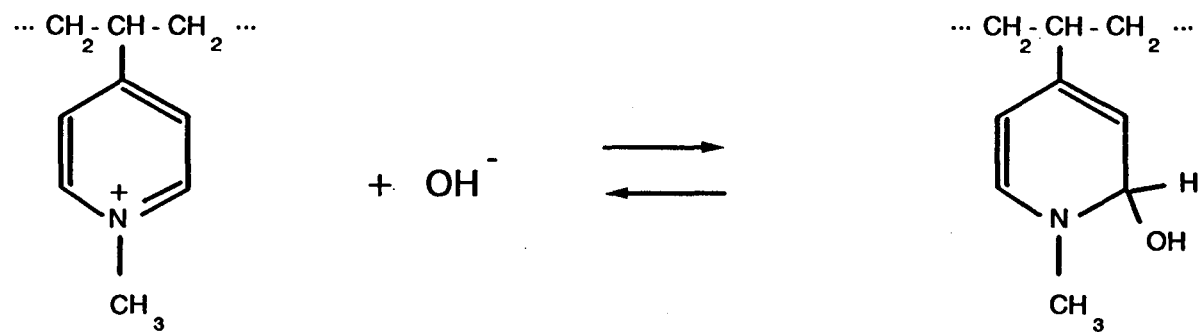


Figure 3-2. Formation of Intermediate in Ring-opening of Reillex HPQ (Perrin et al. [54])

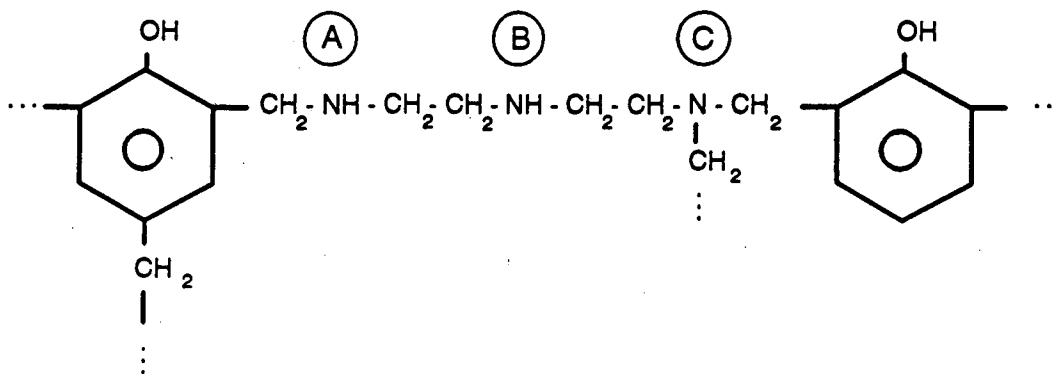


Figure 3-3. Chemical Structure of Duolite A7

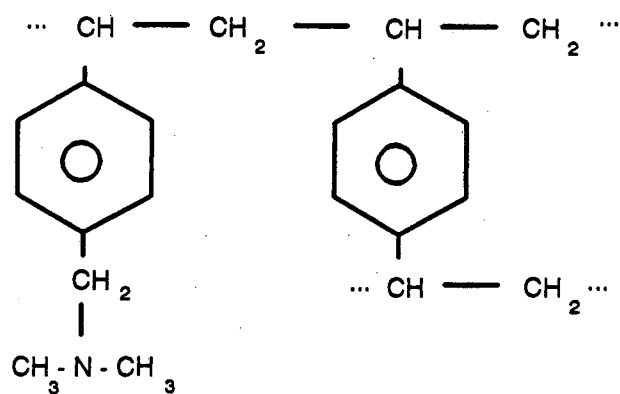


Figure 3-4. Chemical Structure of Dowex MWA-1 and Dowex 66

diethylenetriamine. Figure 3-3 is somewhat misleading in that the resin is actually of a three-dimensional nature, rather than a series of linear chains with crosslinks (51). The sorbent also differs from many other sorbents in that the polymer is produced in bulk and then ground into granules, rather than being produced directly in a bead form. Duolite A7 is marketed as a secondary amine (43), but resins of this type generally exhibit a wide range of functional groups (51, 55). Three possible types of amine groups are shown in Figure 3-3, marked by the letters "A", "B", and "C". Mineral acid titrations support the hypothesis that Duolite A7 is actually a polyamine (56). A high nitrogen content can typically be achieved in phenol-formaldehyde-amine resins, but because many of the functional groups are very closely spaced, under many operating conditions the useable capacity is much lower (51).

Dowex MWA-1 and Dowex 66 are both polystyrene-divinylbenzene resins with primarily tertiary amine groups (48), as shown in Figure 3-4. They are formed by the chlormethylation and subsequent amination of a styrene-divinylbenzene copolymer. During the amination step, two chlormethyl groups sometimes react with one amine molecule, resulting in the formation of a few percent of quaternized groups. Cycling of the resin eventually decreases this strong-base capacity (51).

Bio-Rad AG3-X4 is a cleaned, screened version of Dowex XUS40091 (57), which is closely related to Dowex WGR-2 (52, 58). The exact differences between Dowex XUS40091 and WGR-2 are proprietary information, but are believed to be related to polymer processing and not resin chemistry (58). Therefore, Bio-Rad AG3-X4 is assumed to have the same structure as Dowex WGR-2. The resin is of a general class of epoxy-amine resins, and is formed by the condensation of ammonia and epichlorhydrin (48). This results in a structure containing primarily tertiary amine groups (59). However, this particular resin is also reacted with methyl chloride to add 10% quaternary ammonium groups. The resulting structure is shown in Figure 3-5. The condensation is generally performed in the presence of an organic dispersant, which results in the formation of a porous structure (59). The final product is in

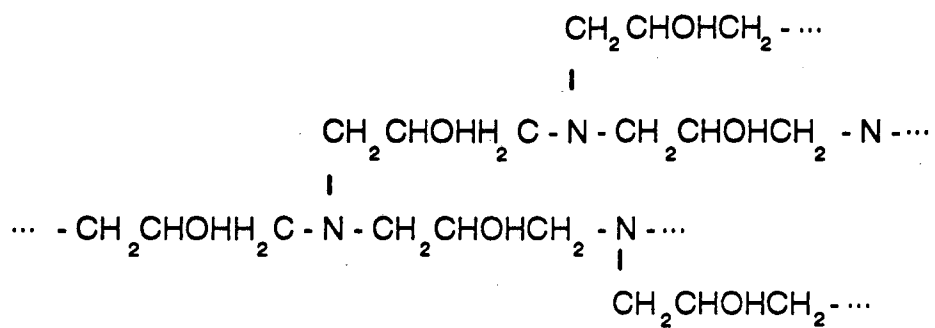
granular form. Like phenol-formaldehyde-amine resins, the epoxy-amine resins have high nitrogen contents, but only part of this capacity can actually be utilized (51).

Amberlite IRA-35 is an acrylic-based resin containing primarily tertiary amine groups (47). Gustafson et al. (60) gives the structure shown in Figure 3-6 for Amberlite IRA-68, which is the gel-form of this resin (52). The structure shows the presence of both amine and amide groups. The polymer is thought to be formed by the reaction of methyl acrylate and divinylbenzene, followed by reaction with dimethylaminopropylamine (52). Communication with a Rohm and Haas representative confirmed the use of dimethylaminopropylamine in the formation of IRA-35 (61).

Finally, Amberlite IRA-910 is a fully quaternized styrene-divinylbenzene resin, or a strong-base ion exchanger (47). Like Dowex MWA-1, it is formed by chlormethylation and subsequent amination of a styrene-divinylbenzene copolymer. Use of a tertiary amine in the amination step results in the formation of a quaternary ammonium site. In general, there are two different types of strong-base anion exchange resins: (1) Type I exchangers, made using trimethylamine and (2) Type II exchangers, made using dimethylethanolamine. The resulting structures are shown in Figure 3-7. Type I resins are more strongly basic and hence more difficult to convert from hydroxide to chloride form, but they are more resistant to thermal and oxidative degradation (51). Amberlite IRA-910 is a Type II resin and was chosen for its lower basicity.

3.2.3 Measured Capacities

Ion exchange capacities were determined experimentally and are presented in Table 3-1, along with the manufacturers' stated minimum capacities. The experimental capacities are divided into strong- and weak-base fractions. Strong-base capacity is associated with fully ionized functional groups, such as quaternary ammonium or N-methyl pyridinium salts, whereas weak-base capacity is associated with uncharged, free base sites, such as amine or pyridine groups. Because they are charged, strong base sites always have an associated



3-5. Chemical Structure of Bio-Rad AG3-X4

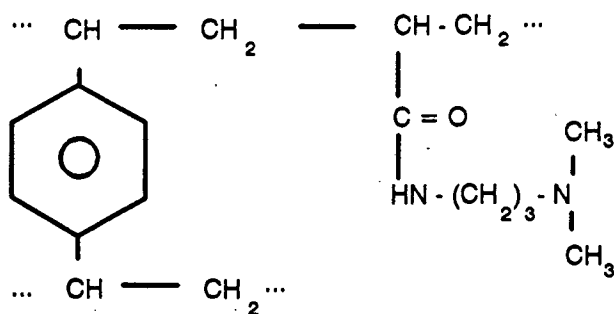


Figure 3-6. Chemical Structure of Amberlite IRA-35

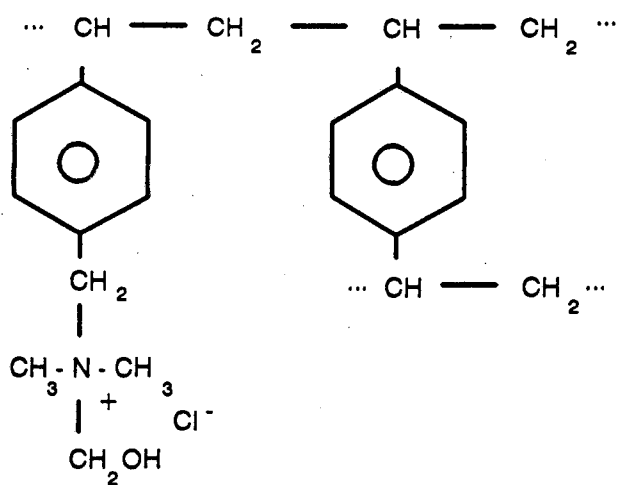
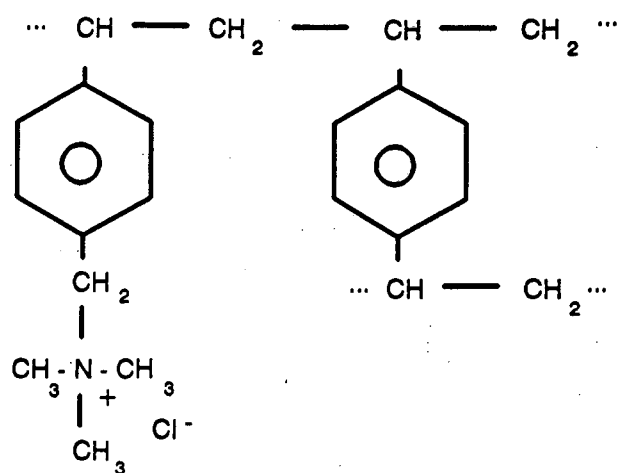


Figure 3-7. Chemical Structures of (a) Type I and (b) Type II Strong-Base Ion Exchangers

counter-ion, such as Cl^- or OH^- . In this work, weak-base capacity is defined operationally as any capacity which sorbs HCl and is regenerable by leaching with aqueous ammonium hydroxide. Strong-base capacity is defined as any capacity which takes up chloride, is not regenerable by leaching with ammonium hydroxide, but is fully regenerable by exchange with nitrate. The procedure for determining these capacities was described in Section 2.3.1.

In most cases, the experimental capacity and the manufacturer's stated value agree reasonably well. Two of the sorbents, Bio-Rad AG3-X4 and Duolite A7, have experimental capacities which are much larger than those of the other resins. These higher capacities are probably related to the fact that phenol-formaldehyde-amine and epoxy-amine resins generally have very high nitrogen contents. Evidently, under the conditions of the capacity determination experiments, much of this nitrogen content is able to complex with HCl. However, some of this capacity may not be useable under other conditions. For example, since carboxylic acid molecules are larger than HCl molecules, some of the measured capacity may not be accessible to carboxylic acid molecules due to steric constraints. Furthermore, because carboxylic acids are much weaker acids than HCl, some of the more weakly basic sites may not be useable in carboxylic acid experiments. A similar argument can be used to explain why the capacity stated by the manufacturer for Bio-Rad AG3-X4 is much lower than the experimentally measured value. The value given by the manufacturer may have been determined under conditions wherein the full capacity was not useable.

Duolite A7, Dowex MWA-1 and Dowex 66 all show small amounts of strong base capacity, despite the fact that they are sold as 100% weak-base resins. The presence of some quaternary ammonium groups is not unusual and results from the manufacturing processes, as described in the previous section. Another interesting observation is that Amberlite IRA-910, which is sold as a fully quaternized strong-base ion exchanger, shows substantial weak-base capacity. This result may be an artifact of the experimental procedure. Type II ion exchangers, the more weakly basic of the two standard types of strong-base ion exchangers,

are sometimes partially regenerable with ammonium hydroxide, at certain concentrations and flow conditions (49).

Finally, Reillex HPQ showed a measurable loss in total capacity when converted from Cl^- to OH^- form, and one-third of the strong-base capacity was converted to weak-base capacity. This is probably due to degradation of the resin through ring-opening reactions, which were described in Section 3.2.2. From Figure 3-2 it is apparent that reactions of this type can convert the charged N-methyl pyridinium salt into an uncharged amine group.

3.2.4 Sorbent Basicities

Sorbent basicities were compared using two measures of pK_a -- experimentally determined "apparent" pK_a values, and monomer pK_a values calculated using a linear free-energy relationship. Garcia and King (22) have shown that both measures of pK_a correlate reasonably well with other measures of sorbent basicity.

3.2.4.1 Apparent pK_a Values

Helfferich (62) discusses the determination of "apparent" pK_a values, where K_a is defined as:

$$K_a = \frac{[\overline{\text{B}^-}] [\overline{\text{H}^+}]}{[\overline{\text{BH}^+}]} \quad (3-1)$$

An "apparent" pK_a value can be determined experimentally through titration of the sorbent with acid in the presence of dissolved salt (e.g. NaCl). Experimental details are given elsewhere (62). The pK_a of the sorbent can be determined from the resulting titration curve through application of the following equation:

$$\text{pK}_a = \text{pH} - \log[\text{Cl}^-] + \log \frac{[\overline{\text{X}}]}{2} \quad (\alpha' = 0.5) \quad (3-2)$$

where $[\overline{\text{X}}]$ represents the concentration of ionogenic groups and α' is the degree of

Table 3-1. Sorbent Capacities (45, 46, 47, 48)

Sorbent	Description	Manufacturer's Stated Minimum Capacity (meq/g)	Measured Capacity (meq/g)	
			Weak base	Strong base
Reillex 425	Pyridine	5.5	6.3	0
Reillex HPQ (Cl ⁻ Form)	Pyridine/ 63% quaternized	1.8 weak base * 3.0 strong base *	1.5	3.0
Reillex HPQ (OH ⁻ Form)	Pyridine/ 63% quaternized	N/A	2.5	1.1
Duolite A7	Phenol- formaldehyde- polyamine	9.5	7.1	0.16
Dowex MWA-1	Polystyrene- divinylbenzene 3° amine	3.9 - 4.3 *	4.3	0.44
Dowex 66	Polystyrene- divinylbenzene 3° amine	3.9 weak base * 0.55 strong base *	4.2	0.49
Bio-Rad AG3-X4	Epoxy-amine 10% quaternized	3.1 - 3.6 *	8.5	0.5
Amberlite IRA-35	Acrylic 3° amine	4.8 *	4.9	0
Amberlite IRA-910 (Cl ⁻ form)	Polystyrene- divinylbenzene 4° ammonium	3.8	1.6	2.2
Amberlite IRA-910 (OH ⁻ form)	Polystyrene- divinylbenzene 4° ammonium	N/A	1.8	2.2

* Calculated from meq/ml using density and moisture content data
 N/A Information not available

dissociation (62). The final two terms in the equation are needed to relate pH in the resin to pH in solution. Some investigators have tried to determine pK_a values from standard titration curves, where pH is plotted versus the amount of titrant added. These experiments give misleading results because they implicitly assume that the pH in the resin is the same as that in the aqueous phase, and that the resin is half converted when half the titrant required for complete conversion has been added. In general, neither of these assumptions is true, and the resulting pK_a values are often highly dependent upon ionic strength (62).

Properly determined apparent pK_a values generally agree reasonably well with pK_a values for aqueous acids and bases. However, the degree of dissociation of the ionogenic groups is affected by other factors, such as electrostatic effects and degree of crosslinking of the resin. Therefore, the apparent pK_a is different from the true, or intrinsic, pK_a . Unfortunately, a determination of intrinsic pK_a values from titration data relies on the use of models containing terms which are difficult to evaluate (62).

Gustafson et al. (60) have determined apparent pK_a values for several weak-base ion exchange resins, including polyvinylpyridine, phenol-formaldehyde-amine, polystyrene-based tertiary amine, acrylic-based tertiary amine, and epoxy-amine resins. The polystyrene- and acrylic-based tertiary amine resins studied have essentially the same chemical structures as Dowex MWA-1 and Amberlite IRA-35, respectively. The polyvinylpyridine resin was poly(2-methyl-5-vinylpyridine), which should have a basicity reasonably close to that of Reillex 425. The phenol-formaldehyde-amine resin investigated was formed with triethylenetetramine rather than diethylenetriamine, but again this resin is expected to have approximately the same basicity as Duolite A7. The epoxy-amine resin was formed from the condensation of epichlorhydrin and triethylenetetramine. This reaction tends to form a mixture of primary, secondary, and tertiary amine functionalities, whereas the reaction with ammonia forms tertiary amine sites much more selectively (59). Therefore, the epoxy-amine resin studied may not give a very close approximation to Bio-Rad AG3-X4.

Gustafson et al. actually determined the quantity pK , which they define as the pH of the aqueous solution in contact with the resin at $\alpha' = 0.5$. The results therefore do not take into account the fact that the pH inside the resin is different from the pH of the external solution. Hence the measured pK values are expected to be low estimates of the apparent pK_a values. Nevertheless, the results should give an indication of the relative basicities of the polymers studied.

The measured values of pK are given in Table 3-2, with the resins arranged in the order of increasing basicity. The name of the sorbent from the current work which is closest in structure to the sorbent studied is shown in parentheses.

Table 3-2. Apparent pK Values (Gustafson et al. [60])

Sorbent	pK
Poly(2-methyl-5-vinylpyridine) (Reillex 425)	3.92
Phenol-formaldehyde-triethylenetetramine (Duolite A7)	5.30
Epichlorhydrin-triethylenetetramine (Bio-Rad AG3-X4)	6.08
Polystyrene-based 3° amine (Dowex MWA-1)	6.70
Acrylic-based 3° amine (Amberlite IRA-35)	8.32

The results indicate a wide range of basicities, with pK values spanning 4.4 units of pH. The polyvinylpyridine resin is the most weakly basic, followed by the phenol-formaldehyde-amine resin. Although the two tertiary amine resins are the most strongly basic, the acrylic-based resin is significantly more basic than the polystyrene-based resin.

The lower basicity of the polystyrene-based resin can be attributed to the proximity of the amine group to the base-weakening styrene ring (54, 60). The acrylic-based resin, on the other hand, has an aliphatic backbone and hence a higher basicity. Gustafson et al. discuss another difference between the two resins. The styrene-divinylbenzene resin has approximately 14% quaternary ammonium groups, which tend to weaken the basicities of nearby amine groups. In contrast, the acrylic-based resin has about 9% carboxylate groups, formed by the hydrolysis of amide groups, which serve to strengthen the basicities of neighboring amine groups.

Garcia and King (22) and Clifford and Weber (56) also measured apparent pK_a values for basic polymeric sorbents, and obtained the results shown in Table 3-3. As expected, the values are generally higher than those obtained by Gustafson et al. The results of Garcia and

Table 3-3. Apparent pK_a Values (Garcia and King [22], Clifford and Weber [56])

Sorbent	Garcia & King	Clifford & Weber
Poly(4-vinylpyridine) (Reillex 425)	4.9	-
Phenol-formaldehyde- triethylenetetramine (Duolite A7)	5.3	-
Phenol-formaldehyde- diethylenetriamine (Duolite A7)	-	7.7
Epoxyamine (Bio-Rad AG3-X4)	7.8/7.9	7.9
Polystyrene-based 3° amine (Dowex MWA-1)	7.6/8.8	7.6
Acrylic-based 3° amine (Amberlite IRA-35)	-	11.1

King show the same general order of basicity given by the Gustafson et al. study, but the epoxy-amine resin appears somewhat more basic, with pK_a essentially the same as that of the

polystyrene-based amine resin. The results of Clifford and Weber yield almost identical pK_a values for the phenol-formaldehyde-amine, the epoxyamine, and the polystyrene-based tertiary amine resins, but the acrylic-based tertiary amine is still significantly more basic. The phenol-formaldehyde-polyamine resin studied by Clifford and Weber was, in fact, Duolite A7 and therefore this result, if accurate, should be the best measure of basicity for this resin.

3.2.4.2 Monomer pK_a Values

A second method of comparing sorbent basicities involves comparing the pK_a values of the monomeric units. Often, the monomeric unit is complex, and experimentally determined pK_a values are not available. For these cases group-contribution methods can be used to predict monomer pK_a values. Predicted monomer pK_a may not be the best measure of sorbent basicity, since it does not account for other effects, such as interactions (electrostatic, steric, etc.) among functional groups and the effects of crosslinking. Furthermore, if the resin has several different types of functional groups in close proximity to one another, it may be difficult to relate calculated pK_a values to an overall "basicity" of the resin. However, the method often has some usefulness, especially with clearly defined monofunctional resins (22).

One method for calculating pK_a values uses a linear free energy relationship (LFER) developed by Perrin et al. (54). The basic idea is that pK_a is directly related to the change in free energy for the ionization, through the expression given in Equation 3-3.

$$\Delta G^\circ = 2.303 RT (pK_a) \quad (3-3)$$

Changes in structure cause a change in free energy and hence in pK_a . For minor structural changes, the effects on pK_a are approximately additive. Therefore, from the pK_a of the parent compound, the pK_a of a related compound can be calculated by adding ΔpK_a values associated with the various substituents. Perrin et al. have tabulated ΔpK_a values for base-

weakening ($\Delta pK_a < 0$) and base-strengthening ($\Delta pK_a > 0$) substituents attached to α - and β -carbon atoms in aliphatic amines and β - and γ -carbon atoms in pyridines. Substituents that are further away from the basic center have much more minor effects, which can generally be approximated using an attenuation factor of 0.4 for each additional $-\text{CH}_2-$ between the substituent and the basic center. Perrin et al. recommend parent compound pK_a values of 10.77, 11.15, and 10.5 for 1°, 2°, and 3° amines, respectively, and 5.25 for pyridines.

The tabulated ΔpK_a values are calculated from a compilation of substituent constants used in the more general Hammett and Taft equations. In some cases, it is preferable to calculate pK_a values directly from the Taft equation, given in Equation 3-4.

$$pK_a = pK_a^\circ - \rho^* \Sigma(\sigma^*) \quad (3-4)$$

where pK_a° is the pK_a of the parent compound, ρ^* is a constant for the particular ionization reaction, and σ^* gives the effect of the substituent.

Table 3-4 presents calculated monomer pK_a values for the five weak base sorbents studied. For Duolite A7, a polyamine, the pK_a value for the strongest basic center is shown.

Table 3-4. Calculated Monomer pK_a Values

Sorbent	pK_a
Reillex 425	6.1
Duolite A7	9.35
Bio-Rad AG3-X4	7.2
Dowex MWA-1/Dowex 66	8.7
Amberlite IRA-35	9.8

The pK_a value for Amberlite IRA-910, the strong base ion exchanger, is expected to be greater than 13 (62). Likewise, the N-methyl pyridinium groups found on Reillex HPQ are expected to have very high pK_a values. The uncharged pyridine groups might be similar in basicity to the groups on Reillex 425, although interactions with neighboring quaternized groups could very well lower these pK_a values.

The calculated pK_a values are consistently higher than the experimental values of Gustafson et al., as expected. The order of basicity is the same, except that Duolite A7 is predicted to be a much stronger base than is indicated by the apparent pK_a . The predicted pK_a value places Duolite A7 between MWA-1 and Amberlite IRA-35 in terms of basicity. The calculated pK_a values are closer in value to the experimental pK_a values obtained by Garcia and King and by Clifford and Weber. However, Duolite A7 is still predicted to be a much stronger base than the results given by either set of experimenters would indicate.

Duolite A7 has at least three different types of basic sites, as shown in Figure 3-3. The amine labelled "B" is predicted to be the strongest of the three, since the pK_a values of the other two amines are lowered by their proximity to the phenol groups. The pK_a value predicted for B using the ΔpK_a method is 9.4. pK_a values calculated for amines A and C from the Taft equation are 7.1 and 6.1, respectively (22). Therefore, B will protonate first. Once B protonates, the pK_a values of the other amines will be lowered even further, since an ammonium ion attached to a β carbon has a ΔpK_a value of 3.6. The pK_a value shown in Table 3-4 is that of the strongest amine group, since the above argument implies that this group will be the major contributor to the overall basicity of the resin. As previously noted, use of this value results in a relative basicity which is not in line with the experimental observations of other researchers. Furthermore, Duolite A7 has been observed to titrate as a polyamine, showing a titration curve with very little inflection (56). It therefore appears that the structure of the resin is more complex than Figure 3-3 would indicate, and hence the pK_a would not be easily predicted.

3.3 Sorption Isotherms

Sorption isotherms were determined for each of the basic polymeric sorbents at 25 °C, over concentration ranges of approximately 0–6 wt. % for succinic acid and 0–12 wt. % for lactic acid. For succinic acid, 6 wt. % represents the approximate solubility limit. Lactic acid is not typically present in fermentation broths at concentrations over 10 wt.%. Uptakes of acid were measured at natural pH without additional buffering agents.

3.3.1 Composite and Individual Isotherms

Two different types of isotherms, composite and individual, are used to describe sorption equilibria. The composite uptake is defined as:

$$\frac{W_o \Delta C_a}{m} = \frac{W_o (C_{a,i} - C_{a,f})}{m} \quad (3-5)$$

where W_o is the initial mass of solution, m is the mass of sorbent used, and $C_{a,i}$ and $C_{a,f}$ are the initial and final weight fractions of solute in solution. The composite isotherm is a measure of the selective uptake of the solute over the solvent and is equivalent to a surface excess (63).

Individual uptakes of solvent (denoted by subscript w) and solute (denoted by subscript a) are defined as:

$$Q_w = \frac{W_o (1 - C_{a,i}) - W_f (1 - C_{a,f})}{m} \quad (3-6)$$

$$Q_a = \frac{W_o C_{a,i} - W_f C_{a,f}}{m} \quad (3-7)$$

where W_o and W_f are the initial and final masses of bulk liquid. The individual uptakes give the total amounts of solute or solvent taken up by the sorbent, including selective uptake at the surface and non-selective uptake due to swelling and pore filling. Calculation of the individual isotherms requires an assumption about the boundary between sorbed and bulk

solution. In this work, the sorbed solution is defined as that solution which is retained by the sorbent after centrifugation for 8 minutes at 2000 rpm.

The relationship between the composite and the individual uptakes is described by Equation 3-8 (63). Examination of the equation reveals that the individual uptake of solute must always be greater than the composite uptake. At low solute concentrations, the composite uptake approaches the individual uptake, and for high water uptakes the two isotherms differ the most.

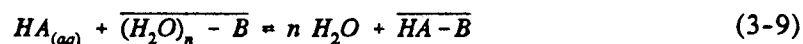
$$\frac{W_o \Delta C}{m} = Q_a (1 - C_{a,f}) - Q_w C_{a,f} \quad (3-8)$$

In this work, composite uptakes were computed directly, using Equation 3-5. Individual uptakes were then computed from Equation 3-8 and the measured total solution uptake ($Q_a + Q_w$) after centrifugation.

3.3.2 Isotherm Models

3.3.2.1 The Langmuir Isotherm

The ideal exchange model is a simple model that can be used to describe sorption of an acid by a basic sorbent (22). This model assumes that each acid molecule competes with one or more water molecules for a basic site on the sorbent, as shown in the following complexation reaction:



where B represents the basic functional group and the overbars denote the solid sorbent phase.

An equilibrium constant for the complexation can be written as follows:

$$K^* = \frac{[\overline{HA-B}][H_2O]^n}{[HA] [(H_2O)_n - B]} \quad (3-10)$$

If it is further assumed that (1) only 1:1 complexes are formed, (2) the solvent activity in dilute solution is constant, (3) the ratio of remaining activity coefficients is constant, (4) there are a fixed number of basic sites, and (5) all of the basic sites have equal basicity and accessibility, the following isotherm results:

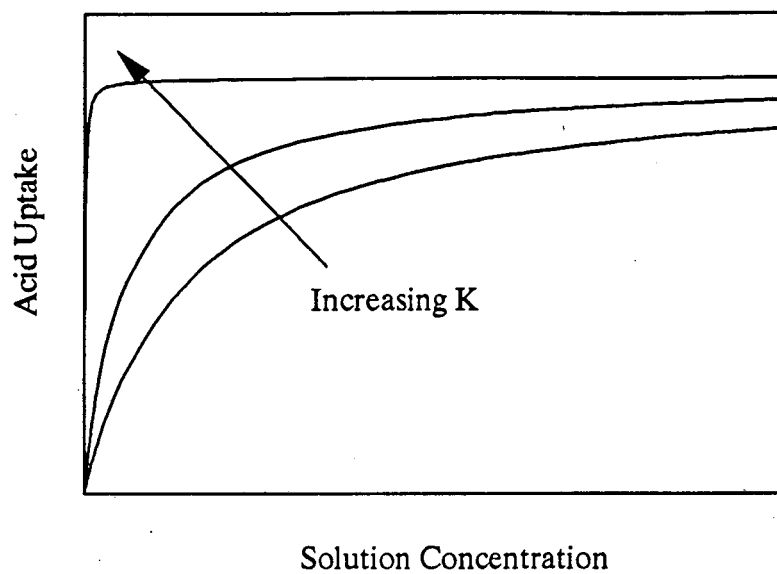
$$\frac{q}{q_m} = \frac{KC_{HA}}{1 + KC_{HA}} \quad (3-11)$$

where

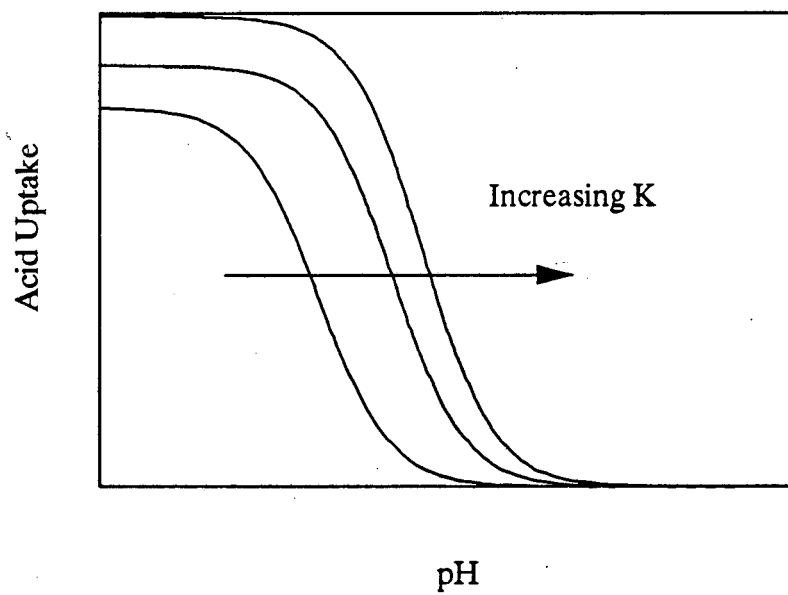
$$K = \frac{K^*}{[H_2O]^n} \quad (3-12)$$

and C_{HA} is the weight fraction of un-ionized acid in the aqueous phase. The uptake q is the selective uptake of acid by the sorbent, or the difference between the individual uptake and the uptake of acid by nonselective mechanisms, such as pore-filling and swelling. This equates conceptually with the composite uptake, except for the possibility of selective, non-chemical uptake.

The isotherm is of the Langmuir form, with parameters q_m , a measure of sorbent capacity, and K , a measure of the strength of complexation. The K value is an important parameter. The value of K is given by the initial slope of the sorption isotherm if q_m is known, and, for complexation with a given acid, should be higher for more strongly basic sorbents. The effect of the K value can be seen in Figures 3-8 (a) and (b). As sorbent K value increases, the initial slope of the sorption isotherm (Figure 3-8 (a)) becomes steeper, and the amount of acid sorbed reaches its maximum value at a very low solution concentration. As shown in Figure 3-8 (b), uptake drops off with increasing pH as the amount of un-ionized acid decreases. However, the more strongly basic the sorbent, the higher the pH value at



(a)



(b)

Figure 3-8. Effect of Sorbent K Value on
(a) Sorption Isotherm (b) Uptake-pH Curve

which this drop begins to occur, because capacity is sustained at low concentrations of un-ionized acid. Therefore, sorbents with high K values sustain capacity to higher values of pH.

A model of the same form can be developed for the uptake of an acid by a strong-base ion exchanger in the OH^- form. The only difference is that the acid-base reaction is written as:



Note that the same five requirements must be met. For di-acids at higher pH this is not always the case, as explained in Section 3.4.1.2.

3.3.2.2 Other Models

If any of the assumptions of the ideal exchange model are violated, the uptake of carboxylic acid by the basic sorbent may not be well-described by a Langmuir isotherm. For example, if the sorbent has more than one type of basic functional group, assumption (5) is unlikely to hold, and the sorption data may not follow a Langmuir curve. If there is reason to believe that the resin contains two types of functional groups, or if only two types of groups are strongly enough basic to give significant uptake of acid, a two-site Langmuir model can be used to describe the data. This model assumes that each type of site sorbs acid independent of the other, following an ideal-exchange mechanism. The resulting model incorporates two values each of K and q_m , as shown in Equation 3-14.

$$q = \frac{q_{m1}K_1C_{HA}}{1+K_1C_{HA}} + \frac{q_{m2}K_2C_{HA}}{1+K_2C_{HA}} \quad (3-14)$$

Other models, having additional values of K and q_m , can be postulated, but the number of parameters can grow large quite quickly, making models of this type somewhat intractable. For sorbents with a wide array of functional groups, a Freundlich isotherm (Equation 3-15) may give nearly as good a fit as a multi-site Langmuir isotherm, but with only two parameters.

$$q = aC_{HA}^n \quad (3-15)$$

There is, in general, no theoretical justification for the Freundlich isotherm, although for dilute solutions a derivation based on the Gibbs equation has been described (63).

The sorption of di-acids might also be poorly described by a Langmuir isotherm. The ideal-exchange model should still apply if each acid molecule pairs with no more than one basic site and if the un-ionized acid is the only species sorbed. However, it is possible that some or all of the sorbed acid molecules may pair with two sites that are in close proximity to each other. Furthermore, when the pH value is such that the acid is partly dissociated, it is possible that both the un-ionized species (H_2A) and the bicarboxylate (HA^-) may complex with the basic sites. If the two species are sorbed with different affinities, the resulting isotherm may not be of the Langmuir form. In this case, a competitive Langmuir isotherm may be used:

$$q = \frac{q_{m,H_2A} K_{H_2A} C_{H_2A} + q_{m,HA^-} K_{HA^-} C_{HA^-}}{1 + K_{H_2A} C_{H_2A} + K_{HA^-} C_{HA^-}} \quad (3-16)$$

Theoretically, q_{m,H_2A} and q_{m,HA^-} must be equal or the result will not be thermodynamically consistent (64, 65). In practice, however, different values are often used.

3.3.3 Fitting of Isotherms to Experimental Data

The ideal-exchange and other models relate the selective uptake of acid to the equilibrium solution concentration. Therefore, in fitting a model to the data, q should be calculated as the difference between the individual uptake and the amount of acid held in the pore volume. Because this second quantity is difficult to determine experimentally, in this work q is equated to the composite uptake (or surface excess). For highly selective uptakes, the composite uptake approaches the actual surface concentration.

Several models, including the Langmuir, 2-site Langmuir, and Freundlich isotherms, were fitted to the experimental data. Least-squares estimates of the parameters were

determined via non-linear regression using the STATGRAPHICS NONLIN procedure, which is based on an algorithm developed by Marquardt (66). For the Langmuir and Freundlich isotherms, fitted parameter values could be determined by linearizing the isotherm equation and performing a linear least-squares regression. For example, the Langmuir equation can be linearized as in Equation 3-17, with the slope determining q_m and the intercept determining the product of K and q_m .

$$\frac{C_{HA}}{q} = \frac{1}{q_m K} + \frac{C_{HA}}{q_m} \quad (3-17)$$

However, because the intercept tends to occur very close to zero and because the linearization alters the way in which points are weighted, it is difficult to obtain an accurate estimate for K using this technique. Therefore, the non-linear regression method was used. The goodness-of-fit of a particular model was evaluated through an examination of the residuals and of the residual standard deviation. Appendix B contains a detailed example.

3.3.4 Results and Discussion

3.3.4.1 Lactic Acid

Experimentally determined composite and individual sorption isotherms are presented for lactic acid in Figures 3-9 through 3-13. The actual data for these and all other experiments can be found in Appendix A. As predicted by Equation 3-8, the individual uptakes are always greater than the composite uptakes, although the two are nearly equal at low solution concentrations.

The models that best describe the composite isotherms for lactic acid are shown as solid curves in Figures 3-9 through 3-13. With the exception of Duolite A7, the sorption data are well described by the Langmuir isotherm. The Duolite A7 data are best described by a two-site Langmuir model, which is not unexpected since this resin is polyfunctional. The

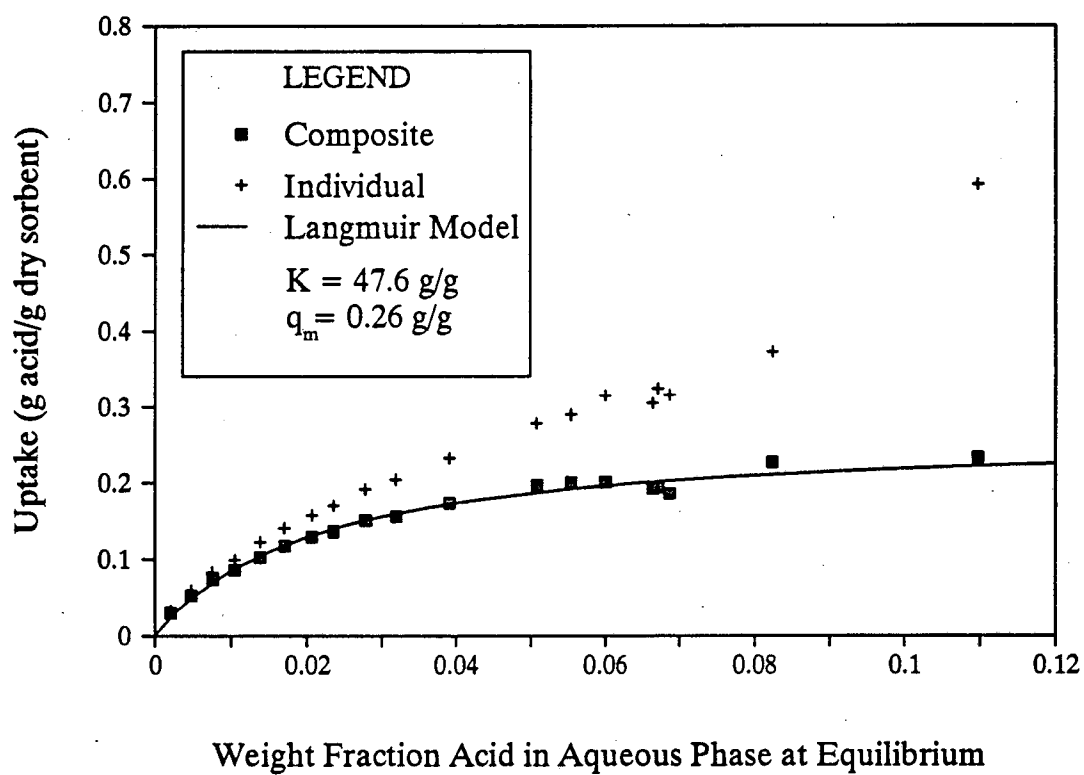


Figure 3-9. Sorption Isotherms for Lactic Acid on Reillex 425

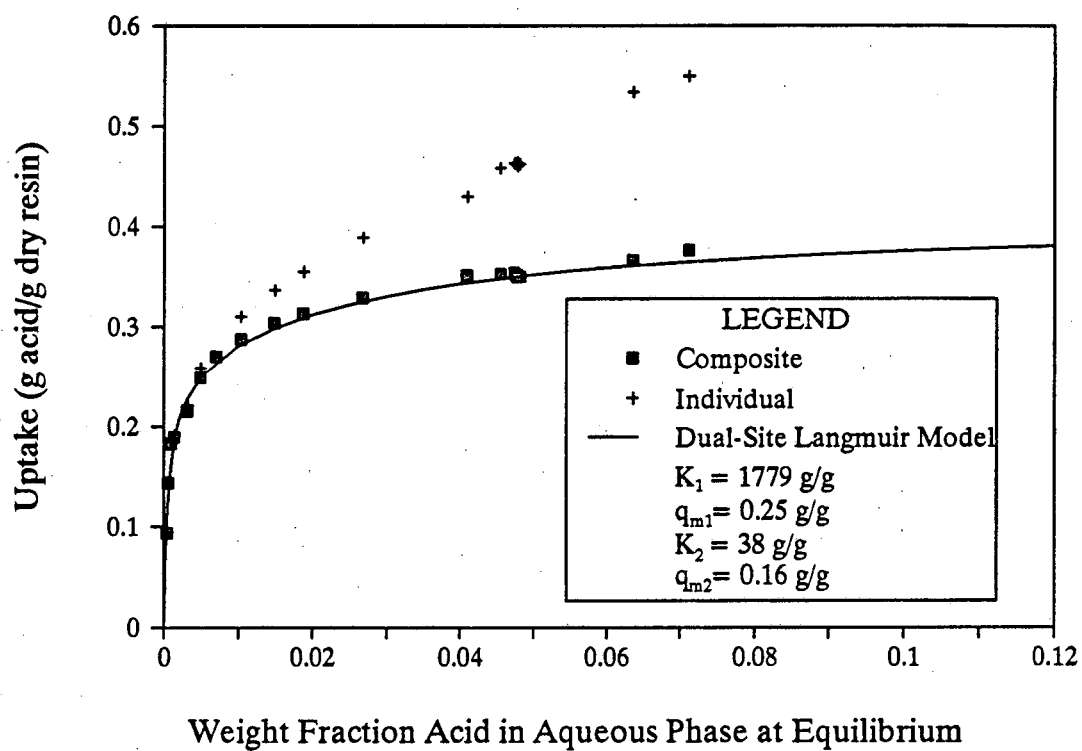


Figure 3-10. Sorption Isotherms for Lactic Acid on Duolite A7

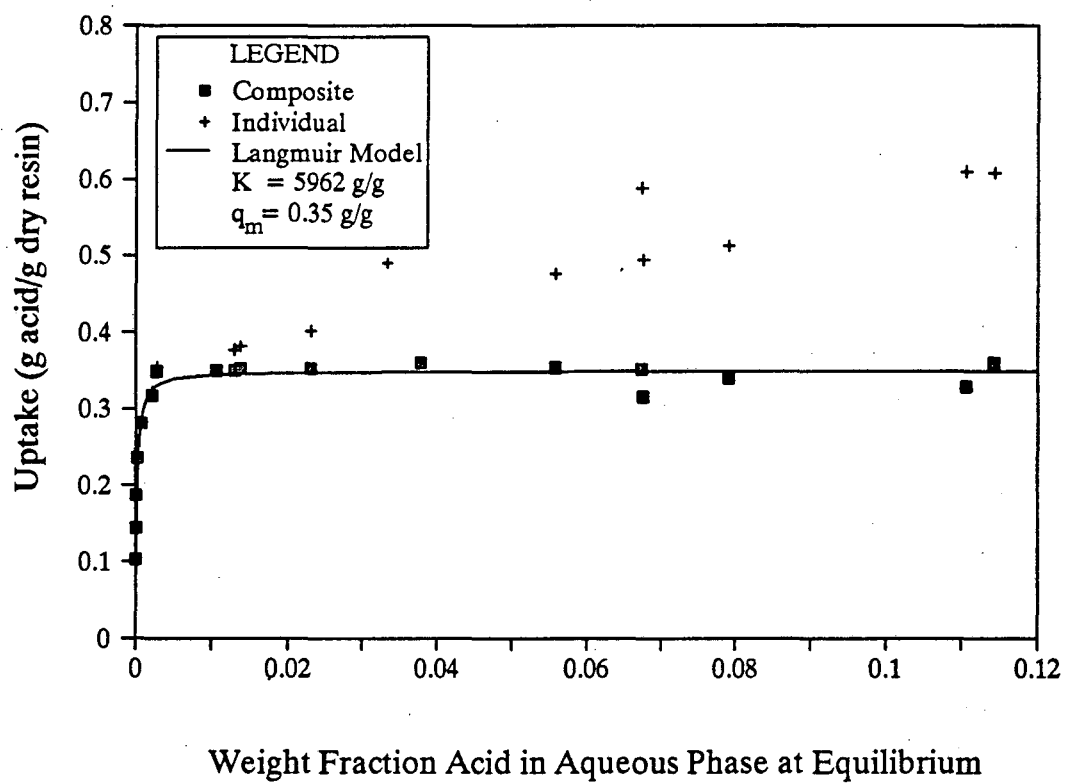


Figure 3-11. Sorption Isotherms for
Lactic Acid on Dowex MWA-1

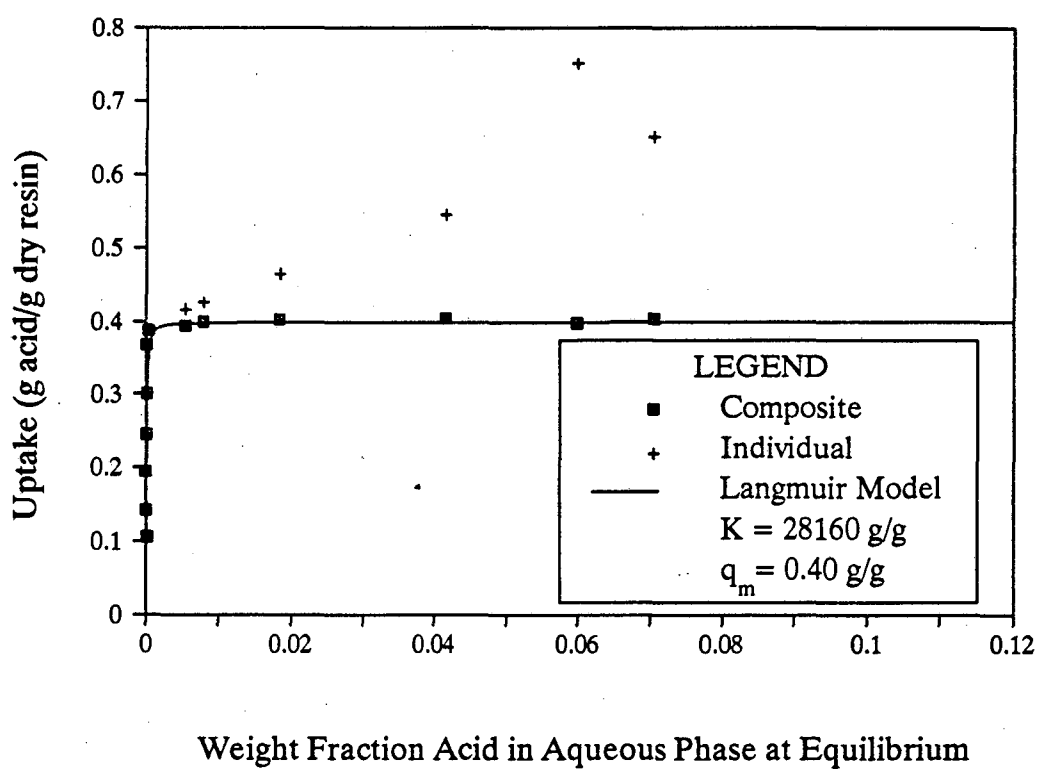


Figure 3-12. Sorption Isotherms for
Lactic Acid on Amberlite IRA-35

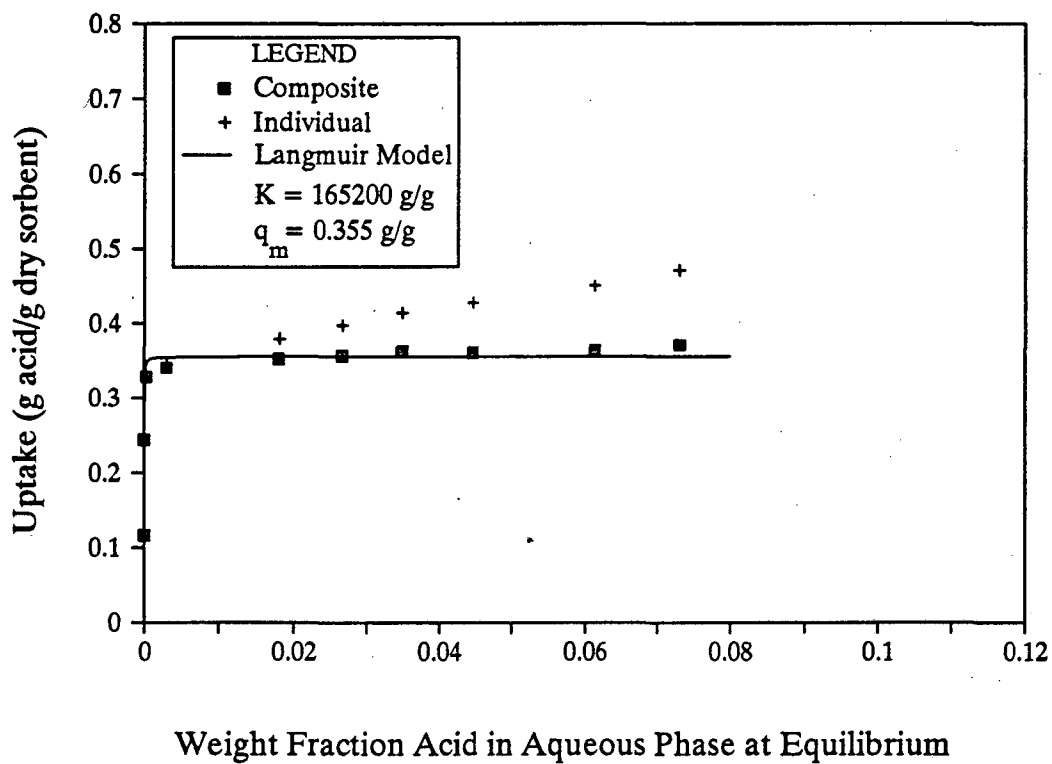


Figure 3-13. Sorption Isotherms for Lactic Acid on Amberlite IRA-910

Freundlich isotherm also gives a reasonable, but significantly worse, fit to the Duolite A7 data.

Table 3-5 lists the K values for the sorption systems. As indicated by Equations 3-10 and 3-12, K is a modified equilibrium constant, the value of which reflects the strength of complexation between the carboxylic acid and the basic site on the sorbent. A comparison of K values for the sorption of the same acid by different sorbents thus gives an indication of the relative basicities of the sorbent functional groups.

In order to compare Duolite A7 (with uptake described by a dual-site Langmuir model) with the other sorbents (with uptakes described by Langmuir models), an "equivalent" K value is needed. The interest here is in ability to sustain capacity at $\text{pH} > \text{pK}_a$, and this ability increases as the initial slope of the sorption isotherm increases. For a simple Langmuir isotherm, K is related to the initial slope by:

$$K = \frac{\left(\frac{\partial q}{\partial C_{HA}} \right)_{C_{HA}=0}}{q_m} \quad (3-18)$$

Extending this idea to a dual-site Langmuir model, an "equivalent K" can be calculated as:

$$\frac{\left(\frac{\partial q}{\partial C_{HA}} \right)_{C_{HA}=0}}{q_{m1} + q_{m2}} = \frac{(q_{m1}K_1 + q_{m2}K_2)}{q_{m1} + q_{m2}} \equiv K_{Ave.} \quad (3-19)$$

Hence, for the purpose of comparing Duolite A7 to other sorbents, an average of K_1 and K_2 , weighted by the corresponding q_m values, can be used. This weighted average is also listed in Table 3-5.

The K values span a wide range and, in general, reflect the order of increasing basicity of the sorbents. The differences in basicities are also visually apparent from the sorption isotherms themselves. The steeper the initial slope of the isotherm, the higher the value of K and the more strongly basic the sorbent functional group. A range of initial slopes

is seen in Figures 3-9 through 3-13, the least steep associated with Reillex 425 and the most steep associated with Amberlite IRA-910.

Table 3-5. K Values for Lactic Acid Isotherms

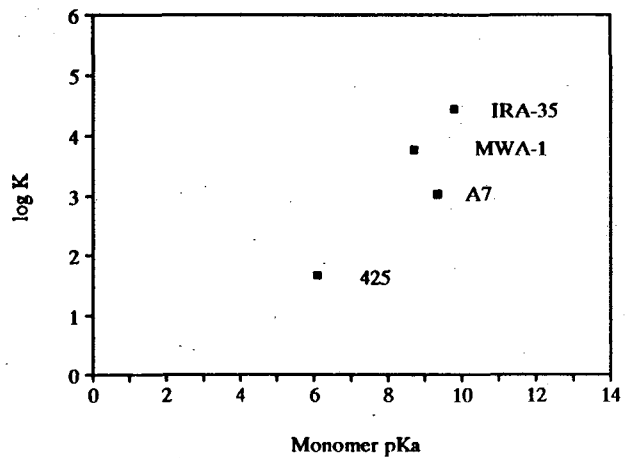
Sorbent	K (g solution/g acid)
Reillex 425	47.6
Duolite A7	$K_1 = 1779$ $K_2 = 38$ $K_{ave.} = 1100$
Dowex MWA-1	5962
Amberlite IRA-35	28160
Amberlite IRA-910	165200

Since the K value is both an equilibrium constant and a measure of sorbent basicity, it should be possible to correlate $\log(K)$ with pK_a via a linear free energy relation (LFER). The general idea behind an LFER is that the free energies of two closely related reaction series are often linearly related. Therefore, the logarithms of the equilibrium or rate constants for one reaction series can be related to those of the second reaction series by an equation of the form:

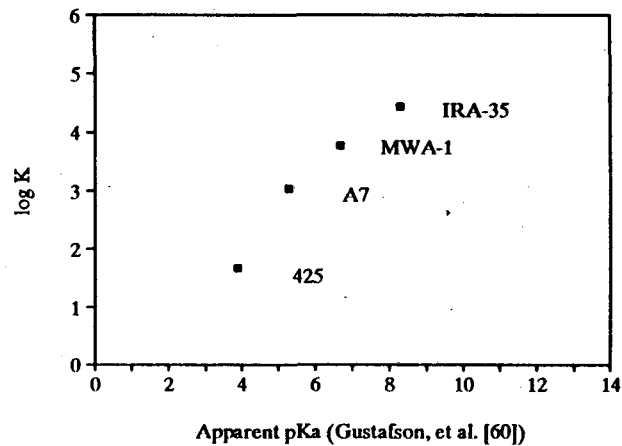
$$\ln k_i^I = a \ln k_i^{II} + b \quad (3-20)$$

where k_i^I and k_i^{II} are equilibrium or rate constants for species i in reaction series I and II (54).

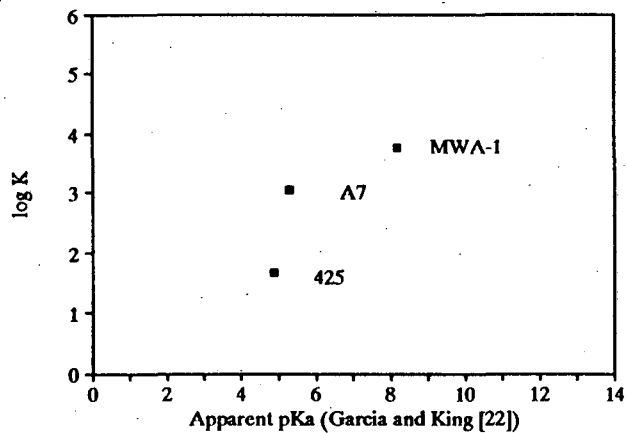
Figure 3-14 presents correlations between $\log(K)$ and various measures of sorbent pK_a . These pK_a values were calculated from the monomer chemistry (Figure 3-14 (a)) and determined experimentally by Gustafson et al. (Figure 3-14 (b)), Garcia and King (Figure 3-



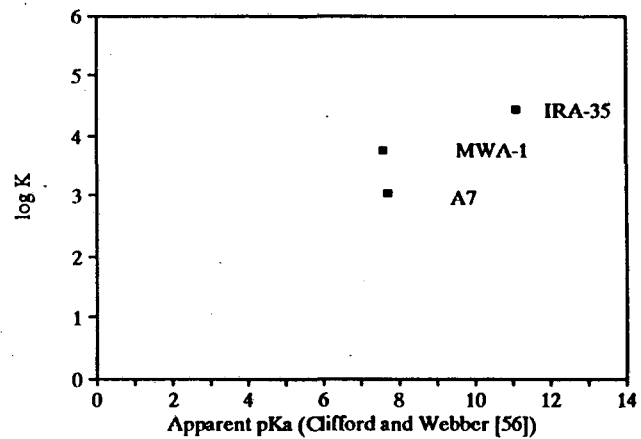
(a)



(b)



(c)



(d)

Figure 3-14. Comparison Between the Experimental K-Values for Lactic Acid and Various Measures of Sorbent pKa

14 (c)), and Clifford and Weber (Figure 3-14 (d)). For Duolite A7, the weighted-average K value was used. Log (K) correlates reasonably well with calculated monomer pK_a , although the data point for Duolite A7 appears somewhat misplaced. As discussed in Section 3.2.4, there is some question as to whether the calculated monomer pK_a value for Duolite A7 is too high. A lower value would result in a better overall correlation. The pK_a values of Gustafson et al. are very highly correlated with log (K). Thus, it appears that the use of the external rather than the internal pH in the calculation may affect the apparent pK_a value approximately linearly. The correlations between log (K) and the pK_a values of Garcia and King and of Clifford and Weber are somewhat weaker, although it is difficult to draw conclusions with only three data points. The data of Gustafson et al. may be more reliable because the aqueous titrant was very carefully buffered, so that pH values could be determined with high reproducibility. Garcia and King and Clifford and Weber used unbuffered titrant, which can make pK_a determinations less reliable (62).

Amberlite IRA-910 was omitted from the above analysis because its pK_a value is difficult to quantify. However, strong-base ion-exchangers typically have $pK_a > 13$. The experimental K value for the sorption of lactic acid by Amberlite IRA-910 is less than one order of magnitude greater than the K value for Amberlite IRA-35. Therefore, the predicted pK_a value, as read from any of the graphs in Figure 3-14, is less than 12. It appears, then, that the experimental K value may be artificially low. The value of K for this resin is, in fact, very difficult to determine with precision because the concentrations in the initial region of the isotherm are all extremely low. Therefore, it is possible that the true K value is higher.

It is interesting to compare the values of q_m from the sorption isotherms with the experimentally determined capacities for HCl, on a mmol/g basis. As seen in Table 3-6, the agreement between the two values is reasonably good for Dowex MWA-1, Amberlite IRA-35 and Amberlite IRA-910. For Reillex 425 and Duolite A7, the full capacity for HCl is not utilized by lactic acid. As discussed in Section 3.2.3, it is not unusual for a sorbent, particularly one with a high concentration of functional groups, to have different capacities

for acids of different sizes and basicities. A final observation concerns the issue of overloading. As will be seen in Chapter 4, organic amine extractants are capable of overloading, or taking up more than one carboxylic acid per amine site. The sorbents shown here show no evidence of overloading. This is typical of an aqueous environment, since water molecules will solvate the acid, preventing a second acid molecule from adding to the complex.

Table 3-6. Comparison Between q_m for Lactic Acid and Capacity Measurements

Sorbent	Experimental Capacity (mmol/g)		q_m (mmol/g)
	Weak	Strong	
Reillex 425	6.3	-	2.9
Duolite A7	7.1	0.16	4.6
Dowex MWA-1	4.3	0.44	3.9
Amberlite IRA-35	4.9	-	4.4
Amberlite IRA-910	1.8	2.2	4.0

3.3.4.2 Succinic Acid

Experimentally determined composite and individual sorption isotherms are presented for succinic acid in Figures 3-15 through 3-22. The models that best describe the composite isotherms are shown as solid curves. As with lactic acid, the Reillex 425 sorption data are well described by a Langmuir isotherm, whereas a two-site Langmuir isotherm is needed to describe the Duolite A7 data. The data for other sorbents are best fit by Freundlich isotherms. Dowex 66 was found to have essentially the same uptake characteristics as Dowex MWA-1 and therefore was not studied further.

For all sorbents except Reillex 425 and Duolite A7, isotherms of the Langmuir form give systematic misfits to the data. A detailed analysis of other models was performed, as described in Appendix B. The lack of fit of a simple Langmuir isotherm to the succinic acid

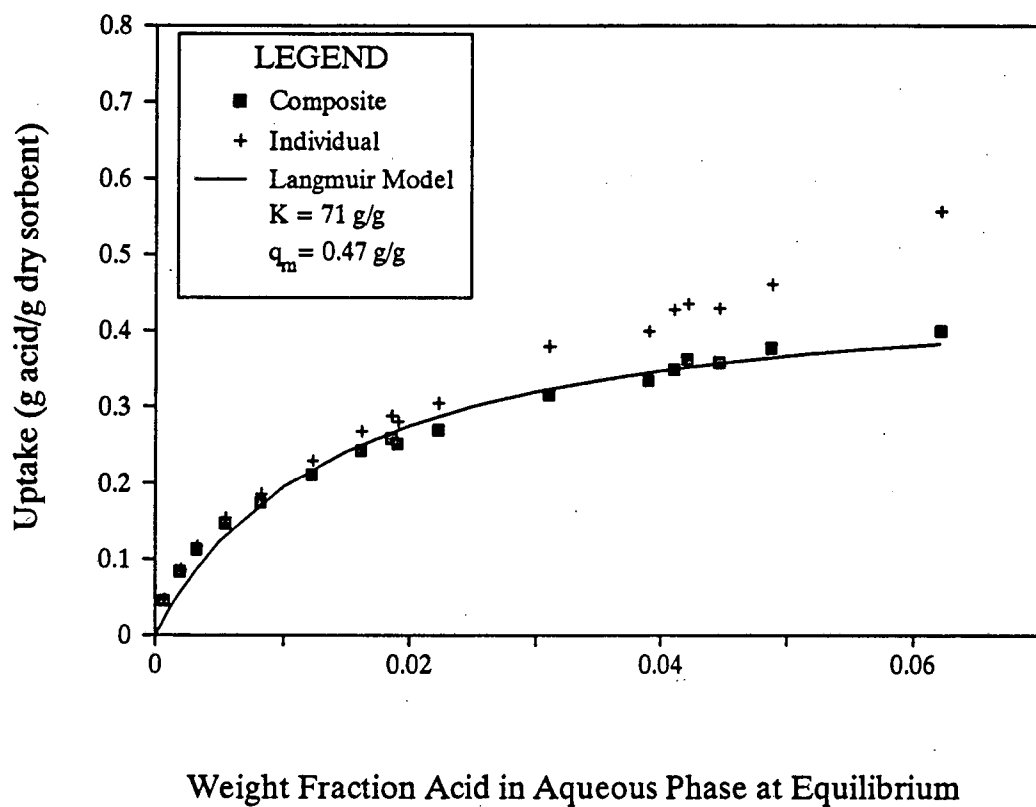


Figure 3-15. Sorption Isotherms for Succinic Acid on Reillex 425

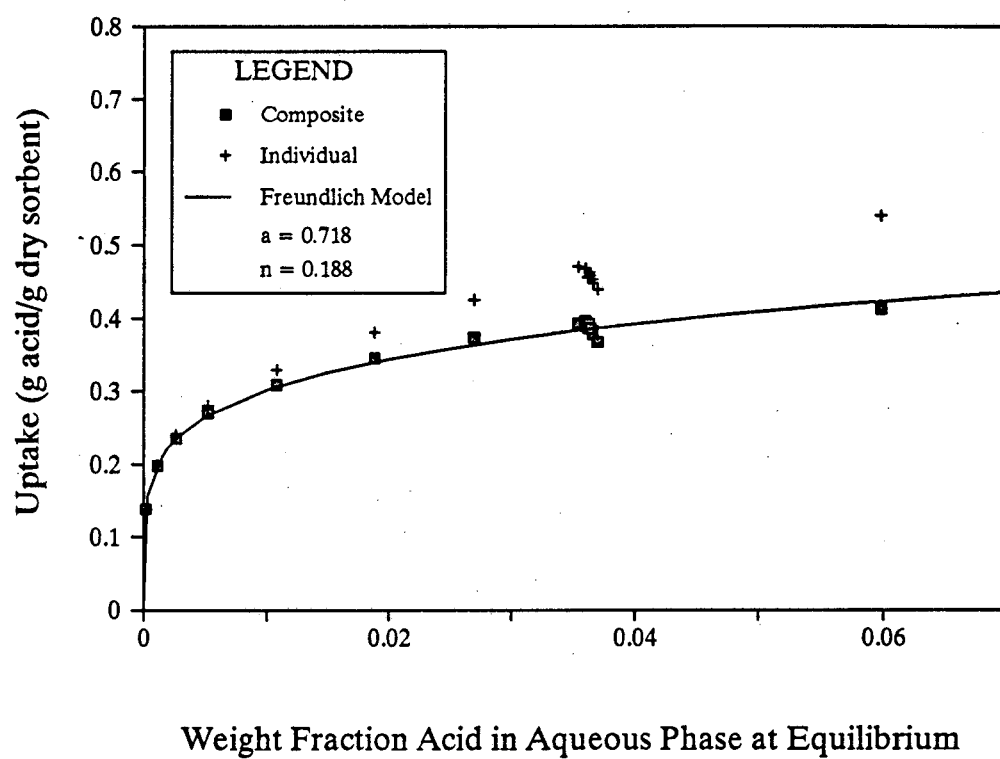


Figure 3-16. Sorption Isotherms for Succinic Acid on Reillex HPQ

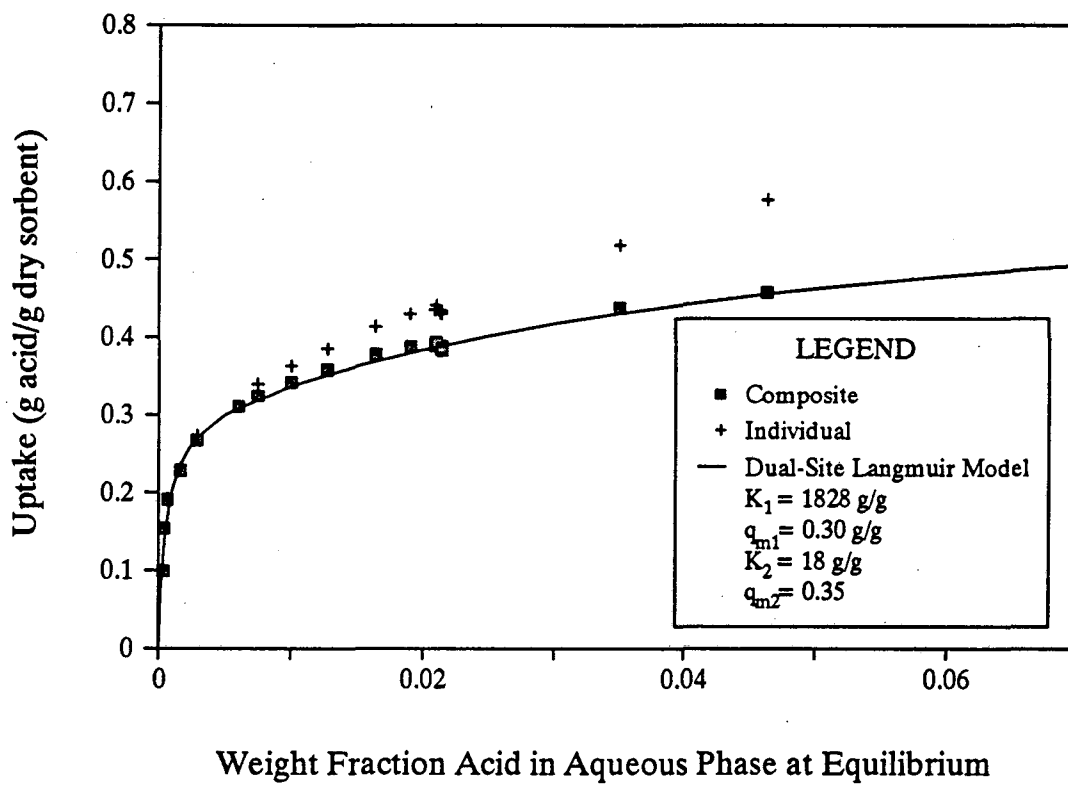


Figure 3-17. Sorption Isotherms for Succinic Acid on Duolite A7

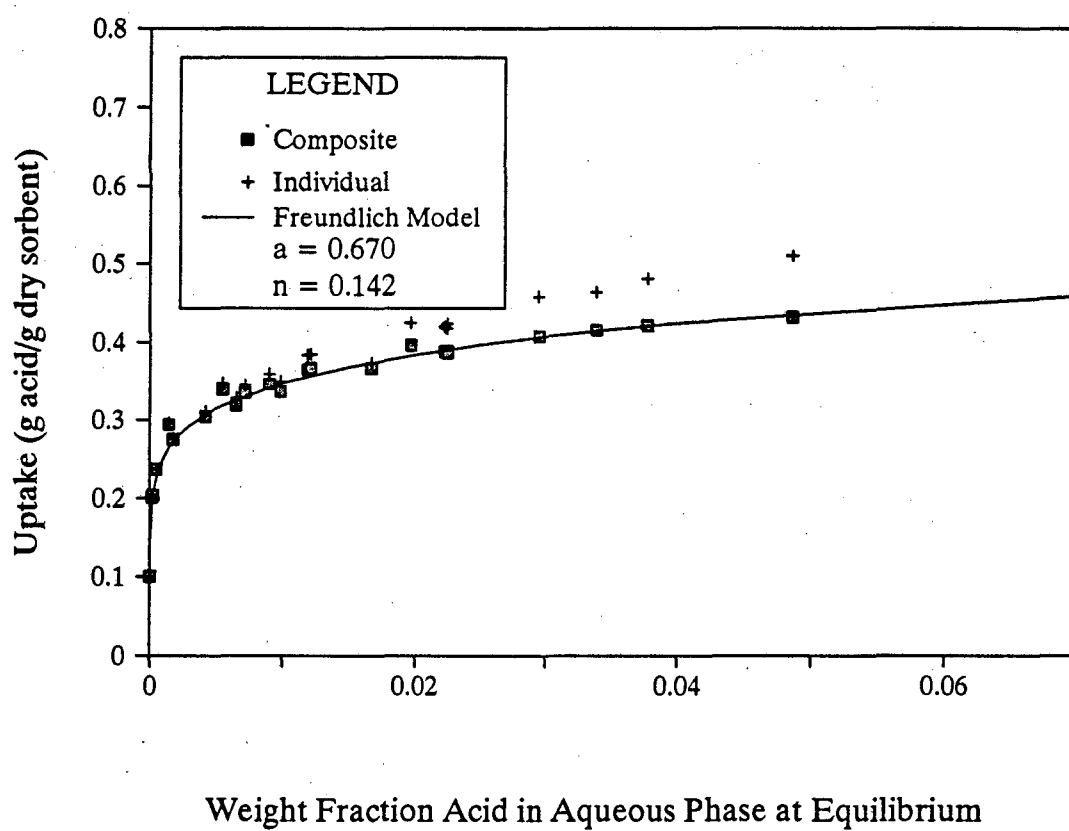


Figure 3-18. Sorption Isotherms for Succinic Acid on Bio-Rad AG3-X4

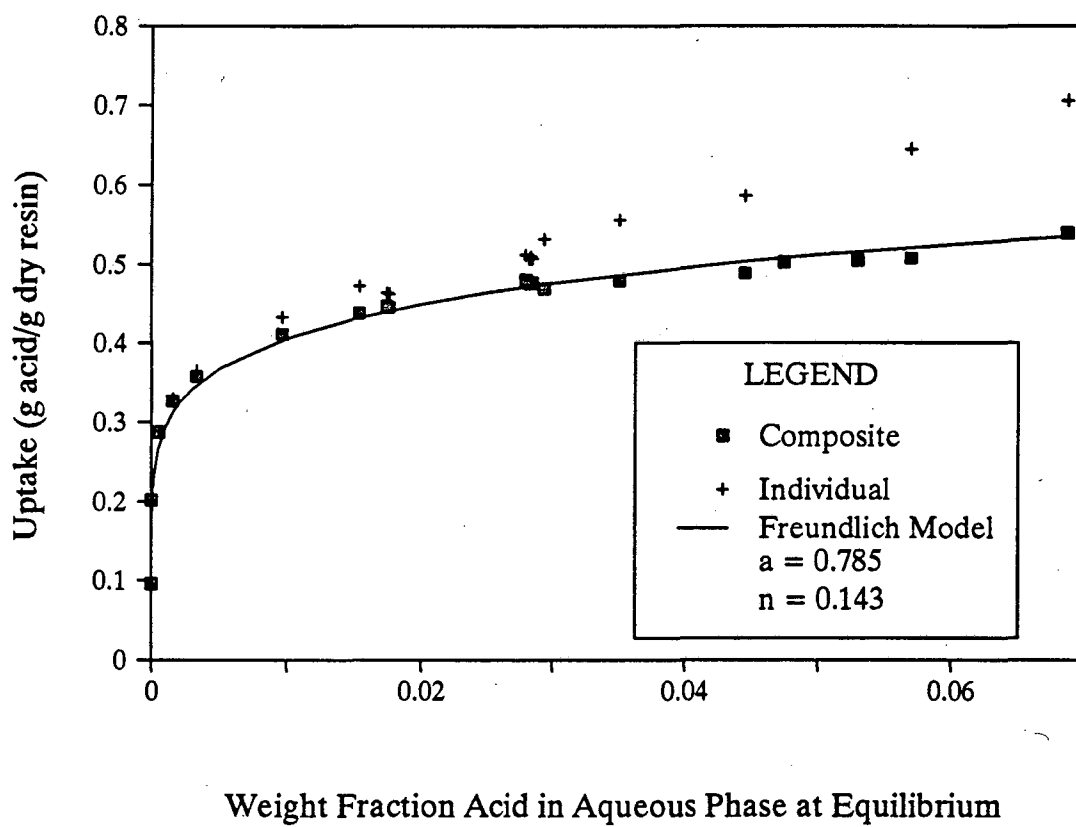


Figure 3-19. Sorption Isotherms for Succinic Acid on Dowex MWA-1

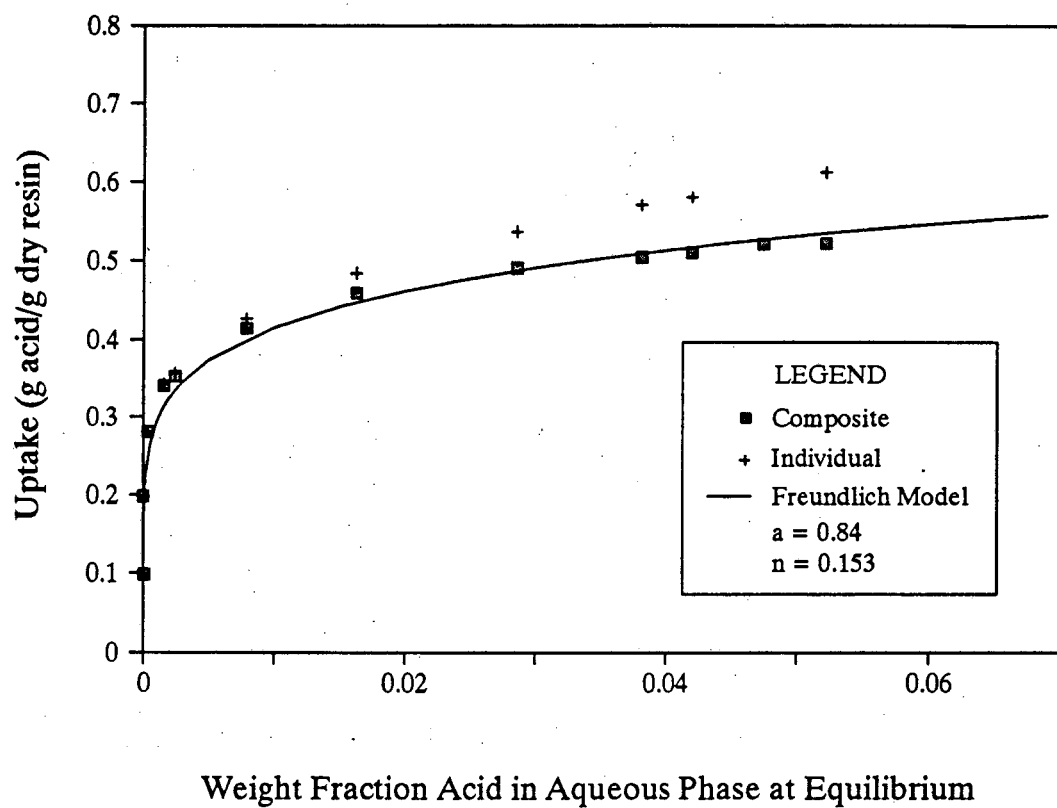


Figure 3-20. Sorption Isotherms for
Succinic Acid on Dowex 66

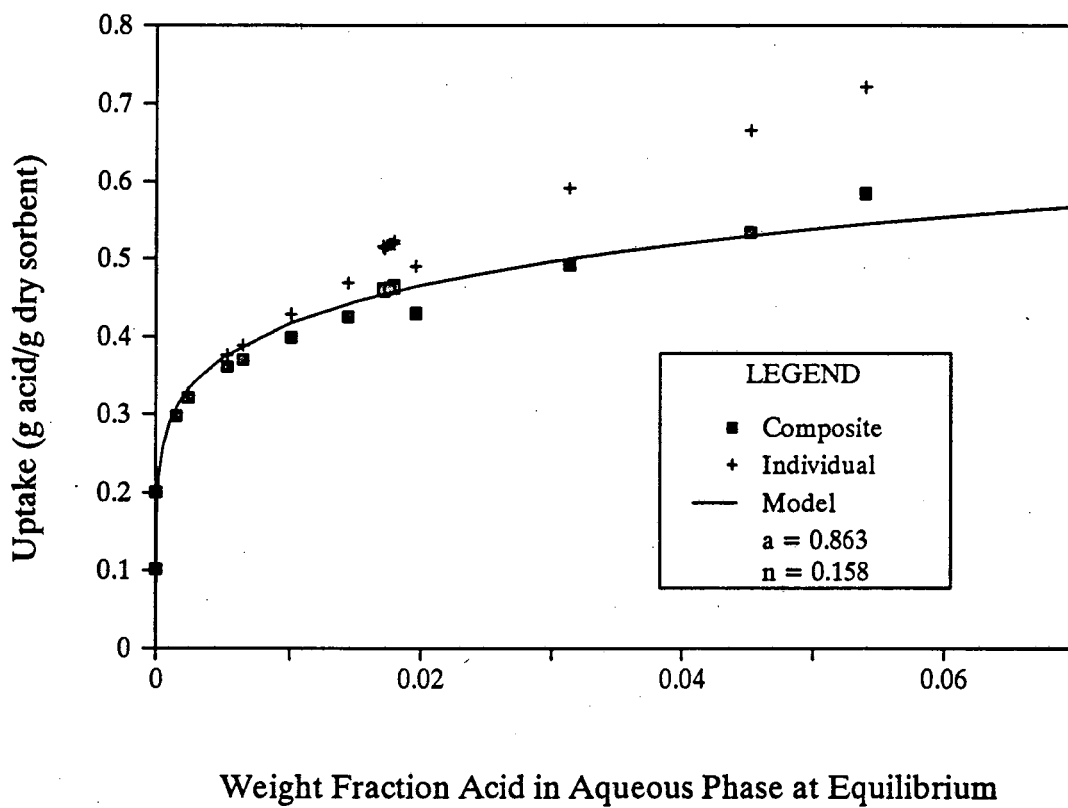


Figure 3-21. Sorption Isotherms for
Succinic Acid on Amberlite IRA-35

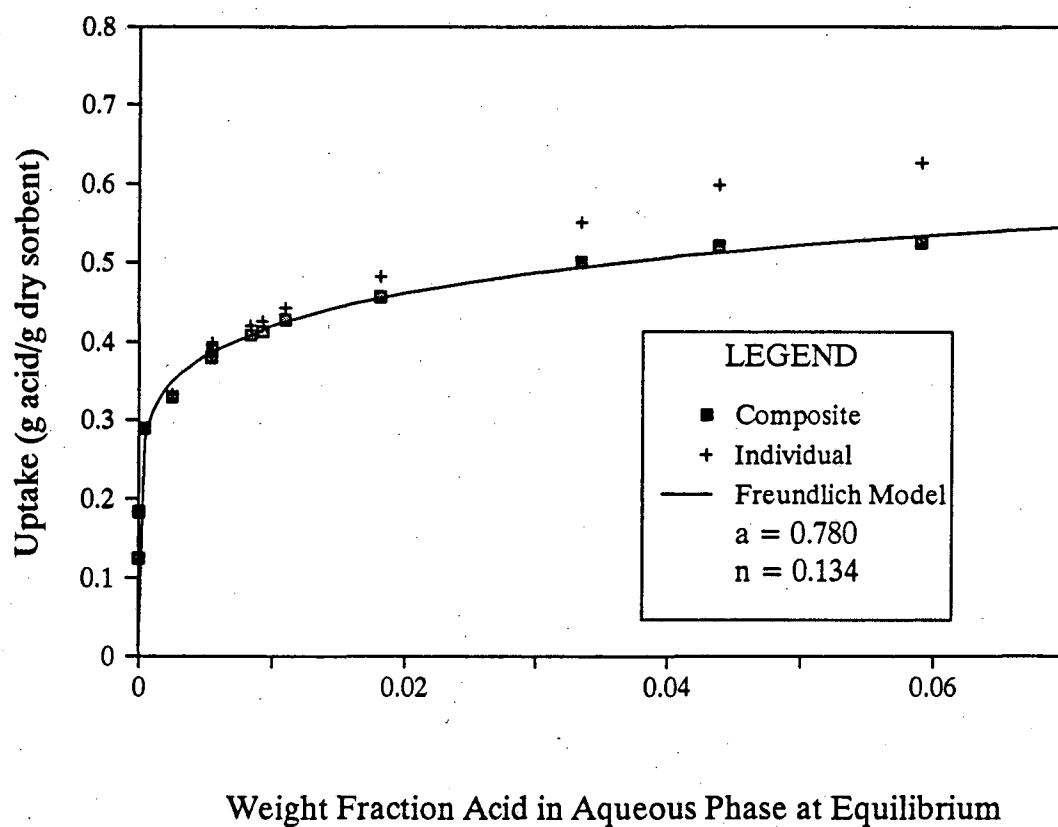


Figure 3-22. Sorption Isotherms for Succinic Acid on Amberlite IRA-910

data is probably related to the fact that succinic acid is a di-acid. Even though all sorption isotherms were generated at low pH (typically around 2.2), calculations based on the dissociation constants for the acid reveal that small amounts of bisuccinate ions are present, especially at lower concentrations of total acid. Competitive Langmuir models, which account for the uptake of both un-ionized acid and bisuccinate ion, were fitted to the data but do not provide a good description of the uptakes. Dual-site Langmuir models generally fit the data well, but there is no clear physical basis for using models of this type, except with Duolite A7. Freundlich isotherms also describe the data well, and with only half the number of parameters as the dual-site Langmuir models. Therefore, the Freundlich isotherm was chosen to describe the sorption data, despite the fact that this isotherm has no theoretical justification.

For lactic acid, the K value, which was obtained directly from the Langmuir or dual-site Langmuir isotherm, was correlated with various measures of sorbent pK_a . The Freundlich isotherm, however, is a purely empirical model and thus neither of its parameters is directly related to the strength of complexation. The initial slope of the sorption isotherm does reflect the sorbent basicity, but for a Freundlich isotherm, the initial slope is infinite. Therefore, for the purpose of comparing sorbent basicities, dual-site Langmuir curves were fitted to each isotherm other than Reillex 425, and a weighted-average K value was calculated as with lactic acid. The resulting K values are shown in Table 3-7:

The order of increasing K values is the same as that displayed for lactic acid, except that for succinic acid Amberlite IRA-35 has a larger K value than IRA-910. This finding is inconsistent with the fact that IRA-910 should be a much stronger base than IRA-35 and is probably due to the experimental error inherent in measuring extremely low concentrations of acid. The K value for Reillex HPQ places it between Duolite A7 and Bio-Rad AG3-X4 in terms of basicity. However, it is difficult to draw any conclusions about this sorbent since it has a mixture of strong- and weak-base groups.

Table 3-7. K Values for Succinic Acid Isotherms

Sorbent	K_1 (g solution/ g acid)	q_{m1} (g acid/ g sorbent)	K_2 (g solution/ g acid)	q_{m2} (g acid/ g sorbent)	$K_{ave.}$ (g solution/ g acid)
Reillex 425	71	0.47			
Reillex HPQ	10360	0.20	73.9	0.26	4546
Duolite A7	1830	0.30	17.9	0.35	853
Bio-Rad AG3-X4	21320	0.26	79.4	0.22	11590
Dowex MWA-1	38350	0.30	67.9	0.26	20600
Amberlite IRA-35	330200	0.25	104	0.32	144900
Amberlite IRA-910	198521	0.28	93.2	0.29	97567

The logarithm of the weighted-average K values can be correlated with various measures of pK_a , as with lactic acid. Such a correlation is shown in Figure 3-23 for all sorbents except Amberlite IRA-910 and Reillex HPQ. It is clear from Figure 3-23 that $\log(K)$ correlates reasonably well with both the predicted monomer pK_a and the apparent pK_a values. The predicted monomer pK_a for Duolite A7 still appears to be high, as seen in Figure 3-23 (a). The correlation between $\log(K)$ and the apparent pK_a values determined by Gustafson et al. (Figure 3-23 (b)) appears to be the strongest of the four, although $\log(K)$ also correlates fairly well with the pK_a values of Garcia and King (Figure 3-23 (c)). The data of Clifford and Weber do not adequately account for differences in basicity amongst Dowex MWA-1, Bio-Rad AG3-X4 or Duolite A7. As a result, the correlation between $\log(K)$ and pK_a is not a strong one (Figure 3-23 (d)).

Amberlite IRA-910 was again omitted from the above analysis because its pK_a value is difficult to quantify. However, by comparing the experimental K value with the correlations in Figure 3-23, it is apparent that the pK_a value corresponding to the

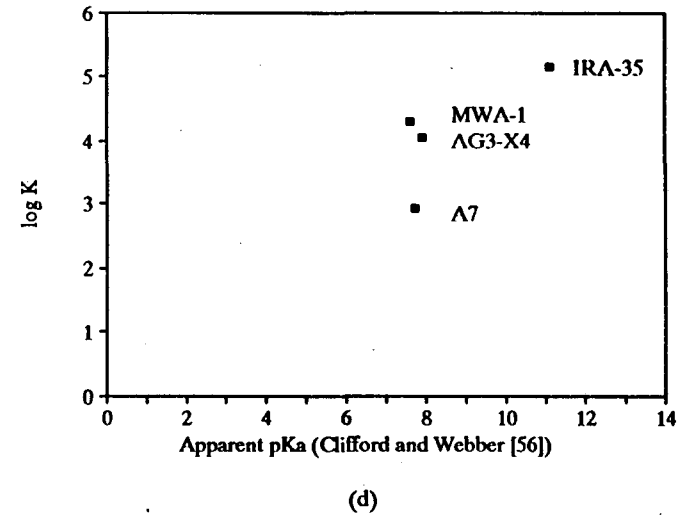
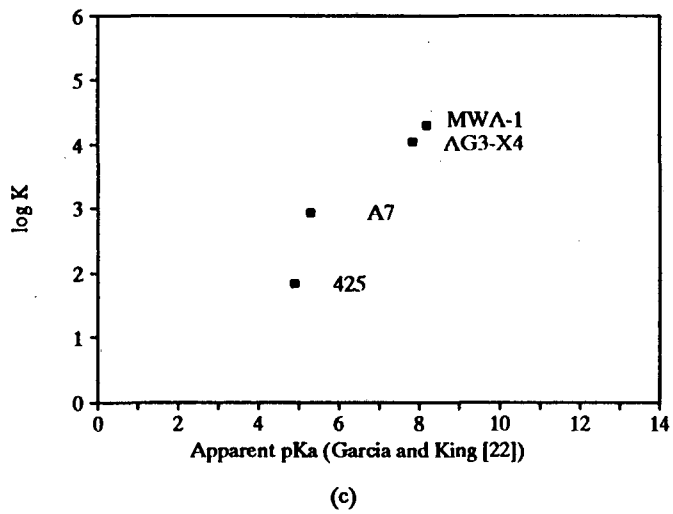
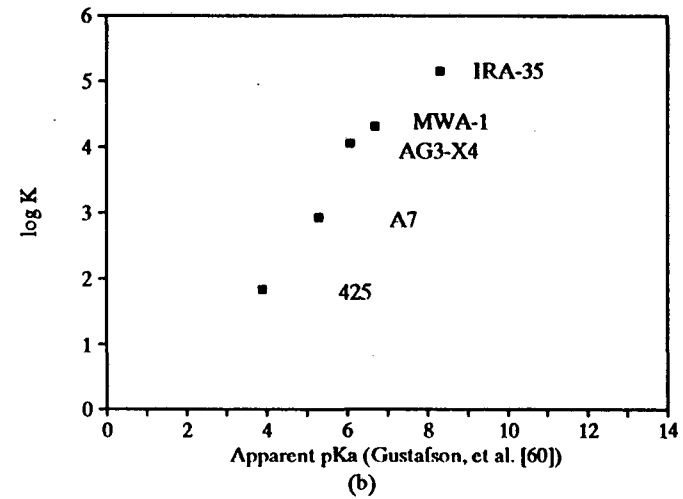
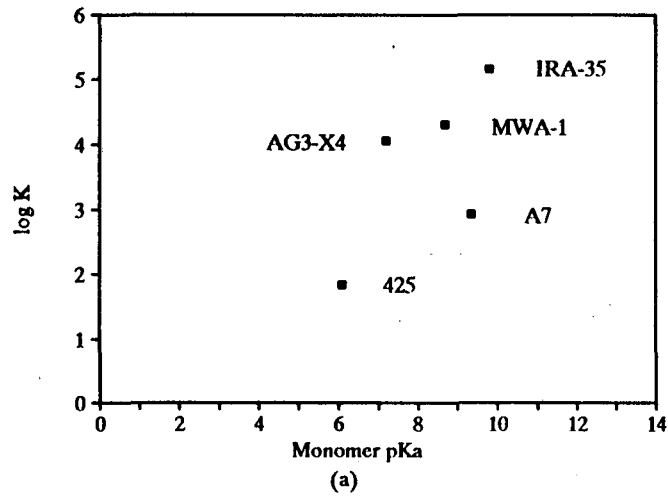


Figure 3-23. Comparison Between Experimental K-Values for Succinic Acid and Various Measures of Sorbent pKa

experimental K value is much lower than 13. It therefore seems that the measured K value is again artificially low. Reillex HPQ was also omitted from the above analysis because it is difficult to predict or measure a single pK_a value for this sorbent. Two different types of groups are present, one of which is a strong base, and it is unclear what happens to the functional groups during conversion to the OH^- form.

Table 3-8 compares the maximum uptake of succinic acid from the sorption isotherm with the experimentally determined capacities for HCl, on a mmol/g basis. Maximum uptakes are used because the Freundlich isotherm has no capacity parameter comparable to q_m . The maximum uptakes of succinic acid are generally 8 to 15 percent higher than the values of q_m obtained for lactic acid, although the value for Duolite A7 is 20 percent lower. For Reillex 425, Duolite A7 and Bio-Rad AG3-X4, all sorbents with high concentrations of functional groups, the full capacity for HCl is not utilized by succinic acid. Otherwise the agreement between the succinic acid uptakes and HCl capacities is good.

Table 3-8. Comparison Between q_m for Succinic Acid and Capacity Measurements

Sorbent	Experimental Capacity (mmol/g)		Maximum Uptake (mmol/g)
	Weak	Strong	
Reillex 425	6.3	-	3.4
Reillex HPQ	2.5	1.1	3.4
Duolite A7	7.1	0.16	3.7
Bio-Rad AG3-X4	8.5	0.5	4.5
Dowex MWA-1	4.3	0.44	3.6
Amberlite IRA-35	4.9	0	4.9
Amberlite IRA-910	-	4.0	4.3

It is clear that, for sorbents other than Reillex 425, Duolite A7 and Bio-Rad AG3-X4, each acid molecule complexes with no more than one basic site. This is an interesting observation because, as a di-acid, succinic acid could potentially complex with two neighboring sites. With Reillex 425, Duolite A7 and Bio-Rad AG3-X4, it is possible that the

acid complexes with more than one basic site, since the uptakes of succinic acid are approximately half the sorbent capacities. However, low uptakes by Reillex 425 and Duolite A7 are also observed with lactic acid, and may simply reflect unutilized capacity. As with lactic acid, there is no evidence of overloading in any of the succinic acid systems.

3.3.4.3 Comparison of Results for Lactic and Succinic Acids

It is interesting to compare the isotherms for the sorption of lactic and succinic acids by the same sorbent. The K value for a particular sorbent is expected to increase with the acidity of the solute. Since lactic acid ($pK_a = 3.86$) is somewhat more acidic than succinic acid ($pK_{a1} = 4.2$, $pK_{a2} = 5.6$), the K values for lactic acid should, barring other effects, be somewhat higher than those for succinic acid. Table 3-9 compares the K values on a 1/mol basis.

Table 3-9. Comparison of K Values for Lactic and Succinic Acids

Sorbent	Lactic Acid K Value (1/mol)	Succinic Acid K Value (1/mol)
Reillex 425	4.3	8.4
Duolite A7	99	101
Dowex MWA-1	537	2432
Amberlite IRA-35	2540	17100
Amberlite IRA-910	14900	11500

For all sorbents except Amberlite IRA-910, the K value for succinic acid is greater than or approximately equal to the corresponding K value for lactic acid. This finding is unexpected, and may be related to the fact that succinic acid is a di-acid. It may also result from the much higher hydrophilicity of lactic acid compared with succinic acid. Garcia and King (22) have shown that the free energy of sorption is linearly related to the sum of the free energy

of the acid-base interaction and the free energy of transfer for the solute from an aqueous phase to a non-polar phase.

3.3.5 Summary

The results of the sorption isotherm experiments indicate that the order of basicity is: Reillex 425 < Duolite A7 < Bio-Rad AG3-X4 < Dowex MWA-1 < Amberlite IRA-35 < Amberlite IRA-910. These results support the earlier observation that, for Duolite A7, the predicted monomer pK_a and the apparent pK_a values of some researchers may be artificially high. Furthermore, K values obtained for IRA-910 appear to be on the low side, probably because of experimental error. For succinic acid, the K value is low enough that Amberlite IRA-910 appears to be less basic than Amberlite IRA-35.

3.4 Uptake-pH Curves

The abilities of the sorbents to sustain capacity at $pH > pK_a$ were evaluated by measuring uptakes as a function of equilibrium pH. The uptakes were measured for a constant initial phase ratio (g solution/g sorbent) and a constant initial concentration of total acid. Curves generated in this manner are not true thermodynamic curves, which would, for example, present uptake as a function of pH at a fixed equilibrium concentration of total acid in the aqueous phase. However, such data are not easy to generate experimentally, since it is very difficult to predict and control the equilibrium acid concentration in the aqueous phase. Zhu et al. (16, 17) used mini-column experiments to control equilibrium pH and acid concentration in experiments with ligand exchangers. Their procedure could also be used with basic sorbents. The goal of the current work, however, was to generate data of the type described, develop models to describe the data, and use these models to generate the desired thermodynamic curves.

3.4.1 Modelling of the Uptake-pH Curves

The uptake-pH curves can be modelled using the appropriate equilibrium and mass-balance equations. These equations are somewhat different for monocarboxylic and dicarboxylic acids.

3.4.1.1 Monocarboxylic Acids

The necessary equilibrium expressions include the equations that describe the dissociation of the acid. For a monocarboxylic acid, there is only one dissociation step, with an equilibrium constant as shown in Equation 3-21.

$$K_a = \frac{[H^+][A^-]}{[HA]} \quad (3-21)$$

The sorption isotherm, which describes the equilibrium between the sorbent and the aqueous phase, is also needed. As discussed in Section 3.3.2, for a monocarboxylic acid the isotherm is generally a function of the concentration of un-ionized acid, as shown in Equation 3-22.

$$q = f(C_{HA}) \quad (3-22)$$

For the lactic acid systems examined, the isotherm is of the Langmuir or dual-site Langmuir form.

An expression for the mass balance, given in Equation 3-23, is needed to complete the model:

$$W_o C_{a,i} - q*m - C_a (W_o - q*m) = 0 \quad (3-23)$$

where $C_a = C_{HA} + C_{A^-}$.

The above equations can be solved simultaneously for q as a function of pH for a given initial phase ratio (W_o/m) and acid concentration ($C_{a,i}$). In this work, the solution was performed using a spreadsheet program and an iterative solution method.

3.4.1.2 Dicarboxylic Acids

The modelling of the uptake-pH curve for a dicarboxylic acid is somewhat more complicated, and the model must be modified if the sorbent function groups are strong-base (quaternized) groups with fixed positive charges. The uptake of dicarboxylic acids by unquaternized sorbents will be considered first.

For a dicarboxylic acid, two equilibrium constants are needed to describe the dissociation of the acid:

$$K_{a1} = \frac{[H^+][HA^-]}{[H_2A]} \quad (3-24)$$

$$K_{a2} = \frac{[H^+][A^{2-}]}{[HA^-]} \quad (3-25)$$

The sorption isotherm may also be a somewhat more complex function than that shown in Equation 3-22. For uptake of dicarboxylic acids by unquaternized sorbents, uptake is primarily a function of the concentration of un-ionized acid. However, for certain di-acids, it may also be a function of the concentration of bicarboxylate ion, because the un-ionized end of a bicarboxylate ion may complex with a basic site. Therefore, the sorption isotherm is represented more generally by:

$$q = f(C_{H_2A}, C_{HA^-}) \quad (3-26)$$

For succinic acid, Equation 3-26 could be a Freundlich isotherm, which was shown to fit the low pH data well. However, at higher pH the amount of bisuccinate increases and its uptake may become an important factor. Thus, Equation 3-26 could also be a competitive Langmuir isotherm of the form shown in Equation 3-16.

The mass balance remains as in Equation 3-23 (with $C_a = C_{H_2A} + C_{HA^-} + C_{A^{2-}}$), and the system of Equations 3-23 through 3-26 can be solved simultaneously, as before, to obtain q as a function of pH for a given initial phase ratio and acid concentration.

For strong-base sorbents, the situation is more complicated. As shown in Figure 3-24, two charged sorbent sites can complex with either one carboxylate ion, as in structure A, or with two bicarboxylate ions, as in structure B. At high pH, the resin is typically in the A form, whereas at lower pH the resin is in the B form. Helfferich (62) discusses the phenomenon of conversion from form A to B, known as site-sharing. As a result of site-sharing, two different equilibrium expressions are needed to define the uptake of acid:



with associated equilibrium constant

$$K_3 = \frac{[\overline{BAB}]}{[\overline{BOH}]^2 [H_2A]} \quad (3-28)$$

and



with equilibrium constant

$$K_4 = \frac{[\overline{BAH}]}{[\overline{BOH}] [H_2A]} \quad (3-30)$$

In the above expressions, the activity of the solvent and all activity coefficients are assumed to be constant and therefore are incorporated into the equilibrium constants. If it is then assumed that there are a fixed number of identical sites available for complexation, Equation 3-31 holds.

$$q_{\max} = 2 [\overline{BAB}] + [\overline{BOH}] + [\overline{BAH}] \quad (3-31)$$

The system is fully defined by Equations 3-28, 3-30 and 3-31, the expressions for the dissociation of the acid given in Equations 3-24 and 3-25, and the mass balance, given in Equation 3-23. These equations can be solved using an iterative method to obtain q ($= [\overline{BAB}] + [\overline{HAB}]$) as a function of pH.

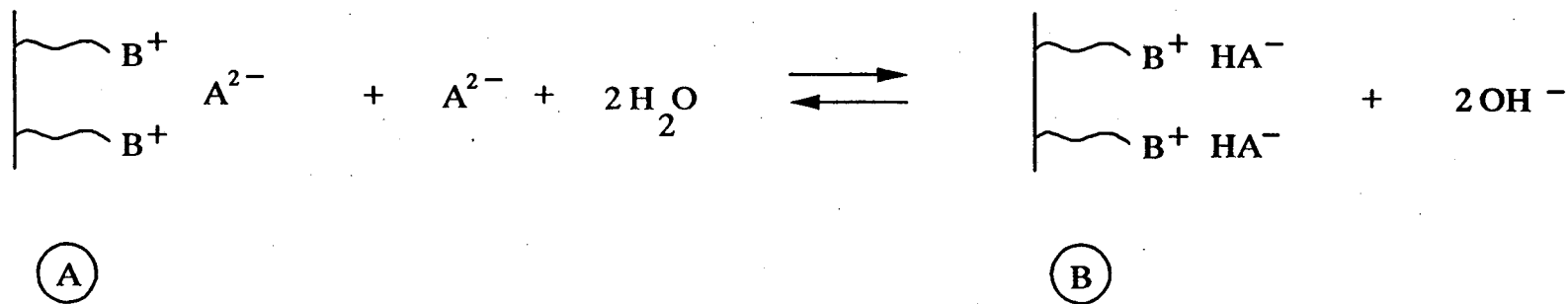


Figure 3-24. Conversion of Strong-Base Site
 from Carboxylate to Bicarboxylate Form
 [Helfferich (58)]

3.4.2 Results and Discussion

3.4.2.1 Lactic Acid

Figures 3-25 through 3-29 present graphs of uptake versus pH for the lactic acid systems at 25 °C. The solid curves were calculated using the model described in Section 3.4.1.1. For all sorbents except Amberlite IRA-910, the best-fit isotherm given in Section 3.3.4.1 was used. The models, which contain no additional fitted parameters, provide an excellent description of the composite-isotherm data. For Amberlite IRA-910, use of the Langmuir isotherm from Section 3.3.4.1 ($K = 1.65 \times 10^5$ g solution/g acid, $q_m = 0.355$ g acid/g sorbent) results in a very poor fit to the uptake-pH data. However, a Langmuir isotherm with $K = 1.52 \times 10^{10}$ g solution/g acid results in a reasonably good fit, as shown in Figure 3-29. This finding is consistent with the earlier observation that the value of K resulting from the sorption isotherm is somewhat lower than expected.

For *in-situ* use in a lactic acid fermentation, the sorbent must demonstrate significant uptake of acid in the pH 5 to 6 range. The uptake in this pH range varies substantially from one sorbent to the next and is strongly dependent upon the basicity of the sorbent, as well as the capacity of the resin. Reillex 425, the weakest base among all the resins, has virtually no selective uptake of acid in the pH 5 to 6 range. Duolite A7, a somewhat stronger base, shows uptakes of 0.18 to 0.08 g acid/g sorbent, and stronger bases exhibit even higher uptakes. The experimental results show composite uptakes of 0.3 to 0.18 g acid/g sorbent for Dowex MWA-1, 0.35 to 0.29 g acid/g sorbent for Amberlite IRA-35, and a constant uptake of about 0.3 g acid/g sorbent for Amberlite IRA-910. On this basis, MWA-1, Amberlite IRA-35, and Amberlite IRA-910 are the best candidates for use for product recovery in a fermentation process, since all show excellent uptake of lactic acid in the pH 5 to 6 range.

The uptakes of lactic acid by all five sorbents are presented as functions of pH in Figure 3-30. The uptakes are shown as fractions of sorbent capacity (obtained from the sorption isotherms) in order to highlight the effects of resin basicity. The order of choice for

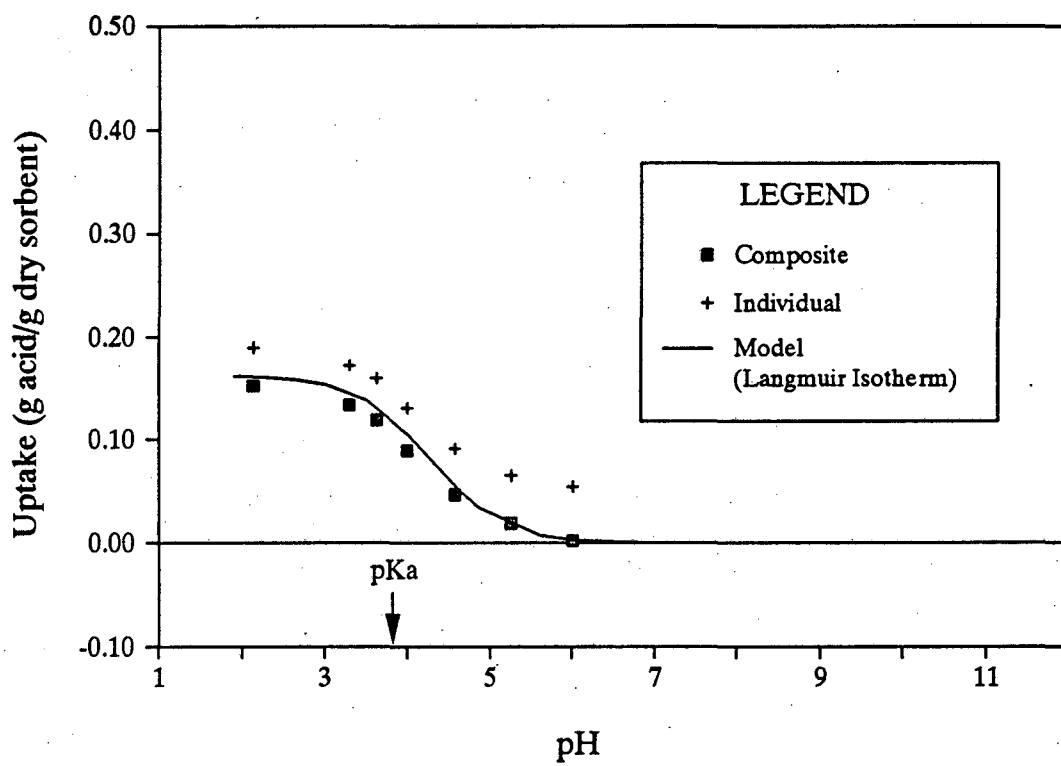


Figure 3-25. Effect of pH on Uptake of Lactic Acid by Reillex 425
 $C_{a,i} = 0.45 \text{ M}$, $W_o/m = 11.0$

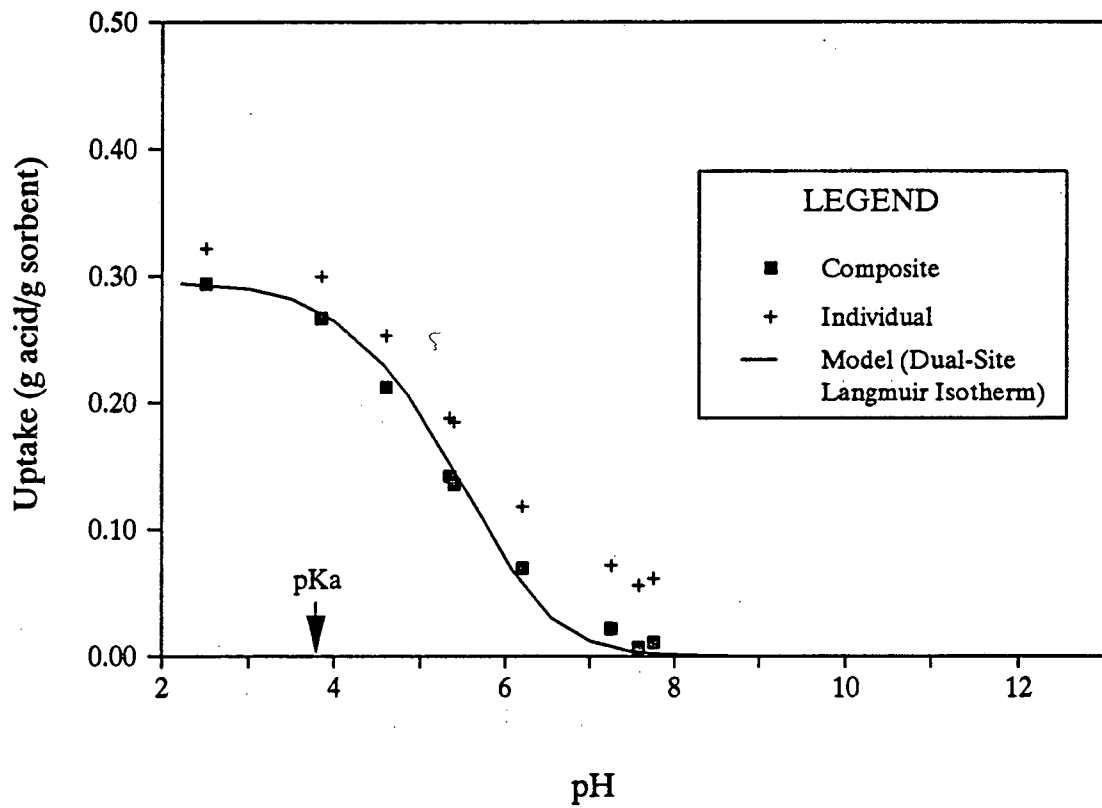


Figure 3-26. Effect of pH on Uptake of Lactic Acid by Duolite A7
 $Ca_i = 0.45 \text{ M}$, $W_o/m = 11.0$

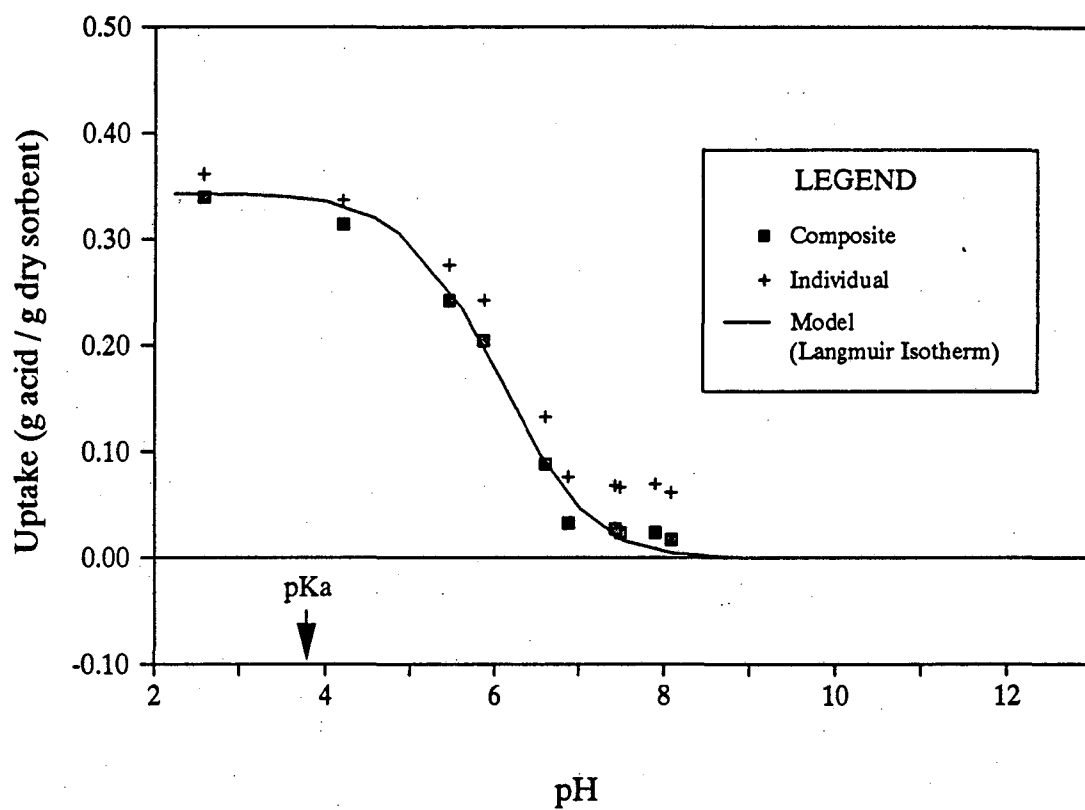


Figure 3-27. Effect of pH on Uptake of Lactic Acid by Dowex MWA-1
 $Ca_i = 0.45 \text{ M}$, $W_o/m = 11.0$

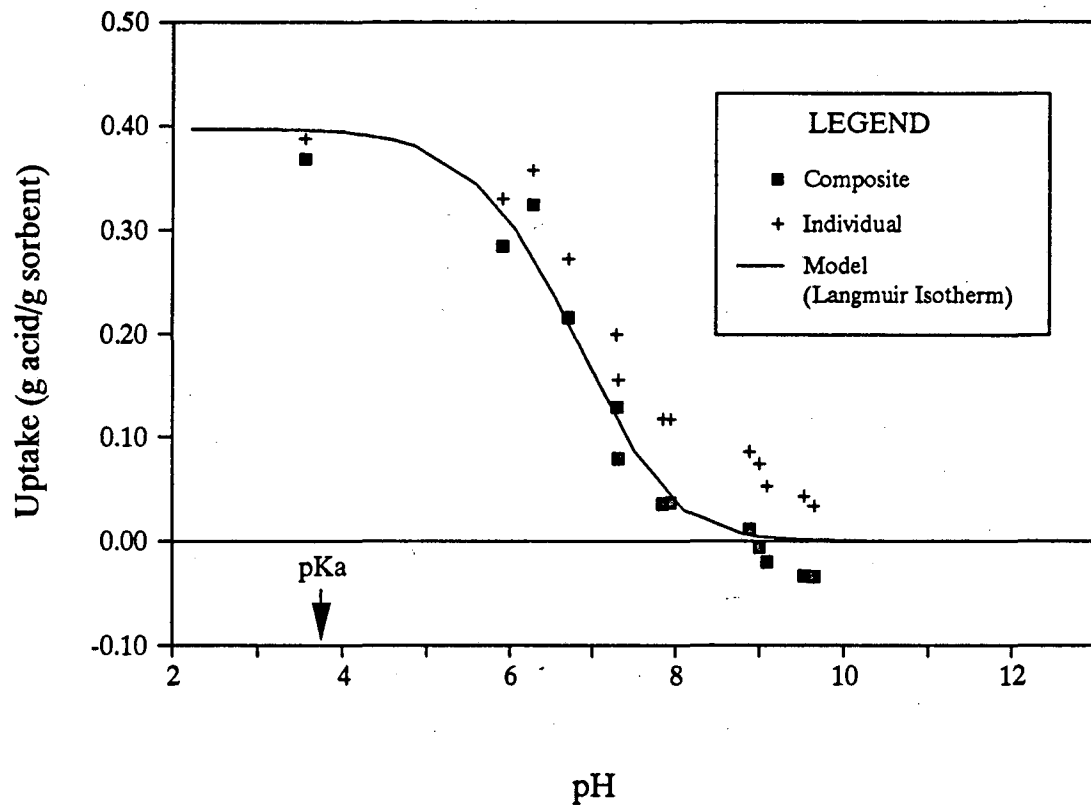


Figure 3-28. Effect of pH on Uptake of Lactic Acid by Amberlite IRA-35
 $Ca_i = 0.45$ M, $W_o/m = 11.0$

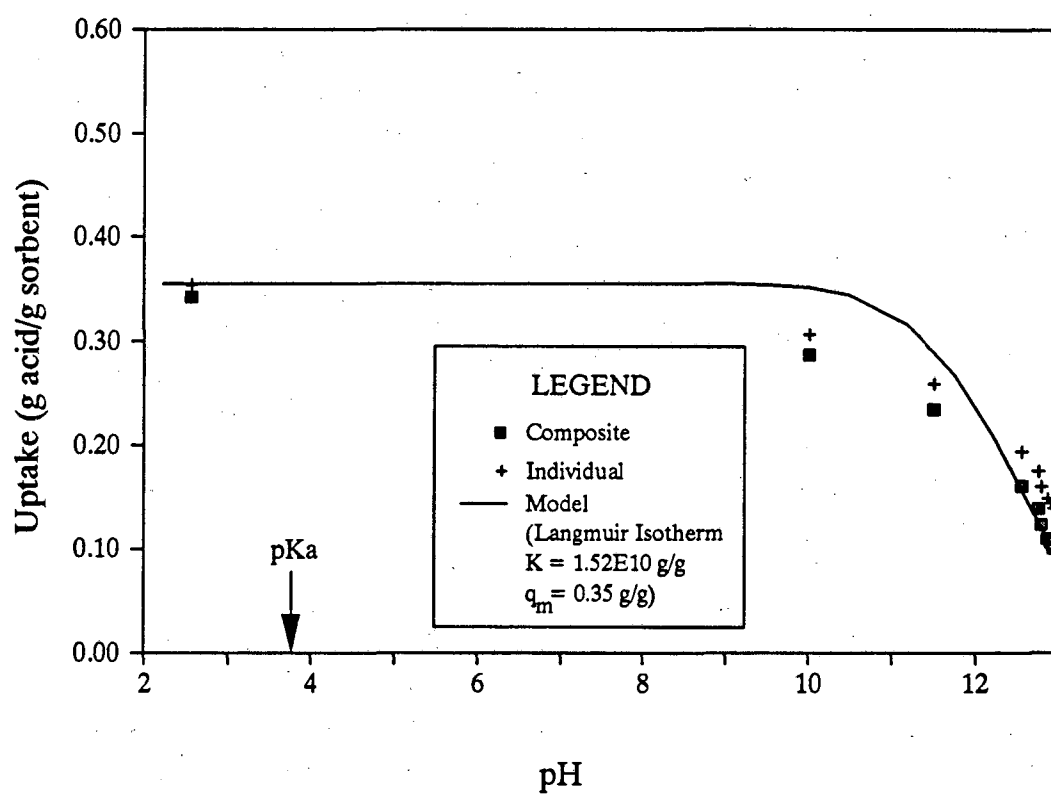


Figure 3-29. Effect of pH on Uptake of Lactic Acid by Amberlite IRA-910
 $Ca_i = 0.45 \text{ M}$, $W_o/m = 11.0$

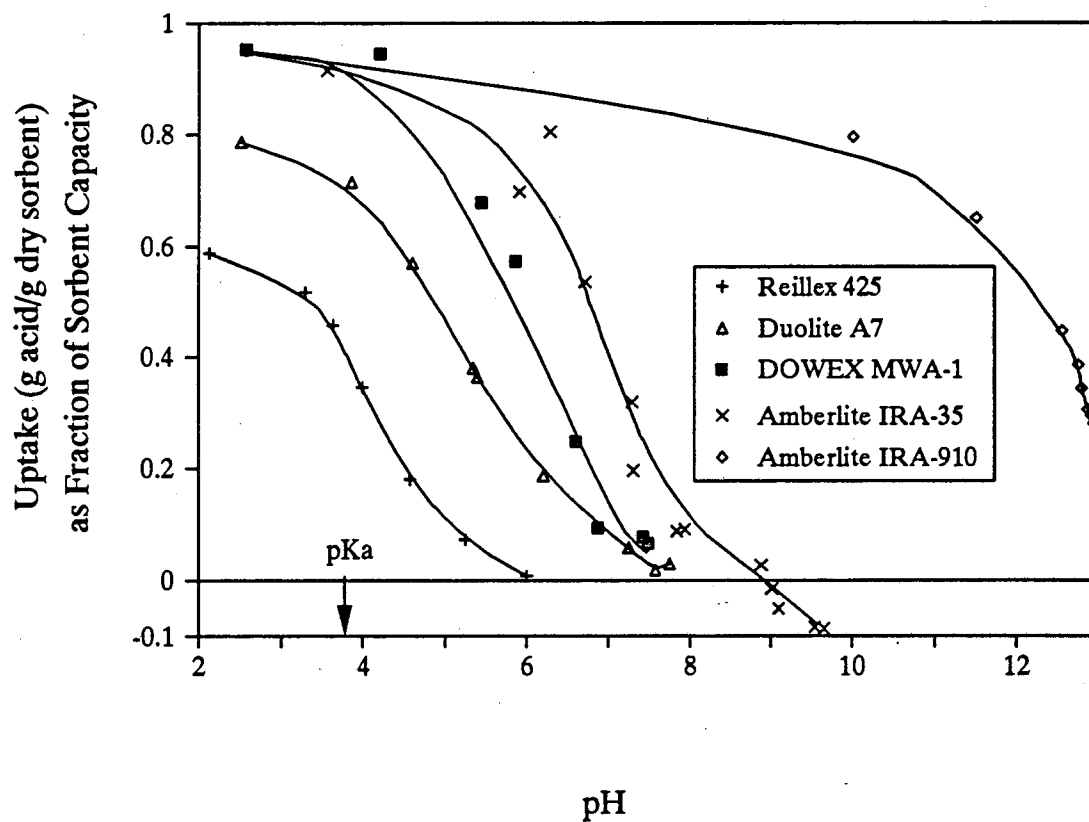


Figure 3-30. Effect of pH on Normalized Uptakes of Lactic Acid
 $Ca_i = 0.45 \text{ M}$, $W_o/m = 11.0$

sustaining capacity with increasing pH is Amberlite IRA-910 > Amberlite IRA-35 > Dowex MWA-1 > Duolite A7 > Reillex 425. This order reflects the relative basicities of the resins and is the same order followed by the experimental K values. It also confirms the earlier hypothesis that Duolite A7 is a relatively weak base, and that some of the measurements and predictions which give it a high pK_a value may be in error.

For design purposes, it is helpful to have graphs of uptake as a function of pH at a fixed equilibrium concentration of total acid in the aqueous phase. These curves can be calculated for each of the five sorbents using the models developed here. Uptakes of lactic acid at an equilibrium acid concentration of 1.0 wt.% are presented in Figure 3-31. Other graphs are easily generated for different solution concentrations.

3.4.2.2 Succinic Acid

Figures 3-32 through 3-41 present uptake-pH curves for the succinic acid systems at 25 °C. The results for Reillex HPQ (Figure 3-32) were not modelled because it is unclear what happens to the functional groups at higher pH. In this case the curve is simply drawn through the data. It does not have a theoretical basis. In the other figures the curve is the theoretical prediction. The composite isotherm results for the unquaternized sorbents (Figures 3-33 through 3-37) are represented reasonably well using the model presented in Section 3.4.1.2 in conjunction with the best-fit isotherm from Section 3.3.4.1 (Langmuir for Reillex 425, dual-site Langmuir for Duolite A7, and Freundlich for Bio-Rad AG3-X4, Dowex MWA-1 and Amberlite IRA-35). The curvature of the Duolite A7 model is somewhat off, and the AG3-X4 curve systematically underestimates the uptake by a few percent. A more serious problem is that the model for Amberlite IRA-35 fails to predict the inflection point which is evident in the experimental uptakes.

Because a model that accounts for uptake of bisuccinate may better describe the experimental data, the use of a competitive Langmuir model was examined. The model, which contains four parameters, was fitted to the data to minimize the residual sum of

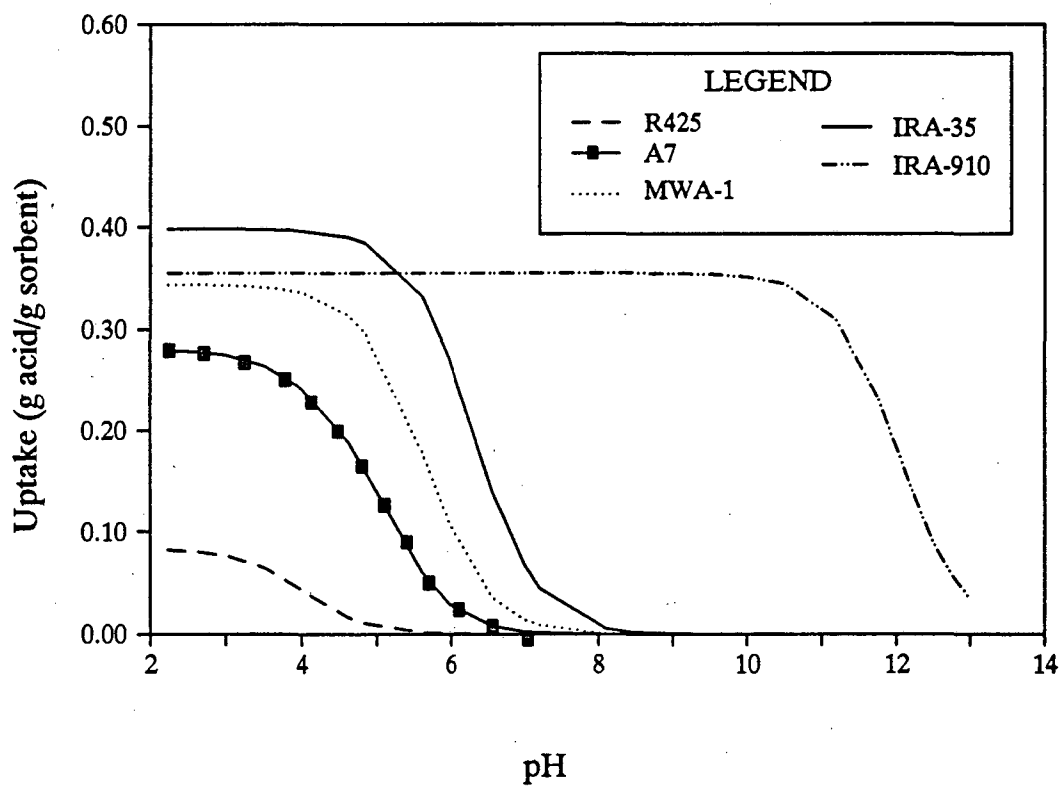


Figure 3-31. Effect of pH on Uptakes of Lactic Acid at Equilibrium Solution Concentration of 1.0 wt. %

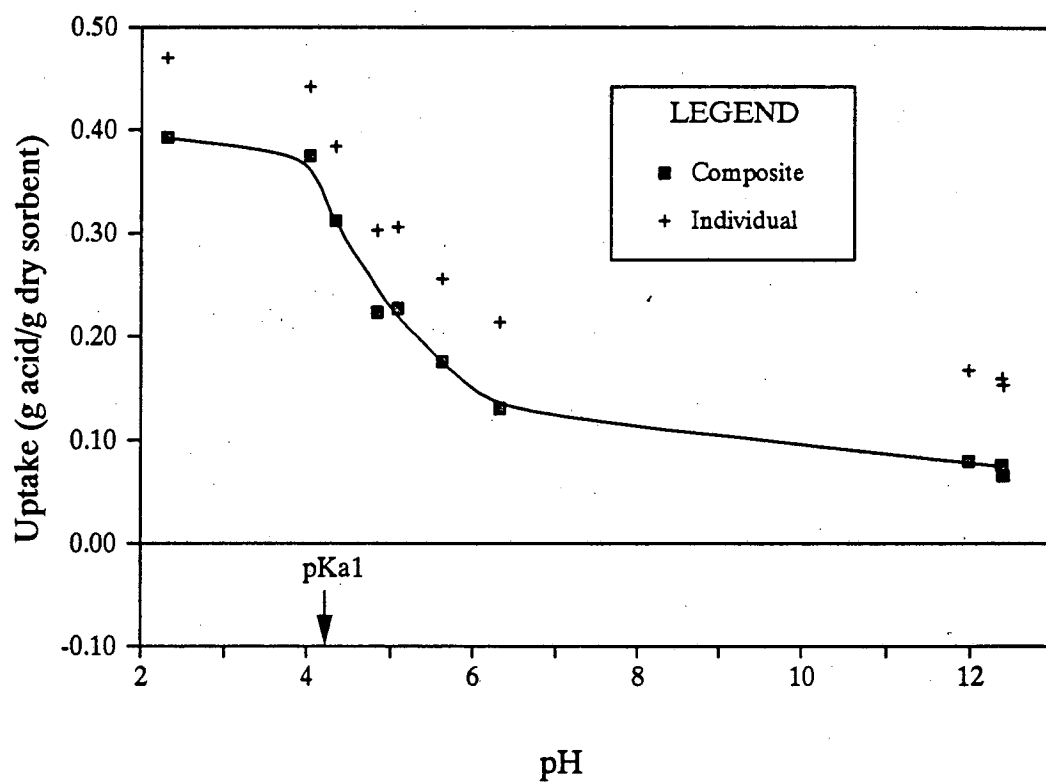


Figure 3-32. Effect of pH on Uptake of Succinic Acid by Reillex HPQ
 $Ca_i = 0.45 \text{ M}$, $W_o/m = 22.5$

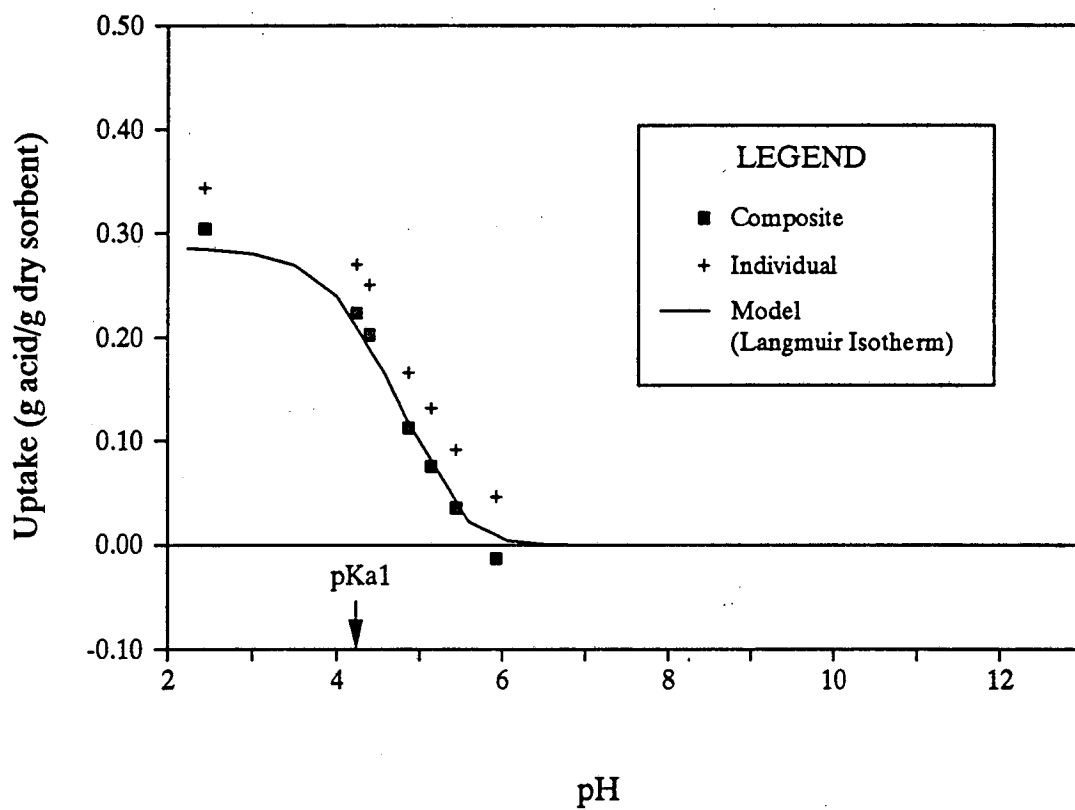


Figure 3-33. Effect of pH on Uptake of Succinic Acid by Reillex 425
 $Ca_i = 0.45 \text{ M}$, $W_o/m = 11.2$

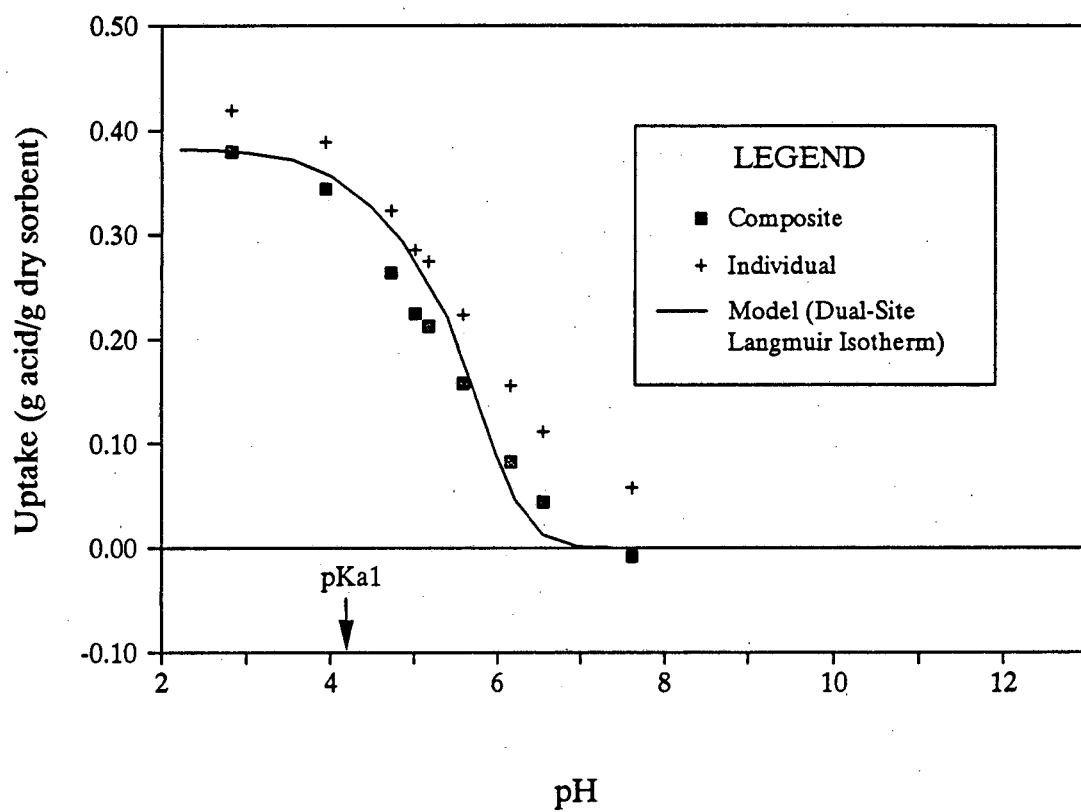


Figure 3-34. Effect of pH on Uptake of Succinic Acid by Duolite A7
 $Ca_i = 0.45 \text{ M}$, $W_o/m = 11.0$

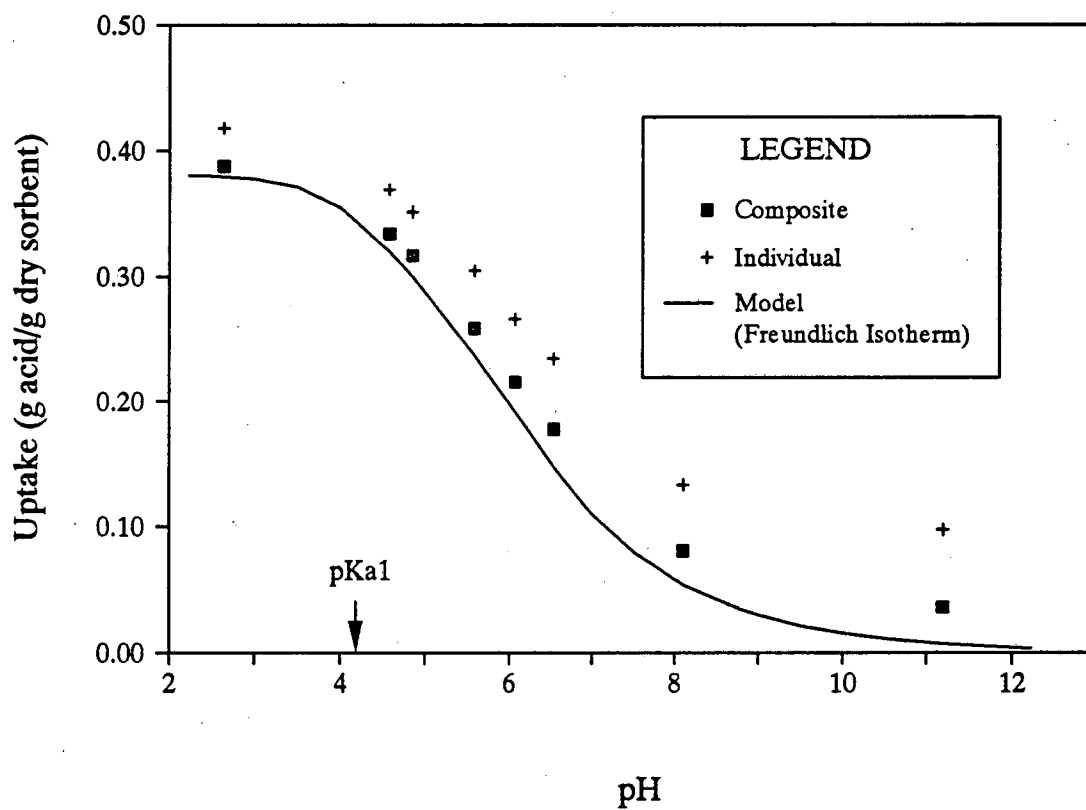


Figure 3-35. Effect of pH on Uptake of Succinic Acid by Bio-Rad AG3-X4
 $Ca_i = 0.45 \text{ M}$, $W_o/m = 10.6$

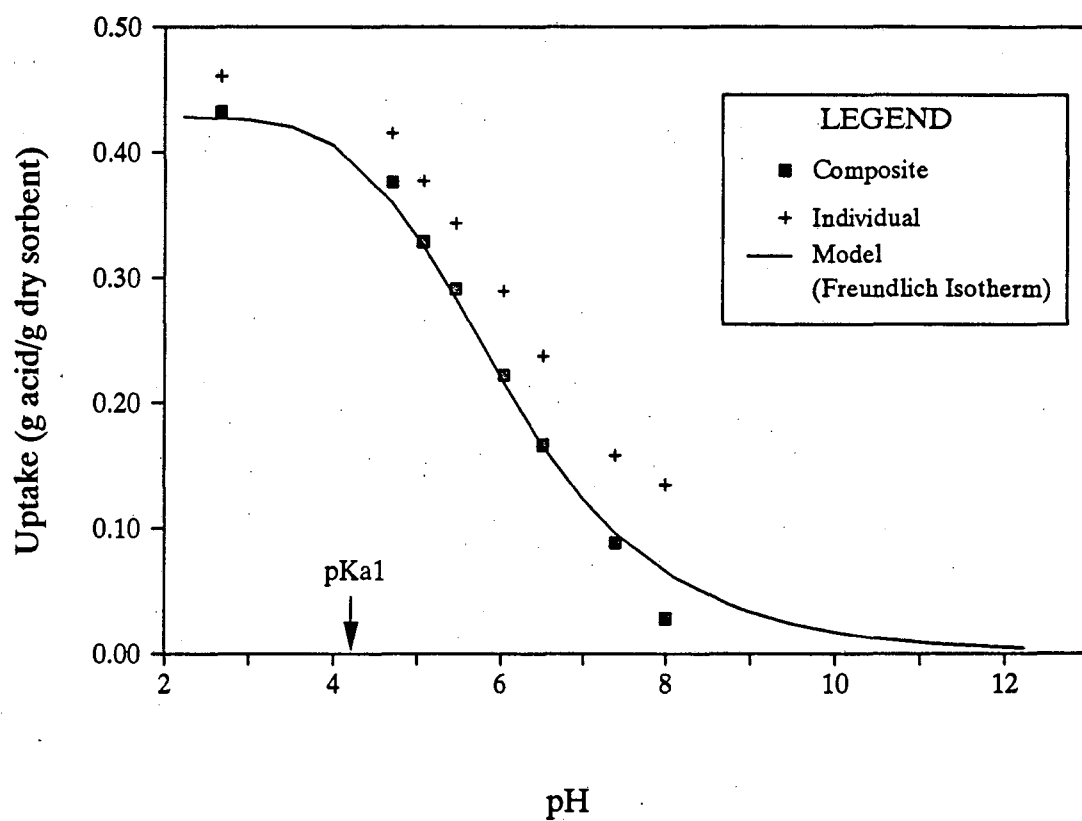


Figure 3-36. Effect of pH on Uptake of Succinic Acid by Dowex MWA-1
 $Ca_i = 0.45$ M, $W_o/m = 11.0$

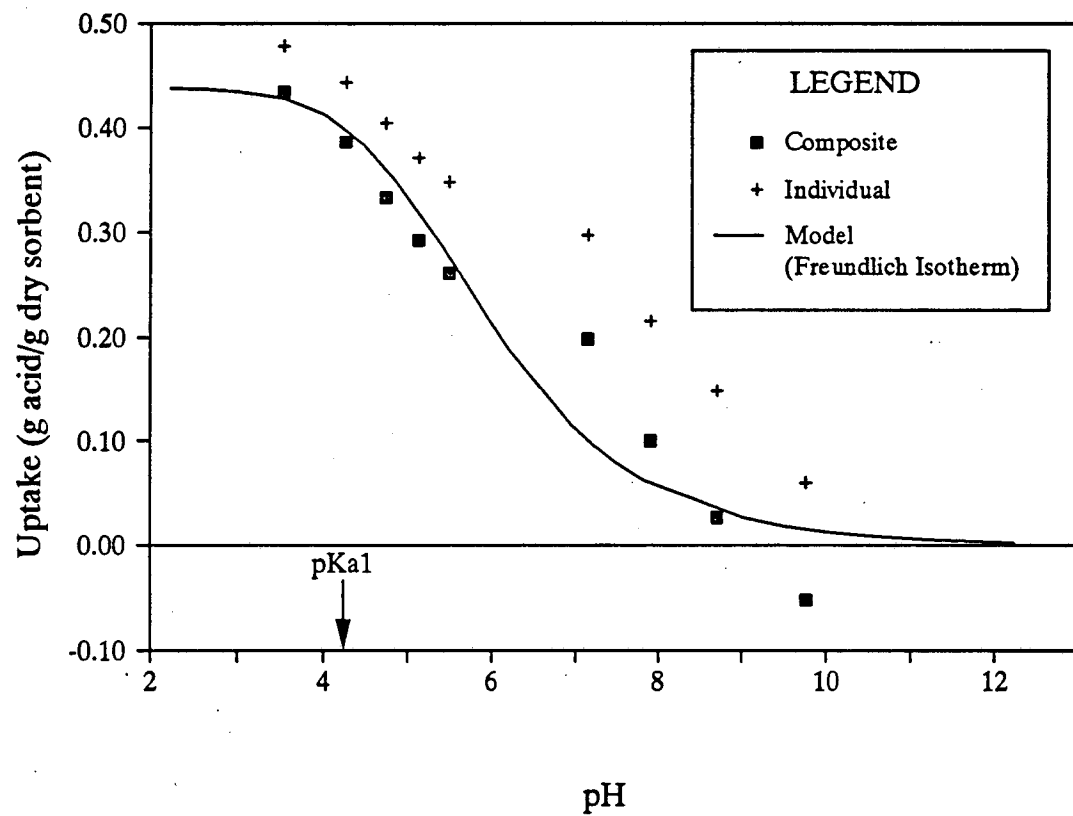


Figure 3-37. Effect of pH on Uptake of Succinic Acid by Amberlite IRA-35
 $Ca_i = 0.45 \text{ M}$, $W_o/m = 11.0$

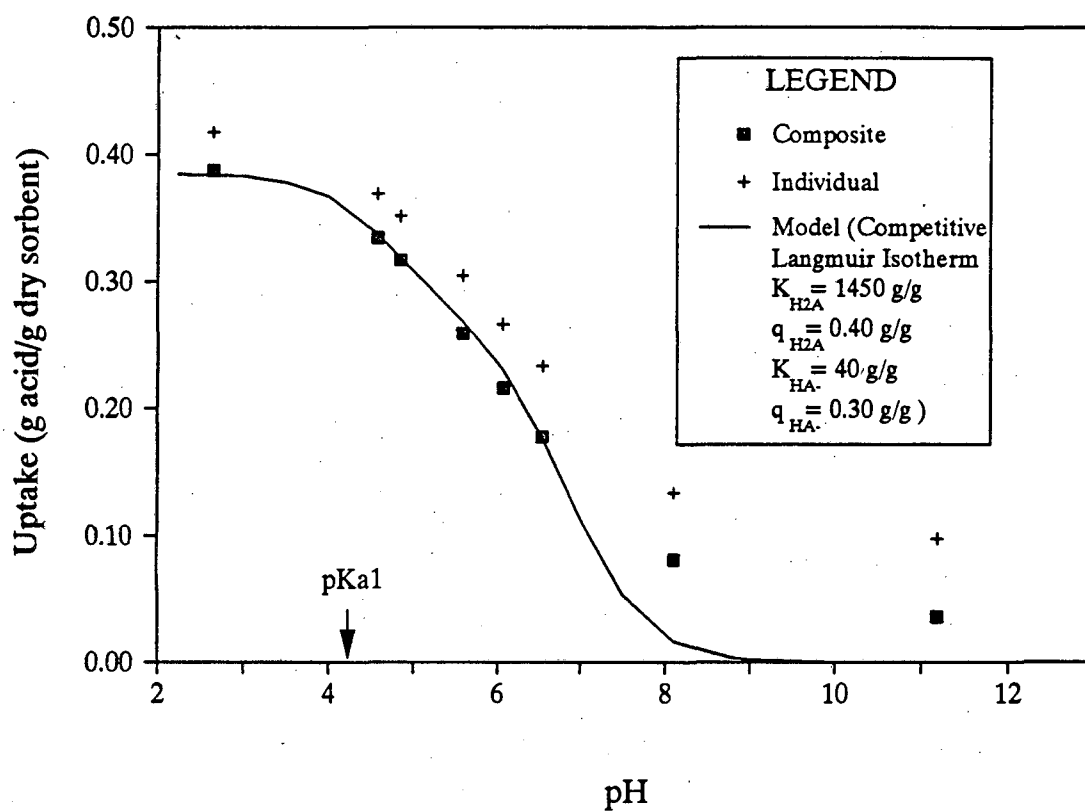


Figure 3-38. Effect of pH on Uptake of Succinic Acid by Bio-Rad AG3-X4
 $Ca_i = 0.45 \text{ M}$, $W_o/m = 11.0$

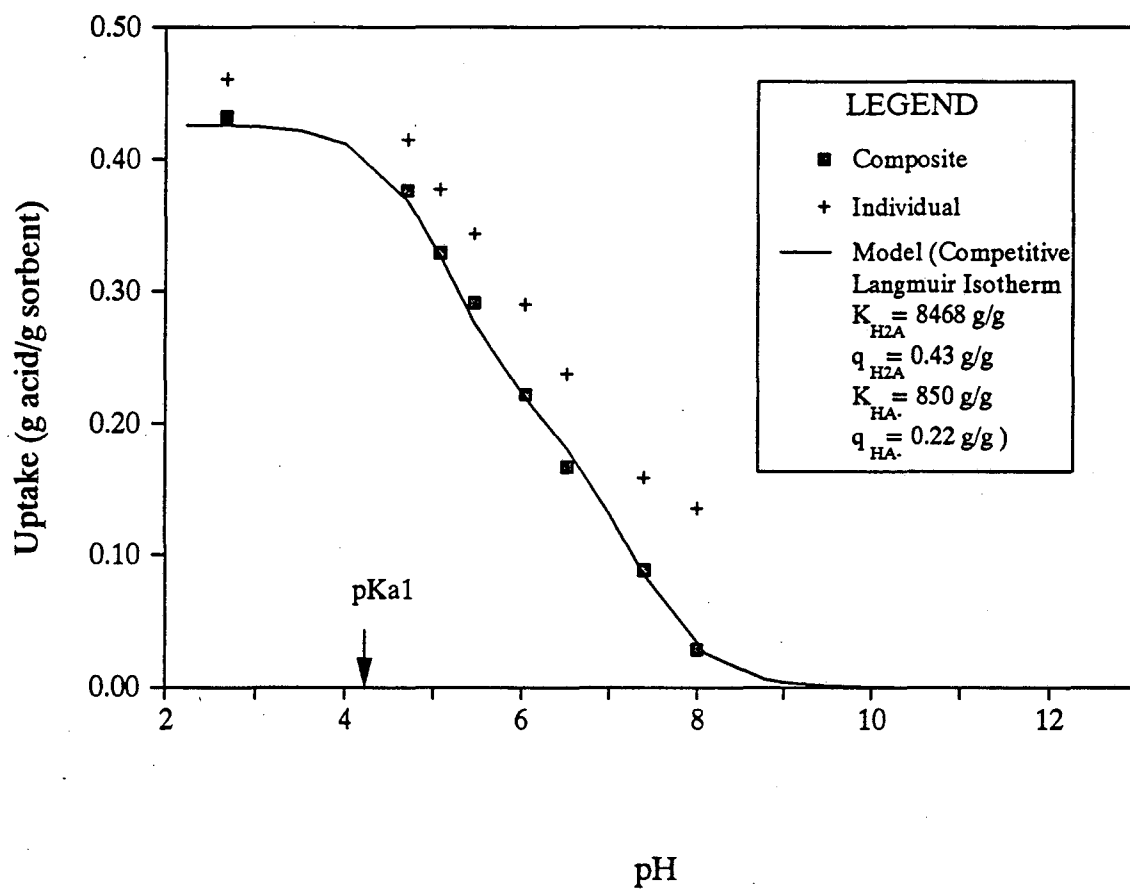


Figure 3-39. Effect of pH on Uptake of Succinic Acid by Dowex MWA-1
 $Ca_i = 0.45 \text{ M}$, $W_o/m = 11.0$

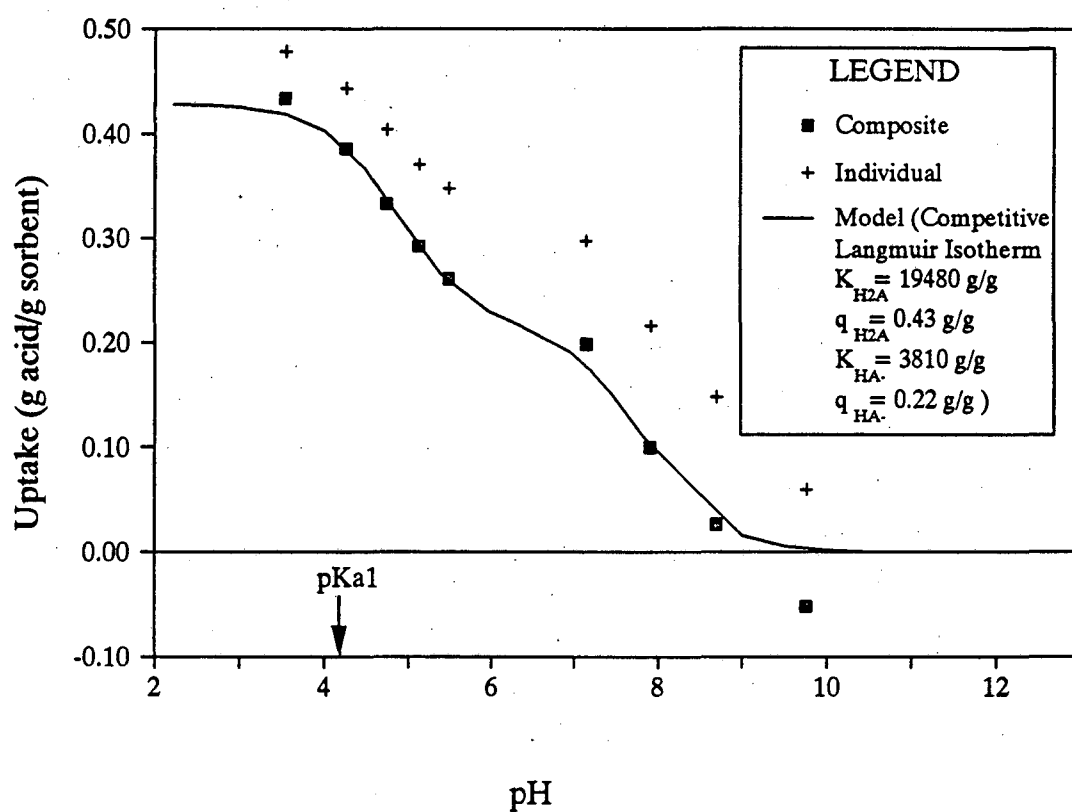


Figure 3-40. Effect of pH on Uptake of Succinic Acid by Amberlite IRA-35
 $Ca,i = 0.45 \text{ M}$, $Wo/m = 11.0$

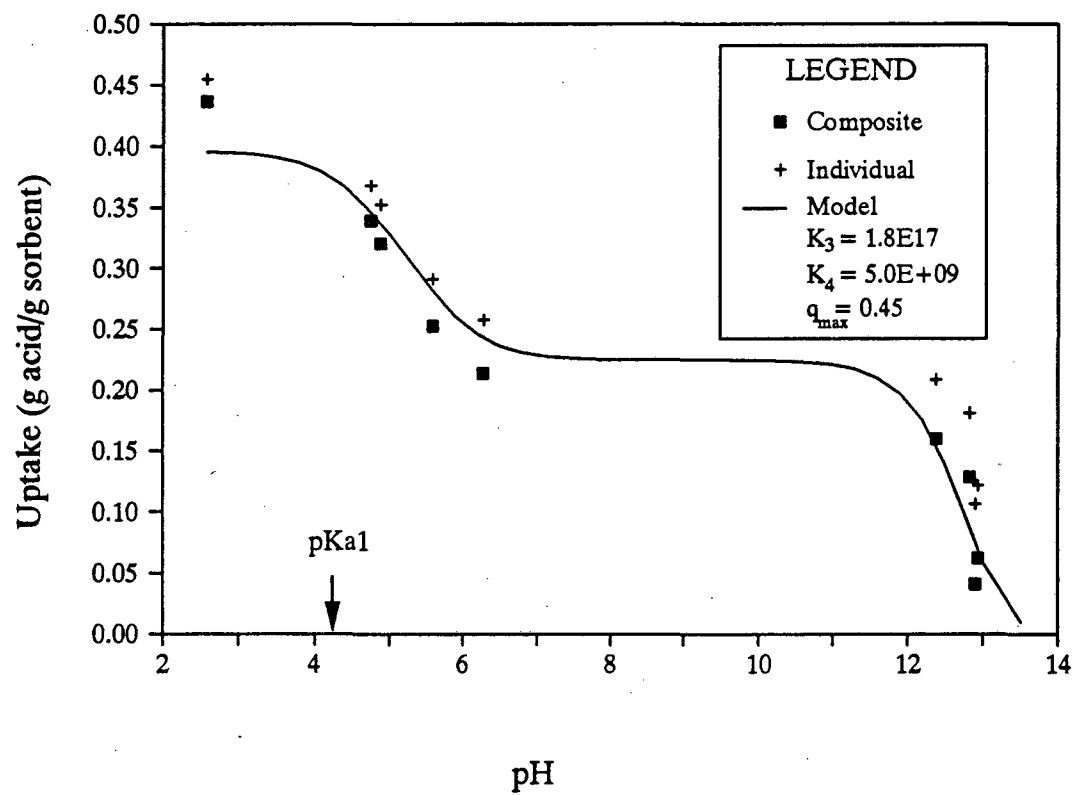


Figure 3-41. Effect of pH on Uptake of Succinic Acid by Amberlite IRA-910
 $C_{a,i} = 0.45$ M, $W_o/m = 11.0$

squares. Figures 3-38 through 3-40 present the fitted models for AG3-X4, MWA-1 and IRA-35, respectively. It is difficult to model the data for AG3-X4 over the entire range of pH values, since this sorbent contains 10% quaternary ammonium groups, and a model which incorporates both strong- and weak-base sites would be quite complex. As a compromise, only data at $\text{pH} < 7$ were used in fitting the competitive Langmuir model, since beyond this point, the quaternary ammonium groups are the major effect. The resulting model fits the data well in the $\text{pH} < 7$ region. The data for MWA-1 and Amberlite IRA-35 were fit over the entire range of pH values, with excellent results. The model for IRA-35 even accounts for the inflection point in the uptake data. An attempt was made to apply the competitive Langmuir models developed here to the isotherms discussed in Section 3.3. However, the resulting curves give a poor description of the uptake data (see Appendix B).

The results of the competitive Langmuir models indicate that the un-ionized acid is the more strongly complexed species. In general, the value of q_{m,HA^-} is only 50 to 75 percent of the value of $q_{m,\text{H}_2\text{A}}$, and the value of K_{HA^-} is lower than that of $K_{\text{H}_2\text{A}}$ by at least an order of magnitude. This result is consistent with the fact that the first ionization constant of succinic acid is an order of magnitude higher than the second ionization constant.

Figure 3-41 presents the uptake-pH curve for Amberlite IRA-910. The model described above for quaternized sorbents was fit to the data, with good results. The value of q_m obtained (0.45 g acid/g sorbent) is slightly lower than the capacity (0.50 g acid/g sorbent) exhibited in the low pH experiments. The values of K_1 and K_2 differ by almost eight orders of magnitude ($K_1 = 1.8 \times 10^{17} (\text{g solution})(\text{g sorbent})/(\text{g acid})^2$ and $K_2 = 5.0 \times 10^9 \text{ g solution/g acid}$), indicating that the succinate form of the resin (species A in Figure 3-24) is the preferred form. Note that there are three distinct regions of the curve. In the first region, from pH 2 to 6, succinate gradually replaces bisuccinate on the sorbent, through the reaction shown in Figure 3-24. In the second region, from pH 6 to 11 or 12, the resin remains in the succinate form. In the third region, at $\text{pH} > 12$, OH^- displaces succinate.

For *in-situ* use in a succinic acid fermentation or use within a recycle loop, the sorbent must demonstrate significant uptake of acid at an average pH of about 6. The uptake at this pH again varies substantially from one sorbent to the next and follows the trend of increasing uptake with increasing sorbent basicity. Reillex 425 demonstrates essentially no selective uptake of acid at pH 6, Duolite A7 shows an uptake of 0.08 g acid/g sorbent, and Reillex HPQ has an uptake of 0.15 g acid/g sorbent. The stronger bases (Bio-Rad AG3-X4, Dowex MWA-1, Amberlite IRA-35 and Amberlite IRA-910) all have uptakes between 0.22 and 0.25 g acid/g sorbent.

The uptakes of succinic acid, as a fraction of sorbent capacity, are presented as a function of pH for all seven sorbents in Figure 3-42. The actual data points have been omitted for reasons of clarity. An interesting observation is that, for each resin, the pH at which the uptake goes to zero is approximately the same for lactic and succinic acids. The order of choice for sustaining capacity with increasing pH is Amberlite IRA-910 > Reillex HPQ > Bio-Rad AG3-X4 > Amberlite IRA-35 > Dowex MWA-1 > Duolite A7 > Reillex 425. This order is consistent with the results for lactic acid and, in general, reflects the relative basicities of the resins. The results again indicate that Duolite A7 is a relatively weak base, and they also confirm that Amberlite IRA-910 is a much stronger base than IRA-35. The one unexpected result is that Bio-Rad AG3-X4, which was predicted to be a slightly weaker base than Dowex MWA-1, sustains capacity to higher values of pH. The sustained capacity of this resin is, in part, due to the 10% quaternary groups, which were ignored in earlier analyses of basicity but account for up to 0.1 g acid/g sorbent of uptake. If the uptake curve for AG3-X4 is shifted downward by this amount, it falls very close to the curve for Dowex MWA-1.

Uptakes of succinic acid, at an equilibrium acid concentration of 1.0 wt.%, are presented for six of the sorbents in Figure 3-43. For Bio-Rad AG3-X4, Dowex MWA-1 and Amberlite IRA-910, the competitive Langmuir model was used in the calculation. A curve

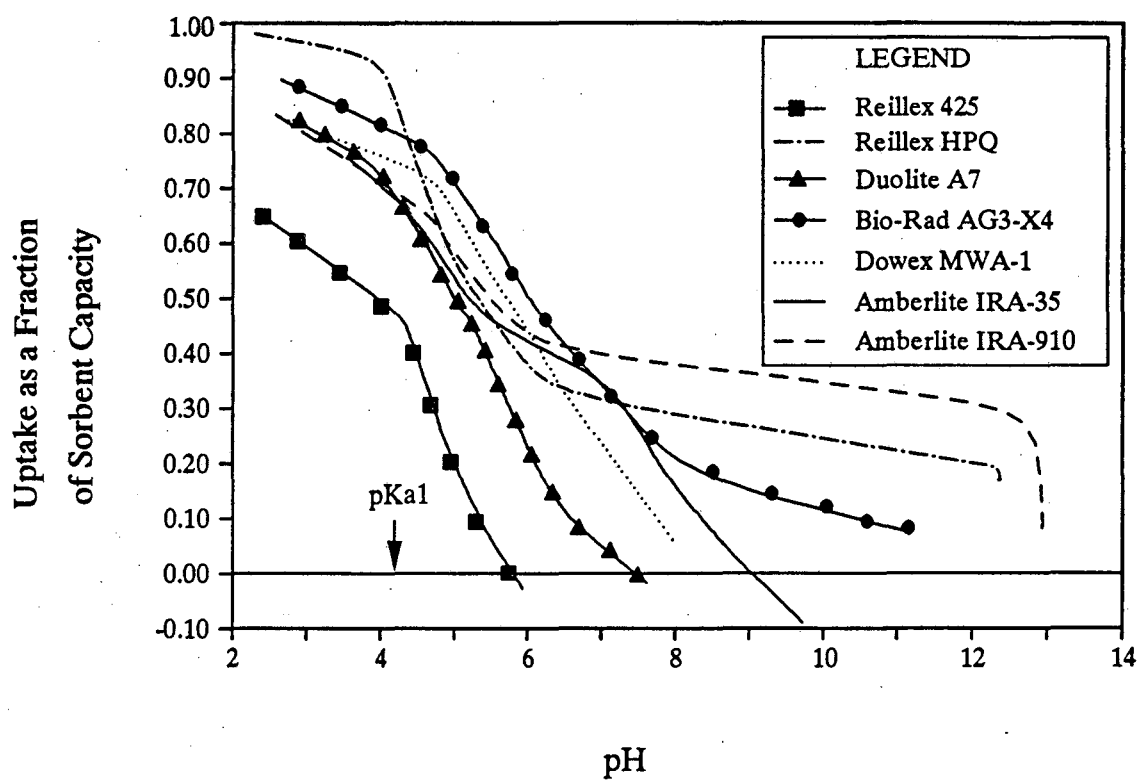


Figure 3-42. Effect of pH on Normalized Uptakes of Succinic Acid
 $Ca_i = 0.45 \text{ M}$, $W_o/m = 11.0$

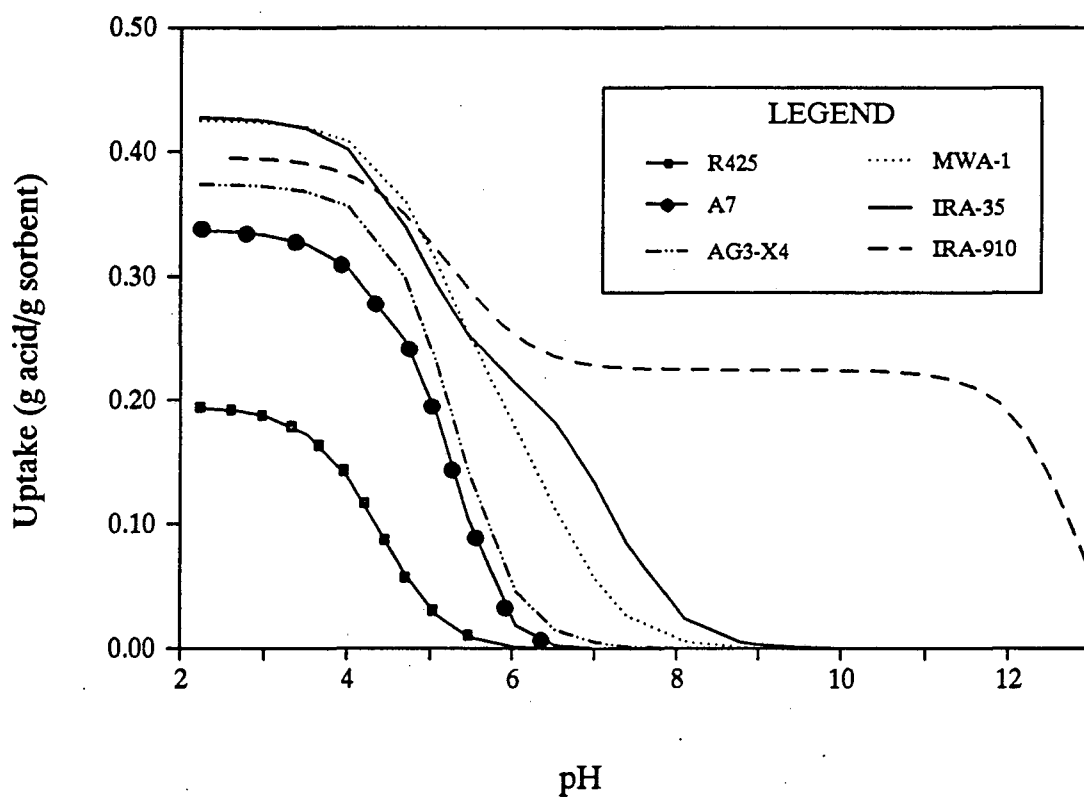


Figure 3-43. Effect of pH on Uptakes of Succinic Acid at Equilibrium Solution Concentration of 1.0 wt. %

for Reillex HPQ is not presented since no appropriate model was developed for this sorbent. Again, other graphs are easily generated for other equilibrium solution concentrations.

3.4.3 Summary

The results for lactic and succinic acids confirm the original hypothesis: Sorbent performance at $\text{pH} > \text{pK}_a$ is dependent upon sorbent basicity. Overall, based on uptake characteristics alone, Bio-Rad AG3-X4, Dowex MWA-1, Amberlite IRA-35, or Amberlite IRA-910 would be excellent for use in a fermentation process. Reillex HPQ has reasonable uptake characteristics but is not a good candidate for use in a fermentation because conversion to the OH^- form results in a loss of capacity.

3.5 TMA Leaching Curves

Sorbent regenerabilities were tested through simple batch equilibrium experiments in which sorbent samples were fully loaded with lactic or succinic acid and then leached with aqueous solutions of TMA of varying concentrations. In this manner, the fractional recovery of the acid was determined as a function of the moles of TMA per mole of acid present in the system.

3.5.1 Modeling of the Leaching Curve

The leaching of the acid from the sorbent phase into an aqueous solution of trimethylamine is described by a set of chemical equilibrium and mass balance equations. The chemical equilibria consist of acid-base equilibria, which describe the dissociation of the carboxylic acid, trimethylammonium, and water; an aqueous-phase charge balance; and the sorption isotherm, which describes the transfer of the acid between the aqueous and sorbent phases. The dissociation of the acid is described by Equation 3-21 for a monocarboxylic acid, and Equations 3-24 and 3-25 for a dicarboxylic acid. The dissociation of water and TMA are represented by Equations 3-32 and 3-33.

$$K_w = [H^+][OH^-] \quad (3-32)$$

$$K_{a,b} = \frac{[TMA][H^+]}{[TMAH^+]} \quad (3-33)$$

The aqueous-phase charge balance is given by Equations 3-34 for a monocarboxylic acid and 3-35 for a dicarboxylic acid.

$$[H^+] + [TMAH^+] = [OH^-] + [A^-] \quad (3-34)$$

$$[H^+] + [TMAH^+] = 2[A^{2-}] + [HA^-] + [OH^-] \quad (3-35)$$

Finally, the sorption isotherm is given by Equation 3-22 for a monocarboxylic acid, Equation 3-26 for a dicarboxylic acid with an unquaternized sorbent, and Equations 3-28, 3-30, and 3-31 for a dicarboxylic acid with a quaternized sorbent.

A mass balance on the acid can be written as:

$$q_{init} - q - \frac{[H_2A] * ASR * MW}{\alpha} = 0 \quad (3-36)$$

where q_{init} is the individual uptake of acid (g acid/g sorbent) during the loading phase, ASR is the aqueous/sorbent phase ratio in g/l, MW is the molecular weight of the acid, and α is given by:

$$\alpha = \frac{1}{1 + \frac{K_{a1}}{[H^+]} + \frac{K_{a1} K_{a2}}{[H^+]^2}} \quad (3-37)$$

For a monocarboxylic acid, K_{a2} is set to 0.

A mass balance on the TMA is needed to complete the model. The balance can be written as:

$$[TMA]_{tot} = \frac{[TMAH^+]}{\beta} \quad (3-38)$$

where $[TMA]_{tot}$ is the total concentration of TMA, in all forms, and β is given by:

$$\beta = \frac{1}{1 + \frac{K_{a,b}}{[H^+]}} \quad (3-39)$$

The above set of equations was solved simultaneously at different pH values to develop a plot of percent acid recovery versus the molar ratio of TMA to acid. The pH was set, and the following equations were solved simultaneously using an iterative procedure -- the equations describing the dissociation of the acid (Equation 3-21 for a monocarboxylic acid, Equation 3-24 and 3-25 for a dicarboxylic acid), the sorption isotherms (Equation 3-22 for a monocarboxylic acid, Equation 3-26 or Equations 3-28, 3-30, and 3-31 for a dicarboxylic acid) and the mass balance on the acid (Equation 3-36). The recovery of acid could then be calculated as:

$$Recovery = \frac{ASR * MW * [H_2A]}{q_{init} \alpha} \quad (3-40)$$

The concentration of TMA corresponding to this pH was then calculated from the dissociation constants for water (Equation 3-32) and TMA (Equation 3-33), the charge balance (Equation 3-34 for a monocarboxylic acid, Equation 3-35 for a dicarboxylic acid), and the mass balance on TMA (Equations 3-38 and 3-39). The molar ratio of TMA to total acid is then given by:

$$\frac{mols \ TMA}{mols \ acid} = \frac{ASR [TMA]_{tot} MW}{q_{init}} \quad (3-41)$$

3.5.2 Results and Discussion

3.5.2.1 Lactic Acid

Figures 3-44 through 3-48 present the experimental data for the leaching of lactic acid from the five sorbents studied into aqueous solutions of TMA at 25 °C. The sorbents were typically fully loaded before the leaching step, and the aqueous/sorbent phase ratio was generally 0.014-0.015 l/g.

For Reillex 425, Duolite A7, and Dowex MWA-1 (Figures 3-44 through 3-46), essentially complete recovery of the acid is achieved when one mole of TMA is present for every mole of acid. These results indicate that the ionized, aqueous TMA is a much stronger base than any of these three sorbents.

For Amberlite IRA-35 (Figure 3-47), slightly greater than a stoichiometric amount of TMA is required for full regeneration. Essentially 100% recovery is achieved when the molar ratio of TMA to acid is equal to 1.45. The fact that regeneration of IRA-35 is more difficult reflects its greater basicity, which apparently approaches that of TMA.

The strongest base, Amberlite IRA-910, proved to be unregenerable by leaching with aqueous TMA. As shown in Figure 3-48, only about 27 percent recovery of the acid was achieved, even with 2.5 moles TMA per mole of acid. This recovery is only slightly better than that achieved by leaching with pure water. These results indicate that IRA-910, a fully ionized strong-base ion exchanger, is a much stronger base than aqueous TMA.

The solid curves in Figures 3-44 through 3-48 are theoretical curves calculated as described in Section 3.5.1. For Amberlite IRA-910, a value of K equal to 1.5×10^{10} was used, as in the pH model. Except in the case of Amberlite IRA-910, the models agree very well with the experimental data. For Amberlite IRA-910, the model predicts a constant recovery of about 18 percent throughout the range of TMA concentrations studied. The lower predicted recoveries are a direct consequence of the lack of fit of the pH model to the uptake-pH curve in the pH 10 to 12 range.

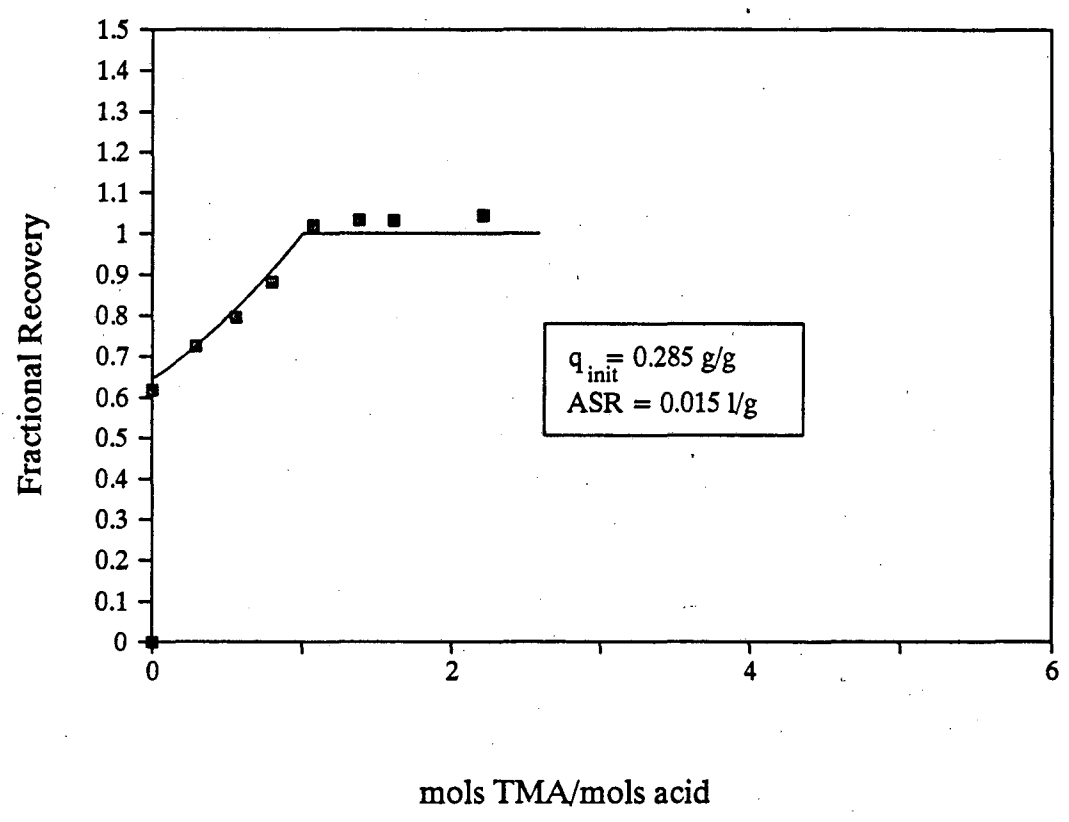


Figure 3-44. Leaching of Lactic Acid from Reillex 425 into Aqueous Solutions of Varying TMA Concentration

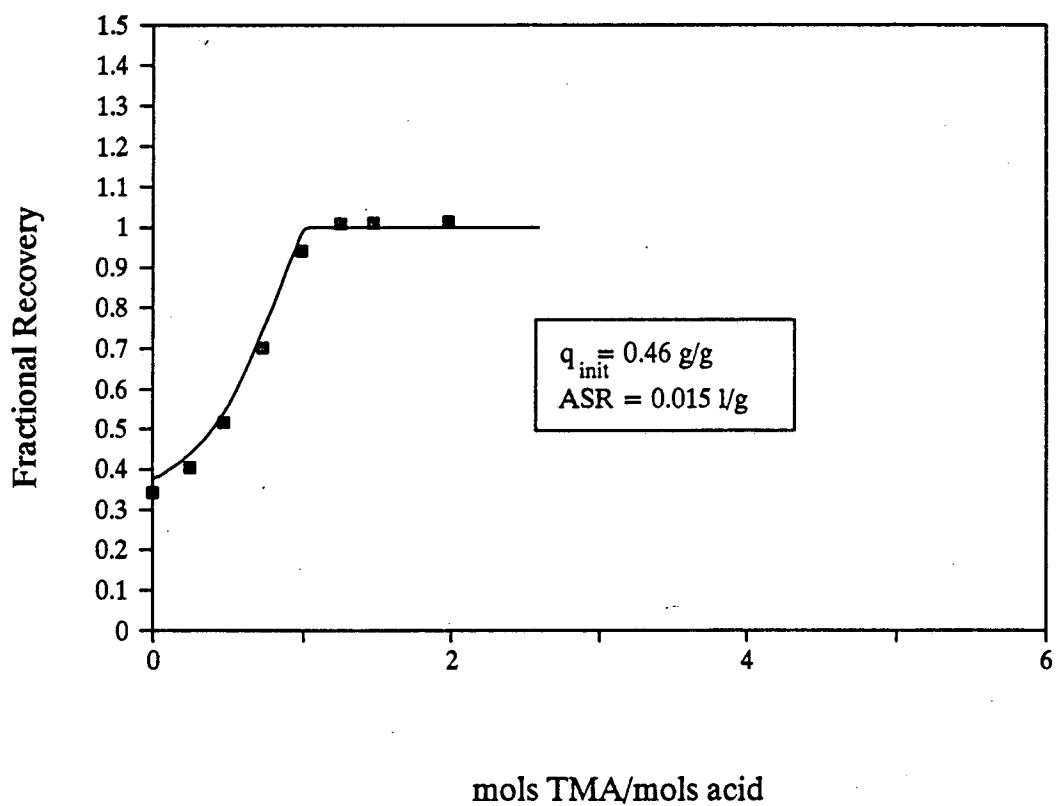


Figure 3-45. Leaching of Lactic Acid from Duolite A7 into Aqueous Solutions of Varying TMA Concentration

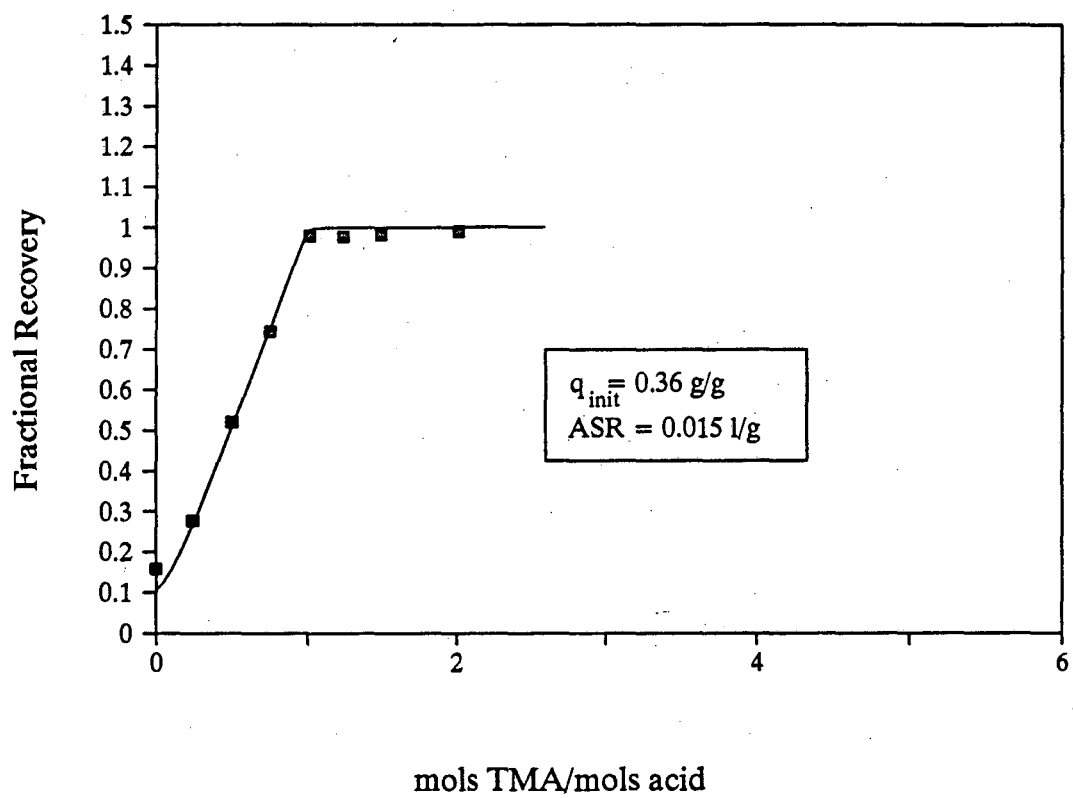


Figure 3-46. Leaching of Lactic Acid from Dowex MWA-1 into Aqueous Solutions of Varying TMA Concentration

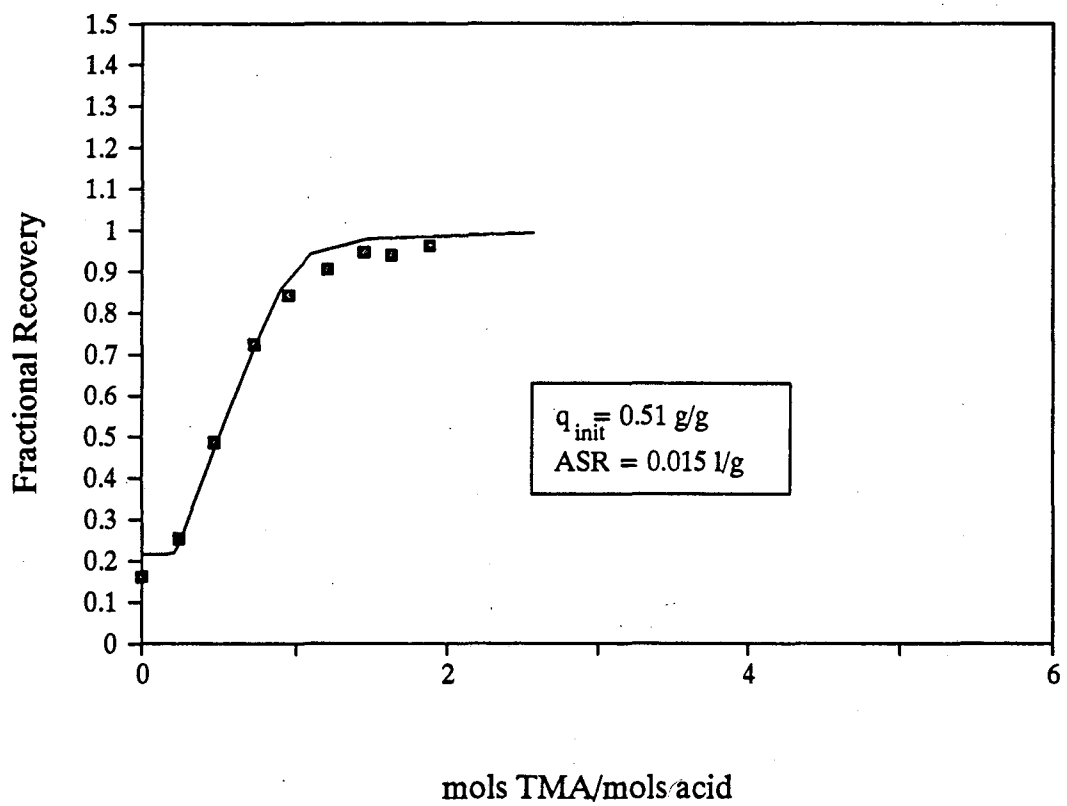


Figure 3-47. Leaching of Lactic Acid from Amberlite IRA-35 into Aqueous Solutions of Varying TMA Concentration

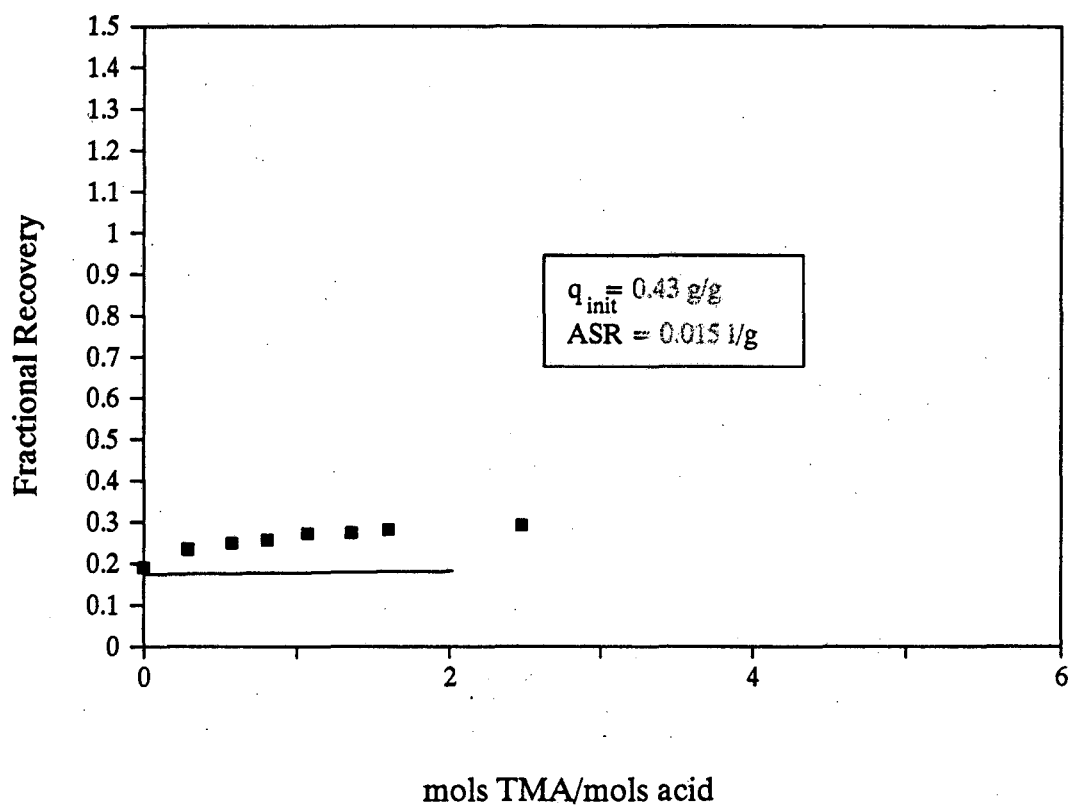


Figure 3-48. Leaching of Lactic Acid from Amberlite IRA-910 into Aqueous Solutions of Varying TMA Concentration

Note that the basicity of the sorbent, and hence its regenerability, is reflected in the fractional recovery at 0 mols TMA/mol acid, corresponding to leaching with pure water. For Reillex 425, leaching with water gives about a 60% recovery of the acid, compared with an 18% recovery for Amberlite IRA-910. This point thus provides a quick visual check of leachability.

3.5.2.2 Succinic Acid

Figures 3-49 through 3-55 present the experimental data for the leaching of succinic acid into aqueous solutions of TMA at 25 °C. The sorbents were again fully loaded before the leaching step, and the aqueous/sorbent phase ratio was generally 0.013-0.016 l/g. For Reillex HPQ, the aqueous/sorbent ratio was 0.025 l/g.

For Reillex 425, Duolite A7, and Dowex MWA-1 (Figures 3-49 through 3-51), essentially complete recovery of the acid is achieved when two moles of TMA are present for every mole of acid. The leaching is stoichiometric, since two moles of TMA are needed to complex with each mole of succinic acid, a di-acid. Again, the results reflect the strong basicity of aqueous TMA.

Reillex 425 was also found to be regenerable by leaching with methanol. Sorbent samples were loaded with approximately 0.4 g succinic acid/g dry resin and leached with 20-30 ml methanol per g dry resin. The recoveries, shown in Table 3-10, range from 89 to 101%. The efficiency of the regeneration would be expected to improve greatly if performed in fixed-bed mode. Therefore, if Reillex 425 could be used in an application wherein a lower pH is required, it could be regenerated by methanol leaching.

For Amberlite IRA-35 (Figure 3-52), essentially 100% recovery is achieved when the molar ratio of TMA to acid is equal to 2.75. As with lactic acid, a slightly greater than stoichiometric amount of TMA is required to regenerate IRA-35 due to its higher basicity. The amount of TMA required is slightly less than twice the amount required to regenerate

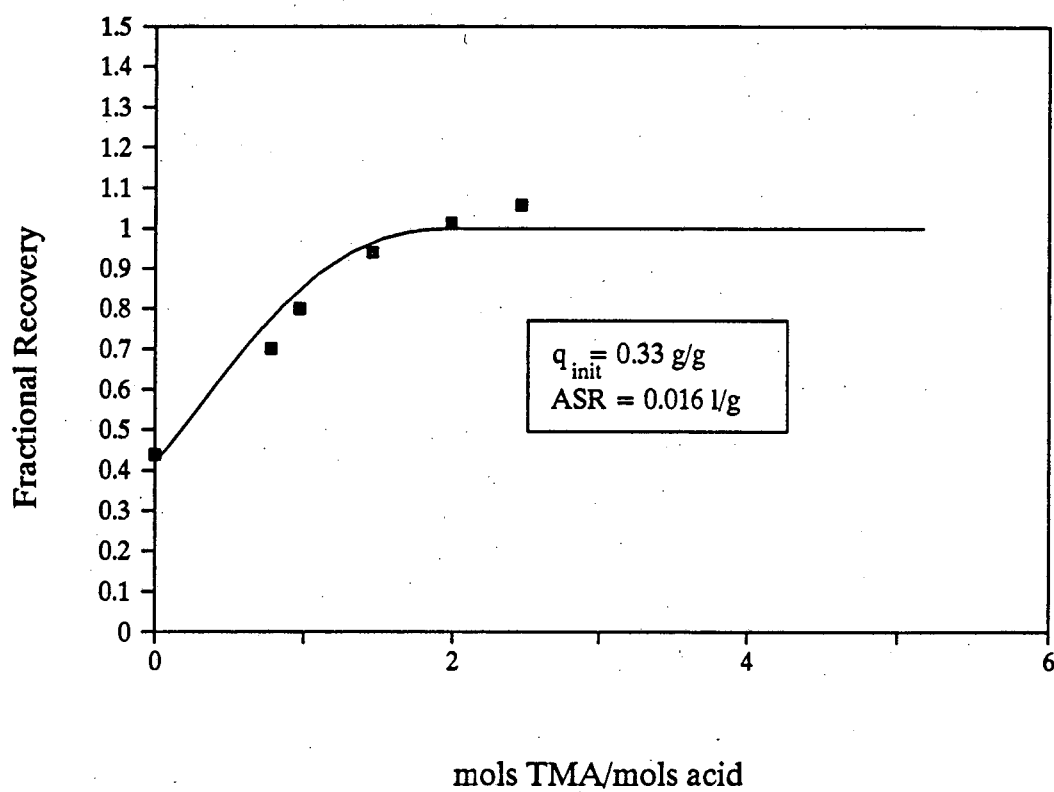


Figure 3-49. Leaching of Succinic Acid from Reillex 425 into Aqueous Solutions of Varying TMA Concentration

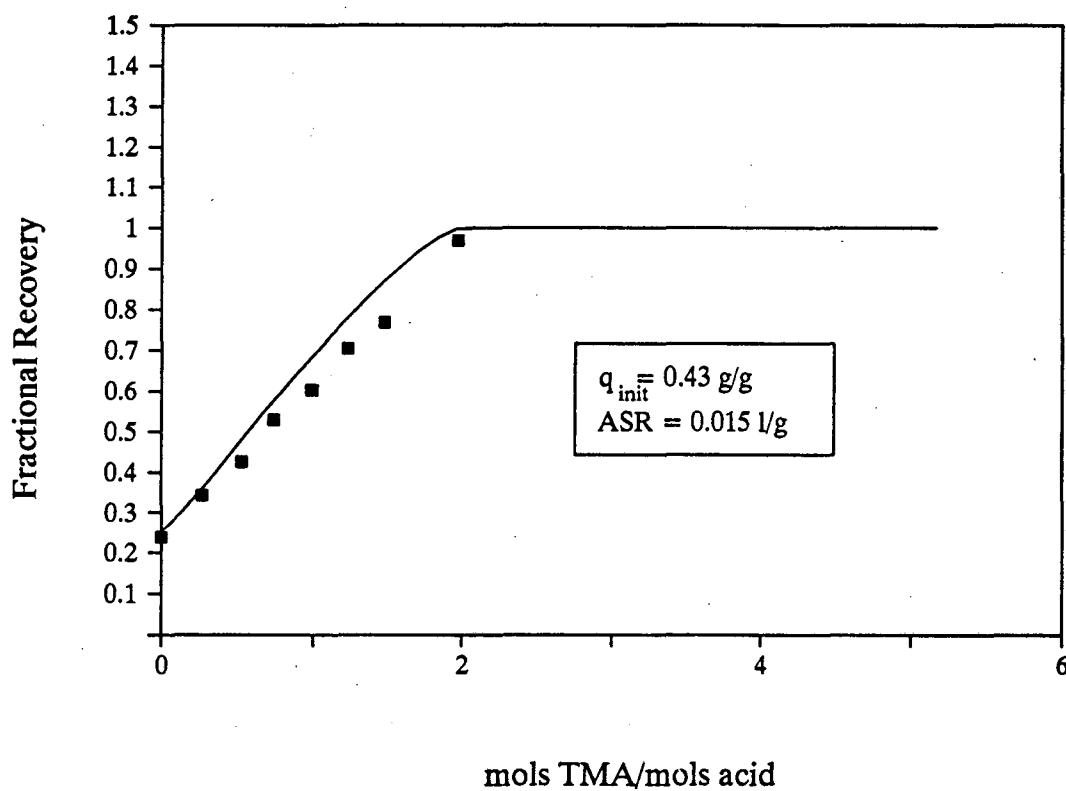


Figure 3-50. Leaching of Succinic Acid from Duolite A7 into Aqueous Solutions of Varying TMA Concentration

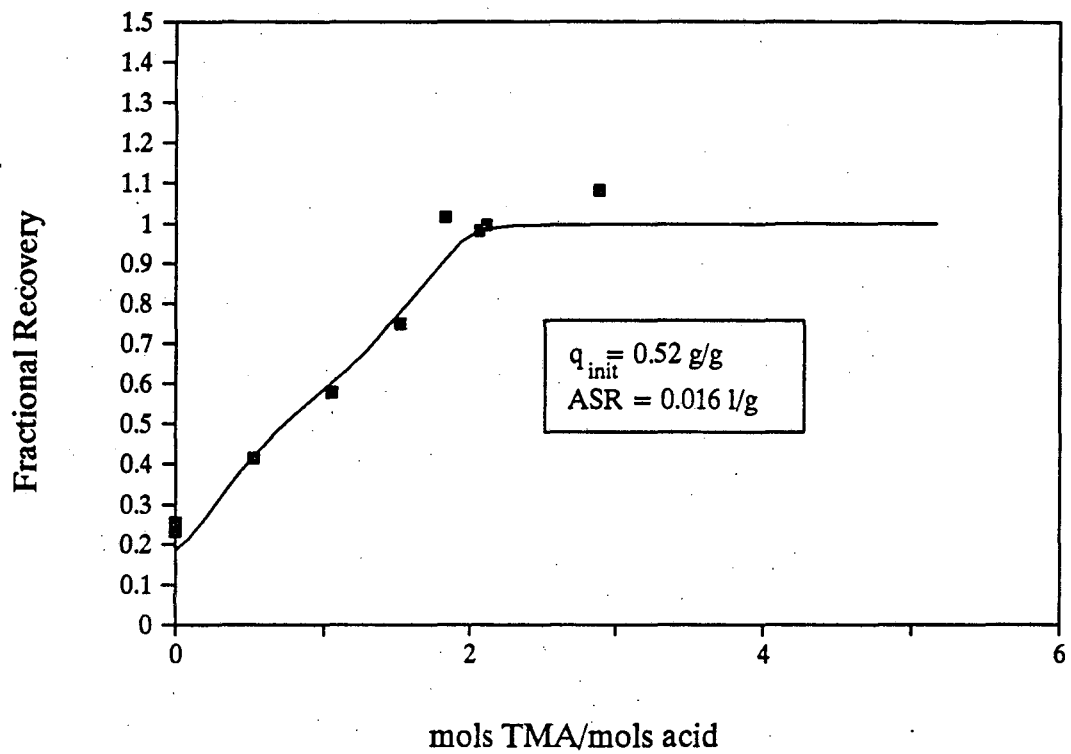


Figure 3-51. Leaching of Succinic Acid from Dowex MWA-1 into Aqueous Solutions of Varying TMA Concentration

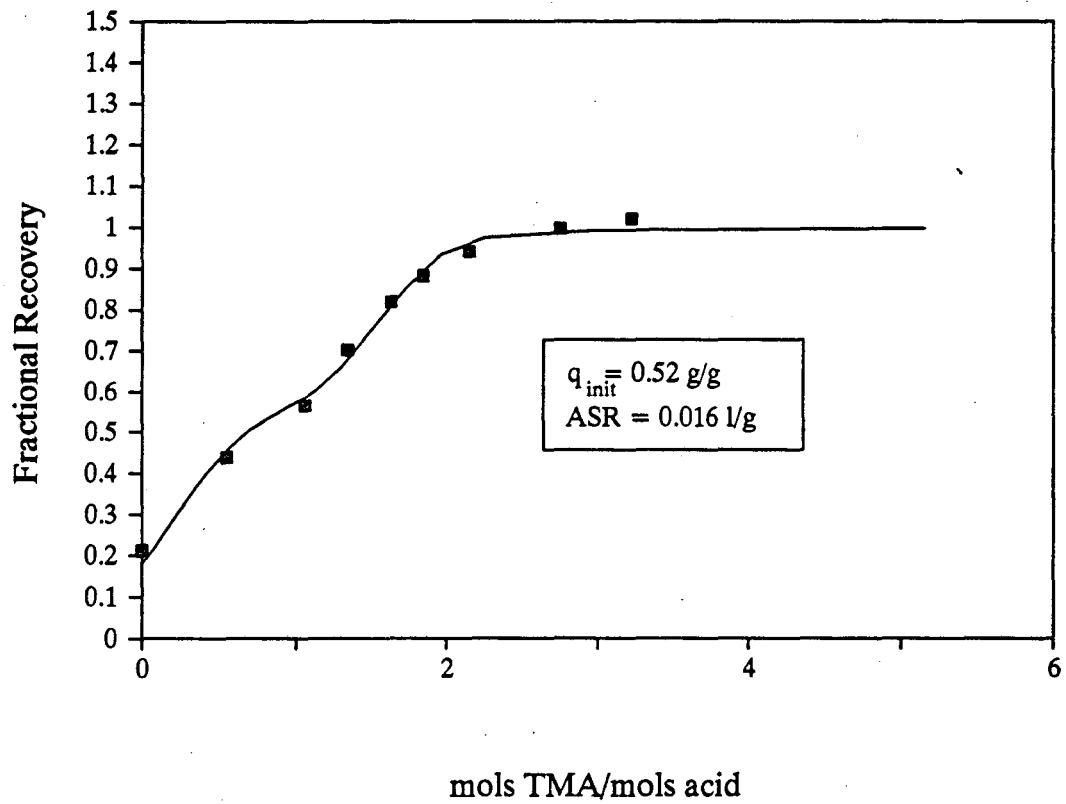


Figure 3-52. Leaching of Succinic Acid from Amberlite IRA-35 into Aqueous Solutions of Varying TMA Concentration

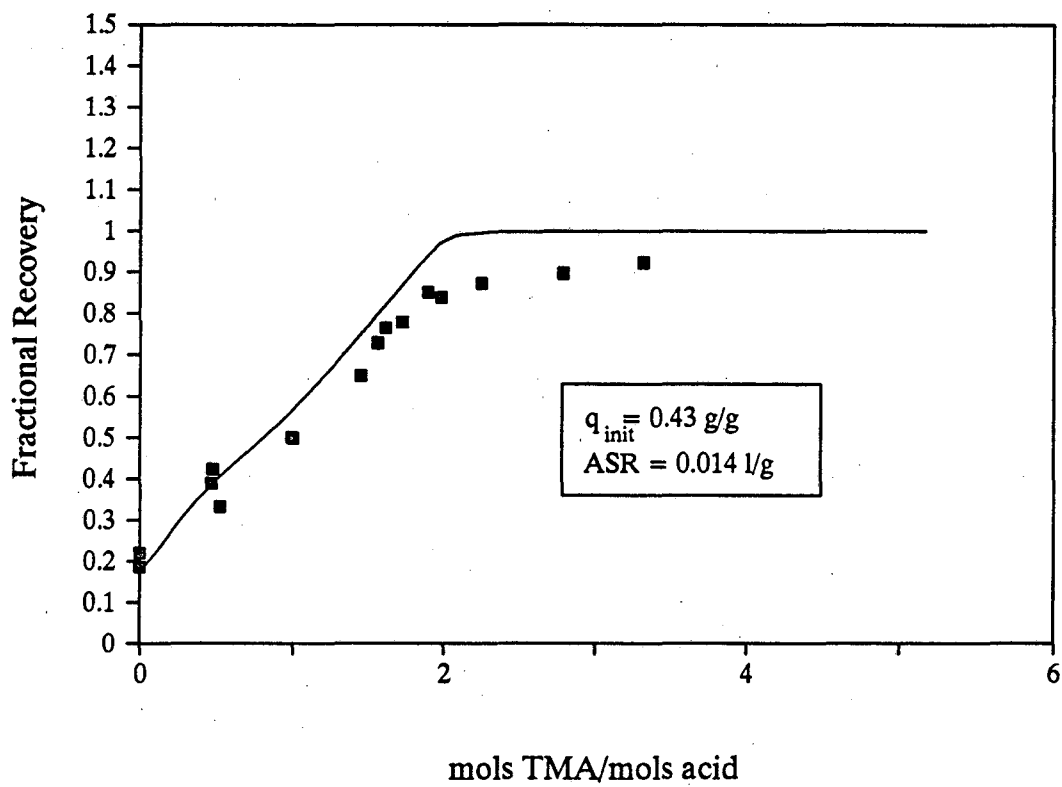


Figure 3-53. Leaching of Succinic Acid from Bio-Rad AG3-X4 into Aqueous Solutions of Varying TMA Concentration

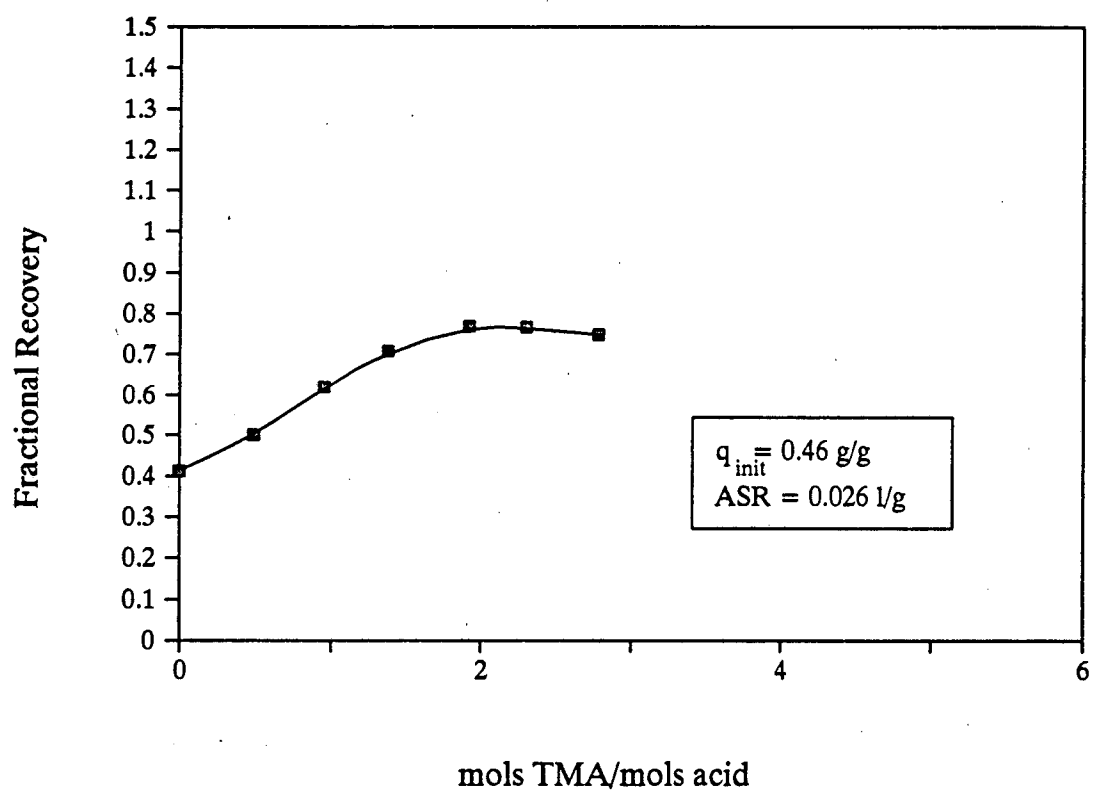


Figure 3-54. Leaching of Succinic Acid from Reillex HPQ into Aqueous Solutions of Varying TMA Concentration

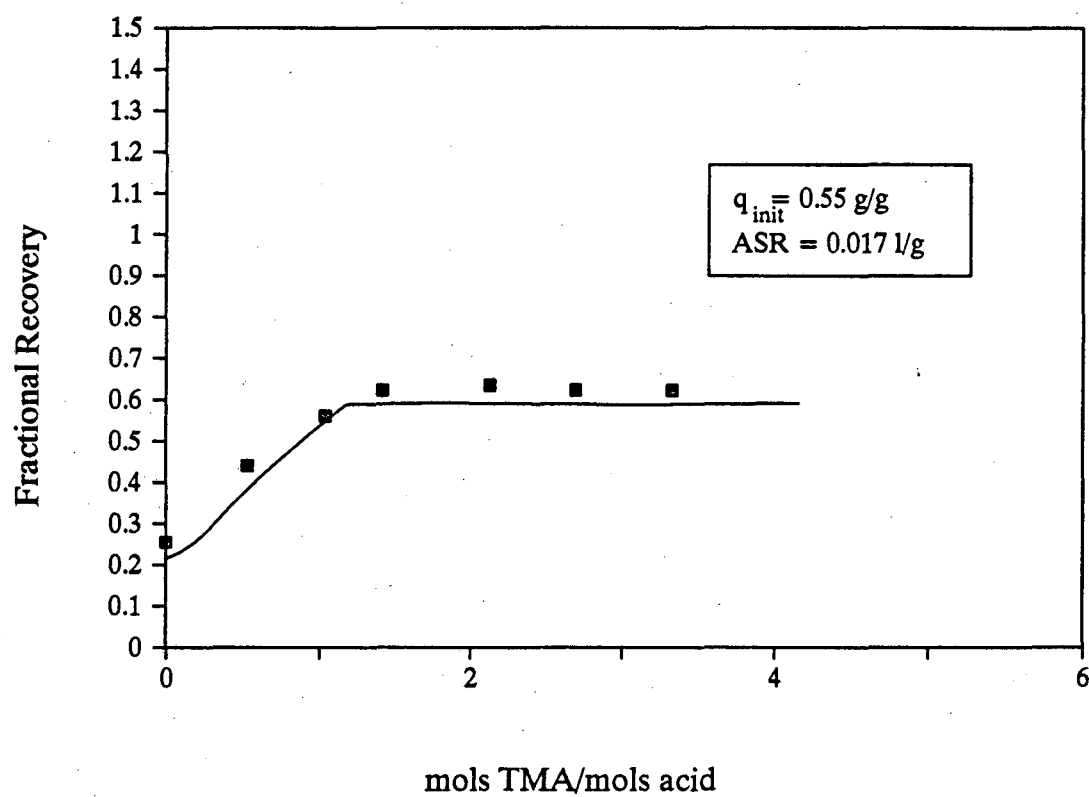


Figure 3-55. Leaching of Succinic Acid from Amberlite IRA-910 into Aqueous Solutions of Varying TMA Concentration

sorbent loaded with lactic acid, perhaps reflecting the somewhat weaker acidity of succinic versus lactic acid.

Table 3-10. Results of Leaching Succinic Acid from Reillex 425 with Methanol

Resin Loading (g acid/g dry resin)	Phase Ratio (ml MeOH/g dry resin)	% Recovery of Acid
0.46	20.7	89
0.43	25.2	92
0.40	22.7	96
0.43	27.1	101

The remaining three resins are not completely regenerable by leaching with TMA. Bio-Rad AG3-X4 (Figure 3-53) is completely regenerable at a molar ratio of TMA to acid of slightly greater than 2, except for about 8 percent of the acid, which is presumably held by the strong-base sites. Reillex HPQ (Figure 3-54) is approximately 75% regenerable when the molar ratio of TMA to acid is 2 or greater. Presumably, acid is effectively leached from the weak-base sites, and some acid is leached from the strong-base sites through the reaction shown in Figure 3-24. That is, as the pH is raised, the resin converts from the bisuccinate to the succinate form. Amberlite IRA-910 (Figure 3-55) is about 62% regenerable when approximately 1.5 moles of TMA are present for every mole of acid. This percent recovery is again consistent with conversion from the bisuccinate to succinate form. The results for these three resins indicate that fully ionized strong-base ion exchange sites are too strongly basic to be fully regenerated by leaching with aqueous TMA. However, conversion from the bicarboxylate to the carboxylate form results in partial regeneration.

The solid curves in Figures 3-49 through 3-55 are theoretical curves calculated as described in Section 3.5.1. However, the leaching curve for Reillex HPQ was not modelled for reasons stated earlier. For Bio-Rad AG3-X4, Dowex MWA-1 and Amberlite IRA-35, the

competitive Langmuir, rather than the Freundlich, isotherm was used. In general, the models agree very well with the experimental data. The model for Bio-Rad AG3-X4 does not account for the presence of 10% strong-base groups on the resin, and hence predicts 100% regenerability. The model for Amberlite IRA-910, however, does account for the strong base groups and gives an excellent representation of the data.

3.5.3 Summary

Overall, the two tertiary amine sorbents, MWA-1 and Amberlite IRA-35, are best suited for use with a fermentation system, as they show excellent capacity at moderate pH and are fully regenerable by leaching with TMA. Bio-Rad AG3-X4 could also be used, but the 10% quaternary ammonium groups are not fully regenerable, and hence it would make more sense to use a similar epoxy-amine resin which is unquaternized.

Very weak base resins like Reillex 425 are not effective in the pH range of interest but may be used at low values of pH. Their advantage is that they are easily regenerable, for instance, by leaching with methanol.

For lactic acid, it is not desirable to use a strong-base ion exchanger like Amberlite IRA-910 because these resins are not regenerable by TMA leaching. However, for di-acids like succinic, it may be possible to use these resins if advantage is taken of the conversion from the dicarboxylate to the carboxylate form at high pH.

3.6 Discussion of Sorbents Not Studied

It is useful to consider how other sorbents, not studied in this work, would perform at $\text{pH} > \text{pK}_a$. Other commercially available resins contain amide, N-oxide and benzimidazole functionalities. Amides are very weak bases (67) and the corresponding polyacrylamide resins are expected to sorb acid much less strongly than polyvinylpyridine. The results of Garcia and King (22) show experimentally that the K value for uptake of acetic acid by

polyacrylamide is about an order of magnitude less than the corresponding K values for several polyvinylpyridine resins.

Poly(N-oxide) is another very weak base. It is meaningless to speak of a pK_a for resins of this type since the N-oxide group does not protonate. However, K values determined by Garcia and King for uptake of acetic acid suggest that poly(N-oxide) resins are somewhat more basic than polyvinylpyridine resins toward carboxylic acids in aqueous solutions, but much less basic than any of the amine resins.

Polybenzimidazole, which has the structure shown in Figure 3-56, has two types of nitrogen sites, one acidic and one basic. Only the basic nitrogen is expected to sorb acid molecules. The predicted pK_a for this resin is given as 5.0 by Garcia and King, which suggests that it is an even weaker base than polyvinylpyridine. However, their results for sorption of acetic acid yield a K value which is about 25% of that for Dowex MWA-1. This suggests that PBI would perform about the same as Duolite A7 at $pH > pK_a$. Chanda et al. (68) examined the sorption of formic ($pK_a = 3.75$), n-butyric ($pK_a = 4.82$), propionic ($pK_a = 4.87$) and acetic ($pK_a = 4.76$) acids by a polybenzimidazole resin. The effect of pH on the uptakes was studied up to only 0.5 pH units above the pK_a values, thus making it difficult to assess the ability of the resin to sustain capacity at $pH > pK_a$. However, there were significant decreases (up to 25%) in the uptakes even over this pH range.

Gustafson et al. (60) determined the pK of a poly[N,N-bis(2-aminoethyl)-vinylbenzene] (AEVBA) resin, the structure of which is shown in Figure 3-57. The sorbent has a wide range of functional groups but is similar to Duolite A7. The experimental pK for this resin is 6.16, placing it between Duolite A7 and Dowex MWA-1 in terms of basicity. The AEVBA resin is therefore expected to demonstrate a decreased ability to sustain capacity at $pH > pK_a$ relative to Dowex MWA-1.

Harris, et al. (69) recently synthesized two novel polyamine resins that are more highly basic than Dowex MWA-1. They investigated the extraction of gold from cyanide solutions using polyamine resins and attempted to increase capacity at high pH by increasing the pK_a

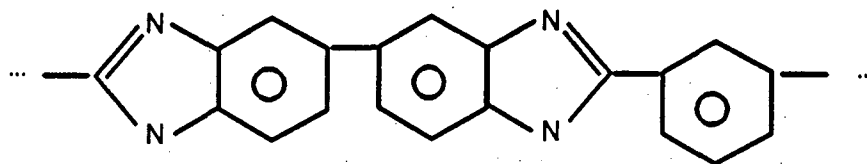


Figure 3-56. Chemical Structure of Poly(benzimidazole) Resin

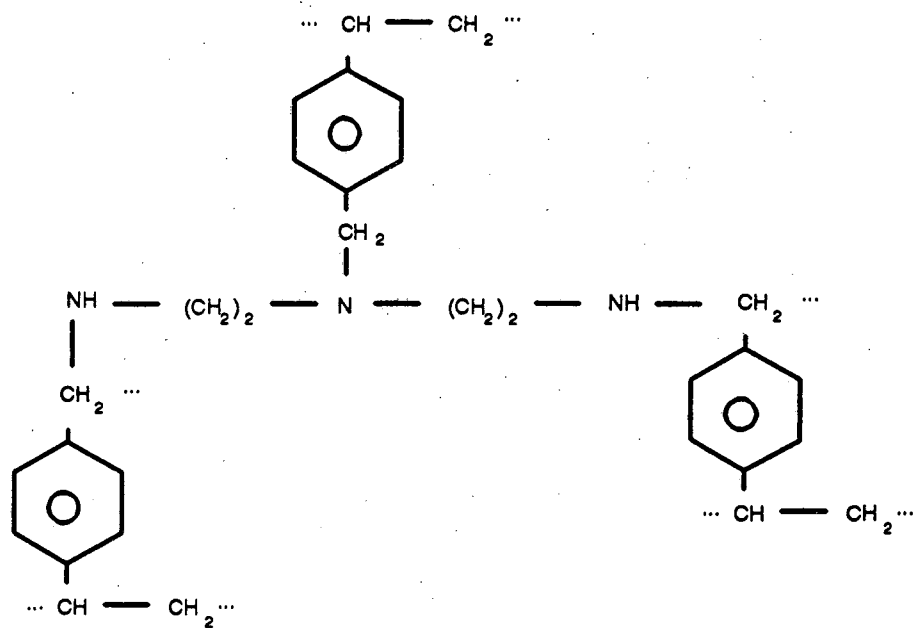
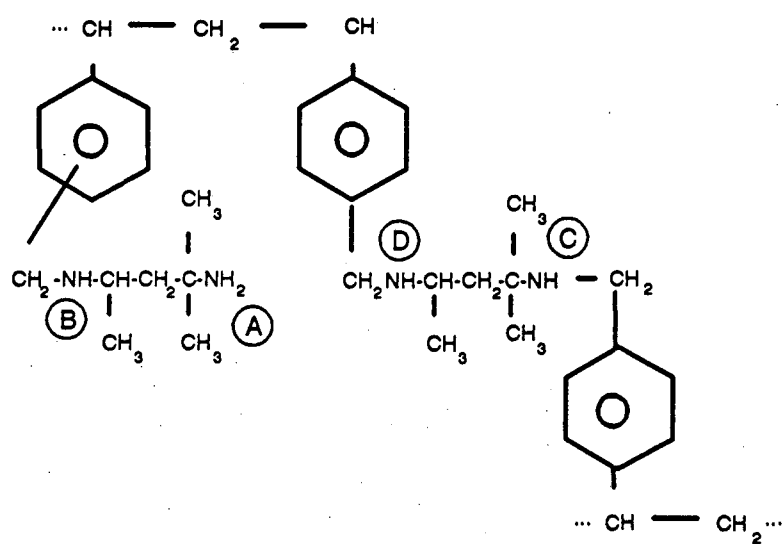


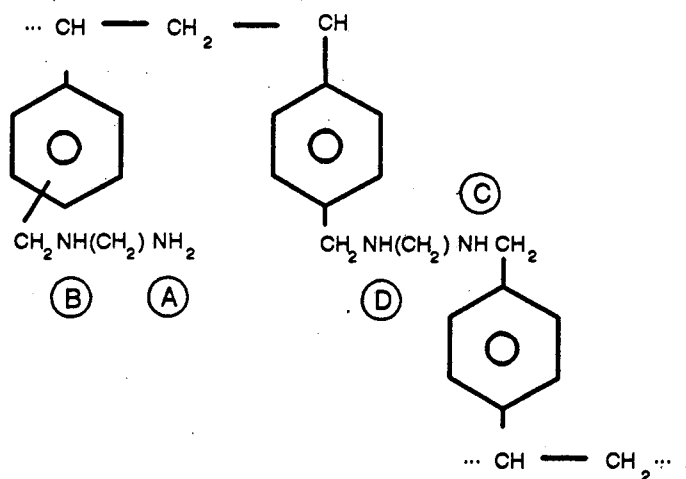
Figure 3-57. Chemical Structure of Poly [N,N - bis(2-aminoethyl) - vinylbenzylamine] Resin

of the resin. Both experimental resins were formed by aminating a macroreticular chloromethylated copolymer of styrene and divinylbenzene. The first resin (DAMP) was formed by reaction with 2,4-diamino-2-methylpentane, and the second (DAP) was formed by reaction with 1,3-diaminopropane. The resulting structures are shown in Figure 3-58. Both resins exhibit monosubstituted and disubstituted (bridged) amine forms. Therefore, at least four different types of amine groups (labelled A-D) are present.

The structures given by Harris et al. were used in the current work to calculate pK_a values for each of the amine groups using the ΔpK_a method. This calculation method results in approximately the same pK_a values for amines A through D on the DAMP resin as for the correspondingly labelled groups on the DAP resins. The calculated values are 10.4 for the primary amine group (A) and 9.4 for the secondary amine groups (B through D). These pK_a values place both resins between Dowex MWA-1 and Amberlite IRA-35 in terms of basicity. Experimentally, Harris et al. found that the DAMP resin sustains capacity for gold to pH values somewhat greater than those for DAP. Both resins perform much better than a resin similar to Dowex MWA-1. Use of a sorbent with pK_a between the values for Dowex MWA-1 and Amberlite IRA-35 is attractive because it might allow increased ability to sustain capacity at $pH > pK_a$ relative to Dowex MWA-1 but a lower flowrate of aqueous TMA in the regeneration step relative to Amberlite IRA-35. The experimental resins are therefore promising possibilities for use in a fermentation broth.



(a)



(b)

Figure 3-58. Chemical Structures of Novel Sorbents
 (a) DAMP Resin (b) DAP Resin (Harris et al. [64])

3.7 Fixed-Bed Experiments

Column experiments were performed to assess the kinetics of the adsorption and regeneration processes. All experiments were performed with Dowex MWA-1, one of the more promising sorbents for use in a fermentation system.

3.7.2 Breakthrough Curves

3.7.2.1 Background

Several researchers have examined sorption rate behavior for carboxylic acids on basic polymeric resins. Chanda et al. (68) looked at the sorption of formic, acetic, propionic and butyric acids on microporous polybenzimidazole and gel-type polyvinylpyridine resins in stirred batch experiments. The polybenzimidazole resin reached 70–85% of the equilibrium sorption within 10 seconds, whereas sorption by the polyvinylpyridine resin was somewhat slower. Stripping of the polybenzimidazole resin with NaOH removed 95% of the acid within 1 minute. Kawabata (70) looked at the breakthrough of adipic acid on resins with polyvinylpyridine, quaternary ammonium, and polyamine functional groups. Sharp breakthrough curves were observed in all cases.

Helfferich (71) discusses the uptake of acids by weak-base ion-exchange resins. For basic polymers, the rate of exchange is typically controlled by a diffusional process within the sorbent phase. Helfferich postulates a shrinking-core mechanism, whereby the resin takes up acid from the outside of the particle inward. As a strong acid is sorbed, an ionized shell builds up, limiting invasion of the co-ion (i.e., H^+) through Donnan forces. The resulting uptake of acid can be quite slow, and the exchange rate depends on the solution concentration. However, for weak monobasic or polybasic acids, rates of uptake are generally faster since diffusion of the un-ionized species is the dominant effect, and such diffusion is unaffected by Donnan forces (72).

Bhandari et al. (73) recently developed a model for the kinetics of sorption of weak acids on weak-base resins. A double layer theory which incorporates flux of both ionized and un-dissociated acid was used to describe uptakes of formic and monochloroacetic acids by amine-type resins. However, the flux of ionized acid is important only at very low solution concentrations ($< 0.05 \text{ kmol/m}^3$) and when there is significant sorption of ionized acid.

3.7.2.2 Modelling of Breakthrough Curves

The fundamental equation for modelling breakthrough curves for fixed-bed adsorption columns is given by a differential fluid phase mass balance (74):

$$\frac{\epsilon}{\rho} \frac{\partial C_a}{\partial t} + \rho_B \frac{\partial q}{\partial t} + \frac{\epsilon v}{\rho} \frac{\partial C_a}{\partial x} = 0 \quad (3-42)$$

where ϵ is the interstitial void fraction of the bed, ρ_B is the bulk density of the sorbent, C_a and q are the solute concentrations in the solution and the sorbent, respectively, and v is the average fluid velocity. Equation 3-42 assumes that the system is isothermal and that plug flow conditions are achieved. To complete the model, an expression is also needed for the rate of sorption:

$$\rho_B \frac{\partial q}{\partial t} = f(q, C_a) \quad (3-43)$$

The rate expression may be a single equation or a set of equations (e.g., diffusion equations and associated boundary conditions). Breakthrough curves (i.e., graphs of C_a vs. t for $x=L$) can be calculated from Equations 3-42 and 3-43, given the concentration of solute in the feed and the initial state of the fluid and sorbent in the bed. Ruthven (64) discusses various proposed models and their solutions. Often, the resulting equations must be solved numerically.

The constant-pattern assumption (64, 74) allows simplification of Equation 3-42 and has been used successfully with many sorption systems. For systems with favorable isotherms,

the concentration profile often reaches an asymptotic form at some distance from the entrance to the column. The length required to reach this "constant pattern" limit depends on the nature of the sorption isotherm and the kinetics of the sorption process. For highly favorable isotherms and rapid kinetics, the distance can be quite small. The advantage of the constant-pattern assumption is that Equation 3-42 can be replaced by the following simple equation:

$$\frac{C_a}{C_{a,o}} = \frac{q}{q_o} \quad (3-44)$$

where $C_{a,o}$ is the feed concentration and q_o is the sorbent-phase concentration in equilibrium with the feed.

The choice of a rate expression is the most important step in modeling a fixed-bed process. In this work, two different models are considered. In view of the discussion in Section 3.7.2.1, it makes sense to use a model in which the rate-limiting step is in the particle phase. A simple model, developed by Glueckauf and Coates (75), assumes a linear driving force in the sorbent phase:

$$\frac{\partial q}{\partial t} = k_p a (q^* - q) \quad (3-45)$$

where k_p is a particle-phase mass transfer coefficient, a is the interfacial area per unit volume of the bed, and q^* is the resin-phase concentration that would be in equilibrium with the solution phase. Solution of Equation 3-45, with the constant pattern condition and a Langmuir isotherm, results in the following expression (64):

$$k_p a (t - t_{1/2}) = \frac{1}{1-R} \ln \left(\frac{C_a}{(C_{a,o} - C_a)} \right) - \ln \left(\frac{2C_a}{C_{a,o}} \right) \quad (3-46)$$

where $t_{1/2}$ is the value of t at which $C_a = C_{a,o}/2$, and R is related to the K value from the sorption isotherm through

$$R = \frac{1}{1 + KC_{a,o}} \quad (3-47)$$

The value of $k_p a$ is roughly related to an effective diffusivity via:

$$k_p a = \frac{60D_{eff}}{d_p^2} \quad (3-48)$$

where D_{eff} is the diffusivity and d_p is the spherical particle diameter.

The linear-driving-force approximation is a crude one, since the true rate expression depends on the distribution of concentrations inside the particle, which are described by unsteady-state diffusion equations. Furthermore, the approximation becomes inadequate for highly non-linear isotherms, especially in the initial region of the breakthrough curve (64). This is a disadvantage because, in industrial operations, it is important to know the time at which breakthrough occurs. Nevertheless, the linear-driving-force model does have the advantage of being simple to use, and it allows for addition of mass-transfer resistances in the case where more than one process is rate-controlling.

A second model assumes that pore diffusion is the rate-limiting mechanism (76). In this model, it is assumed that the amount of solute held in the pores is small compared with the amount sorbed by the solid phase. The system is then described by diffusion of the solute into a porous spherical sorbent particle according to the equation:

$$\left(\frac{\partial \left(\frac{q}{q_o} \right)}{\partial t} \right)_r = \frac{D_{pore}(1-\epsilon)}{\Lambda r^2} \frac{\partial}{\partial r} \left[r^2 \left(\frac{\partial \left(\frac{C_a}{C_{a,o}} \right)}{\partial r} \right)_r \right] \quad (3-49)$$

where D_{pore} is the effective diffusivity in the pore, r is distance in the radial direction, and

$$\Lambda = \frac{q_o \rho_B}{C_{a,o}} \quad (3-50)$$

The pore diffusivity can be related to D_f , the diffusivity in the bulk liquid, by (77):

$$D_{pore} = \frac{D_f x}{2} \quad (3-51)$$

where x is the internal porosity of the sorbent particles.

In general, this problem requires a numerical solution. However, for the special case of constant-pattern conditions and an irreversible equilibrium, an analytical solution can be found. An explicit expression for $C_a/C_{a,0}$ is then given approximately by (76):

$$\frac{C_a}{C_{a,0}} \approx 1 - \left(\frac{1}{3.59}\right)^2 [2.39 - N_{pore,F} (T-1)]^2 \quad (3-52)$$

where

$$N_{pore,F} \equiv \frac{60 D_{pore} (1-e) v}{d_p^2 F} \quad (3-53)$$

and

$$T \equiv \frac{t - (ve/F)}{\Delta v/F} \quad (3-54)$$

A sorption system that follows a Langmuir isotherm with a large K value should approach the behavior of a system with an irreversible equilibrium.

3.7.2.3 Results and Discussion

Since the adsorption isotherms for Dowex MWA-1 are highly favorable, constant-pattern conditions are expected to be achieved fairly rapidly. This hypothesis was tested by generating breakthrough curves for columns of different lengths. Breakthrough curves for 5.25 wt.% succinic acid feeds and a constant flowrate of 1.5 ml/min have the same shape for

column lengths of 18 cm and 29.2 cm, as shown in Figure 3-59. Hence, constant-pattern conditions appear to hold.

The most important feature of the breakthrough curves shown in Figure 3-59 and elsewhere in this section, is that they are indeed self-sharpening due to the highly favorable sorption isotherms (high K values) for Dowex MWA-1. A self-sharpening curve is attractive, since it allows for a high fractional utilization of the column capacity.

For all of the breakthrough curves presented, the capacity of the sorbent was calculated from the area to the left of the breakthrough curve. The values obtained in this manner matched the values from the sorption isotherms within 2.5 % or less for succinic acid and within 5 % for lactic acid.

Breakthrough curves were generated for a variety of conditions, and both linear-driving-force and pore-diffusion models were fitted to the data. In fitting the linear-driving-force model, the K value from the corresponding sorption isotherm was used. For succinic acid, the weighted-average K value from Table 3-7 was used. The breakthrough curves and the corresponding fitted models are shown in Figures 3-60 through 3-64 for the linear-driving-force model and Figures 3-65 through 3-69 for the pore-diffusion model. The values of k_{pa} and D_{pore} obtained are given in Table 3-11. Values of D_{eff} , calculated from Equation 3-48 using the fitted values of k_{pa} and an average particle diameter of 0.06 cm, are also given.

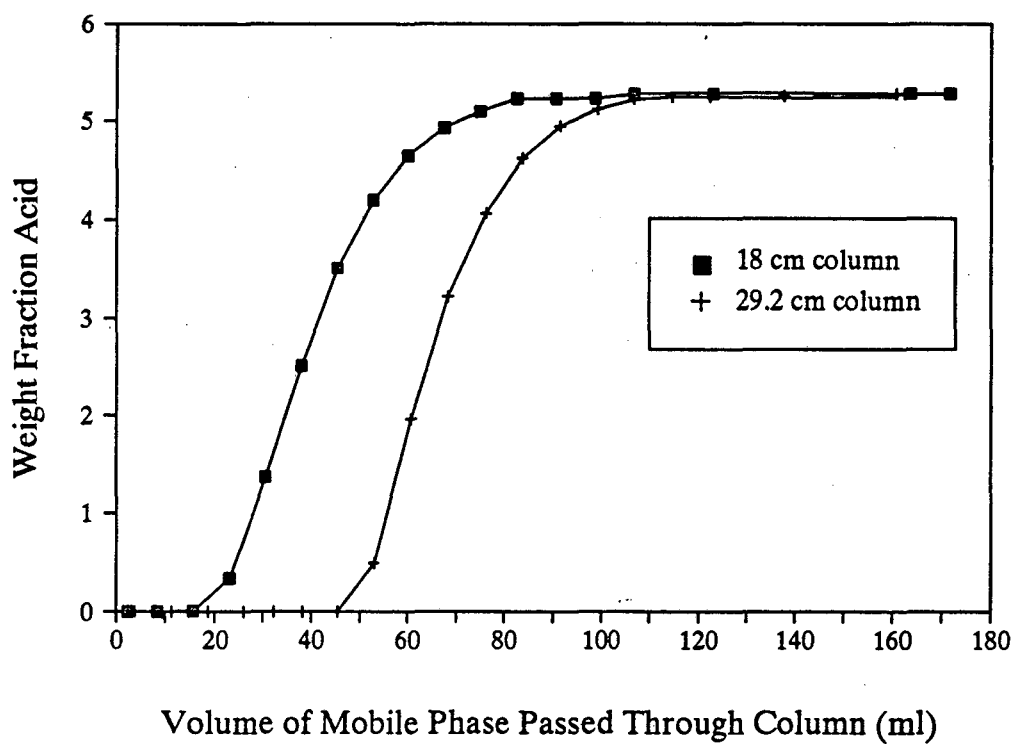


Figure 3-59. Effect of Column Length on Breakthrough of Succinic Acid on Dowex MWA-1
 $F = 1.5 \text{ ml/min}$, $\text{Ca}_0 = 5.25 \text{ wt.}\%$

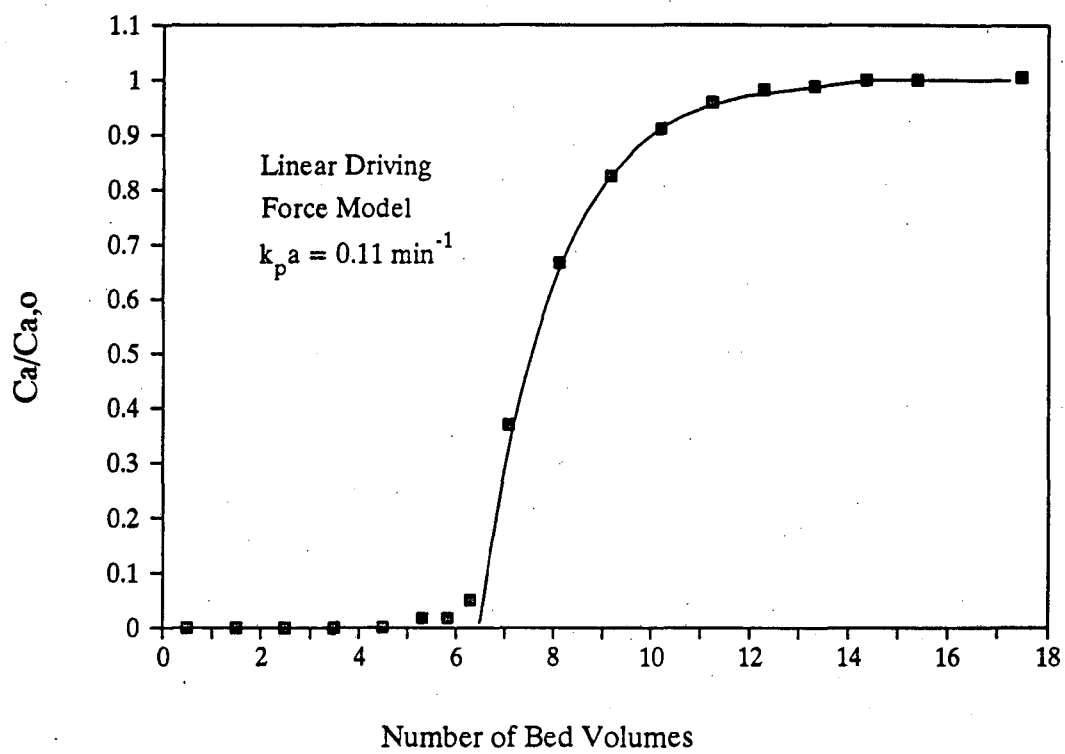


Figure 3-60. Breakthrough of Succinic Acid on Dowex MWA-1.

$F = 1.2 \text{ ml/min}$, $L = 24.5 \text{ cm}$, $\text{Ca}_0 = 5.25 \text{ wt. \%}$

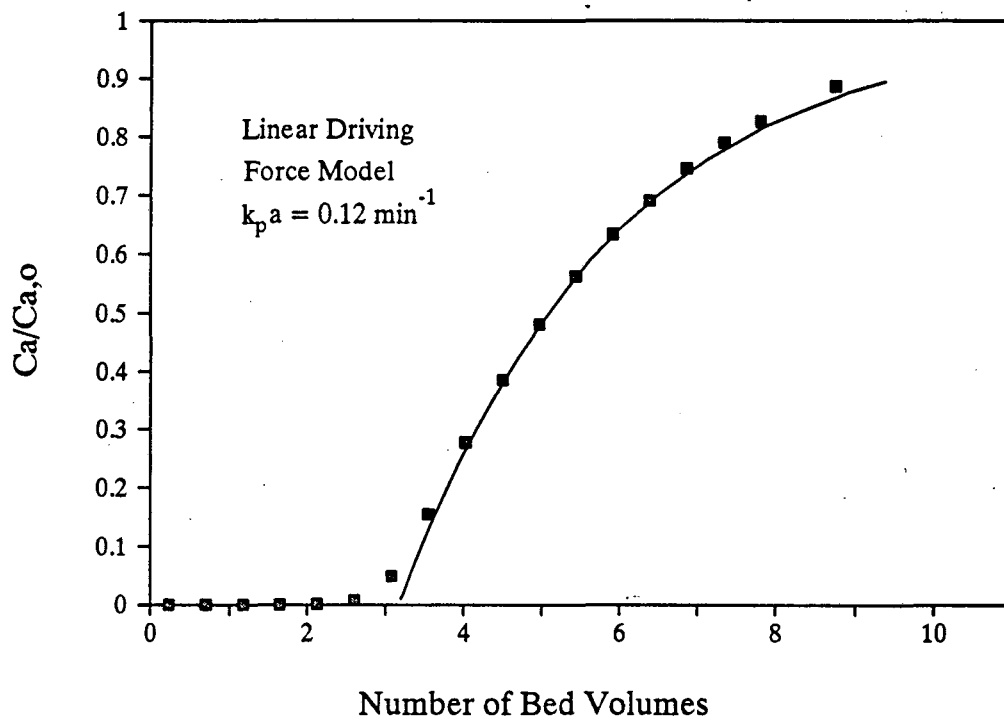


Figure 3-61. Breakthrough of Succinic Acid
on Dowex MWA-1.

$F = 3.1 \text{ ml/min}$, $L = 24.5 \text{ cm}$, $\text{Ca}_o = 5.25 \text{ wt. \%}$

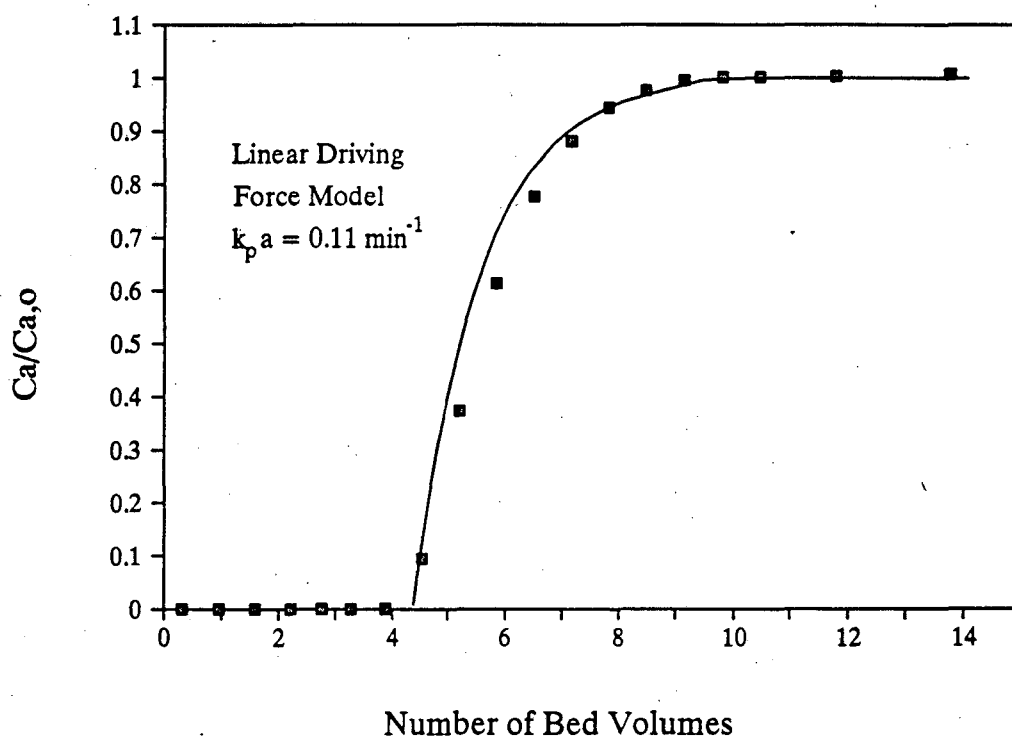


Figure 3-62. Breakthrough of Succinic Acid
on Dowex MWA-1.

$F = 1.54 \text{ ml/min}$, $L = 29.2 \text{ cm}$, $Ca_o = 5.25 \text{ wt. \%}$

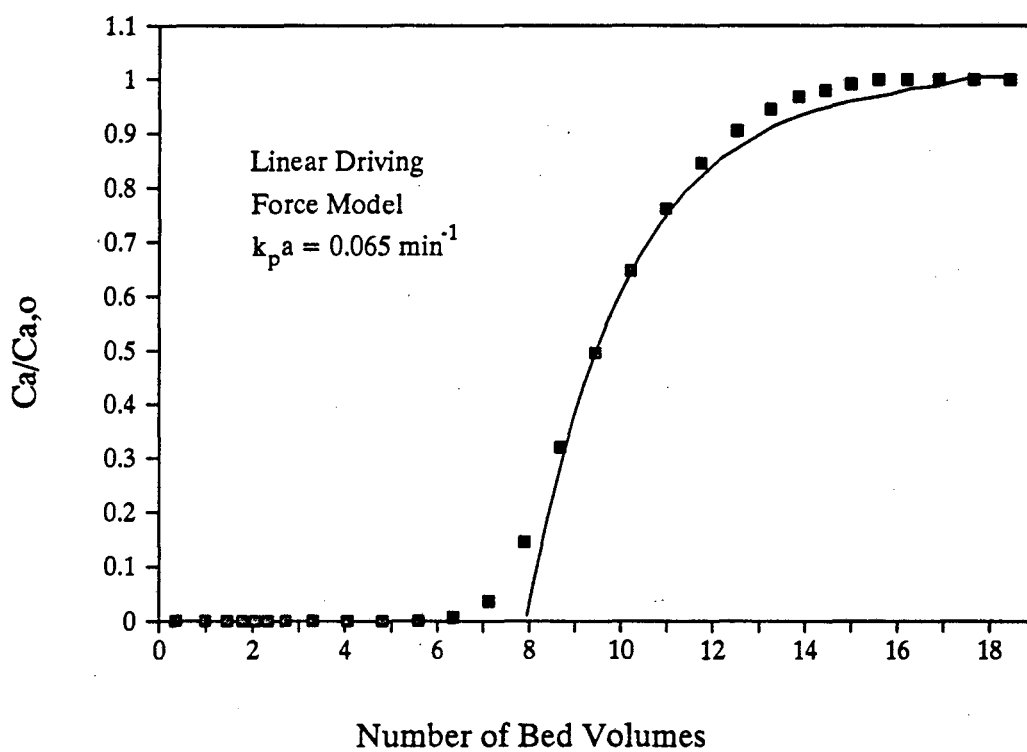


Figure 3-63. Breakthrough of Succinic Acid
on Dowex MWA-1.

$F = 1.4 \text{ ml/min}$, $L = 24.5 \text{ cm}$, $\text{Ca}_0 = 2.53 \text{ wt. \%}$

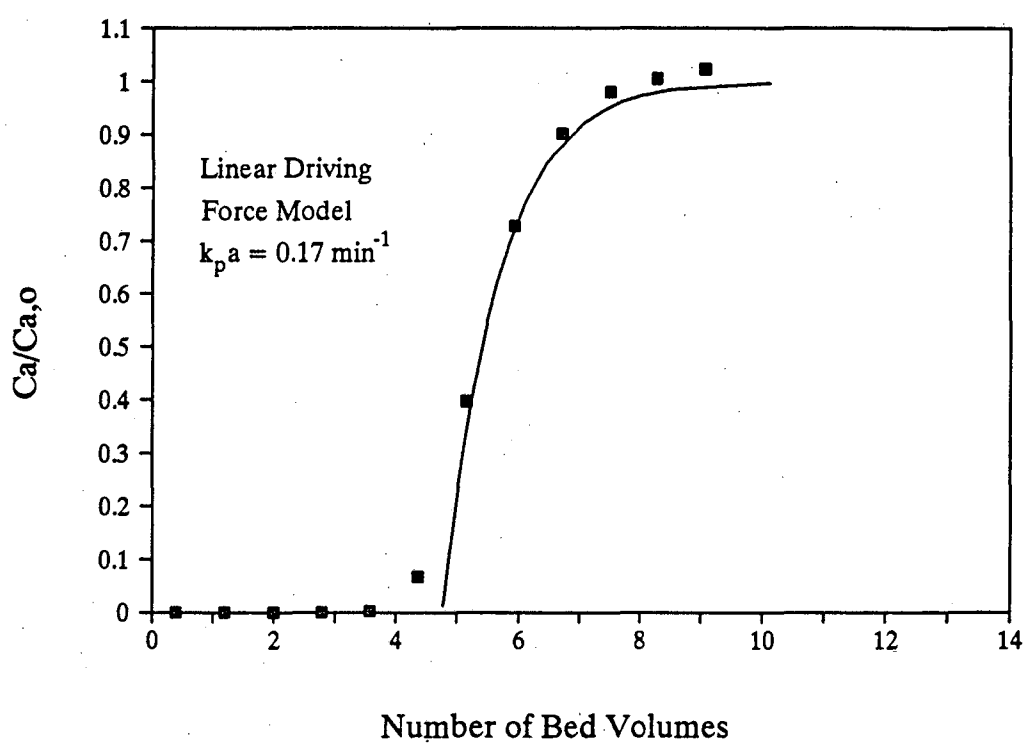


Figure 3-64. Breakthrough of Lactic Acid
on Dowex MWA-1.

$F = 1.5 \text{ ml/min}$, $L = 24.5 \text{ cm}$, $\text{Ca}_o = 4.0 \text{ wt. } \%$

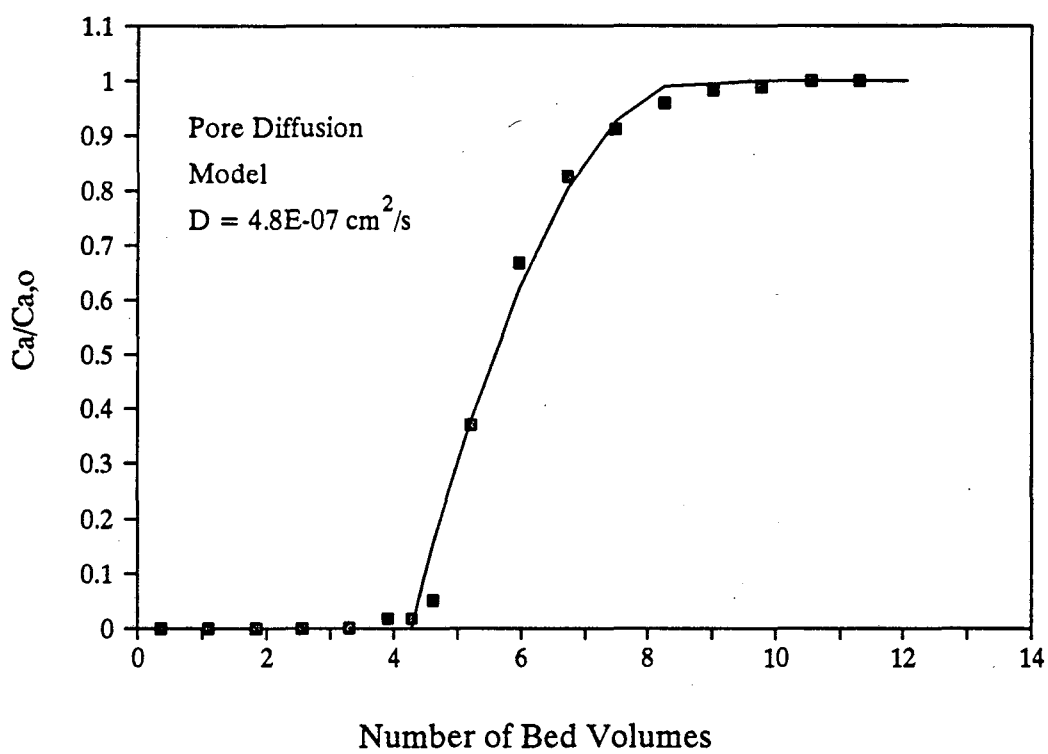


Figure 3-65. Breakthrough of Succinic Acid
on Dowex MWA-1.

$F = 1.2 \text{ ml/min}$, $L = 24.5 \text{ cm}$, $\text{Ca}_o = 5.25 \text{ wt. \%}$

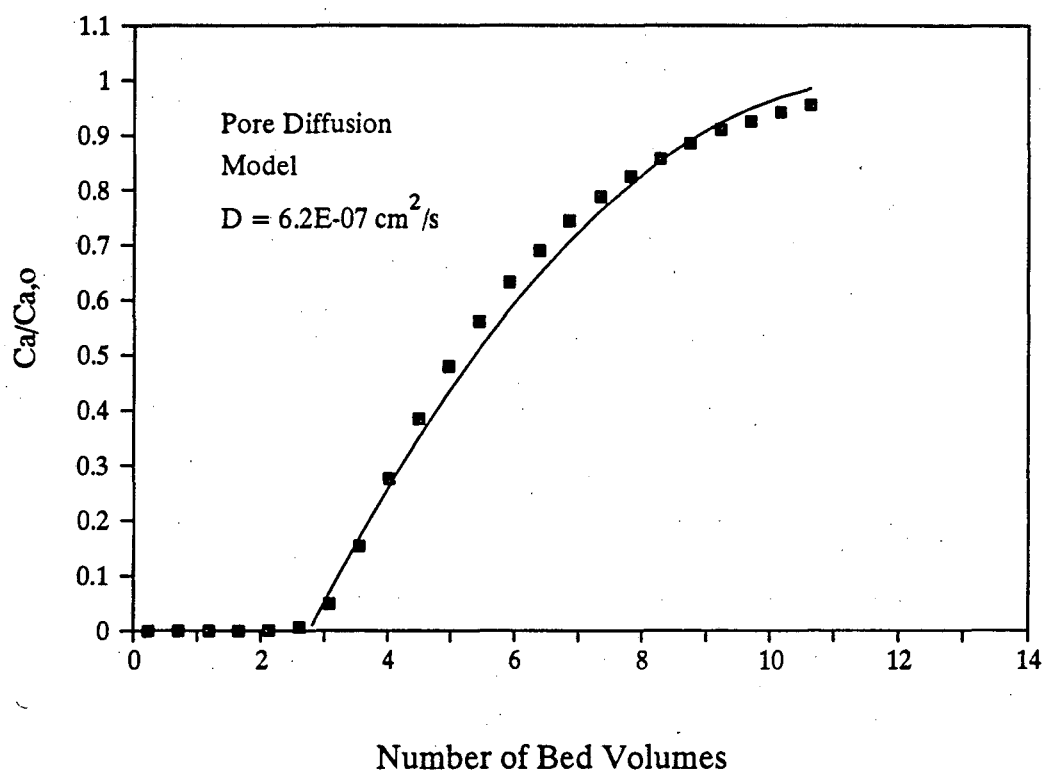


Figure 3-66. Breakthrough of Succinic Acid on Dowex MWA-1.

$F = 3.1 \text{ ml/min}$, $L = 24.5 \text{ cm}$, $\text{Ca}_o = 5.25 \text{ wt. } \%$

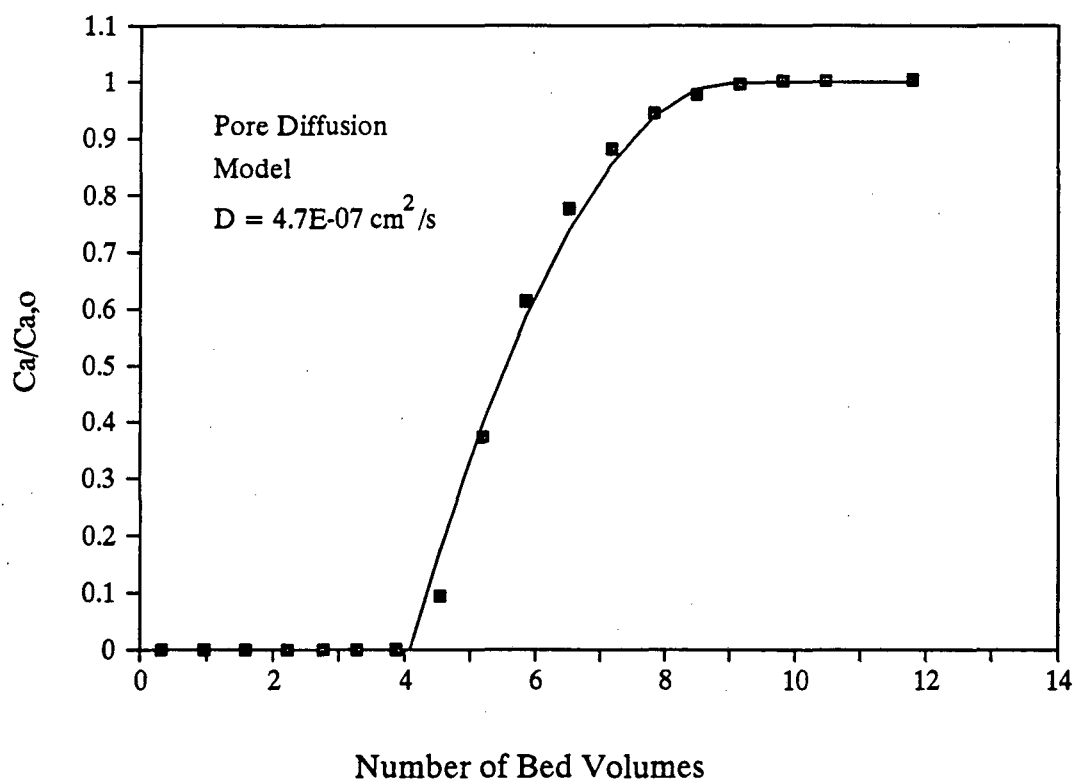


Figure 3-67. Breakthrough of Succinic Acid
on Dowex MWA-1.

$F = 1.54 \text{ ml/min}$, $L = 29.2 \text{ cm}$, $\text{Ca}_0 = 5.25 \text{ wt. \%}$

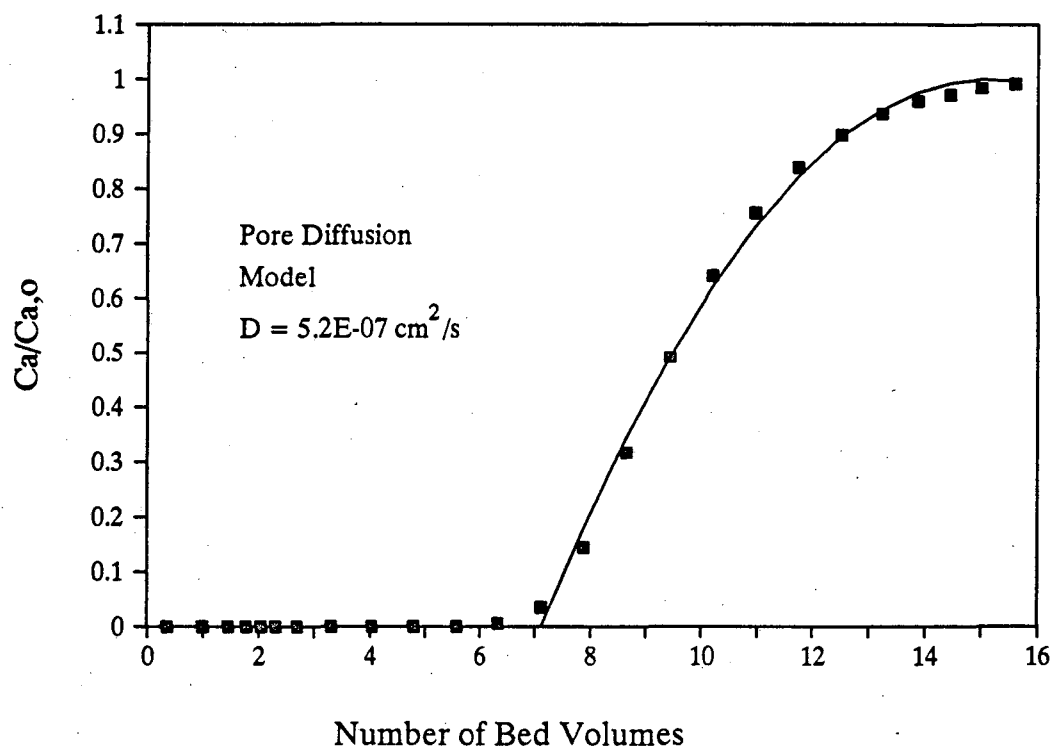


Figure 3-68. Breakthrough of Succinic Acid on Dowex MWA-1.

$F = 1.4 \text{ ml/min}$, $L = 24.5 \text{ cm}$, $\text{Ca}_0 = 2.53 \text{ wt. } \%$

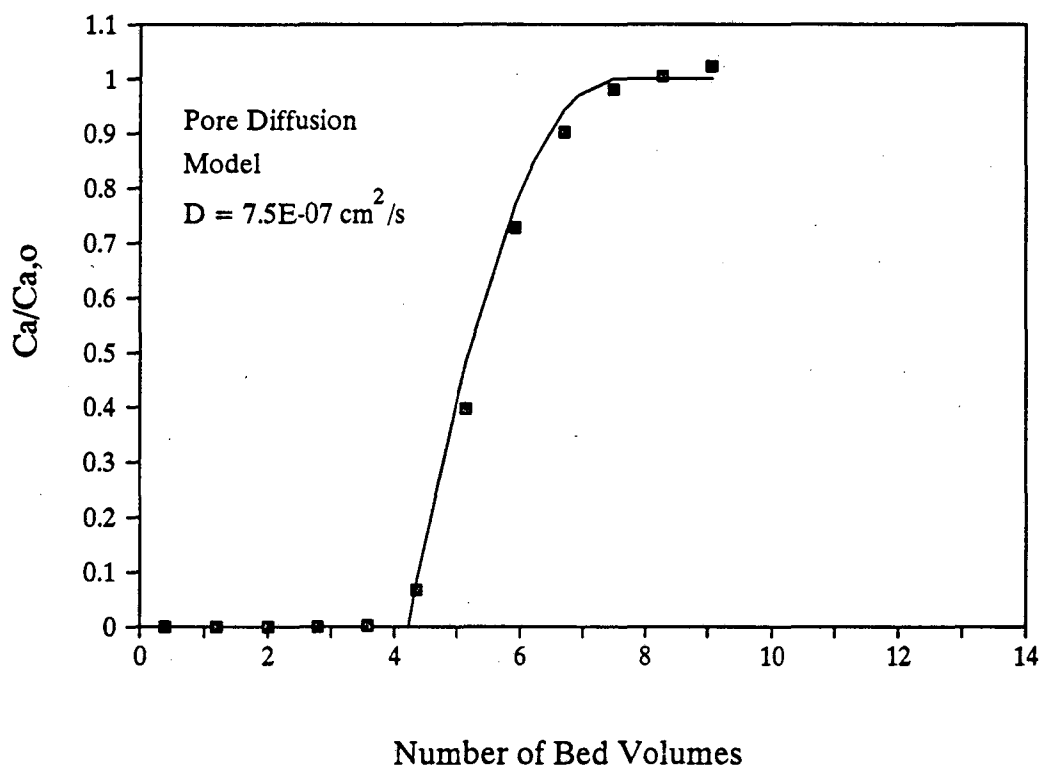


Figure 3-69. Breakthrough of Lactic Acid on Dowex MWA-1.

$F = 1.5 \text{ ml/min}$, $L = 24.5 \text{ cm}$, $\text{Ca}_0 = 4.0 \text{ wt. } \%$

Table 3-11. Breakthrough Curve Results

Run	Figure Numbers	Flow Rate (ml/min)	Column Length (cm)	Acid	Feed Conc. (wt. %)	k_{pa} (min^{-1})	D_{eff} ($10^{-7} \text{cm}^2/\text{s}$)	D_{pore} ($10^{-7} \text{cm}^2/\text{s}$)
1	3-60, 3-65	1.2	24.5	Succinic	5.25	0.11	1.1	4.8
2	3-61, 3-66	3.1	24.5	Succinic	5.25	0.12	1.2	6.2
3	3-62, 3-67	1.54	29.2	Succinic	5.25	0.11	1.1	4.7
4	3-63, 3-68	1.4	24.5	Succinic	2.53	0.065	0.65	5.2
5	3-64, 3-69	1.5	24.5	Lactic	4.0	0.17	1.7	7.5

In general, the linear-driving-force model fits the data reasonably well, although there is some lack of fit, especially in the initial regions of the curves. This result is not surprising, since the sorption isotherms are highly favorable. The same value of k_{pa} was obtained for 5.25 wt.% succinic acid feeds at different flow rates (Runs 1 through 3), as is expected for a particle-controlled process. However, use of a lower feed concentration (2.53 wt.%, in Run 4) results in a value of k_{pa} which is only 55-60% of that obtained at the higher succinic acid concentration. This result indicates that the rate may be affected by mechanism(s) other than simple diffusion within the particle phase. However, it is difficult to draw conclusions about the rate mechanism from a lumped-parameter model. The value of k_{pa} is larger for lactic acid than for succinic acid, indicating that the effective diffusivity of lactic acid is higher.

The calculated values of D_{eff} range from 0.7 to $2 \times 10^{-7} \text{cm}^2/\text{s}$. This is 1.5 to 2 orders of magnitude less than the diffusivity of succinic acid in water, which is $0.94 \times 10^{-5} \text{cm}^2/\text{s}$ (77). Typical effective diffusivities in ion exchangers are 1/10 to 1/10,000 of the values in the liquid phase (77).

Overall, the pore-diffusion model gives a somewhat better fit to the data, especially in the initial regions of the breakthrough curves. For succinic acid, the fitted pore diffusivities are between 4.7 and $6.2 \times 10^{-7} \text{ cm}^2/\text{s}$, and therefore are of the same order of magnitude as the values of D_{eff} obtained from the linear-driving-force model. These diffusivities are much less than what would be predicted using Equation 3-51. Therefore, the mechanism of transport may not be pure diffusion through the pores. Some or all of the solute may diffuse within the adsorbed phase, following the "solid" diffusion mechanism described by Hall et al. (76). However, at the lower flow rates, the value of D_{pore} remains constant at an average value of $4.9 \times 10^{-7} \text{ cm}^2/\text{s}$, independent of the feed concentration, which is consistent with a pore-diffusion mechanism. The model does not fit the high-flow-rate curve (3.1 ml/min, Run 2) as well as it fits the other curves, and a higher value of D_{pore} ($6.2 \times 10^{-7} \text{ cm}^2/\text{s}$) was obtained. It is not clear whether the lack of fit is related to some other resistance (in the fluid phase, for example), to wall effects, or to some other factor.

The model describes the lactic acid breakthrough curve reasonable well. The value of D_{pore} for lactic acid is somewhat higher than that for succinic acid.

3.7.3 Leaching Curves

Figure 3-70 presents the results of a cycling experiment involving breakthrough of 5.25 wt.% succinic acid, regeneration by leaching with 5.25 wt.% TMA, and a second breakthrough step. The graph illustrates several important ideas. First, the two breakthrough curves are virtually identical, and the amount of acid leached (calculated from the area under the leaching curve) is equal to the amount sorbed (calculated from the area to the left of the breakthrough curve) in both cases. This demonstrates that the TMA leaching process is able to regenerate the resin fully without affecting its ability to sorb acid. (A sample of Dowex MWA-1 was also soaked in 25 wt.% TMA for 24 hours, then rinsed and contacted with succinic acid. The uptake of acid was unaffected by contact with even this very concentrated TMA solution.)

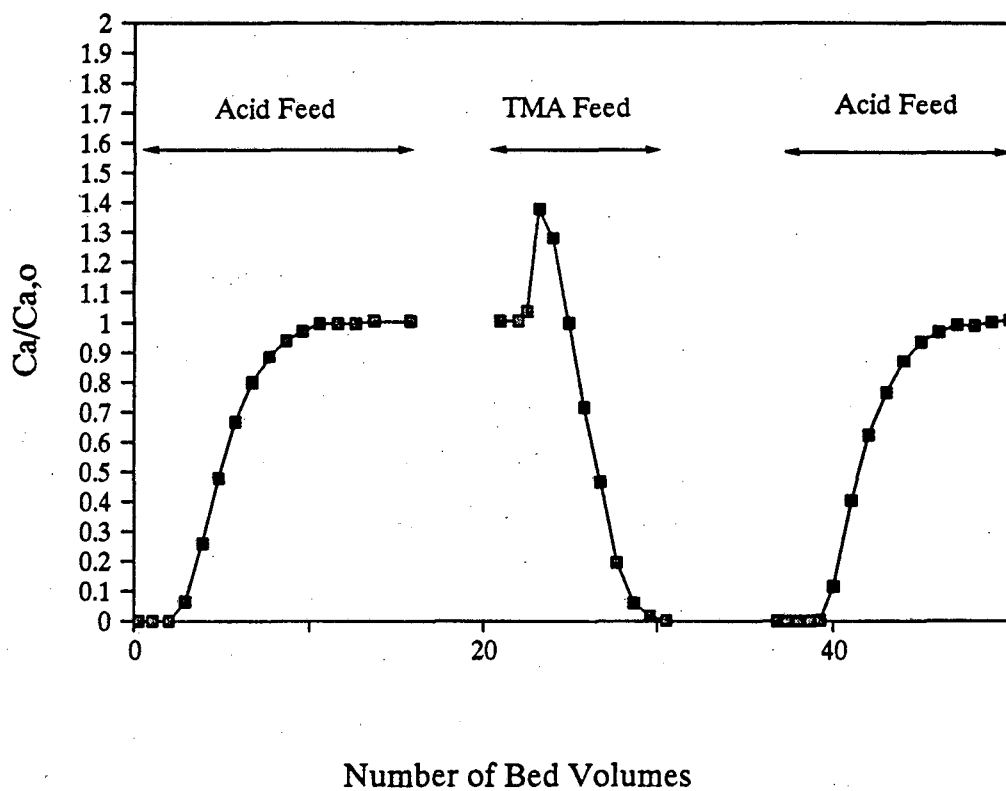


Figure 3-70. Breakthrough and Leaching Curves for Succinic Acid on Dowex MWA-1, $F = 1.5$ ml/min, $L = 18$ cm
5.25 wt. % Acid Feed, 5.25 wt. % TMA Feed

The TMA leaching portion of Figure 3-70 is also quite sharp, reflecting the fact that the leaching process is also a favorable equilibrium. Another interesting feature of the curve is that the concentration of acid at the peak of the leaching curve is much higher than expected. Since the molecular weight of TMA is almost exactly half that of succinic acid, and since one acid molecule pairs with two TMA molecules, the expected value of $C_a/C_{a,o}$ in the column effluent would be 1.0 initially, with a gradual tailing off due to mass-transfer effects. Experimentally, the value of $C_a/C_{a,o}$ reaches 1.4 at the peak of the leaching curve.

This result can be explained in terms of a focusing effect, which has been described by Wankat and co-workers (65, 78). Focusing, or trapping, of a solute wave can occur when there exists some thermodynamic variable (in this case, pH) which, when changed, causes a large change in the amount of solute sorbed. For focusing to occur, the pH wave must move at a velocity which is greater than the solute velocity when it is strongly sorbed (i.e. at low pH) and less than the solute velocity when it is weakly sorbed (i.e. at high pH). Focusing occurs when the pH wave overtakes the slowly-moving solute wave. As the pH wave travels through the column, the pH rises and acid is transferred to the mobile phase. The concentrated solute wave tries to move faster than the pH wave, but if it does so, it will reach a region of low pH and will be forced to slow down. Thus, the solute is trapped at the pH wave front. Figure 3-71 shows the results of a second experiment in which the pH and the concentration of TMA were also monitored. The same focusing phenomenon is observed, and it is apparent that the acid is trapped in front of the pH wave.

In general, the focusing effect will be less pronounced at high TMA concentrations, since the change in concentration due to removing acid from the sorbent is a smaller fraction of the solution concentration. The results of leaching with a solution of 10.2 wt.% TMA are shown in Figure 3-72. If one acid molecule pairs with two TMA molecules, the expected value of $C_a/C_{a,o}$ is 1.94. The observed value is about 1.99, indicating that focusing is not a major factor.

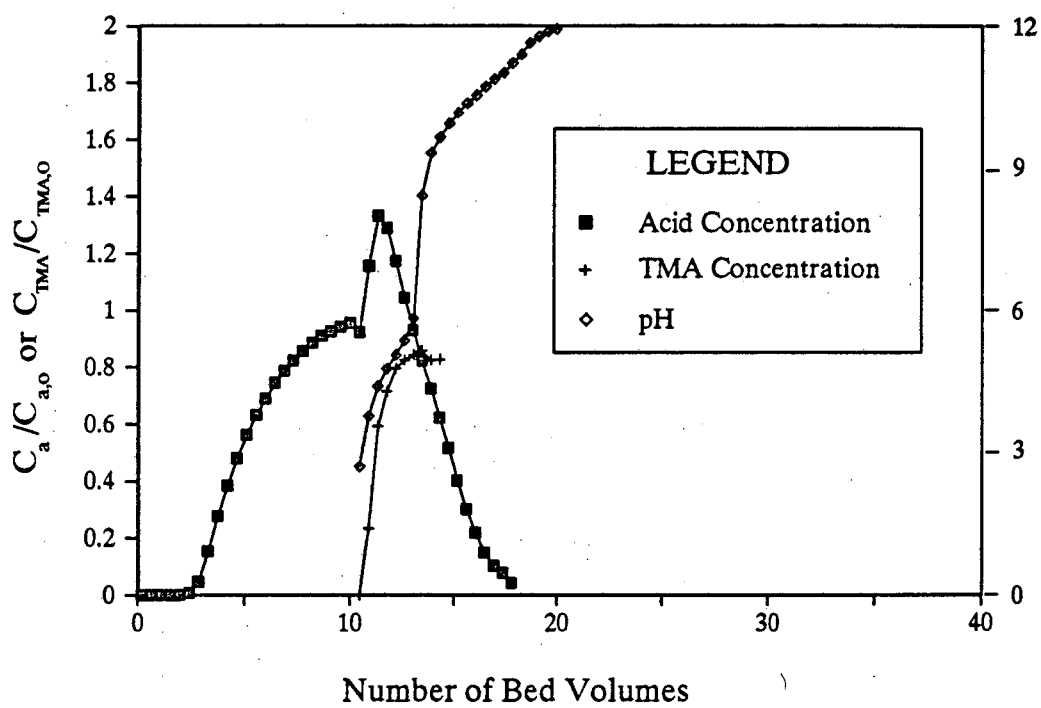


Figure 3-71. Breakthrough and Leaching Curves for Succinic Acid on Dowex MWA-1, $F = 3.1$ ml/min, $L = 24.5$ cm
5.25 wt. % Acid Feed, 5.25 wt. % TMA Feed

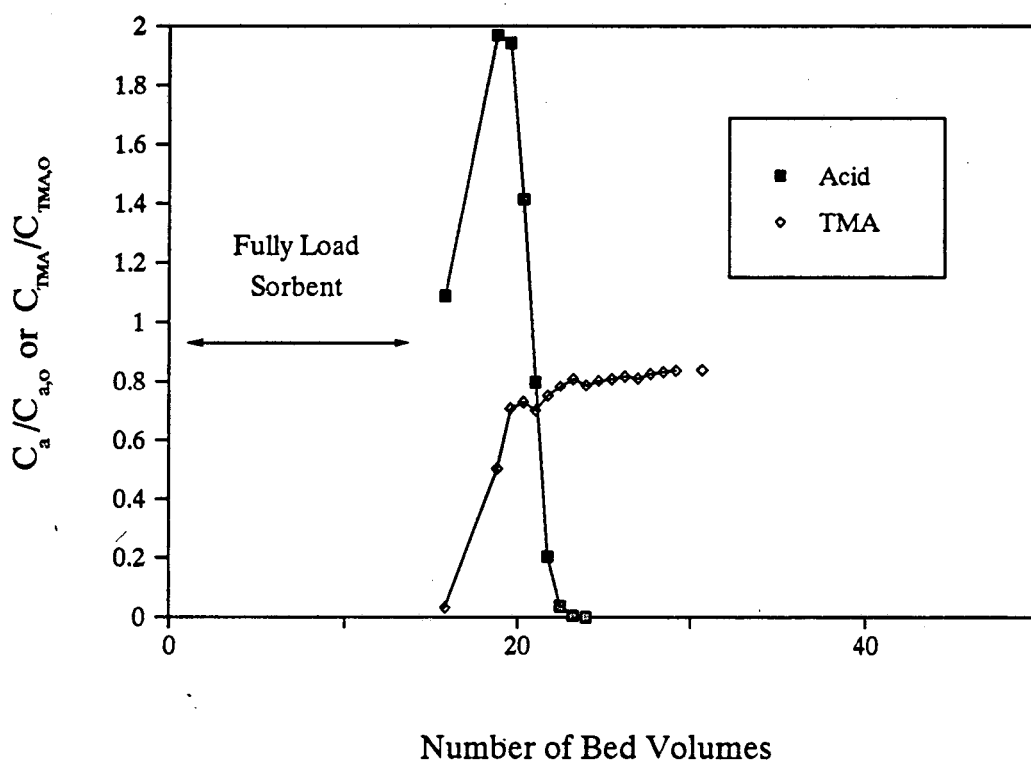


Figure 3-72. Leaching Curve for Succinic Acid on Dowex MWA-1, $F = 1.4$ ml/min, $L = 24.5$ cm
10.2 wt. % TMA Feed

3.7.4 Summary and Conclusions

Fixed-bed experiments have demonstrated that the sorption of carboxylic acids by Dowex MWA-1 shows no major rate limitations. Because of the highly favorable sorption isotherm, the breakthrough curve is self-sharpening and a constant pattern is quickly achieved. The rate-limiting step is most likely diffusion in the particle phase, and a pore-diffusion model fits the data reasonably well. Further studies, preferably using a column with a larger diameter, are needed before an industrial column can be designed. The leaching process is also highly favorable and the resulting leaching curve is sharp. An additional concentration effect is achieved through focusing.

CHAPTER 4. RECOVERY USING LIQUID AMINE EXTRACTANTS

Strongly basic liquid amine extractants are a potential alternative to basic polymeric sorbents in the recovery of carboxylic acids from aqueous solutions at $\text{pH} > \text{pK}_a$. In this chapter, the effects of amine structure and diluent type on the ability of an extractant system to sustain capacity at $\text{pH} > \text{pK}_a$ are explored. Results are presented for two different amine extractants -- Alamine 336 (Henkel Corp.) and Amberlite LA-2 (Rohm and Haas Corp.). Three quite different diluents are also examined -- methylisobutyl ketone (MiBK), 1-octanol, and chloroform. A simple model that relates loading of the amine to equilibrium solution pH is developed. The back-extraction of acid from the extractant using aqueous solutions of trimethylamine (TMA) is also investigated.

4.1 Previous Studies

Long-chain, aliphatic amines are good extractants for the recovery of carboxylic acids from aqueous solutions (26, 36, 40, 79). The amine extractant is typically dissolved in an organic solvent, or diluent, which is useful for controlling the density and viscosity of the organic phase. The diluent can also have a profound effect on the extraction equilibria.

Several researchers have examined the performance of amine extractants at values of pH typical of fermentation systems. Yabannavar and Wang (80, 81) have recovered lactic acid from actual fermentation broths at pH 4.1 - 4.6 using Alamine 336, a tertiary amine extractant, in oleyl alcohol. Two different regeneration methods -- back extraction into aqueous NaOH to produce sodium lactate and displacement of lactic acid with HCl, followed by a distillation step -- were proposed.

Yang et al. (82) investigated the effect of pH on the extraction of several carboxylic acids by Alamine 336 and Aliquat 336 (a long-chain quaternary alkylammonium chloride) in kerosene and 2-octanol diluents. The distribution coefficient for the acid was related to

solution pH via a simple phenomenological model, but rigorous models, based on the various chemical and physical equilibria involved, were not developed.

Reschke and Schügerl (15) studied the extraction of penicillins G ($pK_a = 2.75$) and V and phenoxyacetic acid using Amberlite LA-2 (a secondary amine extractant) and other primary, secondary, and tertiary amine extractants in n-butyl acetate. A range of pH values was investigated, and the results were modelled successfully using acid dissociation equilibria and Law-of-Mass-Action expressions. Secondary amines were found to give the best performances at high pH, followed by tertiary amines and then primary amines. Primary amines were found to have relatively high solubilities in the aqueous phase, and their use often led to the formation of stable emulsions. The effectiveness of Amberlite LA-2 in different diluents was also examined, but no rationale was given for the observed differences in performance. Adogen 464 (a long-chain quaternary alkylammonium compound in Cl^- form) was also investigated but was very difficult to regenerate.

The aim of this work is to develop a better understanding of the extraction equilibria for the uptake of carboxylic acids by basic amine extractants and to use this understanding to identify extraction systems that give sustained capacity at $pH > pK_a$.

4.2 Law-of-Mass Action Modeling of Extraction Systems

Compared with the basic sorbents discussed in Chapter 3, liquid amine extractants afford an environment that is much more organic in nature (83). Therefore, whereas some amine sorbents may be able to sorb bicarboxylate ions, amine extractants typically take up only un-ionized acid molecules (36, 83). (High-molecular-weight quaternary ammonium compounds can function as anion exchangers, exchanging carboxylate anions for, e.g., chloride ions. Ion exchangers *per se* are not considered here due to problems of broth contamination and the ultimate production of a carboxylate salt product. Refer to Section 1.2.3 for further discussion.)

An equilibrium description of the extraction system can be written as a set of reactions of p un-ionized acid molecules (HA) with q base molecules (B) to form (p,q) complexes, with equilibrium constants β_{pq} :



where braces denote species activities and overbars denote organic-phase species. Here and elsewhere in this chapter, H_2A should be substituted for HA in the case of a dicarboxylic acid. For practical purposes, it is often assumed that the ratio of the activity coefficients is constant with respect to composition, so that the species activities in Equation 4-1 can be replaced by concentrations. An apparent equilibrium constant can then be written as:

$$K_{pq} = \frac{[\overline{(HA)_p B_q}]}{[HA]^p [\bar{B}]^q} \quad (4-2)$$

where the brackets denote species concentrations.

The loading of the extractant, Z , is defined as the total molar concentration of acid, in all forms, in the organic phase divided by the total molar concentration of amine, in all forms, in the organic phase, or:

$$Z = \frac{[HA]_{tot}}{[\bar{B}]_{tot}} \quad (4-3)$$

If extraction by the diluent alone is negligible, the loading is given by:

$$Z = \frac{\sum p K_{pq} [HA]^p [\bar{B}]^q}{[B]_{tot}} \quad (4-4)$$

In this work, all reported loadings include physical solvation of acid by the diluent. Note that the value of Z may exceed 1, in which case the amine is said to be overloaded.

"Best-fit" values of the equilibrium constants, K_{pq} , can be determined for sets of experimental loading data using a computer program which minimizes the sum of the squares of the errors between the data points and values calculated from the postulated model. Other programs are designed to minimize other quantities, such as the sum of the absolute values of the errors. Tamada et al. (40) used one such program to find values of K_{pq} for the extraction of several different carboxylic acids by Alamine 336 in various diluents.

It is difficult to generalize the behavior of carboxylic acid-amine extractant systems, since a range of complexes is generally seen. Many carboxylic acid - amine extractant systems appear to exhibit exclusively (p,1) stoichiometries. Overloading of organic amine extractants is extremely common, especially with monocarboxylic acids (36, 40, 79). Spectroscopic evidence indicates that the first acid molecule forms a hydrogen bond or acid pair with the amine, and the second acid molecule then forms a hydrogen bond with the resulting carboxylate, as in Figure 4-1 (40, 79). There are, however, a number of systems that show (p,2) stoichiometries

4.3 Importance of Complexation Constants to Performance at $pH > pK_a$

It is clear from Equations 4-1 through 4-3 that the amount of complexed acid depends not only on the concentrations of un-ionized acid in the aqueous phase and of basic extractant in the organic phase, but also on the magnitude of the equilibrium constants, K_{pq} . The values of the K_{pq} are important, for they determine the performance at $pH > pK_a$. In particular, it is the value of the complexation constant for the reaction of the first acid with the amine

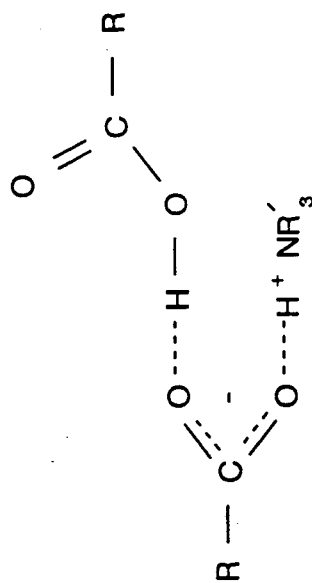


Figure 4-1. Proposed Structure for (2,1)
Acid-Amine Complex

extractant molecule(s) (K_{11} or K_{12}) that is most important in determining performance at $\text{pH} > \text{pK}_a$, since this is the dominant reaction at low concentrations of un-ionized acid.

Figures 4-2 (a) and (b) present schematic graphs of amine loading as a function of pH for a system exhibiting (p,1) stoichiometries. At low pH, there is a high concentration of un-ionized acid and high loadings are achieved. However, at higher values of pH, the concentration of un-ionized acid decreases, resulting in a corresponding decrease in loading. In Figure 4-2 (a), loading-pH curves are presented for two extractants having the same values of K_{21} but different values of K_{11} . The extractant with the higher value of K_{11} is able to sustain capacity to higher values of pH. In Figure 4-2 (b) the effect of K_{21} on the loading is demonstrated. Although the extractant with the higher value of K_{21} does yield higher loadings at low pH, at higher pH the two loading curves are identical. Thus, in the pH range of interest, K_{21} has little effect on loading. Similar results are obtained for systems exhibiting (p,2) stoichiometries. Thus, although higher complexation constants in general result in higher loadings, higher values of K_{11} (or K_{12}) are particularly important in sustaining capacity at $\text{pH} > \text{pK}_a$.

4.4 Factors Affecting Amine Extractant Basicities

There are several factors that influence the values of K_{11} (or K_{12}), including the nature of the acid and of the amine, and the type of diluent. Interactions among these factors can also be important. For the uptake of a given acid by an amine extractant, the value of K_{11} is related to the basicity of the amine extractant, just as the K -value from a sorption isotherm is related to the basicity of the sorbent. The major difference, however, is that the basicity of the sorbent is primarily a function of the nature of the basic functional groups, whereas the basicity of the extractant is a strong function of both the nature of the amine itself and the type of diluent.

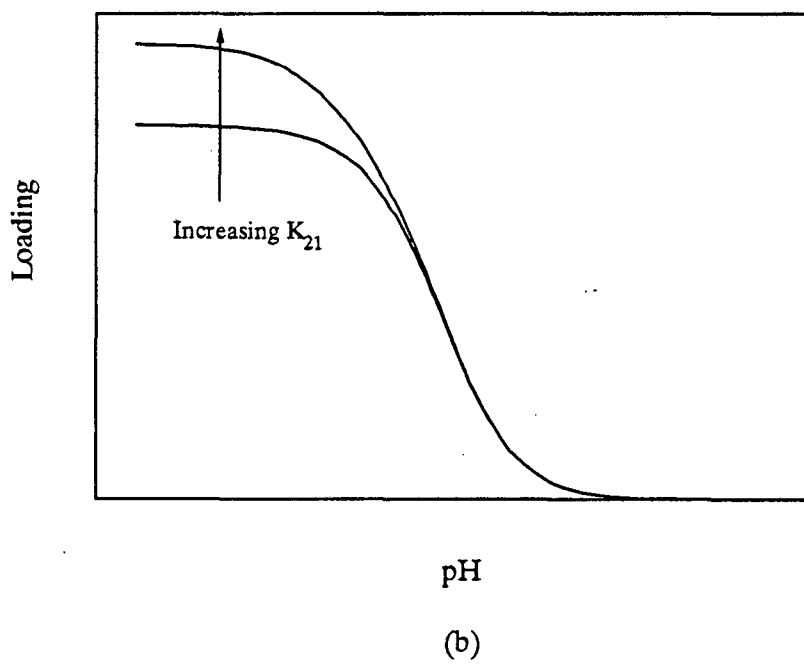
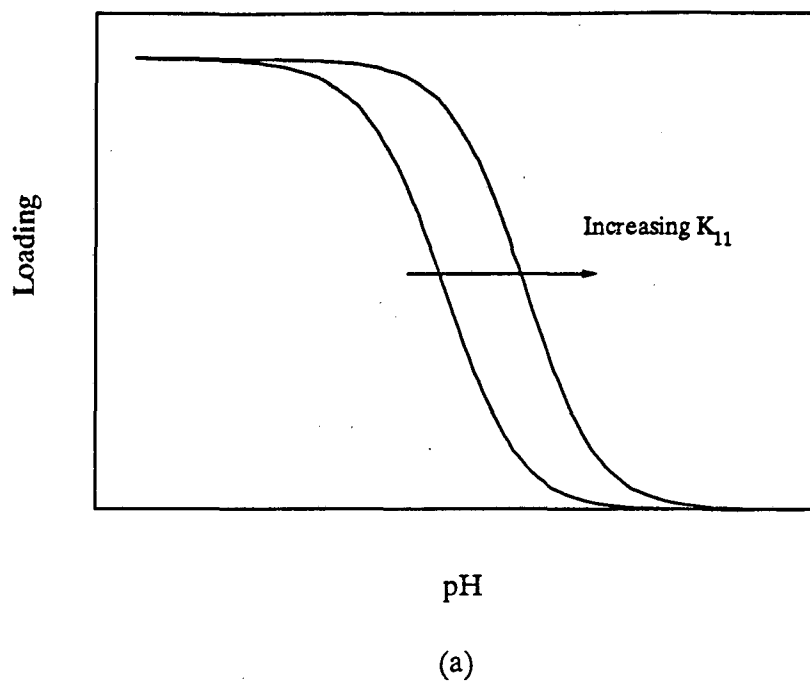


Figure 4-2. Effect of Complexation Constants on Loading
(a) Effect of K_{11} (b) Effect of K_{21}

4.4.1 Diluent Effects

High basicity, and hence increased extraction power, can be achieved in systems in which the diluent is able to stabilize the acid-amine complex more than it stabilizes the uncomplexed amine and acid. Diluents can be classified as "inert" or "active" based upon their degree of interaction with the acid-amine complex. Inert diluents, such as alkanes, benzene, and alkyl-substituted aromatics, are relatively nonpolar and provide very little solvation of the acid-amine complex. Therefore, values of K_{11} for amine extractants dissolved in any of these diluents are generally quite low (40, 79), and the amine extractant is said to have a low basicity. Aromatic diluents generally give somewhat higher values of K_{11} than do alkanes, presumably due to interaction of π electrons with the acid-amine complex (40, 79, 84).

Increased basicity can be achieved with "active" diluents, which are able to solvate or otherwise interact with the acid-amine complex. For example, halogenated aromatic solvents, ketones, and nitrobenzene are polar and therefore provide a good solvating medium for the ion pairs. Thus, values of K_{11} for amine extractants in these diluents are typically much higher than the corresponding values in inert diluents (40, 79). Other diluents provide more stability than can be accounted for by polarity alone. For example, protic halogenated hydrocarbons, such as chloroform, and alcohols, such as 1-octanol, appear to interact with the acid-amine complex through hydrogen bonding, as in Figure 4-3, thus providing further stability (40, 79, 85, 86, 87, 88). The resulting values of K_{11} are therefore quite large. Spectroscopic evidence for hydrogen bonding has been observed in systems comprising mono-, di- or tri-ethylamine, chloroform, and acetic acid (86, 87, 88).

It is difficult to quantify the effect of diluent type on the extraction power or "basicity". Several researchers have correlated the Hildebrand solubility parameter with extracting power, but the correlation does not apply to diluents like chloroform, which interact specifically with the acid-amine complex (79, 85). Schmidt and co-workers (89, 90,

91) have used linear free-energy relationships to account for solute, extractant and diluent effects on extraction equilibria.

4.4.2 Effects of Amine Type

The nature of the amine itself is also an important factor in determining extractant basicity. In inert diluents, the order of basicity typically reflects the various inductive, substituent and steric effects associated with the amine molecule. Thus, for straight chain amines without substituents, the order of basicity is usually tertiary > secondary > primary, since substitution of a hydrogen atom by an aliphatic chain increases basicity via the inductive effect. Grinstead and Davis (92) observed this order for dilute solutions of aliphatic amines in toluene. Barring steric effects, branched chains increase basicity more than straight chains with the same number of carbon atoms (93). Electron-withdrawing substituents, on the other hand, decrease the basicity of the amines to which they are attached. Consequently, aromatic amines are more weakly basic than aliphatic ones. Steric effects can also be important, and may counteract the inductive effect when exceptionally bulky molecules are involved. Steric effects are less of a concern with primary and secondary amines than with tertiary amines (93).

In more active diluents, other effects often outweigh the effects discussed above. Pearson and Vogelsong (94) looked at the complexation of primary, secondary and tertiary amines with 2,4-dinitrophenol in various diluents. They showed that primary and secondary amines are stronger bases in oxygenated solvents than in non-oxygenated solvents with the same dielectric constant. Tertiary amines, on the other hand, were equally basic in the two types of solvents. The researchers suggest that oxygenated solvents stabilize the primary and secondary amine complexes by forming a hydrogen bond with the amine protons, as in Figure 4-4 (a). Tertiary amines, however, have no additional protons with which an oxygenated diluent can form hydrogen bonds (Figure 4-4 (b)). As a result of this structural difference,

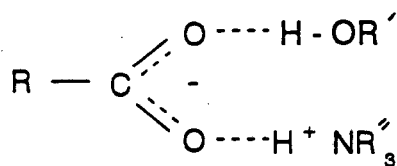


Figure 4-3. Stabilization of Amine-Carboxylic Acid Complexes Through Hydrogen-Bonding with an Alcohol

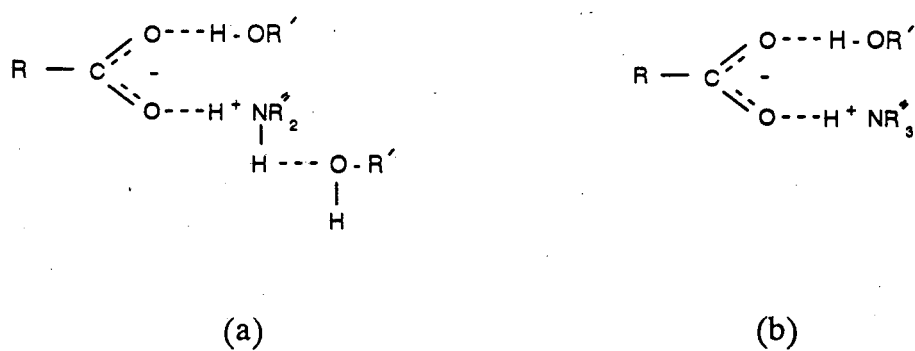


Figure 4-4. Stabilization by Oxygenated Diluents
 (a) Secondary Amine (b) Tertiary Amine

primary amines were found to be slightly more basic than secondary amines in ethyl acetate, and both were much more basic than tertiary amines. In chloroform, which is not oxygenated, the order tertiary > secondary > primary was observed.

Other authors have also noted that primary and secondary amines are generally stronger bases than tertiary amines in solvents that strongly solvate substituted ammonium cations (95, 96). The diluents that are able to solvate these cations are all electron donors -- oxygen-containing organic solvents (alcohols, ethers, esters, ketones, etc.) and organic bases (amines, dioxane, nitrobenzene, etc.) (96).

4.5 Choice of Extraction Systems for Study

Both a tertiary and a secondary amine extractant were chosen for study; primary amines were not considered due to their high water solubilities (15, 41) and tendency to form emulsions (15). The chosen amines, Alamine 336 (Henkel Corp.) and Amberlite LA-2 (Rohm and Haas Co.), are both commercially available and have proven abilities to extract carboxylic acids from aqueous solutions. Alamine 336 is a straight-chain tertiary amine with a mixture of about 67% C₈ and 33% C₁₀ side chains. Its solubility in water levels out at less than 10 ppm after repeated contact with aqueous solutions (42). Initial solubilities are higher due to the presence of low-molecular-weight amine impurities (see Section 2.1.1). Amberlite LA-2 is an asymmetric alkyl amine with one straight C₁₂ chain and one highly-branched chain of 12-15 carbon atoms (41). Its limiting solubility is also 10 ppm or less (42) and is higher initially due to impurities.

Three different diluents were also studied -- methylisobutyl ketone (MiBK), chloroform and 1-octanol. These diluents were chosen to provide a variety of interactions with the amine-carboxylic acid complexes. All three diluents are polar and hence should provide general solvation of the ion-pairs. Chloroform and 1-octanol are capable of a more specific interaction with the amine-carboxylic acid complex through hydrogen bonding with

the carboxyl group on the acid. Furthermore, two of the solvents (MIBK and 1-octanol) are oxygenated and thus may interact differently with secondary amines versus tertiary amines.

A high-molecular-weight quaternary alkylammonium extractant, Aliquat 336 (Henkel Corp.) was also pre-screened for use in this study. The extractant is essentially equivalent to Alamine 336, except that it has been quaternized through reaction with methyl chloride (44). In order to avoid the problems associated with using this compound as an ion exchanger, it is necessary to convert the alkylammonium chloride to hydroxide form. Due to the high affinity of the alkylammonium cation for chloride, this conversion process proved to be exceedingly difficult. Successive contacts of a 0.3 M Aliquat 336 solution in toluene with a concentrated sodium hydroxide solution resulted in a conversion of less than half the functional groups to OH^- form, as measured by the amount of chloride displaced.

The regenerability of Aliquat 336 was also briefly tested, since it was expected that this extractant would be difficult to regenerate. A 0.3 M solution of Aliquat 336 (Cl^- form) in toluene was contacted with an equal volume of 0.45 M lactic acid at pH 5.1. A loading of 0.23 was achieved. The extract was then contacted with an equal volume of aqueous solution containing a large excess of TMA (mol TMA/mol acid = 4.8). Only 13% of the acid was back-extracted by the TMA. Thus, the extractant is not efficiently regenerable by this method. In light of the above findings, the use of a quaternary alkylammonium extractant was not studied further.

4.6 Previous Results for Alamine 336

Tamada et al. (40, 79) studied the extraction of several carboxylic acids by solutions of Alamine 336 in various diluents. The fitted equilibrium constants for some of the systems studied are given in Table 4-1.

Table 4-1. $\log(K_{pq})$ Values for Extraction of Lactic and Succinic Acids by Alamine 336 in Various Diluents (Tamada et al. [40])

(p,q)	Lactic Acid		Succinic Acid		
	MiBK	Chloroform	MiBK	Chloroform	1-Octanol
(1,1)	1.31	2.57	1.39	2.44	-
(2,1)	1.52	2.12	1.91	1.49	-
(3,1)	1.17	-	-	-	-
(1,2)	-	-	-	-	3.50
(2,2)	-	-	-	-	4.91

The ratio of K_{11} to K_{21} is dependent on the diluent. Chloroform and 1-octanol tend to inhibit overloading, probably because they contain acidic protons which compete with the proton of the second acid for the carboxylate binding site on the first acid (40, 79). MiBK, on the other hand, promotes overloading. Except for the succinic acid/1-octanol system, there is no evidence that complexes with more than one amine per acid molecule are formed.

Physical extraction of the acids by the various diluents was also considered. The solubility of the acid in pure diluent can be represented by the partition coefficient, P , which is defined as:

$$P = \frac{[\overline{HA}]}{[HA]} \quad (4-5)$$

The values of P reported by Tamada are given in Table 4-2.

Table 4-2. Partition Coefficients (Tamada [97])

Acid	Diluent	P
Lactic	MiBK	0.11
Lactic	Chloroform	0.010
Succinic	MiBK	0.192
Succinic	1-Octanol	0.264
Succinic	Chloroform	-

4.7 Loading of Amine Extractants as a Function of pH

The abilities of the two extractants to sustain capacity at $\text{pH} > \text{pK}_a$ were evaluated by measuring the loadings of 0.3 M amine solutions in various diluents as a function of equilibrium pH. The loadings were measured for a constant phase ratio (volume of aqueous phase/volume of organic phase) and a constant initial concentration of total acid.

4.7.1 Results and Discussion

4.7.1.1 Lactic Acid

The loadings of Alamine 336, in various diluents, with lactic acid at 25 °C are presented as functions of equilibrium pH in Figure 4-5. Smooth curves have been drawn through the data. At low pH, 100 % loading of the amine is achieved for all diluents. Of the three diluents, MiBK shows a decrease in loading at the lowest pH. Chloroform and 1-octanol sustain significant capacity to two or more pH units above the pK_a of the acid, which is 3.86. In particular, at pH 5.5, where a typical fermentation might occur, the loading is 0.61 for chloroform and 0.50 for 1-octanol. The corresponding value for MiBK is only 0.15. Overall,

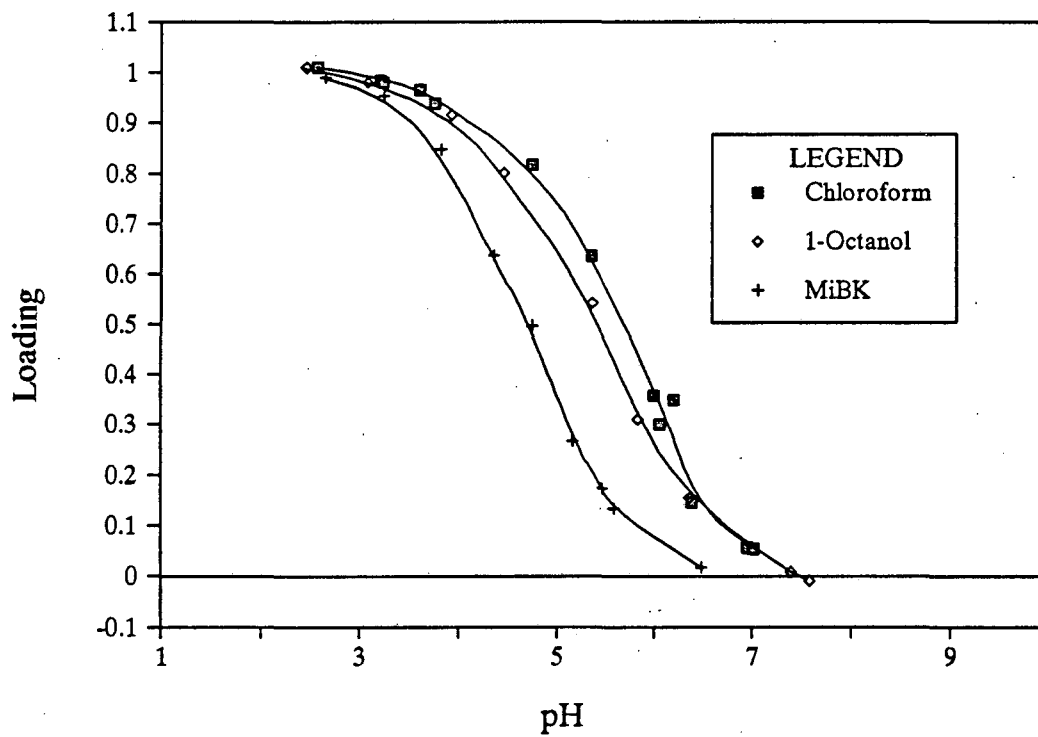


Figure 4-5. Effect of pH on the Extraction of Lactic Acid by Alamine 336 in Various Diluents
[HA]_{tot} = 0.45 M, [B]_{tot} = 0.30 M, Phase Ratio = 1.0

chloroform gives slightly better performance than 1-octanol, but, on the basis of uptake alone, either would be acceptable for use in connection with a lactic acid fermenter.

The observed differences in performance from one diluent to the next reflect the relative abilities of the diluents to stabilize the acid-amine complex. MiBK is polar and thus provides good general solvation of the acid-amine ion pair. Chloroform and 1-octanol are able to form hydrogen bonds with the complex, providing additional stabilization. Therefore, these two extraction systems are more basic and hence sustain capacity to higher values of pH. From the data, it appears that chloroform provides somewhat stronger stabilization of the ion pair than does 1-octanol.

Figure 4-6 presents the corresponding results for lactic acid and Amberlite LA-2. At low pH, the amine is again at least 100% loaded. With the MiBK diluent, a small degree of overloading is observed. This result is consistent with the findings of Tamada et al., who showed that ketones tend to promote overloading. Amberlite LA-2 in 1-octanol would give excellent performance in a fermentation system, with a loading of 0.72 at pH 5.5. Chloroform would give the same good performance ($Z = 0.61$) as with Alamine 336. The Amberlite LA-2/MiBK system shows improved performance over the Alamine 336/MiBK system, but the loading at pH 5.5 is only 0.32.

Comparison with Figure 4-5 reveals that the MiBK and 1-octanol curves are shifted toward significantly higher pH values, whereas the chloroform curve is essentially the same. These shifts are made more apparent in Figures 4-7 through 4-9, which compare, for each diluent, the results for the two amines. The shifts in the MiBK and 1-octanol curves are expected, since LA-2 is a secondary amine and therefore has an additional proton available for solvation by an appropriate diluent. As discussed in Section 4.4, oxygenated compounds, such as alcohols and ketones, provide the greatest solvation power for amine cations. Thus, in MiBK and 1-octanol, Amberlite LA-2 is a stronger base than Alamine 336, and hence the pH curves shift toward higher pH values. Chloroform, on the other hand, cannot interact

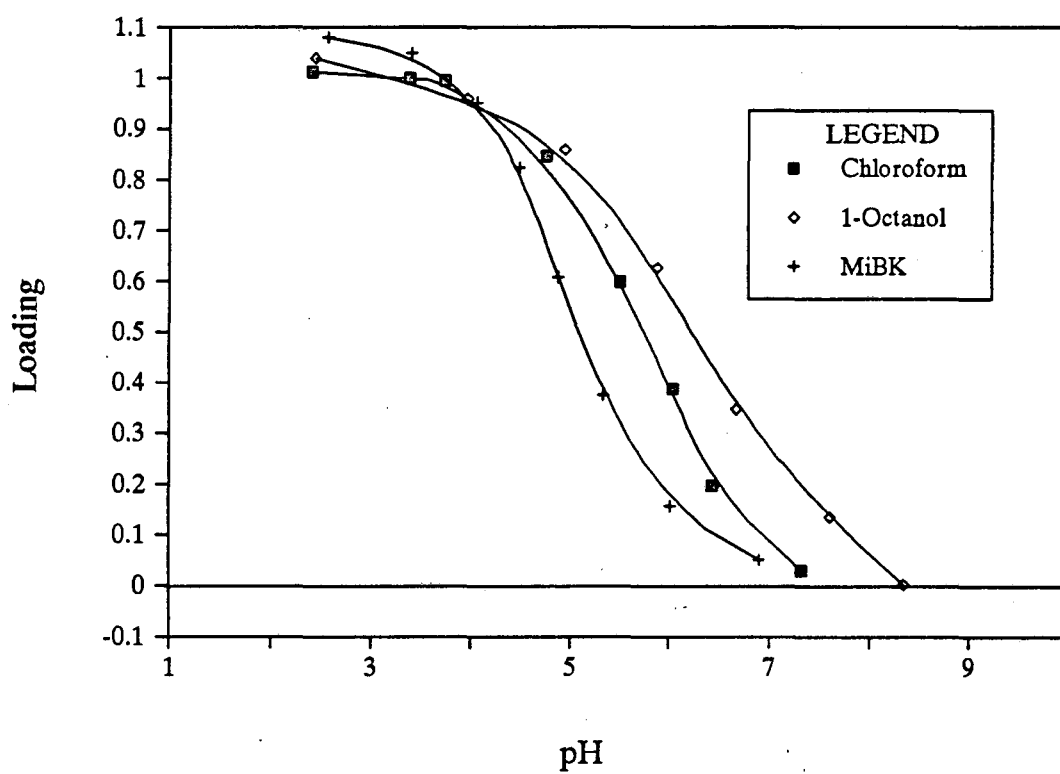


Figure 4-6. Effect of pH on the Extraction of Lactic Acid by Amberlite LA-2 in Various Diluents
[HA]_{tot} = 0.45 M, [B]_{tot} = 0.30 M, Phase Ratio = 1.0

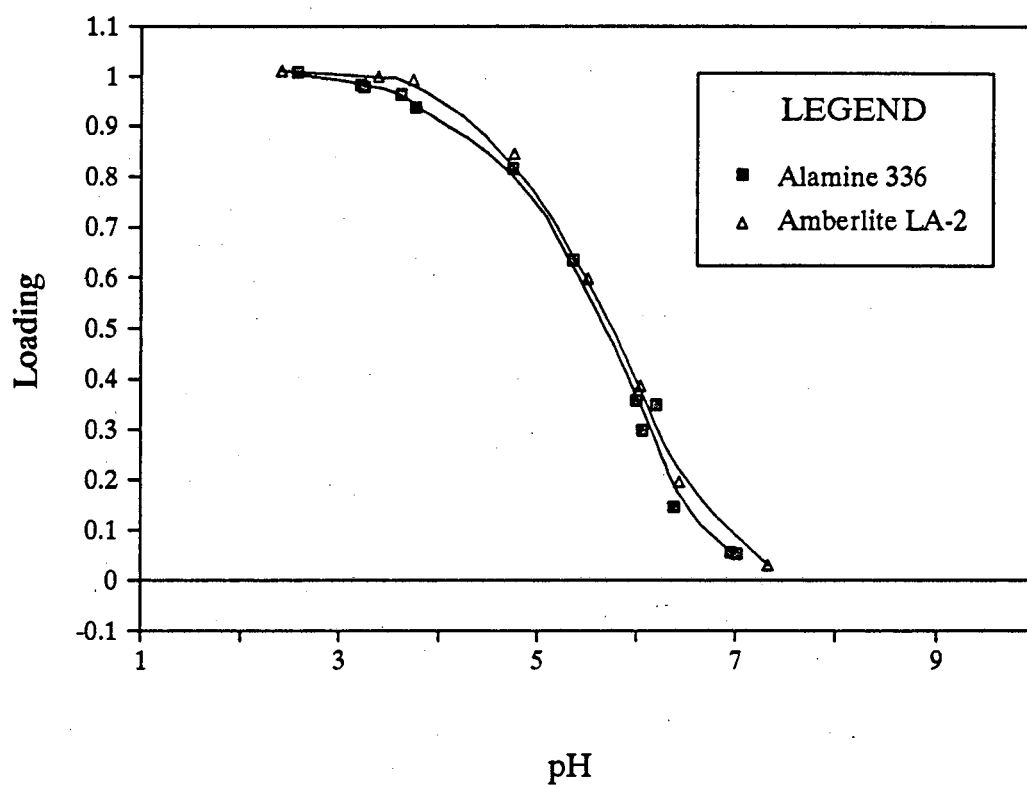


Figure 4-7. Effect of Amine Type on Uptake of Lactic Acid Using a Chloroform Diluent
[HA]_{tot} = 0.45 M, [B]_{tot} = 0.30 M, Phase Ratio = 1.0

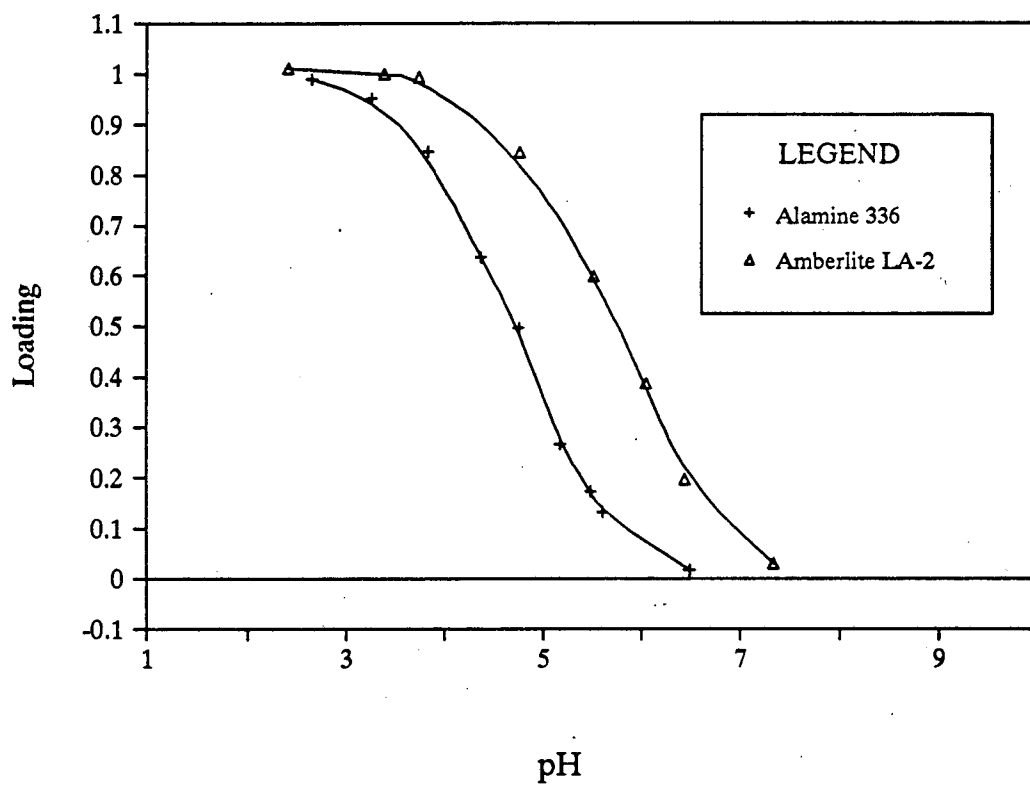


Figure 4-8. Effect of Amine Type on Uptake of Lactic Acid Using an MiBK Diluent
[HA]_{tot} = 0.45 M, [B]_{tot} = 0.30 M, Phase Ratio = 1.0

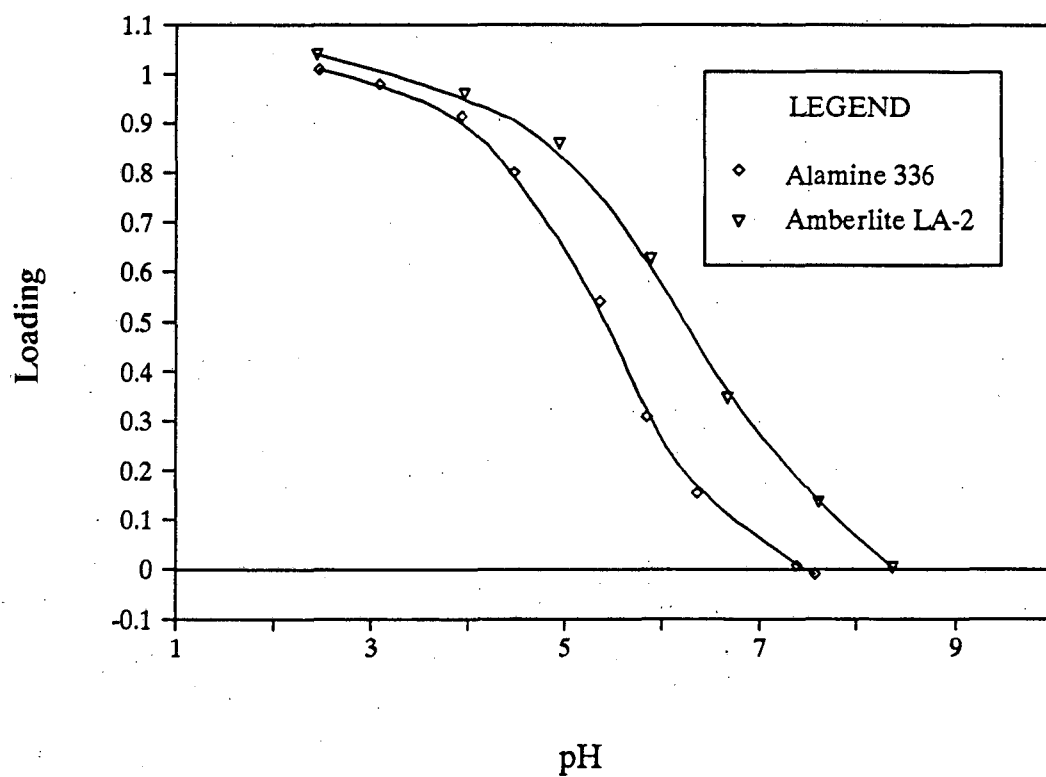


Figure 4-9. Effect of Amine Type on Uptake of Lactic Acid Using a 1-Octanol Diluent
[HA]_{tot} = 0.45 M, [B]_{tot} = 0.30 M, Phase Ratio = 1.0

effectively with the additional hydrogen and hence Amberlite LA-2 is no stronger than Alamine 336 in this diluent. (Pearson and Vogelsong [94] found that, in chloroform, tertiary amines were actually stronger bases than secondary amines, and this is what is expected on the basis of the inductive effect alone. However, other factors are also important. For example, Amberlite LA-2 is a branched amine, which may give it increased basicity over the straight-chain Alamine 336 [93].)

4.7.1.2 Succinic Acid

The loading of Alamine 336 with succinic acid at 25 °C is presented as a function of pH in Figure 4-10. The loading at low pH differs from one diluent to the next. This observation is consistent with the work of Tamada et al., who observed promotion of overloading with MiBK, and formation of complexes with more than one amine per acid with 1-octanol. Otherwise, the results are similar to those for lactic acid, in that chloroform and 1-octanol sustain capacity to higher pH than does MiBK. The relative drop-off in loading with increasing pH is less steep in 1-octanol than in chloroform. This behavior is related to the relative tendencies to form (1, 2) and (2, 2) complexes. If the tendency to form (2, 2) complexes (i.e., the value of K_{22}) were higher, the uptake at low pH would be greater, and the relative-drop off with increasing pH would be steeper.

Overall, the performance of the extractants is somewhat poorer than with lactic acid, with chloroform and 1-octanol sustaining capacity to barely two pH units above pK_{a1} , which is 4.2. This behavior is not unexpected, since succinic is a weaker acid than lactic, and hence the strength of complexation is expected to be lower. Nevertheless, Alamine 336 in chloroform or 1-octanol gives reasonable performance in the pH range of 5 to 6. At pH 5.5, loadings of 0.49 and 0.32 are observed for chloroform and 1-octanol, respectively. In MiBK the loading is less than 0.1.

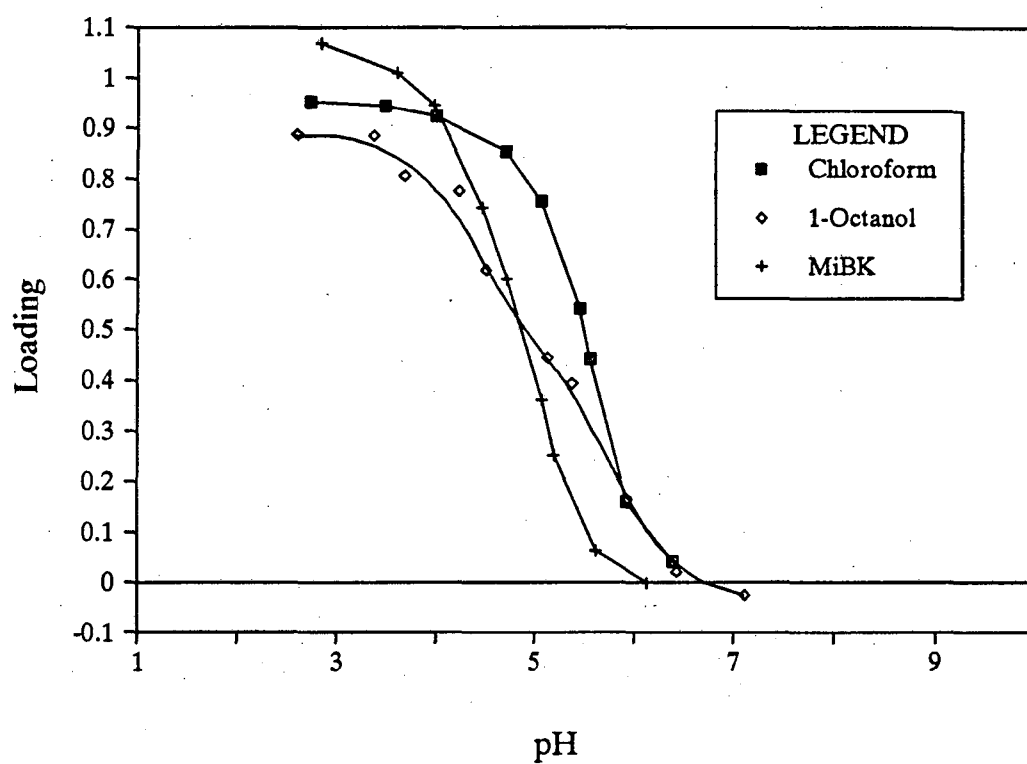


Figure 4-10. Effect of pH on the Extraction of Succinic Acid by Alamine 336 in Various Diluents
[H₂A]_{tot} = 0.45 M, [B]_{tot} = 0.30 M, Phase Ratio = 1.0

Finally, Figure 4-11 presents the results for succinic acid and Amberlite LA-2. Even at low pH, the loading of Amberlite LA-2 in 1-octanol is significantly lower than the loading of Alamine 336 in the same diluent. Amberlite LA-2 may have a greater tendency to form complexes with more than one amine per acid. Several researchers (87, 88, 98) have reported that primary and secondary amines are more likely to form multi-amine complexes than are tertiary amines. As a result of the unusual shape of the 1-octanol curve, chloroform exhibits higher loadings than 1-octanol in the pH 5 to 5.5 range, but 1-octanol shows higher loadings the pH 6 to 7 range. At pH 5.5 the loadings of chloroform, MiBK and 1-octanol are 0.49, 0.35 and 0.35, respectively.

As with lactic acid, the curves for MiBK and 1-octanol are shifted toward higher pH values relative to those for Alamine 336, whereas the chloroform curve is almost the same. Figures 4-12 through 4-14 show these effects more clearly.

4.7.2 Modeling of Loading-pH Curves

The loading-pH curves can be modelled using the appropriate equilibrium and mass-balance equations. The necessary equilibria include the equations describing the dissociation of the acid, which are given in Equation 3-21 for a monocarboxylic acid and Equations 3-24 and 3-25 for dicarboxylic acids. It is again helpful to express the concentration of un-ionized acid in the aqueous phase as the product of the concentration of total acid in the aqueous phase and the quantity α , where

$$\alpha = \frac{1}{1 + \frac{K_{a1}}{[H^*]} + \frac{K_{a1}K_{a2}}{[H^*]^2}} \quad (3-37)$$

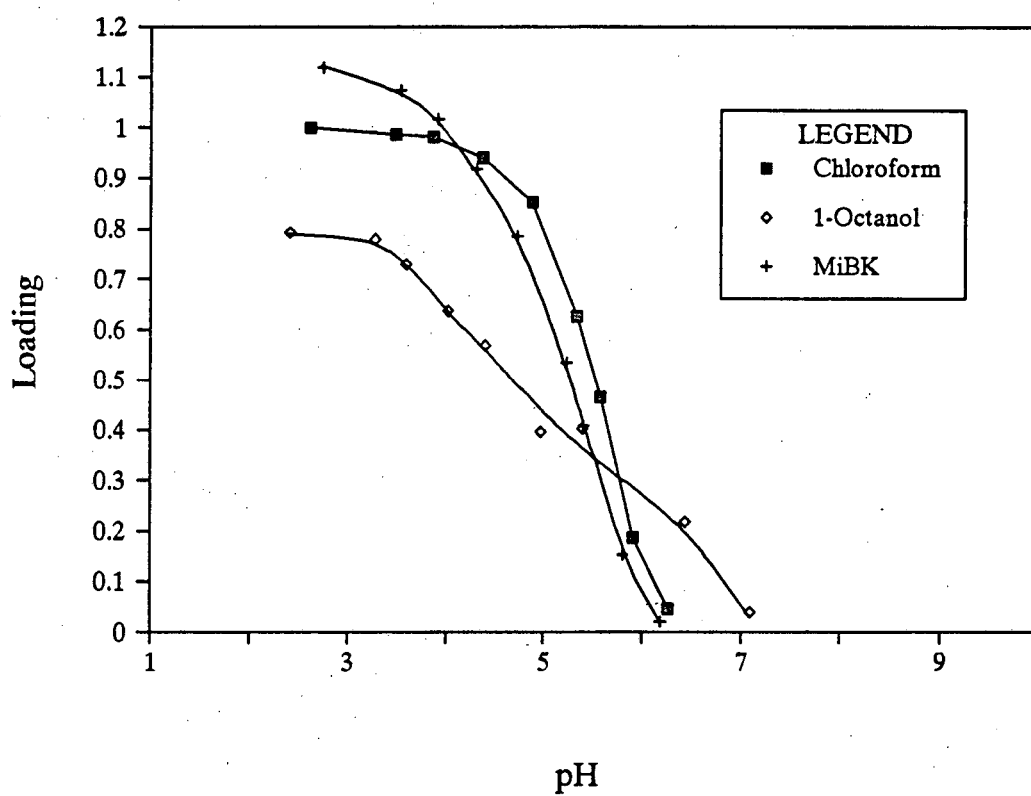


Figure 4-11. Effect of pH on the Extraction of Succinic Acid by Amberlite LA-2 in Various Diluents
[H₂A]_{tot} = 0.45 M, [B]_{tot} = 0.30 M, Phase Ratio = 1.0

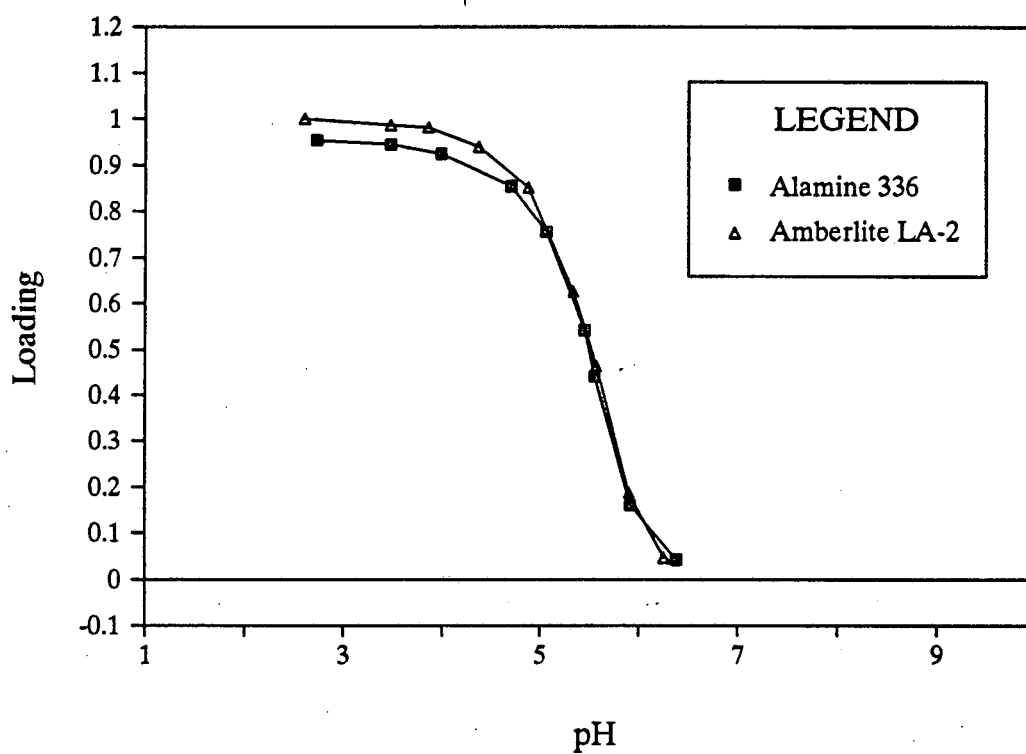


Figure 4-12. Effect of Amine Type on Uptake of Succinic Acid Using a Chloroform Diluent
[H₂A]_{tot} = 0.45 M, [B]_{tot} = 0.30 M, Phase Ratio = 1.0

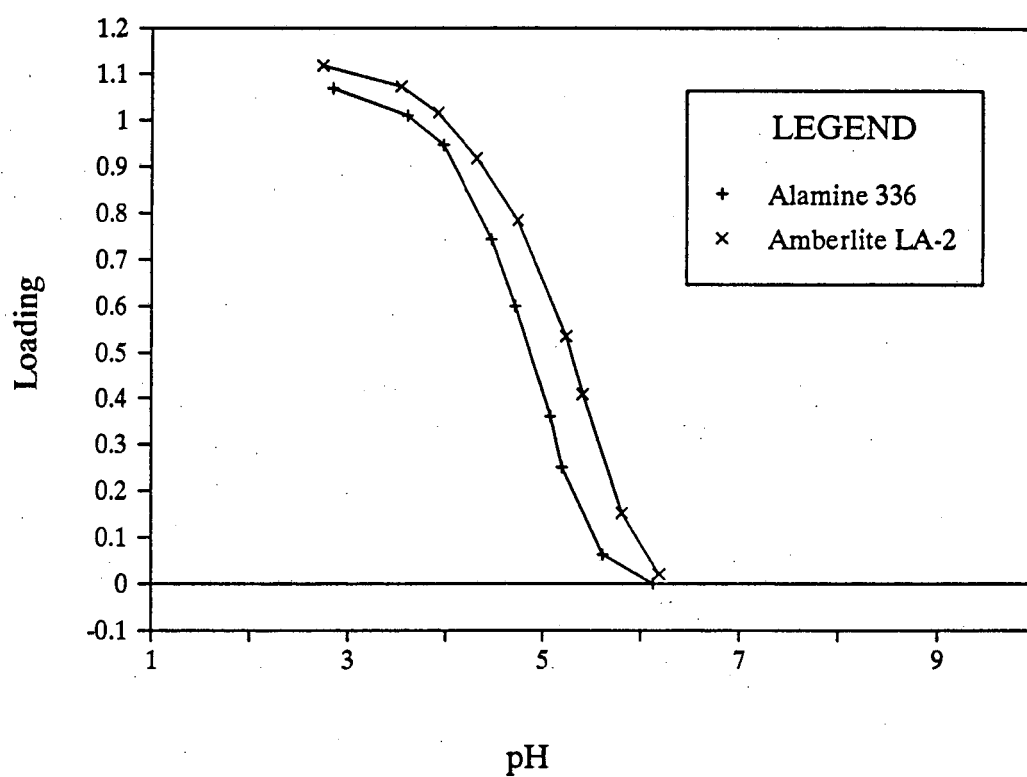


Figure 4-13. Effect of Amine Type on Uptake of Succinic Acid Using an MiBK Diluent
[H₂A]_{tot} = 0.45 M, [B]_{tot} = 0.30 M, Phase Ratio = 1.0

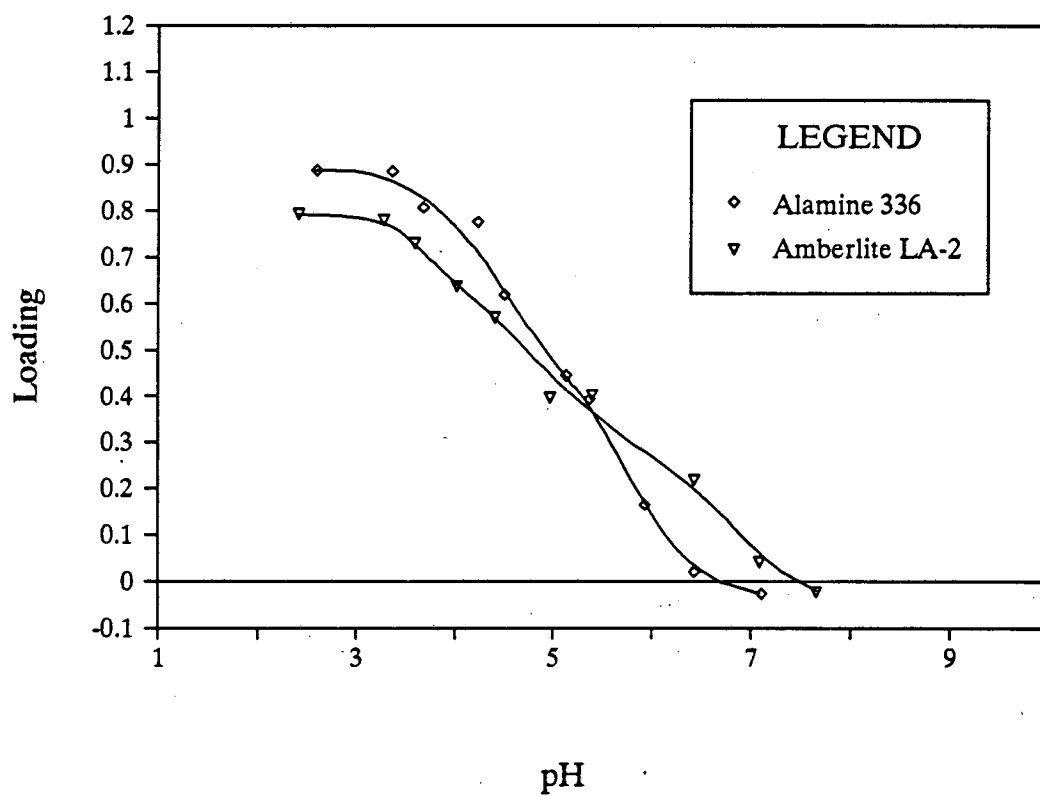


Figure 4-14. Effect of Amine Type on Uptake of Succinic Acid Using a 1-Octanol Diluent
[H₂A]_{tot} = 0.45 M, [B]_{tot} = 0.30 M, Phase Ratio = 1.0

Also needed are the equations describing the equilibrium between the aqueous and organic phases. The chemical equilibrium equations describing the formation of the acid-amine complexes are given in Equations 4-1, with equilibrium constants in Equations 4-2. Physical extraction of the acid by the diluent must also be accounted for, using the expression for the partition coefficient, given in Equation 4-4. Physical extraction by the amine is assumed to be negligible.

Finally, mass balances for the acid and the amine are needed to complete the model. The mass balance on the acid is given by:

$$WS [HA]_{tot,i} = \Sigma p[(HA)_p B_q] + \Phi P[HA] + \frac{[HA] WS}{\alpha} \quad (4-6)$$

where $[HA]_{tot,i}$ is the concentration of total acid, in all forms, in the initial solution, Φ is equal to the volume fraction of diluent in the organic phase, and WS is equal to the aqueous-to-organic phase ratio. Note that this expression assumes no change in the volume of either phase in the course of the equilibration, a criterion which was met in all of the experiments performed in this work. The model could be adjusted easily to account for measured changes in volume.

The mass balance on the amine extractant is given by:

$$[\bar{B}]_{tot} = \Sigma q[(HA)_p B_q] + [\bar{B}] \quad (4-7)$$

where $[\bar{B}]_{tot}$ is the total concentration of amine extractant, in all forms, in the organic phase. The above expression assumes that no amine extractant is lost to the aqueous phase. For all practical purposes this assumption is accurate.

If the values of the equilibrium constants and the partition coefficient are known, the above equations can be solved simultaneously for the concentrations of all species as a

function of pH, given the initial concentration of total acid in the aqueous phase ($[HA]_{tot,i}$), the total concentration of amine extractant ($[\overline{B}]_{tot}$), and the aqueous-to-organic phase ratio (WS). The loading can then be calculated from Equation 4-3.

The values of the equilibrium constants, K_{pq} , and the partition coefficient, P , are generally obtained from separate experiments performed without pH adjustment and covering a range of acid and amine concentrations. In this work, the values of K_{pq} determined by Tamada et al. were used to model the results for most of the Alamine 336 systems. Values of K_{pq} were not available for the lactic acid/Alamine 336/1-octanol system, nor were they available for any of the Amberlite LA-2 systems studied.

The theoretical curves, calculated from the above model and the values of K_{pq} shown in Table 4-1, are presented in Figures 4-15 through 4-19. The experimental loadings were calculated using both the organic phase and aqueous phase concentration measurements. It is clear from the figures that the two values agree closely, although the values calculated from the aqueous phase measurements are systematically lower than those calculated from the organic phase measurements.

Overall, the models give a good description of the data. The fit for the lactic acid/Alamine 336/MiBK system (Figure 4-15) is excellent. For the other systems, the model predicts somewhat higher loadings than were seen experimentally, and the difference between the model and the experimental data increases somewhat with increasing pH. Good agreement between model and data in the loading-pH experiments requires a good fit of the Law-of-Mass-Action model to the low-concentration data in the experiments performed at low pH. The method used by Tamada et al. to obtain the fitted values of K_{pq} does not necessarily stress the low-concentration data to the extent that is necessary to achieve a good fit to the loading-pH curve in the high pH region. Other methods of fitting may yield better results for this application. Overall, though, the differences between model and data are not major, except possibly in the case of the succinic acid/Alamine 336/1-octanol system. Tamada et al. (79)

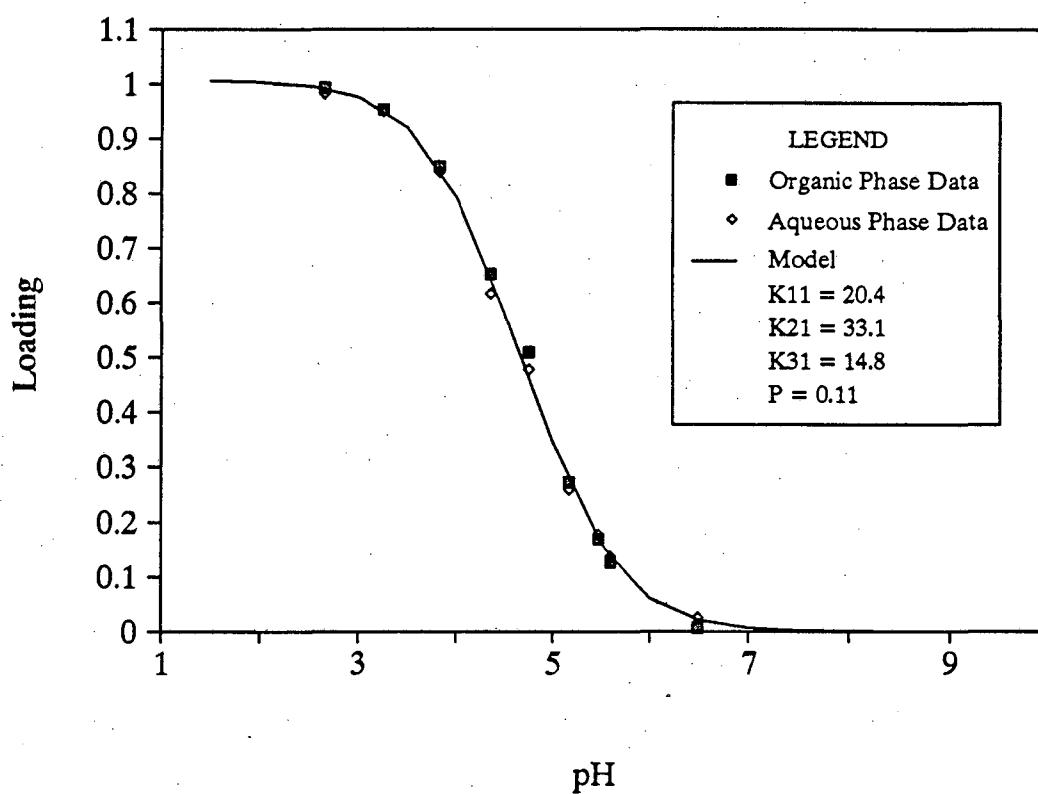


Figure 4-15. Modeling of the Effect of pH on the Extraction of Lactic Acid by Alamine 336 in MiBK
[HA]_{tot} = 0.45 M, [B]_{tot} = 0.30 M, Phase Ratio = 1.0

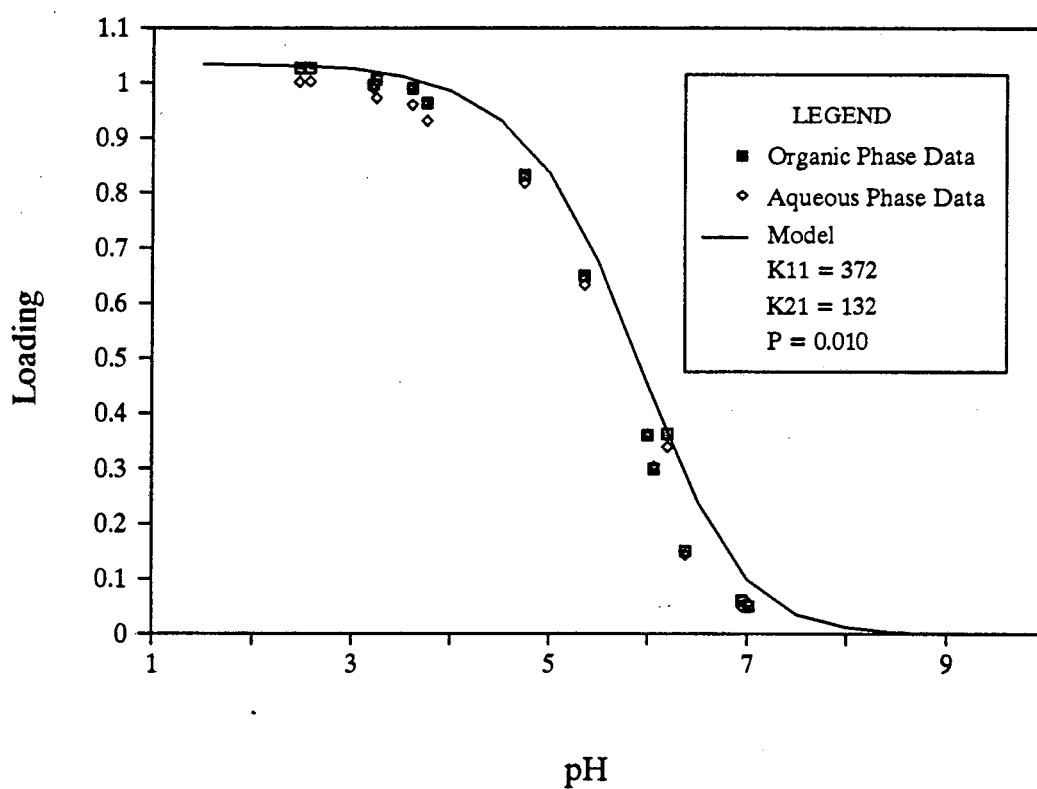


Figure 4-16. Modeling of the Effect of pH on the Extraction of Lactic Acid by Alamine 336 in Chloroform $[HA]_{tot} = 0.45$ M, $[B]_{tot} = 0.30$ M, Phase Ratio = 1.0

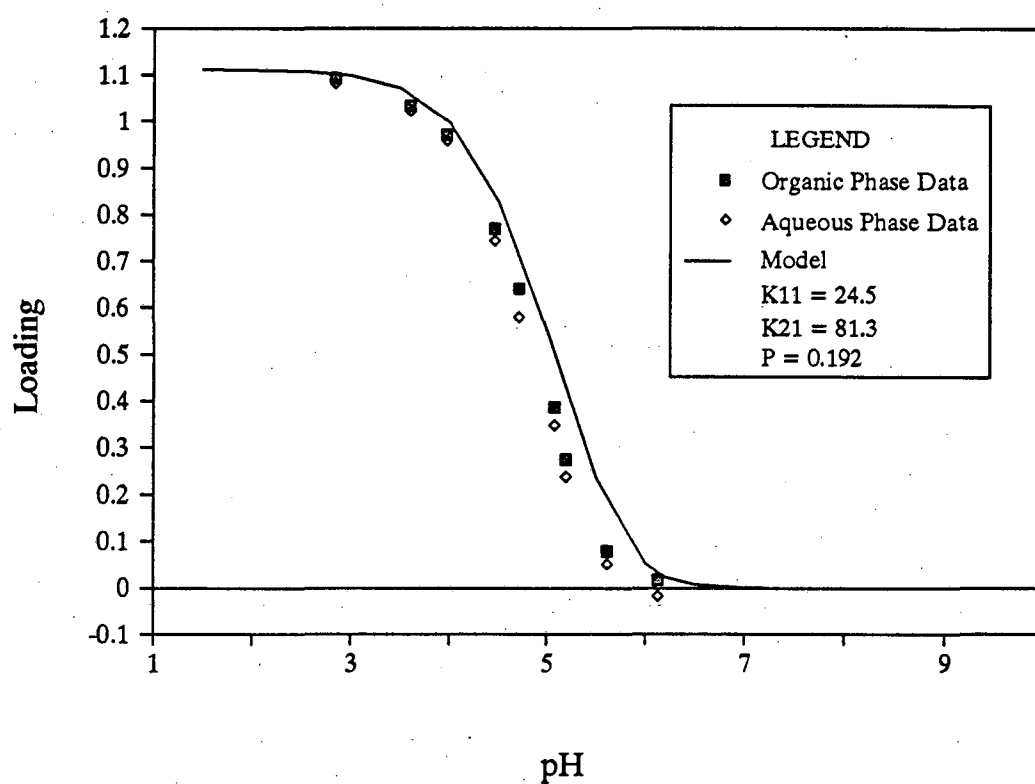


Figure 4-17. Modeling of the Effect of pH on the Extraction of Succinic Acid by Alamine 336 in MiBK
[H₂A]_{tot} = 0.455 M, [B]_{tot} = 0.30 M, Phase Ratio = 1.0

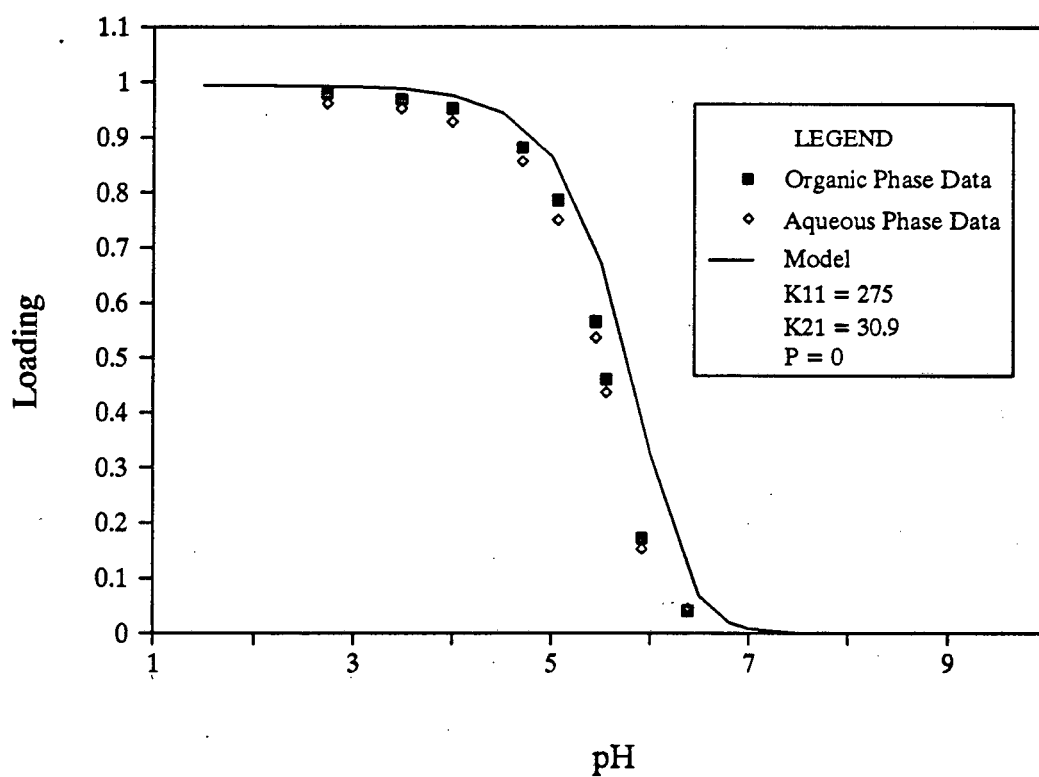


Figure 4-18. Modeling of the Effect of pH on the Extraction of Succinic Acid by Alamine 336 in Chloroform
[H₂A]_{tot} = 0.45 M, [B]_{tot} = 0.30 M, Phase Ratio = 1.0

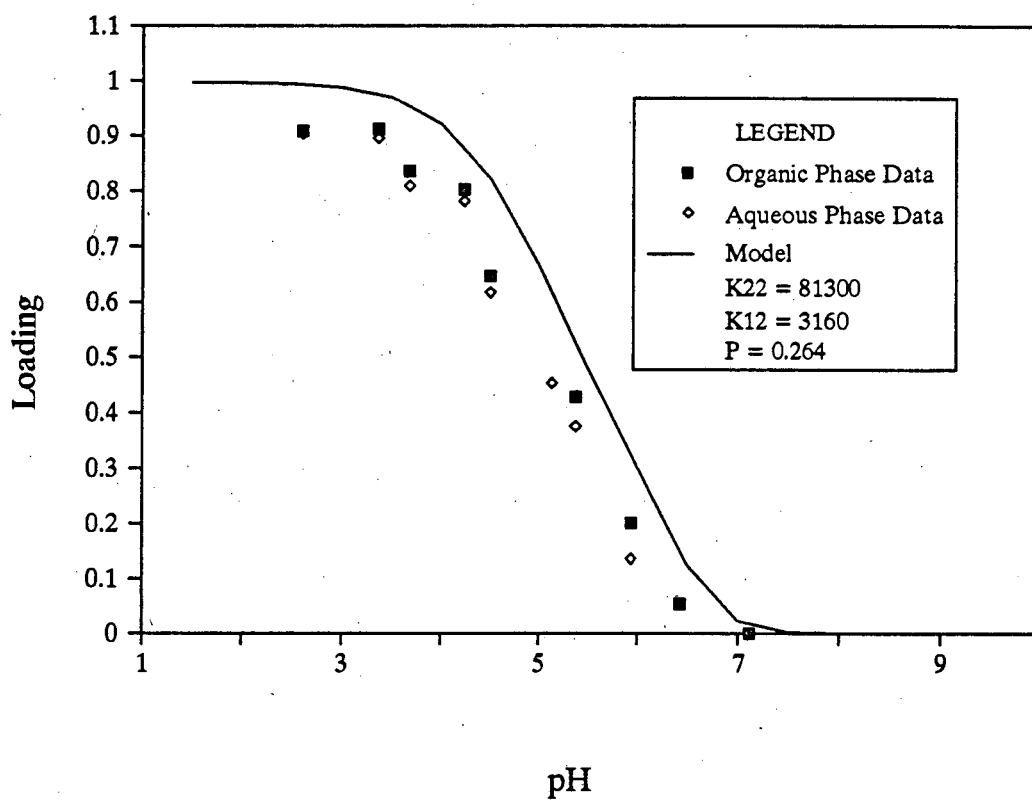


Figure 4-19. Modeling of the Effect of pH on the Extraction of Succinic Acid by Alamine 336 in 1-Octanol
[H₂A]_{tot} = 0.45 M, [B]_{tot} = 0.30 M, Phase Ratio = 1.0

state that there are large uncertainties in the fitted values of K_{pq} for this system.

For design purposes it is helpful to have graphs of loading as a function of pH at a fixed equilibrium concentration of total acid in the aqueous phase. The model presented above can be used to generate such curves. Sample curves are shown in Figures 4-20 and 4-21 for lactic and succinic acid at equilibrium acid concentrations of 0.1 M (approximately 0.9 wt. % lactic acid or 1.2 wt. % succinic acid). Similar curves could be generated for Amberlite LA-2 systems if values of K_{pq} are determined in separate experiments.

4.8 Regenerability of Extracts

4.8.1 Results and Discussion

Poole and King (30) demonstrated that Alamine 336/MiBK extracts of lactic and succinic acids are regenerable by back-extracting with aqueous solutions of TMA. In this work, further experiments were performed to verify that other extracts are also regenerable. Amberlite LA-2/1-octanol extracts of lactic acid were chosen for the back-extraction studies since it is this system for which the strength of complexation is greatest, as evidenced by the fact that there is some degree of loading up to pH 8. A sample of 0.3 M Amberlite LA-2 in 1-octanol was fully loaded with lactic acid ($Z=1.04$) and then back-extracted with aqueous solutions of TMA of varying concentrations. The fractional recovery is shown as a function of the molar ratio of TMA to lactic acid in Figure 4-22. Full recovery of the acid is achieved when at least one mole of TMA is present per mole of acid.

4.8.2 Modeling of Back-Extraction

The curve shown in Figure 4-22 is a smooth curve drawn through the data; it was not possible to calculate a theoretical curve because the values of the various complexation constants are unknown. For systems for which the complexation constants are known, a

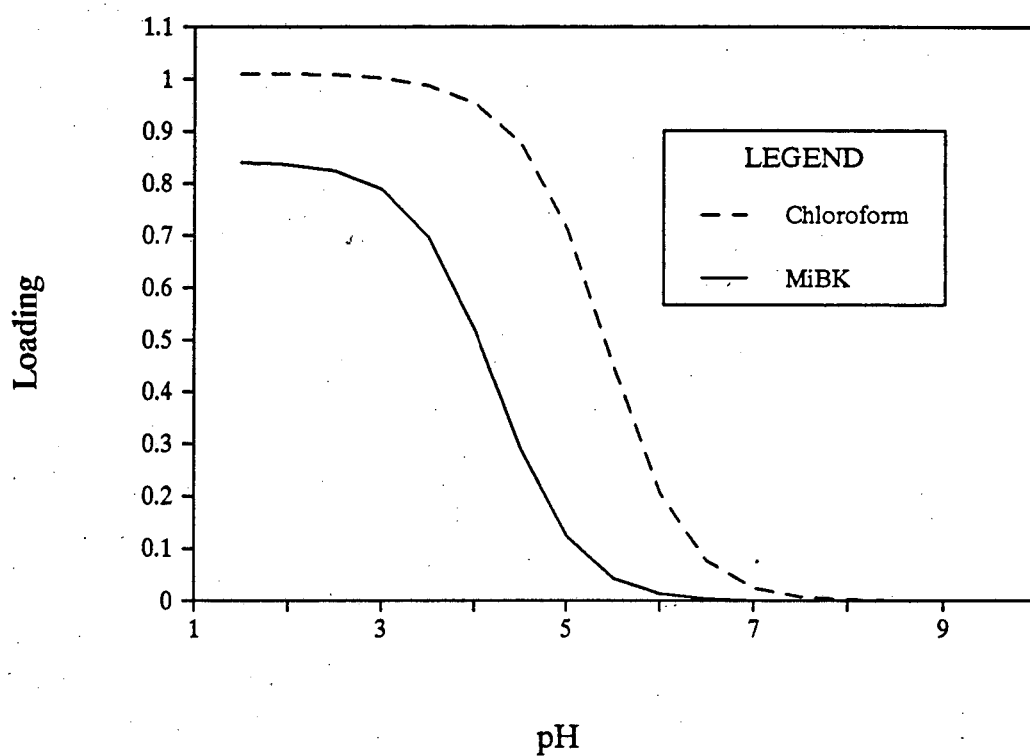


Figure 4-20. Effect of pH on the Loading of 0.3 M Alamine 336 in Various Diluents by Lactic Acid at an Equilibrium Solution Concentration of 0.10 M

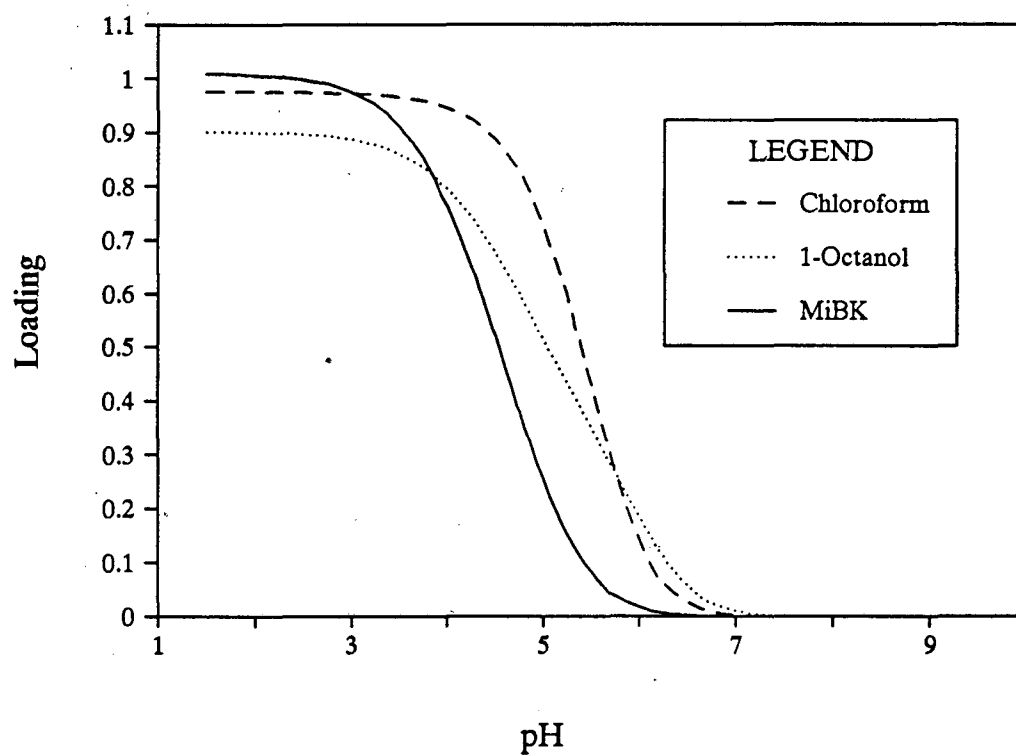


Figure 4-21. Effect of pH on the Loading of 0.3 M Alamine 336 in Various Diluents by Succinic Acid at an Equilibrium Solution Concentration of 0.10 M

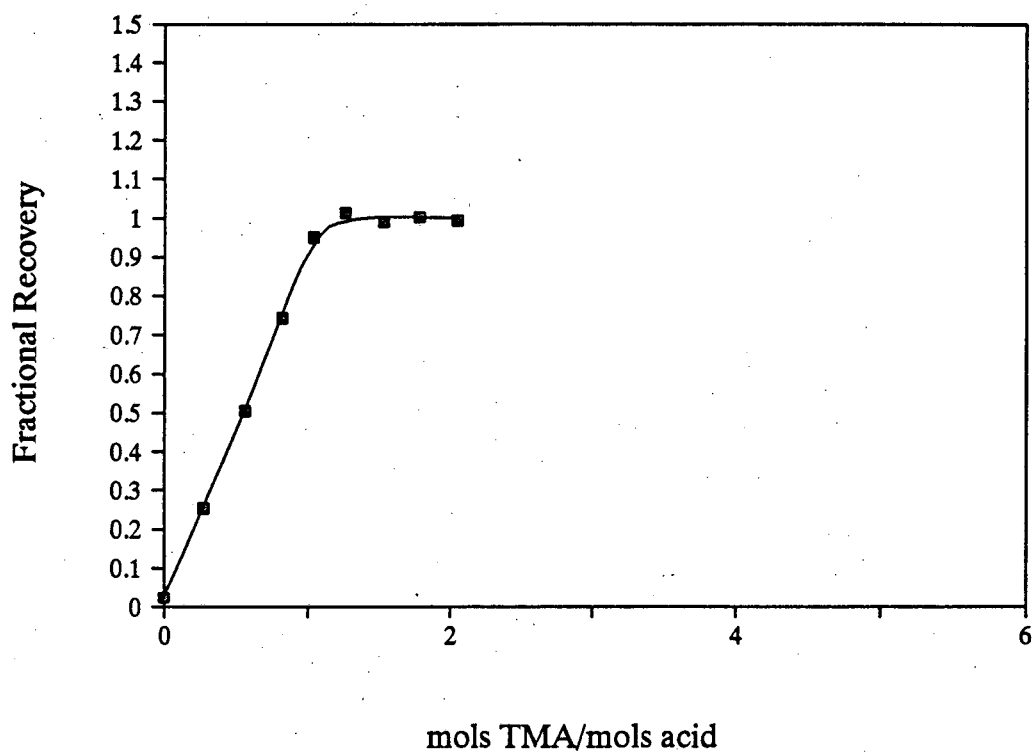


Figure 4-22. Back-Extraction of Lactic Acid from Loaded Amberlite LA-2 in 1-Octanol ($Z = 1.04$) with Aqueous TMA Solutions

theoretical leaching curve can be calculated easily. For a fixed pH, the model presented in Section 4.7.2, with a modified version of Equation 4-6, is solved for the concentration of all species. Equation 4-6 is modified to account for the fact that the acid is initially in the organic phase, and the equation becomes:

$$[\overline{HA}]_{tot,i} = \sum p[(\overline{HA})_p B_q] + \Phi P[HA] + \frac{[HA]WS}{\alpha} \quad (4-8)$$

where $[\overline{HA}]_{tot,i}$ is the concentration of total acid initially present in the organic phase. The recovery of acid is then calculated as:

$$Recovery = \frac{WS * [HA]}{\alpha [\overline{HA}]_{tot,i}} \quad (4-9)$$

The concentration of TMA corresponding to this pH is then calculated exactly as for the sorbent systems (see Section 3.5.1), from the equations for the dissociation of water (Equation 3-32) and TMA (Equation 3-33), the charge balance (Equation 3-34 for a monocarboxylic acid or Equation 3-35 for a dicarboxylic acid) and the mass balance on TMA (Equations 3-38 and 3-39). The molar ratio of TMA to total acid is then given by:

$$\frac{mols \ TMA}{mols \ acid} = \frac{WS [TMA]_{tot}}{[\overline{HA}]_{tot,i}} \quad (4-10)$$

4.9 Process Issues

Two different process issues are touched upon briefly here. In extraction systems, it is important that an efficient separation of the organic and aqueous phases be achieved. The formation of stable emulsions or third phases is thus highly undesirable. In this work, there were no major problems with separation of the organic and aqueous phases. For the succinic acid/Amberlite LA-2/MiBK system, formation of a small amount of a third phase was observed. However the amount of acid in this third phase was low enough that no discernible effect on the mass balance was noted. Tamada et al. (40) report the formation of a coacervate (a third, surface-area-dependent phase) for the succinic acid/Alamine 336/1-octanol system. No such coacervate was observed in this work. Phase-separation characteristics can often be improved through addition of a small amount of an organic modifier to the extractant phase. However, care must be taken to avoid adversely affecting the extraction equilibrium.

A second issue of importance industrially is the rate of the extraction. Previous work with Amberlite LA-2 and carboxylic acids indicates that the complexation reaction itself is instantaneous and thus the extraction rate depends on the rate of mass transfer (99, 100). For this reason, the rate of extraction is highly dependent upon the extraction device used.

Work performed by other researchers with Alamine 336 revealed no problems with rate limitations. In this work, samples of 0.3 M Alamine 336 in 1-octanol contacted with equal volumes of 0.45 M lactic acid on a magnetic stirrer were found to reach equilibrium within 15 minutes or less.

4.10 Summary

Strongly basic extractants, such as Alamine 336 and Amberlite LA-2, can be used to recover carboxylic acids at $\text{pH} > \text{pK}_a$. Furthermore, these extractants can be completely regenerated by leaching with an aqueous solution of trimethylamine. Amine extractants function best in highly active diluents, such as chloroform and 1-octanol, which can stabilize

the acid-amine complex through specific interactions like hydrogen bonding. Secondary amines perform better than similar tertiary amines if the chosen diluent is capable of strongly solvating the additional proton. Such is the case with oxygenated solvents.

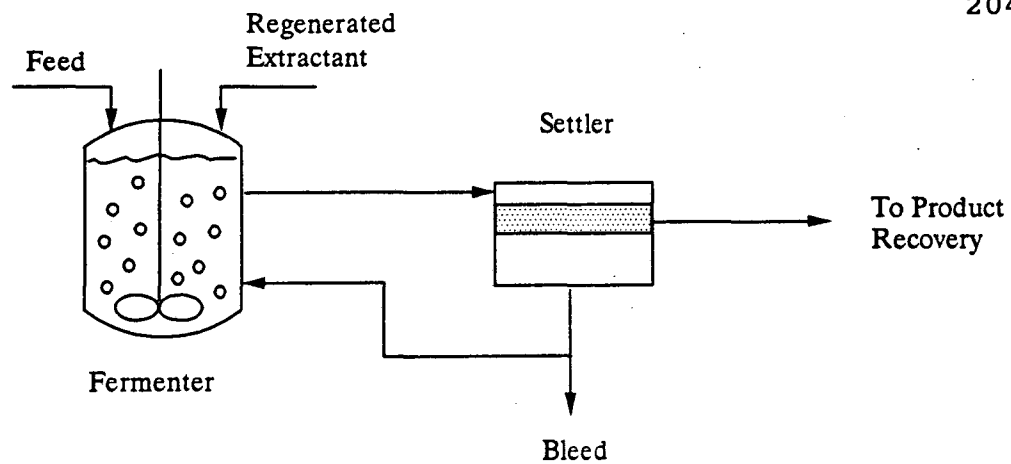
CHAPTER 5. ACTUAL FERMENTATION SYSTEMS

In this chapter issues related to actual fermentation systems are examined. Methods of implementing the sorption/extraction process are described, and complications introduced by using actual fermentation broths are considered. These complications include competitive uptake of other broth components, temperature effects on the sorption/extraction equilibria, and possible toxicity concerns.

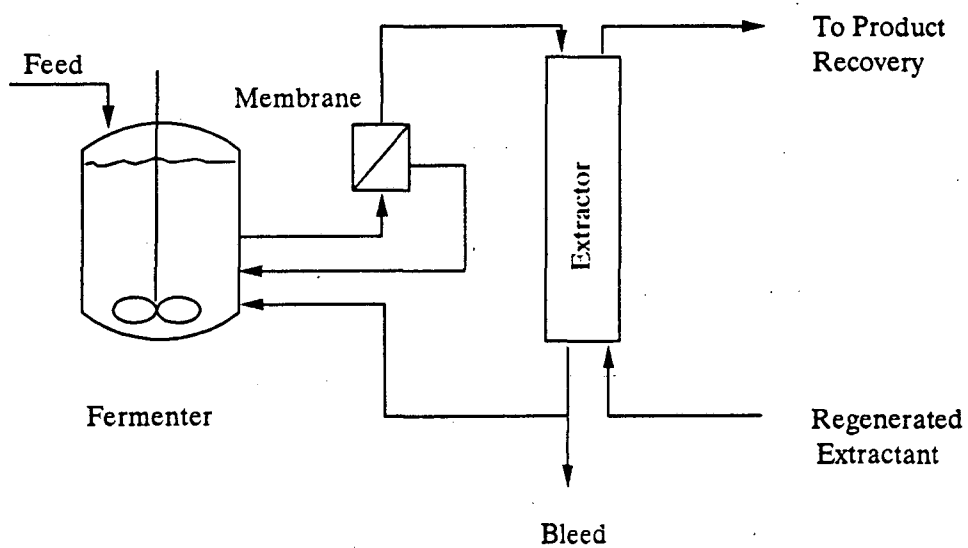
5.1 Implementation of Sorption/Extraction Process

There are at least two basic methods for implementing an extractive fermentation -- *in-situ* and in an external recycle loop. Schematics of these processes are shown in Figure 5-1. Although the fermentations shown are continuous ones, the same basic extraction processes could be used in conjunction with batch fermentations. In Figure 5-1(a), which shows a continuous *in-situ* extraction, the extractant is added directly to the fermenter, and the contents are agitated to promote contact between the two phases. A stream is withdrawn continuously from the fermenter and sent to a settling tank, where the extract and raffinate are separated. The raffinate is returned to the fermenter after a fraction of the stream is bled off. Meanwhile, the extract is sent to a product recovery step, and regenerated extractant is recycled to the fermenter.

The second method of implementation uses an external recycle loop, as shown in Figure 5-1(b). In this case, a stream of broth is withdrawn from the fermenter and sent to an external extraction device, such as a mixer-settler or an extraction column. Whole broth, containing cells, may be sent to the extractor, or a membrane may be inserted, as shown, to remove cells from the broth before the extraction step. In the latter case, the retentate is recycled to the fermenter and the permeate is sent to the extractor. From the extractor, the raffinate stream is recycled to the fermenter. The extract is sent to a product recovery stage,



(a)



(b)

Figure 5-1. Methods of Incorporating Solvent Extraction Process
(a) In-Situ Extraction (b) External Recycle Loop

and regenerated extractant is recycled to the extractor. An important point is that the behavior of an external-recycle-loop process should approach that of an *in-situ* process as the rate of recycle of broth to the fermenter becomes infinitely large.

Roffler et al. (9) discuss some of the advantages and disadvantages of the two approaches. A multi-stage extraction column, used in an external loop, allows for a more efficient use of solvent than the single-stage *in-situ* process. However, if a membrane is used to separate cells from the broth prior to extraction, additional pumping requirements are created and complications such as membrane fouling or degradation may develop. Adding solvent directly to the fermenter is a simpler approach, but the high levels of agitation that are usually employed may result in emulsion formation (9). Moreover, direct contact with solvent may have deleterious effects on the cells. This issue will be discussed in greater detail in Section 5.5.

Examples of both types of processes can be found in the literature, but the use of an external recycle loop seems to have been more prevalent in recent years. Yabannavar and Wang (80) produced lactic acid in an extractive fermentation using an Alamine 336/oleyl alcohol extractant in an external recycle loop. Wang et al. (101) also used an external loop to recover lactic acid from a simulated fermentation broth using a TOPO/kerosene extractant. They used a membrane extractor to prevent direct contact between the extractant and the microorganisms. Seevaratnam et al. (18) used *in-situ* extraction with a batch lactic acid fermentation. They also performed a continuous fermentation with an external recycle loop, using a hollow-fiber filter to remove the cells from the broth prior to the extraction step.

Processes similar to those shown in Figure 5-1 exist for sorptive fermentations, but solids handling problems may make *in-situ* sorption more difficult to implement. When *in-situ* sorption is used with traditional fermenters, there is no simple method for adding and removing sorbent to the fermenter, and attrition of the sorbent particles may be a problem both during the addition and removal steps and in the fermenter itself, due to the action of

the impeller (102). A different approach for *in-situ* implementation, used by Davison and Thompson (8) in a lactic acid fermentation, employs a biparticle fluidized-bed bioreactor (FBR). In this type of reactor, shown in Figure 5-2, sorbent particles are added as a slurry to the top of the fermenter and withdrawn from the bottom, through a star valve. As the sorbent particles fall, they sorb acid from the broth. A bi-particle FBR can be used only if the density and particle size of the sorbent particles are significantly different from those of the cells, so that the settling velocities are different. Otherwise, either cells will be lost from the reactor, or sorbent particles will build up in the column. To a certain extent, differences in size and density can be controlled, for example by immobilizing the cells in an alginate gel bead. However, immobilization may introduce rate limitations. The use of a bi-particle FBR solves the problem of how to remove sorbent from the fermenter. However, attrition of the sorbent particles remains a concern.

A simpler approach may be to use a sorption column in an external recycle loop. Unlike the extractive fermentation shown in Figure 5-1(a), sorptive fermentation with a single column cannot be run as a truly continuous process. However, if two columns are used, with each alternating between sorption and regeneration/product-recovery modes, a continuous process can be achieved. A simulated-moving-bed process, such as the Sorbex process (65), could also be utilized.

If a packed column is used, the broth must be filtered to remove cells and other solids before the stream is sent to the column. The column can become plugged if even low levels of solids are present in the feed (103). An alternate approach is to use a fluidized bed adsorber, which allows cells and other broth solids with the proper density and particle size to pass through the bed. Gailliot et al. (103) used fluidized bed adsorption to recover immunomycin from unfiltered fermentation broths. The fluidized bed adsorber functions in essentially the same manner as the biparticle FBR. Although, in this case, the sorption

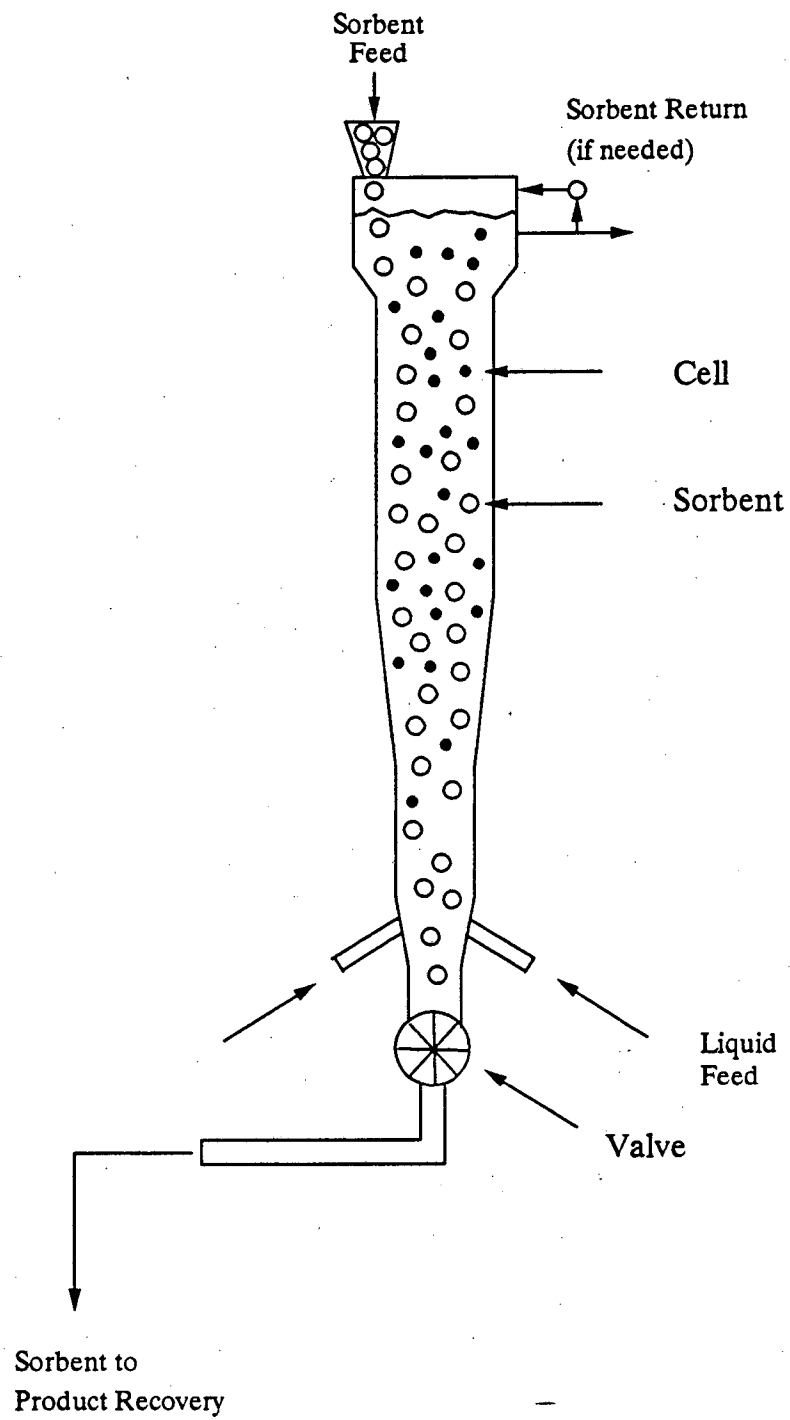


Figure 5-2. Biparticle Fluidized-Bed Bioreactor
(from Davison and Thompson [7])

technically does not take place in the fermenter, this process is very much like an *in-situ* sorption process, since cells and sorbent particles come into direct contact with each other.

5.2 Nature of the Fermentation Broth

All of the experimental results presented in Chapters 3 and 4 were for model solutions, containing only the carboxylic acid of interest and, in experiments in which solution pH was adjusted, sodium ions. Moreover, all experiments were performed at 25 °C. Real fermentation broths differ from model solutions in several key respects. In general, fermentation broths are quite complex, containing many other chemical species in addition to the carboxylic acid product. Competitive uptake of other species by the extractant or adsorbent therefore may be an issue. In addition, the fermentation is routinely run at temperatures higher than ambient. Since equilibrium uptakes of acid by basic sorbents and extractants are a function of temperature, it is clear that the effect of temperature on the sorption/extraction equilibria must be considered. Finally, real fermentation broths contain living microorganisms, which may be sensitive to chemicals with which they come in contact. Thus, potential toxic effects of sorbents and extractants must be considered.

5.3 Competitive Uptake of Other Species

5.3.1 Broth Compositions

Broth compositions differ from one fermentation system to the next and are a function of the type of microorganism, the desired product and the choice of substrate. Listings of typical media for selected microorganisms are given by several sources (104, 105).

A typical broth must contain sources of carbon, nitrogen, phosphorous and sulfur, as well as sources of energy. Various organic compounds function as carbon and energy sources, and phosphorous can be supplied in the form of phosphate salts. The form in which nitrogen

and sulfur are supplied depends on the needs of the microorganism. Many bacteria can utilize nitrates and sulfates, but some require a reduced form. Nitrogen is therefore commonly supplied in the form of ammonium salts. Requirements for reduced sulfur are somewhat rarer. Often, nitrogen and sulfur can be obtained from amino acids or peptones (protein degradation products) (106).

Various metallic elements, including potassium, magnesium, calcium, iron, manganese, cobalt, copper, molybdenum and zinc, are also required by almost all microorganisms (106). Potassium, magnesium, calcium and iron are required in larger amounts and are usually included as cations of inorganic salts in the broth formulation. The remaining elements are required in only trace amounts, if at all (106).

Other growth factors that may be required are amino acids, purines and pyrimidines (building blocks of nucleic acids) and vitamins (106). Often, yeast extract is used to provide amino acids, peptides, vitamins, nucleic acid fractions and carbon compounds (105).

Broths are often buffered with, for example, phosphate salts. Low levels of buffering must be used since most microorganisms can tolerate only 5 g/l of potassium phosphates at the most (106). In acid-producing fermentations, this buffer capacity is consumed quickly. Thus, although broths may be described as "buffered", often they are not (106).

Other species present in the broth include any side-products of the fermentation. For example, some lactic acid bacteria are homofermentative, producing only lactic acid, whereas others are heterofermentative, producing lactic acid and other by-products such as acetic acid, carbon dioxide, ethanol and glycerol (3).

Finally, the composition of broth will also depend on the nature of the raw material (substrate) used in the fermentation. Common substrates in lactic acid fermentations are refined sucrose and dextrose. Ultimately, however, it would be desirable to use other (waste) biomass, such as corn starch, beet sugar, whey, etc. These raw materials are, of course, much more complex, and introduce a myriad of components into the broth.

Three examples of typical broths for *L. delbreuckii* are given in Table 5-1. Some species, such as unessential cations that serve as counter-ions for essential anions, have been omitted. Most ionic species are present at 0.5 wt.% or less, and some, like Fe^{3+} , are present at extremely low levels. The concentration of phosphate is at most 0.37 wt.% (equivalent to 5.3 g/l KHPO_4), and that of sulfate less than 0.05 wt.%.

Table 5-1. Compositions of Representative Fermentation Media for *L. delbreuckii*

Component	Concentrations in Wt.%		
	MRS Broth (107)	ATCC 1006 Broth (104)	ATCC 80 Broth (104)
Yeast Extract	0.5	0.5	0.5
Peptone	1.0	-	-
Trypticase	-	1.0	1.0
Tryptose	-	0.3	-0
L-Cysteine HCl	-	0.02	-
Glucose	2.0	0.5	1.0
Tween 80	0.1	0.1	-
PO_4^{3-}	0.11	0.37	0.06
SO_4^{2-}	0.01	0.03	0.02
Acetate	0.22	0.07	0.90
Citrate	0.16	-	-
NH_4^+	0.04	-	-
Mg^+	0.002	0.006	0.004
Mn^+	0.001	0.004	0.0004
K^+	0.09	0.2	0.04
Fe^{3+}	-	0.0007	0.0004
Cl^-	-	-	0.0006

5.3.2 Expected Interferences

The interaction between the carboxylic acid molecule and the basic amine extractant or sorbent is a highly specific one, and major interferences are expected to come primarily from other acids. Interfering acids include by-products, such as acetic acid, and any other acids that are added to the medium initially, such as citric acid. Furthermore, anions of strong acids, such as sulfate, phosphate, and chloride, may also be taken up, as the corresponding acids, by basic sorbents and extractants. San-Martín, et al. (108) looked at the extraction of lactic acid by Alamine 336 in toluene in the presence of sodium chloride and lactose. They found that the presence of lactose had no effect on the extraction of lactic acid, but the presence of sodium chloride resulted in lower levels of extraction. Reschke and Schügerl (109) also observed that, in the extraction of penicillin G ($pK_a = 2.75$) by Amberlite LA-2, some co-extraction of citrate and phosphate buffer components occurred. However, in a separate paper (15), they note that the presence of (unspecified) buffer and chloride ions does not greatly influence the extraction of penicillin.

Other, non-acidic broth components may also be taken up by strongly basic sorbents or extractants. In the case of polymeric sorbents, for example, some species may be sorbed through hydrophobic interactions with the polymer backbone. Such effects are expected to be relatively minor. However, Kaufman et al. (23) do report significant uptakes of glucose by Reillex 425 in lactic acid fermentations. Certainly, basic polymeric sorbents and extractants are expected to take up carboxylic acids much more selectively than non-functionalized polymeric sorbents, activated carbons, or physical solvents.

5.3.3 Experiments with an Actual Fermentation Broth

An actual fermentation broth was used in a simple screening experiment designed to identify which components of the broth are most likely to interfere with the uptake of the carboxylic acid product by basic sorbents and extractants. The broth, obtained from the

Bioprocessing Research and Development Center at Oak Ridge National Laboratory, is from a fermentation of glucose to lactic acid by *L. delbreuckii*. The initial composition of the medium is given in Table 5-2.

During the fermentation, a value of pH greater than 5 was maintained through periodic addition of NaOH. The final concentration of lactic acid was 9.9 g/l, and small amounts of acetic acid (0.38 wt.%) and ethanol (0.29 wt.%) were also present. The broth was centrifuged to remove the cells and filter-sterilized before shipping (110).

Table 5-2. Initial Composition of Fermentation Broth Used in Experiments

Component	Concentration in Wt.%
Glucose	1.0
Yeast extract	0.5
(NH ₄) ₂ SO ₄	0.05
MgSO ₄	0.03
KH ₂ PO ₄	0.20
K ₂ HPO ₄	0.20

Dowex MWA-1 was tested for its ability to sorb lactic acid from this fermentation medium. Compared with industrial fermentation broths, this broth contains a relatively low concentration of lactic acid and relatively high phosphate and sulfate concentrations. Therefore, for the sorption experiments, the broth was diluted to sulfate concentrations of 0.051 wt.% or less and phosphate concentrations of 0.21 wt.% or less. The solutions were then supplemented with additional lactic acid, bringing the total lactic acid concentration to 1.4 wt.%, which is within the range typical of industrial fermentations. The pH of the initial

solution varied somewhat depending upon the relative amounts of original broth and added lactic acid.

In each experiment, 18.3 g solution were contacted with 0.5 g sorbent, and the equilibrium uptakes of lactic acid, acetic acid and ethanol were measured. The uptakes of sulfate and phosphate were not measured because, at the time this experiment was performed, no quantitative analytical technique was available for measuring the concentrations of these species. Qualitative measures of these concentrations were obtained by monitoring the size of the appropriate peaks on the high-performance liquid chromatogram, but reliable, quantitative results could not be obtained because the peaks emerged at the void volume of the chromatography column.

The experimental results are summarized in Table 5-3. The experimental uptakes of lactic acid are shown, as are the uptakes predicted from the sorption isotherm at the equilibrium pH. Initial concentrations of sulfate and phosphate were calculated from the concentrations given for the initial broth and from the known dilution factor. The actual concentrations may be somewhat higher or lower, but the relative concentrations from one sample to the next will remain the same.

Table 5-3. Results of Sorption Experiments with Actual Fermentation Broth

Initial Solutions				Final Solutions		$W_o\Delta C/m$ (g/g)	Predict- ed q (g/g)
Wt.% SO_4^{2-}	Wt.% PO_4^{3-}	Wt.% Acid	pH	pH	Wt.% Acid		
0.051	0.211	1.46	3.99	5.71	1.15	0.114	0.169
0.012	0.049	1.43	3.15	3.80	0.63	0.292	0.333
0.003	0.013	1.42	2.73	3.16	0.52	0.330	0.336

The difference between the experimental and predicted uptakes increases as the initial concentrations of phosphate and sulfate increase. The experimental chromatographs also

showed a decrease in the areas of the sulfate and phosphate peaks from the initial to the final solutions. Therefore, it appears that the lower-than-predicted lactic acid uptakes are due to competitive uptake of sulfate and/or phosphate.

In all cases, no discernable amounts of acetic acid or ethanol were sorbed. It is possible that at higher concentrations, these species would be sorbed significantly. However, ethanol, which has no acidic functional groups, is not expected to compete with lactic acid for basic functional groups.

5.3.4 Phosphate/Sulfate Uptake Experiments

Additional experiments were performed to quantitate the effects of sulfate and phosphate on the sorption and extraction of lactic acid. The ion chromatograph was used to obtain quantitative measures of sulfate and phosphate concentrations. The initial experiments were performed with the sorbent Dowex MWA-1. In later experiments, separation factors were determined for the two amine extractant systems as well.

5.3.4.1 Phosphate/Sulfate Uptake by Dowex MWA-1

Figures 5-3 and 5-4 present sorption isotherms for the uptakes of sulfuric and phosphoric acids by Dowex MWA-1. The isotherms show very steep initial slopes, indicating that both species are strongly sorbed. The slopes both appear to be greater than the initial slope from the comparable isotherm for lactic acid (Figure 3-10). This observation is consistent with the fact that both phosphoric and sulfuric acids are more strongly acidic than lactic acid. The initial slope for phosphoric acid appears to be steeper than that for sulfuric acid, which is not expected based on acid strength alone. However, with very steep isotherms, it is difficult to determine the initial points with great precision. Furthermore, the slopes may be affected by the di- and tri-functionalities of sulfuric and phosphoric acids, respectively.

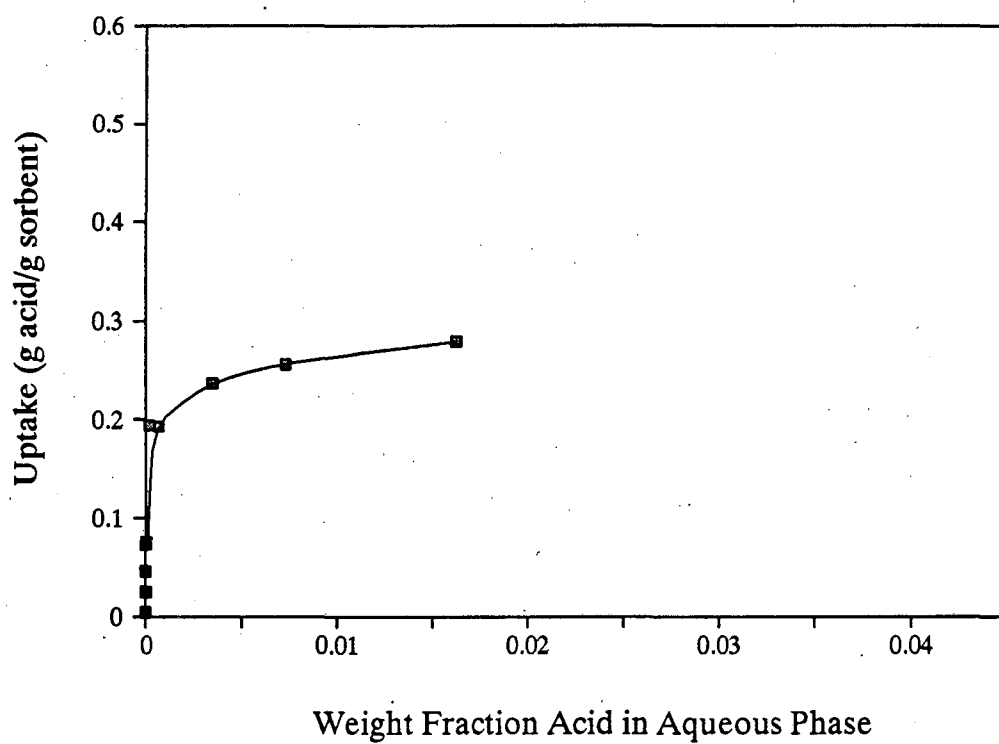


Figure 5-3. Uptake of Sulfuric Acid by Dowex MWA-1

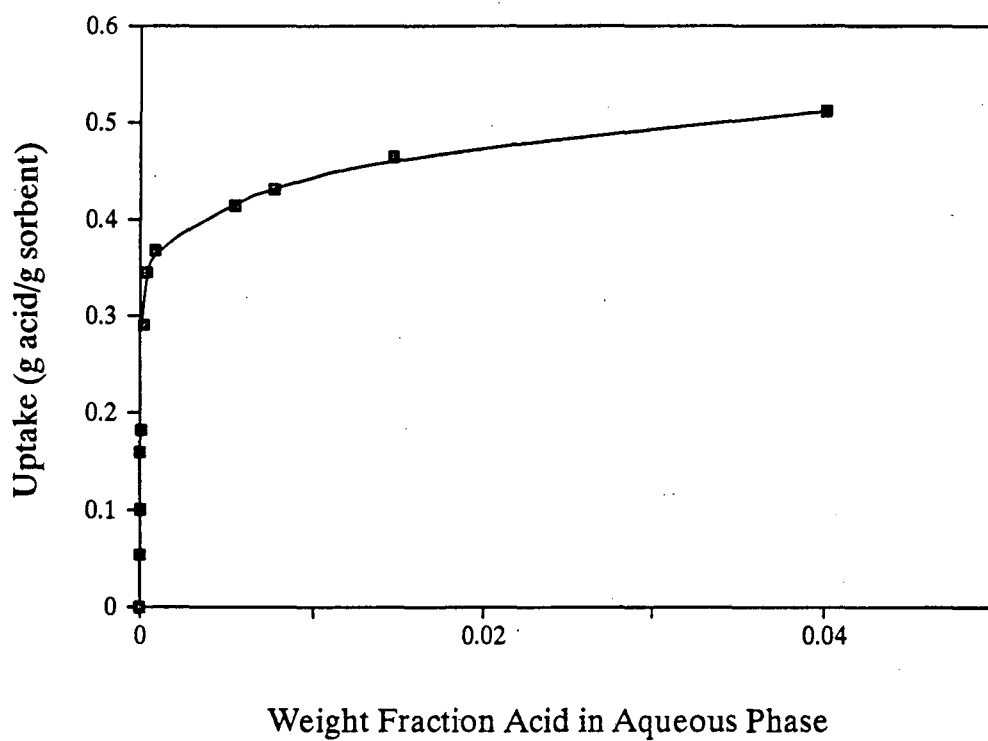


Figure 5-4. Uptake of Phosphoric Acid by Dowex MWA-1

Breakthrough curves were also generated for solutions of lactic acid and sodium phosphate or sodium sulfate on Dowex MWA-1. In Figure 5-5, breakthrough of a solution containing 4.00 wt.% lactic acid and 0.06 wt.% SO_4^{2-} is compared with that of a similar lactic acid solution containing no SO_4^{2-} . The pH values of both feed streams were unadjusted. Although the concentration of the added sulfate is on the high end of what would be seen in an actual fermentation broth, the effect on the breakthrough curve is minimal. Figure 5-6 shows a similar set of curves comparing breakthrough of 4.00 wt.% lactic acid alone and with 0.25 wt.% PO_4^{3-} , which is near the expected maximum concentration. In this case, because of the much higher anion concentration, there is a significant effect on the breakthrough curve. Lactic acid begins to break through at only one bed volume in the presence of phosphate, whereas breakthrough occurs between three and four bed volumes in the absence of phosphate.

Figures 5-7 and 5-8 present breakthrough and TMA leaching curves for experiments performed with lactic acid and very high concentrations of sodium sulfate and sodium phosphate. In these experiments, the concentrations of sulfate and phosphate, as well as the concentration of lactic acid, were monitored. In the phosphate experiment, pH was also monitored. The anion concentrations (0.6 wt.% SO_4^{2-} and 0.64 wt.% PO_4^{3-}), which are much higher than those found in actual fermentation broths, were chosen to magnify the observed effects.

Several important observations can be made. In both graphs, lactic acid breaks through very quickly, while the inorganic anion takes much longer to emerge from the column. The lactic acid that breaks through initially must be in the ionized (lactate) form, since a proton originally associated with a lactic acid molecule must pair with the inorganic anion before it can be sorbed. This hypothesis is confirmed by the pH measurements shown in Figure 5-8, which show much higher values of pH in the first few bed volumes than would be expected for the breakthrough of lactic acid alone. The breakthrough of lactate also

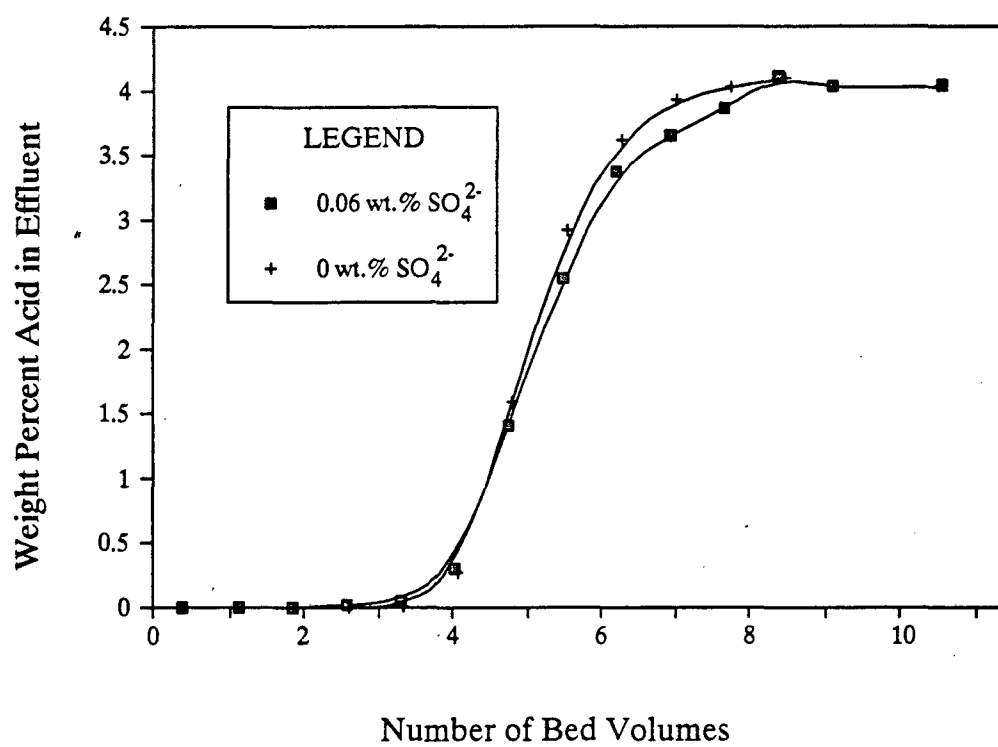


Figure 5-5. Effect of Sulfate on Breakthrough of 4.00 wt.% Lactic Acid on Dowex MWA-1

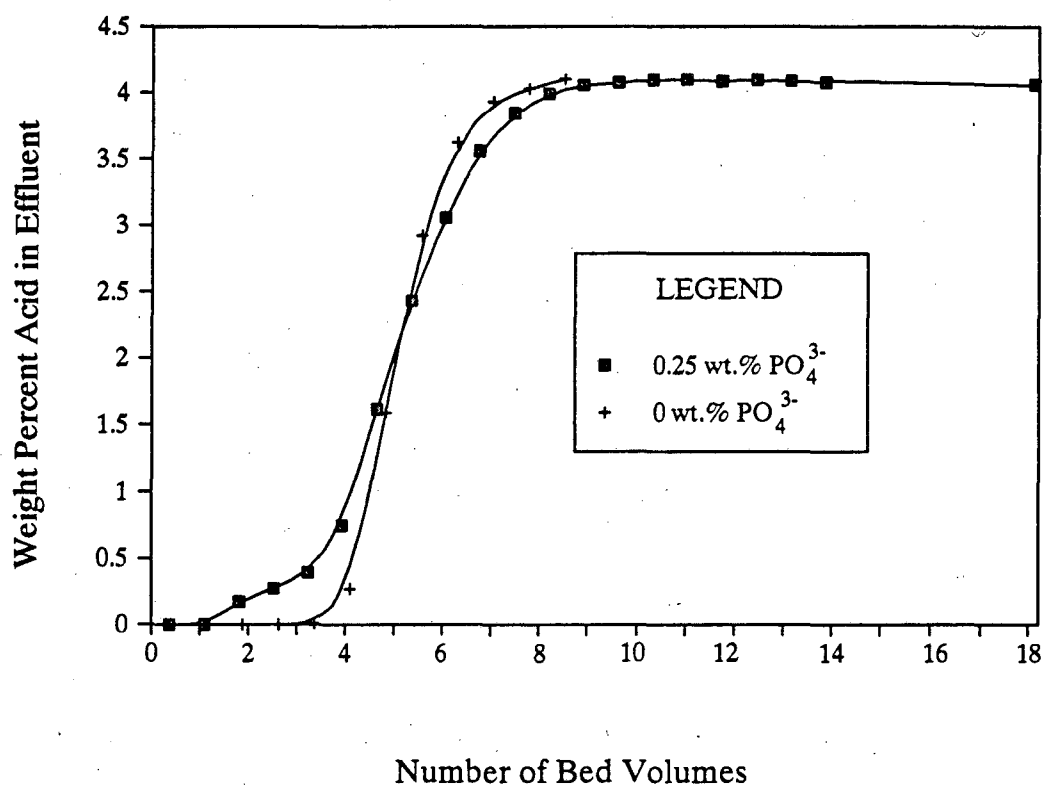


Figure 5-6. Effect of Phosphate on Breakthrough of 4.00 wt.% Lactic Acid on Dowex MWA-1

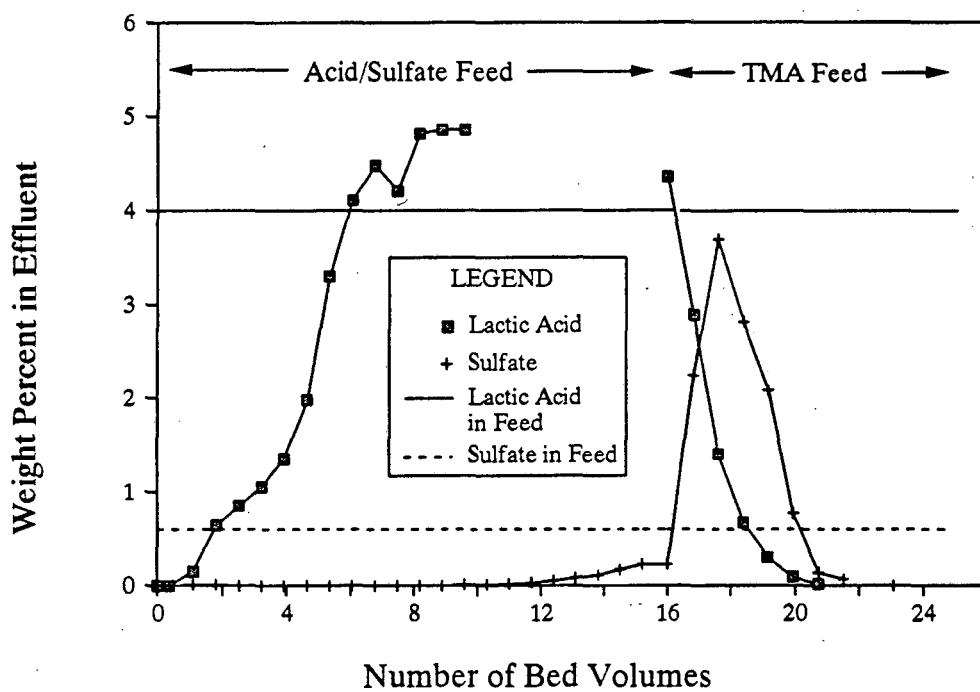


Figure 5-7. Breakthrough and Leaching Curves for Lactic Acid and Sulfate on Dowex MWA-1, $F = 1.5$ ml/min, $L = 24.5$ cm
 Feed: 4.00 wt.% Lactic Acid, 0.60 wt.% Sulfate; TMA Feed: 4.82 wt.%

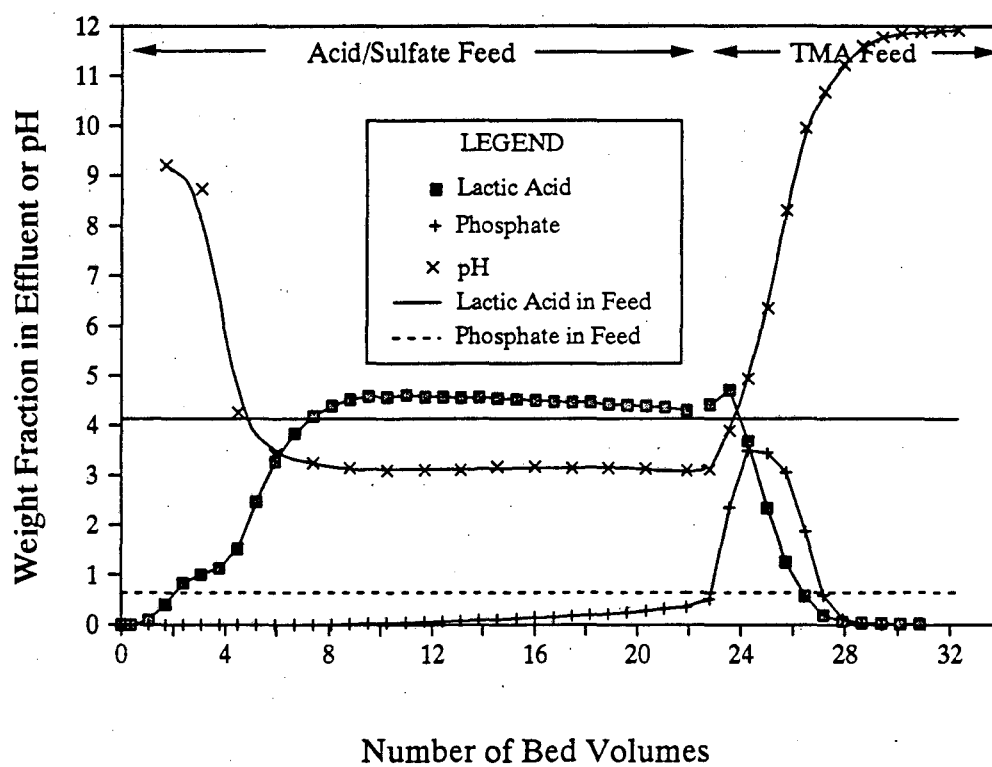


Figure 5-8. Breakthrough and Leaching Curves for Lactic Acid and Phosphate on Dowex MWA-1, $F = 1.5$ ml/min, $L = 24.5$ cm
 Feed: 4.13 wt.% Lactic Acid, 0.64 wt.% Phosphate; TMA Feed: 5.36 wt.%

accounts for the inflection point observed in the initial part of all the breakthrough curves involving inorganic anions.

It should also be noted that, after about six bed volumes, the concentration of lactic acid in the effluent reaches a value greater than that of the feed. This concentration effect occurs both because sulfate is being removed from solution and also, presumably, because sulfate displaces acid that was sorbed earlier in the process.

The above discussion points to methods for overcoming the effect of strong-acid anions on the sorption of lactic acid. A small pre-column could be used before the lactic acid-recovery column to remove the anions in the form of their acids. The effluent from this column would contain all non-sorbable species, lactic acid, and small amounts of lactate associated with some counter-ion(s) (e.g., Na^+ , K^+). This stream could then be passed through a small bed of cation exchange material, which would remove the cations and replace them with H^+ . The stream would then be sent to the lactic acid-recovery column. Both pre-columns would, of course, need to be regenerated, and the recovered ions would have to be recycled back to the broth. However, since the concentrations of these ions are extremely low, it is not expected that large volumes of material will need to be processed.

Figures 5-7 and 5-8 also present curves for experiments in which the loaded sorbent was leached with a solution of aqueous TMA. Both lactic acid and the inorganic ions are recoverable by this method. Furthermore, the results indicate that there is an additional separating effect in this stage of the process, evidenced by the fact that the lactic acid and sulfate or phosphate peaks do not completely overlap. This observation is consistent with the fact that lactic is the weaker of the two acids. The percent recoveries calculated from the areas under the curves are 112% for sulfate and 95% for phosphate. If these recoveries are assumed to represent 100% recovery within experimental error, there is no evidence of irreversible build-up of strong acids on the column.

Because of the uncertainties in the values of percent recovery obtained from the column leaching experiments, the leachabilities of these strong acids were also tested in separate batch studies. Samples of Dowex MWA-1 were loaded with sulfuric acid and leached with aqueous TMA, using a molar ratio of TMA to acid equal to 2.7. Samples were also loaded with phosphoric acid and leached with TMA using a ratio of 2.0 moles TMA per mole acid. In both cases, 100% recovery of the acid was achieved.

5.3.4.2 Separation Factors

Batch equilibrium experiments were used to determine separation factors for sulfate/lactic acid and phosphate/lactic acid in sorbent and extractant systems. The separation factor, α , is a measure of the relative partitioning of the two species between the aqueous and organic phases and, for sulfate-containing systems, is given by:

$$\alpha = \frac{\overline{C_{SO_4}}/C_{SO_4}}{\overline{C_a}/C_a} \quad (5-1)$$

where C_{SO_4} is the concentration of sulfate, C_a is the concentration of lactic acid, and the overbars denote the organic phase. The value of α for phosphate-containing systems is calculated in an analogous manner. For sorbent systems, the concentration in the organic phase is given by the composite uptake. It is understood that uptake of these anionic species occurs through the acid form.

Tables 5-4 and 5-5 present the experimentally determined values of α for sulfate- and phosphate-containing systems, respectively, at lactic acid concentrations of 2 wt.%. One sorbent (Dowex MWA-1) and two extractants (Amberlite LA-2 and Alamine 336) were examined. The sulfate and phosphate in these systems were supplied in the form of the sodium salt, and the pH values of the solutions were not adjusted. The sulfate concentrations

(0.1-0.2 wt.%) and phosphate concentrations (0.5-0.6 wt%) are somewhat higher than what would typically be found in a fermentation broth.

Table 5-4. α Values for Sulfate/Lactic Acid

Sorbent/Extractant	Wt. % Lactic Acid	Wt. % SO ₄	α
Dowex MWA-1	2	0.1	124
Amberlite LA-2 /MiBK	2	0.2	5.4
Amberlite LA-2/ 1-Octanol	2	0.2	11.1
Alamine 336/ MiBK	2	0.2	4.2
Alamine 336/ 1-Octanol	2	0.2	13.2

The results indicate that uptake of sulfate is generally much stronger than uptake of phosphate, despite the fact that the phosphate was present at higher concentrations. In fact, in extractant systems, competitive uptake of phosphate was not observed. Furthermore, uptake of both anions is much greater for sorbents than for extractants, presumably because the sorbent provides an aqueous environment whereas the extractant provides a more organic one. The organic environment tends to favor organic molecules, such as lactic acid, over inorganic acids like sulfate and phosphate. There are no major differences in behavior between systems containing Amberlite LA-2 and Alamine 336. There does, however, appear to be a diluent effect. The less active, less polar diluent MiBK takes up anions to a lesser extent than the more active, more polar diluent 1-octanol. Unfortunately, if a less active diluent is chosen to minimize the competitive uptake of strong-acid anions, the effectiveness of the extractant at $\text{pH} > \text{pK}_a$ is also reduced.

Table 5-5. α Values for Phosphate/Lactic Acid

Sorbent/Extractant	Wt. % Lactic Acid	Wt. % PO ₄	α
Dowex MWA-1	2	0.5	3.8
Amberlite LA-2 /MiBK	2	0.6	0
Amberlite LA-2/ 1-Octanol	2	0.6	0
Alamine 336/ MiBK	2	0.6	0
Alamine 336/ 1-Octanol	2	0.6	0

5.3.5 Summary and Conclusions

Competitive uptake of anions by basic sorbents and extractants is an issue that must be addressed in a commercial fermentation process. Fortunately, these anions are, in general, present at very low concentrations. Uptake of anions of strong acids, such as sulfate, pose the greatest problems, and competitive uptake in general is more of a concern with sorption than with extraction. There are several possible means for dealing with sulfate and/or phosphate in feed streams. As discussed in Section 5.3.4.1, a pre-column could be used before the actual recovery column to remove anions. A cation-exchange column could also be used to re-supply the protons that were pulled out of solution. Alternatively, a mixed bed could be used to perform both operations simultaneously. This would be a relatively simple procedure given the low levels of anions present in the broth.

A second approach would be to use a sorbent that is selective for lactic acid over sulfuric and phosphoric acids. Metal ligand exchangers show some promise in this respect but appear to have other major disadvantages, which were described in Chapter 1.

5.4 Temperature Effects

Due to the nature of the microorganisms used, the optimum operating temperatures for many carboxylic acid fermentations are higher than ambient. Lactic acid, for example, is typically produced at temperatures of 45-60 °C for *L. delbreuckii* and 43 °C for *L. bulgaricus* (3). Yabannavar and Wang (80) did, however, perform a lactic acid fermentation using *L. delbreuckii* at 37 °C. Obviously, it is important to have an understanding of the effects of temperature on the sorption and extraction equilibria.

5.4.1 Effects of Temperature on Sorption/Extraction Equilibria

Tamada and King (26) studied the effects of temperature on the extraction of lactic and succinic acids by Alamine 336 in MiBK and chloroform. Values of K_{pq} were determined for these systems at temperatures ranging from 0 to 55 or 75 °C. In this work, the values of K_{pq} given by Tamada and King were used to calculate amine loading as a function of pH at different temperatures. The effects of temperature on the loading of 0.3 M Alamine 336 in chloroform by succinic and lactic acids are shown in Figures 5-9 and 5-10, respectively. The equilibrium acid concentrations in the aqueous phase are 0.10 M. For succinic acid, only values of K_{11} were used in the calculations, since Tamada and King do not give values of other K_{pq} at temperatures other than 25 °C. Thus, the curve given for succinic acid at 25 °C may be somewhat different from that shown in Figure 4-21.

It is clear from Figures 5-9 and 5-10 that increased temperatures lead to lower overall loadings. Furthermore, since values of K_{11} decrease as temperature is increased, extractants show decreased ability to sustain capacity at $\text{pH} > \text{pK}_a$. The results of Tamada and King indicate that the apparent enthalpies of formation of amine-carboxylic acid complexes are more exothermic for succinic acid than for lactic acid and more exothermic in chloroform than in MiBK. Values of K_{pq} , and hence uptakes of carboxylic acid, will be more sensitive to increases temperature for systems with more exothermic enthalpies of complex formation.

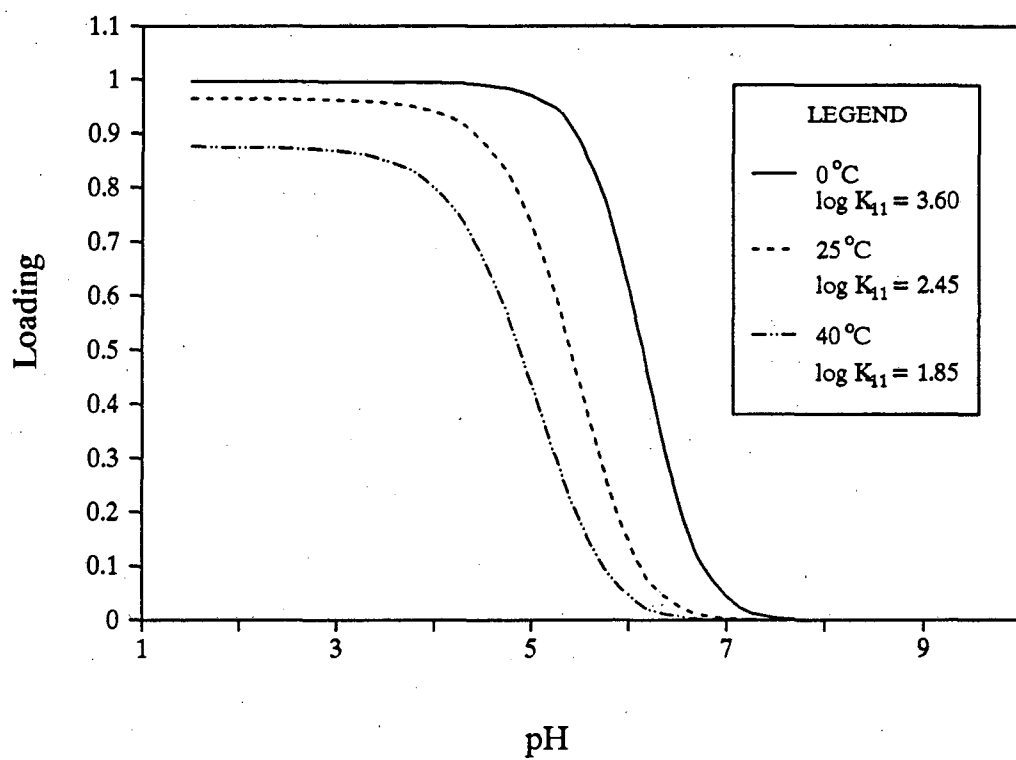


Figure 5-9. Effect of Temperature on the Loading of 0.3 M Alamine 336 in Chloroform with Succinic Acid at an Aqueous Phase Concentration of 0.1 M

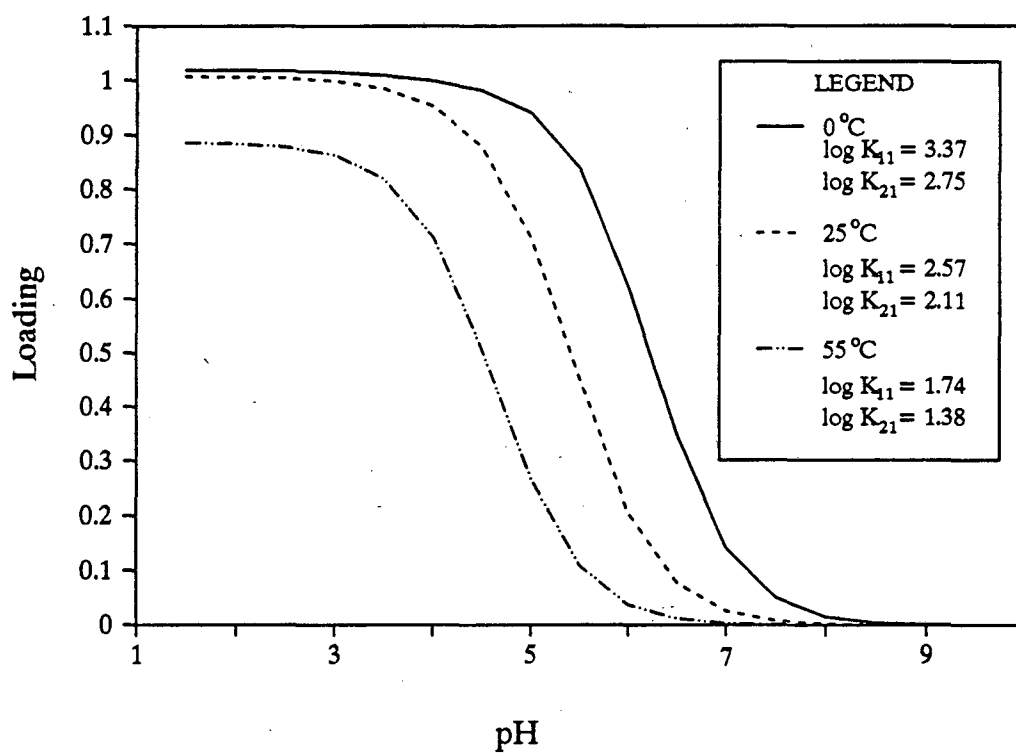


Figure 5-10. Effect of Temperature on Loading of 0.3 M Alamine 336 in Chloroform with Lactic Acid at an Aqueous Phase Concentration of 0.10 M

The effect of temperature on the sorption of lactic acid by Dowex MWA-1 was explored briefly in this work. Figure 5-11 presents acid uptakes at 25 °C and 37 °C. There is a slight decrease in uptake at the higher temperature, but the effect is not a major one. More extensive studies of the effects of temperature on other sorbent systems are needed. Kaufman, et al. (23) have investigated the effects of temperature on the uptakes of lactic acid by Reillex 425 and other resins. They were able to regenerate loaded Reillex 425 partially by leaching with water at 90 °C. More strongly basic sorbents, such as Amberlite IRA-35, were not regenerable using that method.

5.4.2 Thermal Stabilities of Sorbents and Extractants

The thermal stability of the sorbent or extractant must also be considered. The sorbent/extractant must be stable, for extended periods of time, at the temperature at which the extraction will be performed. Furthermore, if the sorbent/extractant is to contact whole cells, it must first be sterilized. For sorbents, in particular, heat sterilization, often at 120 °C (106) is the preferred method. Therefore, it is important that the sorbent/extractant be stable, for shorter periods of time, at the sterilization temperature. If the sorbent/extractant contacts only cell-free broth, sterilization is often not necessary. In this case, the broth can be sterilized, by heat treatment or filtration, after it passes through the sorption column (111).

The suggested maximum operating temperatures for the sorbents studied in this work were given in Table 2-4. These temperatures are those recommended for extended periods of operation. Many of the sorbents may be able to withstand higher temperatures for shorter periods of time. Most of the sorbents have maximum operating temperatures of about 100 °C or above, but a few have much lower operating temperatures. Duolite A7, for example, should be operated at temperatures of 40 °C or less. Of the sorbents of interest for use at $\text{pH} > \text{pK}_a$, Dowex MWA-1, with a maximum operating temperature of 100 °C, is more heat-stable than Amberlite IRA-35, which has a maximum operating temperature of only 60 °C.

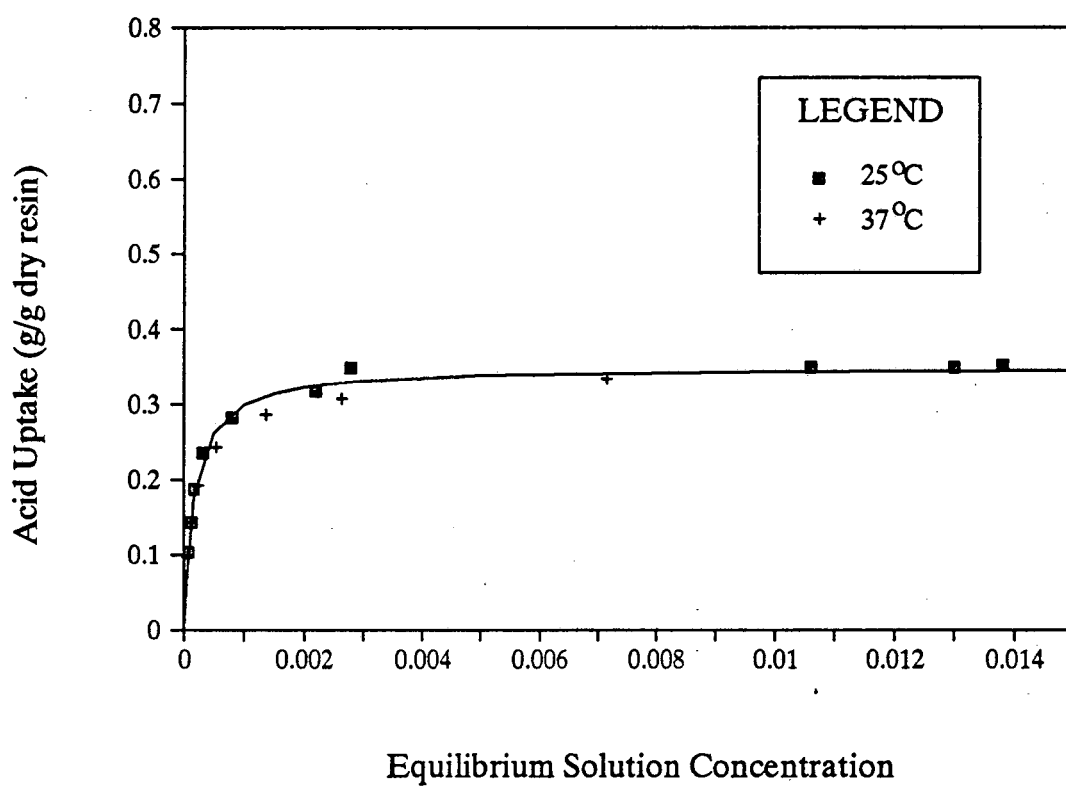


Figure 5-11. Effect of Temperature on Uptake of Lactic Acid by Dowex MWA-1

Organic extractants, by themselves, are much more heat-stable than sorbents. However, primary and secondary amine extractants can react with carboxylic acids at elevated temperatures to form amides (39, 41, 112). The reaction is slow at 37 °C but results in irreversible losses of acid and amine (112). One advantage of using tertiary amine extractants is that amide formation is not possible. Another possible interference is reaction of alcohol diluents with carboxylic acids to form esters (39, 41, 112). Again, this reaction is slow at 37 °C, but may be a problem at higher temperatures (112).

5.4.3 Process Considerations

If the operating temperature for a particular fermentation would result in poor sorption/extraction, degradation of the sorbent/extractant, or irreversible by-product formation, it may be preferable to use an external recycle loop and to provide for cooling of the stream prior to the extraction/sorption step. The stream would, of course, have to be heated before it was returned to the fermenter. The heating and cooling could be accomplished through heat exchange between the stream leaving the fermenter and the stream returning to it. In general any heating/cooling loads would not be large, since most fermentation temperatures are less than 60 °C, if not closer to 40 °C. The heating loads would be greater if the broth were raised to the sterilization temperature with every pass.

5.5 Toxicity to the Microorganism

Toxicity to the microorganism may be an obstacle to be overcome before *in-situ* sorption or extraction can be successfully implemented. Toxicity effects vary substantially from one system to the next and depend on both the natures of the microorganism and product and the type of extractant or adsorbent used. For extraction systems, both the extractant and the diluent can influence the viability and productivity of the cells.

Solid sorbents are, in general, considerably less toxic to microorganisms than are extractants. Holst and Mattiasson (111) discuss two potential problems associated with sorbent use -- leaching of residual monomer from the resin into the broth and adsorption of essential nutrients from the broth. The former could be eliminated by pretreatment of the resin, while the latter could be controlled by careful resin selection or, in some cases, by presaturating the resin with the nutrient. Seevaratnam et al. (18) showed that Bonopore, a hydrophobic solid resin, sorbed essential nutrients from yeast extract in a *L. delbrueckii* fermentation. This effect was eliminated by pre-saturating the sorbent with yeast extract. Pre-saturation makes sense only when the equilibrium uptake is a small fraction of the total resin capacity. For nutrients that are adsorbed more strongly, another approach is needed. If the nutrient is present in small amounts, and the sorption is being carried out in an external recycle loop, the nutrient can be removed by a small pre-column placed before the acid-recovery column. The nutrient must then be recovered from the pre-column and recycled back to the broth. This option was discussed as a method for dealing with uptake of phosphate and sulfate.

In-situ use of sorbents could also cause disturbances in cell metabolism if cells attach themselves to the sorbent surface (111). Srivastava, et al. (113) report no effect of the presence of Amberlite IRA-400, a Type I strong-base anion exchange resin used in OH⁻ form, on the growth of *L. delbreuckii* in a sucrose-yeast extract medium. They do note, however, that there was no apparent cell adsorption on the surface of the resin (18). If cell adsorption is a problem, the cells could be immobilized in hydrogel beads (113), although this could introduce rate limitations.

Extraction systems can pose more severe toxicity problems. The extractant can affect the microorganism through both the water-immiscible and the water-soluble portions (81, 114). In addition, uptake of nutrients can be a problem, but one which can be controlled using similar techniques to those outlined for sorbent systems.

The immiscible portion of the extractant can coat the cell wall, thereby disturbing the diffusion of nutrients into and waste products out of the cell, and it can disrupt the cell wall through increases in interfacial tension (114). Other effects may exist but are not fully understood at this time (81). There are several alternatives for minimizing these effects, including cell immobilization (115) or the use of a membrane (116). Yabannavar and Wang (115) demonstrated that Alamine 336 in oleyl alcohol was less toxic to cells immobilized in a κ -carrageenan gel than to free cells. Lewis and Yang (114) extracted propionic acid from a fermentation broth using Alamine 336 in 2-octanol. They observed very little detrimental effect on acid production when the extractant was contacted with cell-free broth in an external loop. However, decreased production rates were observed when the extractant was used *in-situ* in the fermentor. They therefore recommend avoiding direct contact between cells and extractant.

The water-soluble portion of the extractant can interfere with cell metabolism by changing the permeability of the cell membrane, by inhibiting enzymes, or through other mechanisms (81, 114). Since it can be difficult to choose an extractant and diluent that show good acid uptakes and are completely insoluble in the aqueous phase, there have been attempts to limit the effects of the water-soluble portion of the extractant on the cell. Yabannavar and Wang (115) demonstrated that *L. Delbrueckii* entrapped with soybean oil in κ -carrageenan gels show higher growth rates and lactic acid productivities than cells entrapped without soybean oil. Apparently the oil acts as a scavenger for dissolved solvent that diffuses into the gel.

Studies of solvent biocompatibility in extractive fermentations have shown varying results that are highly dependent on the particular microorganism used. Another important point is that, in most toxicity studies, little or no effort was made to purify the solvent or extractant being tested. As was discussed in Section 2.1.2, commercial amine extractants, such as Alamine 336 and Amberlite LA-2, in general contain highly water-soluble impurities, including lower molecular weight tertiary amines and primary and secondary amines. Without

initial washing steps under conditions that reliably remove these impurities, it is impossible to differentiate between the toxic effects of these impurities and any toxic effects of the principal amine extractant itself. Thus, the results of extractant toxicity studies presented here must be viewed with caution.

Researchers generally agree that solvents with high molecular weights and low polarities tend to be more biocompatible. Laane et al. (117) related biocompatibility to the octanol-water partition coefficient, P . They suggest using solvents with $\log P > 4$ to minimize toxic effects. Yabannavar and Wang (81) followed this heuristic in choosing diluents for the extraction of lactic acid from broths containing *L. delbrueckii*. They found that dodecane, Isopar-M and oleyl alcohol showed no toxicity to the cells. Tri-octyl phosphine oxide (TOPO) and Alamine 336 showed some toxic effects, although immobilization minimized these.

Datta (118) studied solvent toxicity effects on anaerobic acidogenic bacteria. He saw no effect of diesel oil, toluene or amyl acetate, with or without TOPO or Alamine 336. Roffler et al. (9) examined systems containing *L. delbrueckii*. While several hydrocarbons had no effect on the fermentation, ketones (diisobutyl ketone, octanone and undecanone) decreased cell growth rate or stopped growth altogether. TOPO and tributylphosphate showed toxic effects at saturation concentrations but had no effect at 10% of saturation. Roffler et al. also studied several amine extractants. At 10% of saturation, Adogen 363 (trilaurel amine), Adogen 283 (ditridecylamine) and Adogen 381 (triisooctylamine) had no effect on cell growth rate, although Adogen 381 did decrease lactic acid yield. At saturation conditions, all of the amines inhibited cell growth, with straight-chain amines having more of an effect than branched amines. Roffler et al. also found Aliquat 336, a quaternary amine, to be toxic even at only about 1% of saturation.

Playne and Smith (119) studied the toxic effects of 30 different solvents on a mixed culture of facultatively anaerobic, acid-producing bacteria. Several solvents were nontoxic even when supplied in amounts greater than necessary to saturate the aqueous phase. These

included several paraffins, phthalates, phosphorus-based compounds, Freon 113, Aliquat 336, diisoamyl ether, and trioctylamine. Primene JMT (a primary amine) and Amberlite LA-2 were partially toxic, but only at levels in excess of saturation. Several alcohols, ketones, benzene derivatives, isoamyl acetate and diisopropyl ether were toxic, but not completely so unless present at levels in excess of saturation conditions.

5.6 Summary

Competitive uptake of other species, temperature effects, and toxicity to the microorganism are issues which must be considered in designing a sorption/extraction process for recovering a carboxylic acid product from an actual fermentation broth. To a certain extent, the chosen method of implementing the sorption/extraction process determines the degree of flexibility that one has in dealing with these issues. If implementation is through an external recycle loop, the sorption/extraction can operate at a temperature different from that of the fermentation. In addition, direct contact between the microorganism and the sorbent/extractant can be prevented through the use of a membrane, and intermediate clean-up steps can be performed before recycling the broth to the fermenter. Competitive uptake of anions can also be controlled, for example, by use of a pre-column. What is gained in flexibility, however, is countered by increased complexity and cost. *In-situ* sorption/extraction, by contrast, offers less flexibility, but is simpler and less expensive to implement. It should therefore be considered a viable option if at all possible.

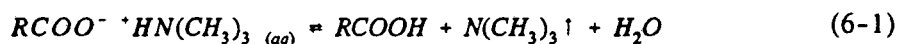
CHAPTER 6. CRACKING OF THE TRIMETHYLAMMONIUM CARBOXYLATE

This chapter examines the third step in the proposed process, the cracking of the trimethylammonium carboxylate complex. The focus of this work is on the cracking of trimethylammonium lactate, since previous efforts to crack this complex have not been entirely successful. Two novel methods of recovering lactic acid from the trimethylammonium salt are considered -- thermal cracking with solvent addition and esterification by reaction with an alcohol. Experimental results are presented and analyzed, and process recommendations are made.

6.1 Simple Thermal Cracking

6.1.1 Background

In the final step of the proposed process, the aqueous trimethylammonium carboxylate is thermally decomposed, or cracked, yielding both TMA vapor for recycle and product carboxylic acid. The cracking reaction is shown in Equation 6-1.



As described in Section 1.3.2, Poole and King (30) were able to achieve essentially complete removal of TMA during the cracking step for acids, such as succinic and fumaric, which precipitate from solution. It is more difficult to remove TMA in the case of lactic acid, which is highly soluble and tends to polymerize at higher concentrations. In this work, two different methods of recovering lactic acid and TMA from the trimethylammonium lactate solution are investigated. First, however, as a basis for comparison, the simple thermal cracking process is re-examined.

6.1.2 Experimental Results and Discussion

Several simple thermal cracking experiments were performed, following the procedure given in Section 2.5.1. The initial solutions typically contained 0.076 moles each of lactic acid and TMA, and 3.5 moles water. During the course of the experiment, essentially 100% of the total water and an average of 65% of the total TMA present initially were recovered overhead. The final solution was viscous and contained, on average, 0.27 mol TMA/mol acid, as determined by elemental analysis. This value is somewhat lower than the value calculated from the amount of TMA recovered overhead, indicating that some TMA may have been lost from the apparatus.

Figure 6-1 presents the results of a typical simple thermal cracking experiment performed at 470 mm Hg abs. under a nitrogen atmosphere. The rate of evolution of TMA is slow until most of the water (totaling 63 ml) has been driven off, at which point the temperature of the solution rises, and TMA is evolved at a higher rate. It is likely that the cracking reaction will occur at a significant rate only at elevated temperatures. However, it is also possible that the presence of water helps to stabilize the trimethylammonium lactate ion-pair, making cracking less thermodynamically favorable. If the increased rate of cracking is attributable to a temperature effect, it may be possible to crack the complex at a greater rate by operating at a higher pressure. Of course, the overall cracking time could also be decreased by heating the solution at a higher rate initially.

There are several possible reasons for the incomplete removal of TMA during the simple thermal cracking. The cause may be a thermodynamic one. For example, the ratio of lactic acid to TMA increases throughout the experiment, which may reduce the volatility of TMA (30). It is also possible that irreversible by-products are formed, although there is no evidence of this. On the other hand, kinetic and/or transport limitations may prevent complete removal of TMA. At lower concentrations of TMA, the driving force for the reaction may become so low that the reaction will not occur at a significant rate.

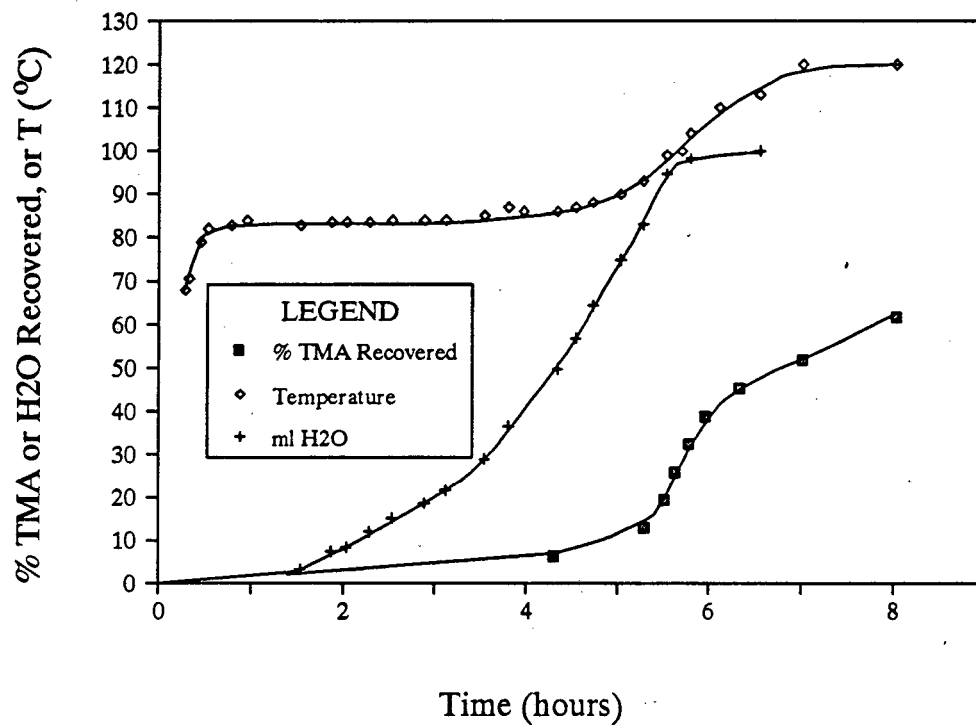


Figure 6-1. Simple Thermal Cracking of Trimethylammonium Lactate
0.076 mol lactic acid, 0.077 mol TMA, 3.5 mol water initially present
P = 470 mm Hg abs.

Alternatively, the formation of a viscous solution may introduce transport limitations, which inhibit the removal of TMA (30). The cause of the incomplete conversion is not clear from the cracking experiments alone.

Discoloration of the final solution was also a problem. In a preliminary experiment, the temperature of the solution was allowed to exceed 145 °C, and at one point reached 210 °C for a brief period of time. The resulting product contained only 0.11 mol TMA/mol lactic acid but was dark brown and caramel-like. This is consistent with an observation by Schopmeyer (120), who discusses the steam distillation of lactic acid under high vacuum. He states that lactic acid can decompose during distillation, yielding a residue that is "a black tarry mass which is largely anhydride, etc. and has a limited recovery value."

When the temperature of the solution was allowed to reach, but not exceed, 120 °C, the final solution was yellow in color. However, when the temperature was kept below 110 °C, the solution was colorless. It is possible that the yellow color may come from lactoyllactic acid (the dimer of lactic acid), which is reportedly pale yellow and can be prepared by heating lactic acid at 120 °C for 10 hours (121). Oxidation of one or more species is also a possible source of color. Although a nitrogen environment was used in the experiments, no special precautions were taken to ensure that the reaction vessel was free of oxygen. However, a more likely source of color is a caramelization reaction involving lactic acid and/or trace amounts of sugar and/or TMA. Discoloration of lactic acid upon heating is common, except with special "heat stable" grades, and usually occurs in the presence of residual sugars (3). Sugars themselves decompose, yielding colored products, at temperatures above 100 °C (122). A study of the mechanism of caramelization of reducing sugars in alkaline solutions has shown that organic acids are formed during a preliminary induction period, and that the addition of organic acids, such as lactic acid, to a decomposing sugar decreases the length of this induction period (123). Furthermore, other work has demonstrated that, in the presence of amino acids, the rate of decomposition of reducing

sugars and the intensity of the color are increased through the Maillard reaction (122). Thus, the discoloration observed in the final product of the cracking reaction may be due to interactions between trace amounts of residual sugars present in the original lactic acid and/or TMA and/or lactic acid.

6.1.3 Summary and Conclusions

It appears that the cracking process will occur more quickly and possibly to a greater extent if it is run at a higher temperature. Unfortunately, in these experiments, higher temperatures led to severe polymerization, caramelization and color formation. However, the experiments were performed in batch mode, and, as a result, the lactic acid solution was allowed to reach very high concentrations near the end of the cracking process. It might be possible to operate at high temperature, in a continuous mode, feeding additional water into the system to maintain a relatively low concentration of lactic acid. This approach should, at a minimum, reduce the extent of polymerization. Color formation may still be a problem at higher temperatures. However, many compounds can produce color even at very low solution concentrations, and these minor impurities may be removable using standard procedures, such as treatment with activated carbon.

6.2. Thermal Cracking with Solvent Addition

6.2.1 Background

Poole and King (30) examined methods of further purifying succinic and fumaric acid crystals. The method that was found to give the highest overall yields and greatest purities involved recrystallization from MiBK. The crystal mass, with adhering residual solution, was dissolved in MiBK and then heated to 80 °C under vacuum to drive off MiBK. Crystals of fumaric acid containing 0.05 moles of TMA per mole acid were obtained, with an overall

yield of 81.0%. The levels of TMA were reduced an order of magnitude by further recrystallization.

Poole and King suggest that the MiBK recrystallization serves to drive any remaining trimethylammonium carboxylate toward the uncomplexed acid and TMA. Dissolution of the concentrated residue in MiBK lowers the concentration of all species, which tends to drive the equilibrium shown in Equation 6-1 toward the right. Furthermore, the ionization of TMA should be suppressed in the organic solvent, making the TMA more volatile and driving the equilibrium toward the uncomplexed forms.

The above work can be extended to the trimethylammonium lactate system. It may be possible to remove the TMA remaining in solution after concentration of the aqueous trimethylammonium lactate by using a similar dissolution/vaporization method. The residual solvent could then be driven off, leaving behind a concentrated solution of lactic acid in free and polymeric forms. In that case another effect of the ketone would be that it solvates the carboxylate salt only somewhat, but interacts more strongly with the product acid, helping further to drive the cracking reaction. This approach was investigated experimentally in the current work.

6.2.2 Experimental Results

The final solutions from the simple thermal cracking experiments were heated in the presence of organic solvents, according to the procedures described in Section 2.5.2. Figure 6-2 presents the results of an experiment performed using MiBK as the solvent. The initial solution contained 0.076 mol lactic acid, 0.02 mol TMA and less than 0.01 mol water. MiBK was added to the solution in 30-40 ml aliquots and evaporated by heating at 445 mm Hg abs. under a nitrogen atmosphere. The solution temperature was not allowed to exceed 110 °C. As can be seen in Figure 6-2, with each addition of solvent, additional TMA was driven from solution. After three successive rounds of solvent addition and evaporation, 60 ml MiBK

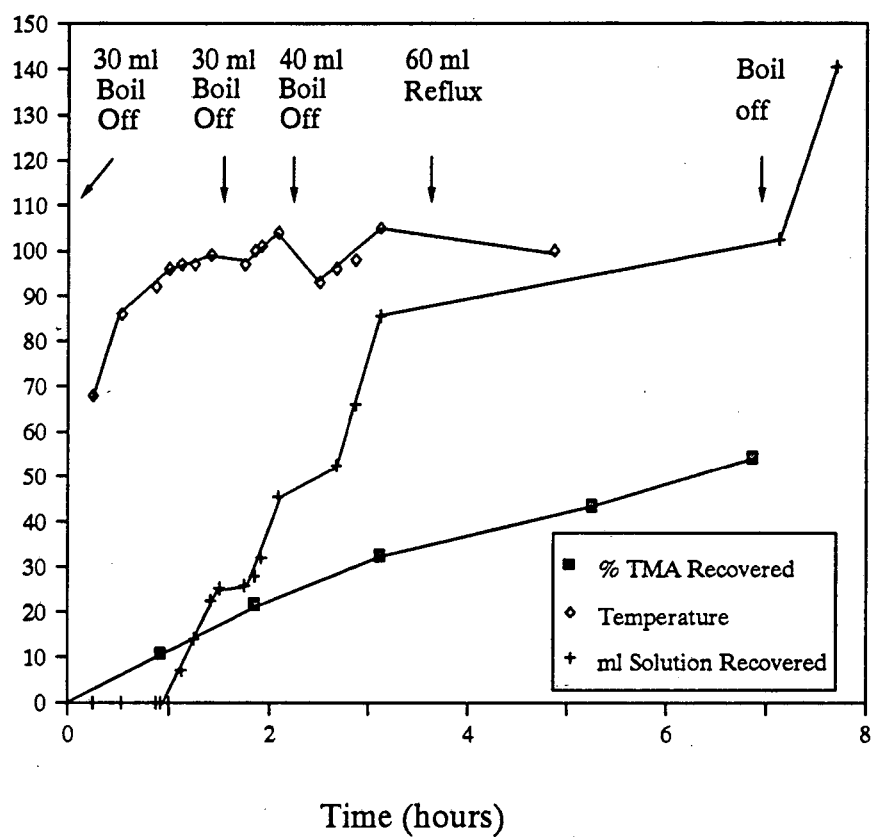


Figure 6-2. Cracking with MiBK Addition
 0.076 mol lactic acid, 0.02 mol TMA, < 0.01 mol water
 initially present, P = 445 mm Hg abs.

were added and the solution was heated under total reflux conditions. Some additional TMA was evolved during this period, but at a very slow rate. Finally, when the evolution of TMA appeared to have ceased, most of the remaining MiBK was evaporated from the solution. It was necessary to stop the evaporation process before all the MiBK was removed in order to avoid charring of the lactic acid mixture. Nevertheless, the solution became discolored during this step. Overall, 55% of the TMA present in the initial solution was recovered. The resulting product was dark yellow in color and contained 0.09 mol TMA/mol lactic acid by elemental analysis. A mass balance on the TMA closed within 11%.

In a second experiment, 40 ml butyl acetate were added to a solution containing 0.076 mol lactic acid, 0.03 mol TMA, and less than 0.01 ml water. The mixture was heated under total reflux conditions at 470 mm Hg abs. for almost 6 hours. As shown in Figure 6-3, the temperature remained constant at about 92 °C during this period, and TMA was gradually evolved. When the evolution of TMA appeared to have ceased, the solvent was evaporated from solution. During this period, the solution temperature was not allowed to exceed 120 °C, but, nevertheless, the solution became discolored. No additional TMA was evolved during this time. Overall, 64.9% of the TMA present in the initial solution was recovered. The final solution was yellow and contained 0.13 mol TMA/mol lactic acid, by elemental analysis. The mass balance on the TMA closed within 2%.

An analogous experiment was performed using ethyl acetate. The temperature of the solution during reflux was only 62 °C. No additional TMA was driven from solution using this method, probably because the temperature was too low for cracking to occur at any detectable rate.

6.2.3 Discussion and Conclusions

Cracking with solvent addition does remove additional TMA from the viscous mixture obtained from the simple thermal cracking. However, the removal process is a slow one, and

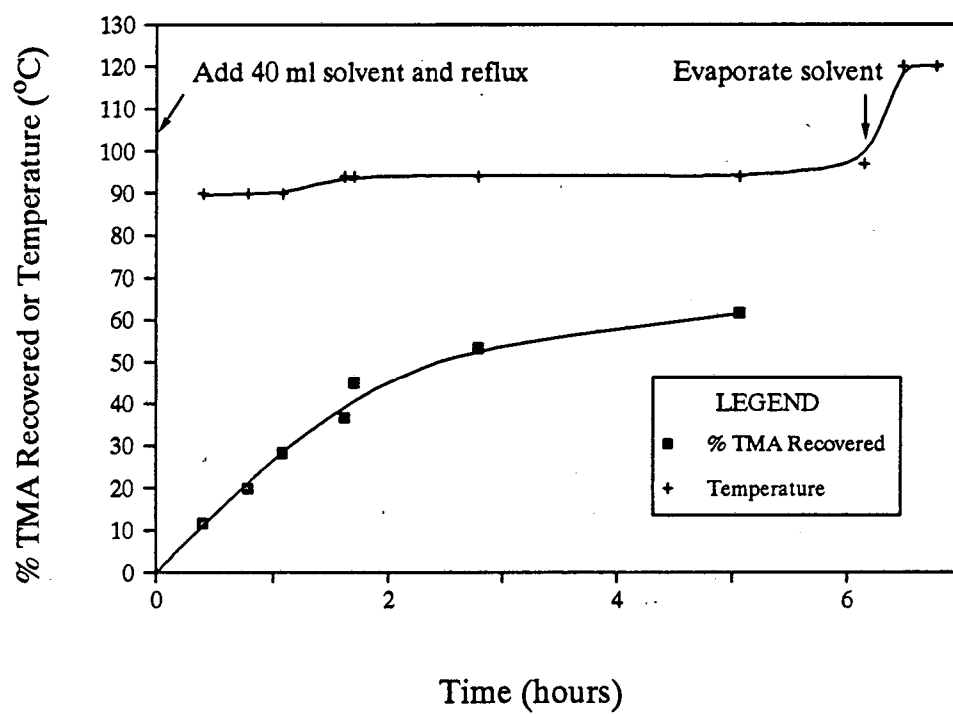


Figure 6-3. Cracking with Butyl Acetate Addition
0.076 mol lactic acid, 0.03 mol TMA, < 0.01 mol water
initially present, P = 470 mm Hg abs.

significant amounts of TMA remain in the final product. Possible explanations for the incomplete removal of TMA include the thermodynamic and kinetic limitations discussed in conjunction with the simple thermal cracking. Lower levels of TMA might be achieved by running the process at a higher temperature, either by using a higher-boiling solvent or by running the process under pressure. However, temperatures greater than about 110 - 120 °C may result in discoloration of the final product.

A solvent other than the ones studied may also be useful in driving off more TMA. For example, it is possible that if the solvent stabilizes the uncomplexed lactic acid and TMA over the trimethylammonium lactate, the reaction may be driven toward the uncomplexed TMA. Both MiBK and butyl acetate are expected to solvate the acid much more than the carboxylate salt. However, it is clear from the discussion in Chapter 4 that trimethylammonium lactate would be even less stable in MiBK than in an oxygenated solvent like butyl acetate. MiBK was, in fact, more effective than butyl acetate in driving off additional TMA, but it is not clear whether the improved performance is due to destabilization of the complex or to the somewhat higher temperatures reached in the MiBK experiment.

It is important that the chosen solvent not react with lactic acid or trimethylamine. Alcohols, for example, can form esters with lactic acid, thus complicating the final recovery procedure. Lactic acid can also react with esters to form transesterification products. For this reason, ethyl and butyl acetates may not be the most appropriate choices of solvent for use in a process of this sort.

If, through the appropriate choice of solvent and operating temperature, complete removal of TMA is achieved, there remains the question of how to recover the acid from the resulting mixture of solvent and lactic acid. In the experiments described, the solvent was evaporated from solution under moderate vacuum. Problems of discoloration and,

undoubtedly, polymerization were encountered. This is typical of processes in which lactic acid is distilled, even under high vacuum (120, 124).

The extent of polymerization and/or caramelization could probably be decreased if the concentration of lactic acid were kept reasonably dilute during the final evaporation step. Since an aqueous product is desired, the added diluent would be water. The chosen solvent must therefore have a lower boiling point than water. Use of a low-boiling solvent would mean that the cracking step would need to be performed under pressure. The final evaporation could be carried out at atmospheric pressure or under vacuum.

An alternative would be to use a solvent that is higher boiling than water but that forms a minimum-boiling azeotrope with it. The azeotrope would preferably be heterogeneous and contain primarily solvent. After the TMA was completely removed from the solvent-trimethylammonium lactate mixture, water could be added to the system, and the azeotrope could be distilled off. A sufficient quantity of water would have to be added so that the solvent would be entirely driven off before all the water was. The remaining solution would then be an aqueous lactic acid solution, perhaps containing some polymers, but hopefully similar to commercial 85% syrup.

Finally, a significant drawback of the thermal cracking approaches is that the lactic acid product is taken off the bottom of a distillation column, where impurities tend to concentrate. This problem is addressed in the next section, where a different approach is discussed.

6.3 Esterification

A second potential method of recovering lactic acid from trimethylammonium lactate involves the formation of a lactate ester by reaction with an alcohol, as in Equation 6-2.



The reaction would be driven to the right by removal of water and TMA. The resulting mixture would then be distilled to recover excess alcohol and the lactate ester. The ester could be taken as the ultimate product, or it could be hydrolyzed back to form aqueous lactic acid and alcohol. The alcohol would be removed by distillation and recycled to the reactor.

There are several potential advantages to this process. First, the lactate ester is taken off the top of a distillation column and hence should be recoverable as an extremely pure (USP-grade) product. This is an improvement over the thermal cracking processes, in which the product was always taken from the bottom of a distillation column. A further advantage is that the esterification of lactic acid itself is a well-understood process that has been carried out industrially. Thus, it may be possible to apply some of the existing equipment and technology to the proposed process. This is particularly true of the hydrolysis step, which is identical to the hydrolysis performed in a lactic acid esterification process.

6.3.1 Background

6.3.1.1 Simple Esterification

Most esterification reactions are highly reversible and therefore, to obtain high yields, the equilibrium must be forced to the right through removal of water and/or ester. Although the hydrolysis is catalyzed by both acid and base, a base-catalyzed esterification mechanism is not known. Common catalysts include strong mineral acids, tin salts, organo-titanates, silica gel and cation exchange resins. Strong acid catalysts, such as sulfuric or hydrochloric acids, can lead to the formation of alkyl chlorides and can promote polymerization, isomerization, and dehydration side-reactions. Therefore, weaker acids (e.g. sulfonic acids),

are often used as catalysts industrially. In general, the rate of reaction is proportional to the concentrations of alcohol, organic acid and acid catalyst (7).

The formation of azeotropes is common in esterification processes. With the exception of methanol, most alcohols with less than twenty carbons form azeotropes with water. Many of these azeotropes are heterogeneous and hence allow for easy removal of water from the system and recycle of alcohol to the reactor. However, azeotropes of water and ethanol, n-propyl, isopropyl, allyl, or t-butyl alcohols are homogeneous. When these alcohols are used, a hydrocarbon, such as benzene or toluene, may be needed to entrain water from the system through azeotropic distillation. The details of azeotropic distillation processes are discussed elsewhere (125). Alternatively, a desiccant, such as bauxite, can be used (7). For other alcohols, including 1-butanol, heterogeneous azeotropes are formed. This is an advantage, since the vapor can be condensed, the water layer removed, and the alcohol layer recycled back to the reactor.

The esterification of lactic acid usually produces both lactic and polylactic esters. The formation of polymers can be minimized by using an excess of alcohol. The esters can be recycled back to the reactor and re-reacted, so yields generally remain high (7, 124).

There are several known industrial examples of lactic acid esterification. USP-grade lactic acid has been produced industrially from crude lactic acid through the methyl ester. The acid can be refluxed with methanol in the presence of the acid catalyst, or methanol vapor can be passed through the acidified lactic acid solution. In the second case, methyl lactate is volatilized, driving the equilibrium. The resulting methyl lactate is hydrolyzed with water, with continuous removal of the more volatile methanol (7). Several sources describe processes for producing purified lactic acid through the methyl ester (121, 126, 127, 128, 129, 130). Schopmeyer (120) cites problems of corrosion of stainless steel equipment by the lactic acid. Keyes (130) discusses a method for manufacturing ethyl lactate, using benzene to increase the ratio of water to alcohol in the vapor phase.

6.3.1.2 Esterification of Ammonium Lactates

Filachione and Costello (131) investigated the esterification of ammonium lactate with a variety of alcohols. They refluxed mixtures of ammonium lactate and alcohol, driving the equilibrium through removal of ammonia and water. The reaction was continued until water was no longer detected in the condensed vapor. With water-soluble alcohols, such as iso-butyl and sec-butyl alcohol, toluene was used to entrain water. In general, primary alcohols gave higher conversions than secondary alcohols, and high-boiling alcohols gave higher conversions than low-boiling ones.

In particular, Filachione and Costello found that when 2.5 moles 1-butanol were reacted with 1 mole ammonium lactate (as a 73.6% aqueous solution), a 67% conversion was achieved within 4 hours. In a control experiment, performed with 1 mole lactic acid and 2.5 moles 1-butanol, 62% conversion was achieved within 2.5 hours. Boric acid, trihexylamine, basic aluminum acetate and silica gel were weak catalysts, reducing reaction time by a factor of about one half.

Filachione and Costello recovered the ester product by distilling the reaction mixture under vacuum. The residue from this distillation was reacted again with fresh 1-butanol and ammonium lactate. After seven such cycles, an overall conversion of 85% was achieved.

Filachione et al. (132) also studied the esterification of several alkylammonium carboxylates. The salts were prepared from non-volatile, long-chain amines, such as tributylamine and decylamine, and hence the amines were not removed overhead.

6.3.2 Esterification Step

The goal of the current work was to determine whether it is practicable to recover lactic acid by conversion of trimethylammonium lactate to an ester. 1-Butanol was chosen for the experimental work since the formation of a butanol-water azeotrope facilitates the

removal of water from the system. Experiments were performed to measure both the reaction equilibrium and the rate of reaction. The hydrolysis and distillation steps were also examined.

6.3.2.1 Conversion Experiments

6.3.2.1.1 Results

Esterification experiments were performed according to the procedure described in Section 2.6.1. In most experiments, a concentrated trimethylammonium lactate solution was prepared from a more dilute solution (about 1.5 M) by heating the solution at 420 mm Hg abs. During this step, a fraction of the trimethylammonium lactate was cracked thermally, and TMA was driven from solution. The amount of TMA removed depended on the amount of evaporation of the solution but was between 13.3% (when the solution volume was reduced by a factor of 2.4) and 38.7% (when the solution volume was reduced by a factor of 5.1).

In most of the experiments, concentrated trimethylammonium lactate was reacted with 1-butanol using a molar ratio of butanol to lactate equal to 2.5. The reactions were performed at atmospheric pressure and in a nitrogen environment. During the course of the reaction, water and TMA were driven from solution. Heating of the solution was stopped when the evolution of TMA and water ceased. In general, the temperature of the solution had increased to about 140 °C at this point. Discoloration of the solution began to occur at about 130 °C, and the final solution was dark yellow. The percent conversion to butyl lactate was calculated from a measurement of the butyl lactate in the final solution and from the amount of lactic acid originally added to the system. An average conversion of $(68.3 \pm 4.1) \%$, at the 95% confidence level, was achieved. This value is close to that achieved by Filachione and Costello with ammonium lactate.

Additional TMA was driven from solution during the esterification. An average of $(76.8 \pm 7) \%$ of the TMA present at the start of the esterification was recovered overhead.

During both the initial concentration and the esterification stages an average of (81.5 ± 5.3) % of the total TMA present was recovered. There was a fairly large amount of scatter in the measured amounts of TMA recovered overhead, especially in the first few experiments. Therefore, three of the final solutions were analyzed for residual nitrogen using elemental analysis. Based on these analyses, the average amount of TMA removed during both the cracking and esterification stages was calculated to be (89.9 ± 2.5) % of the original TMA present in the system.

The effects of several variables on the conversion to butyl lactate were investigated, again using 2.5 moles of 1-butanol per mole lactate. The conversion was unaffected by the presence of several potential catalysts, including silica gel, alumina, sulfuric acid and a strong cation exchange resin. The pre-concentration step also had no effect on the conversion. Unconcentrated trimethylammonium lactate (1.5 M) was reacted with 1-butanol to give a conversion of 70.0%. Finally, an experiment was performed using a molar ratio of 1-butanol to lactate equal to 10.0. The equilibrium conversion was 64%, which is not significantly different from the conversion achieved using 2.5 moles butanol per mole lactate.

As a control, a solution containing lactic acid and no TMA was reacted with 1-butanol, using a molar ratio of butanol to lactic acid equal to 2.5. The color of the final solution was a much lighter yellow than the final solution from the reaction with trimethylammonium lactate. A conversion of 75.3% was obtained. This value is somewhat higher than that obtained with the trimethylammonium lactate solution, although the difference between the two values is just barely significant statistically. The result of the lactic acid esterification may be somewhat high, since Filachione and Costello performed the same experiment and achieved a conversion of only 62%. Thus, there is no conclusive evidence that the reaction of trimethylammonium lactate with 1-butanol gives a lower conversion than the reaction of lactic acid with 1-butanol.

An overall material balance on the system generally closed within 5 - 10%. The final mass was usually somewhat lower than the initial mass, probably due to holdup of liquid in the packed column and/or minor losses of vapor through small leaks. The amount of 1-butanol in the final solution was always significantly lower than that expected based on the percent conversion to butyl lactate. On average, the amount of 1-butanol present was only about 78% of the amount expected. Even the fact that the liquid holdup in the packed column is primarily 1-butanol does not account for the low value. The "missing" 1-butanol does, however, support the idea that other, longer-chain esters are formed. Further support of this hypothesis comes from the gas chromatograms of the final solutions, which show a small, wide peak at a high retention time, perhaps corresponding to a long chain ester or esters.

6.3.2.1.2 Discussion

Theoretically, it should be possible to drive the esterification reaction to completion through removal of water and/or TMA. Complete conversion of lactic acid was not achieved in any of the reactions with trimethylammonium lactate, nor in the reaction with lactic acid. This incomplete conversion is most likely due, at least in part, to the formation of long-chain esters. It is also possible that, once a majority of the water and TMA have been driven off, the driving force for the esterification is so small that the rate of the esterification becomes extremely slow.

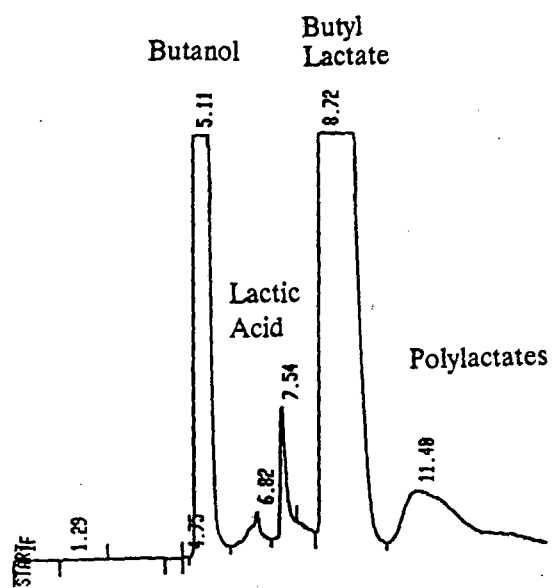
The important issue is whether or not by-products are formed irreversibly in the reaction. The production of lactic acid or butyl lactate polymers is not problematic, since these polymers can be fed back to the esterification reaction, where, under more dilute conditions, they will eventually be converted to butyl lactate (7, 124, 131). It would, of course, be desirable to limit the production of polymers so that a higher percent conversion per pass could be achieved. Polymer formation typically is decreased when an excess of

alcohol is used (7). However, in this case, increasing the ratio of 1-butanol to lactate from 2.5 to 10.0 did not affect the conversion.

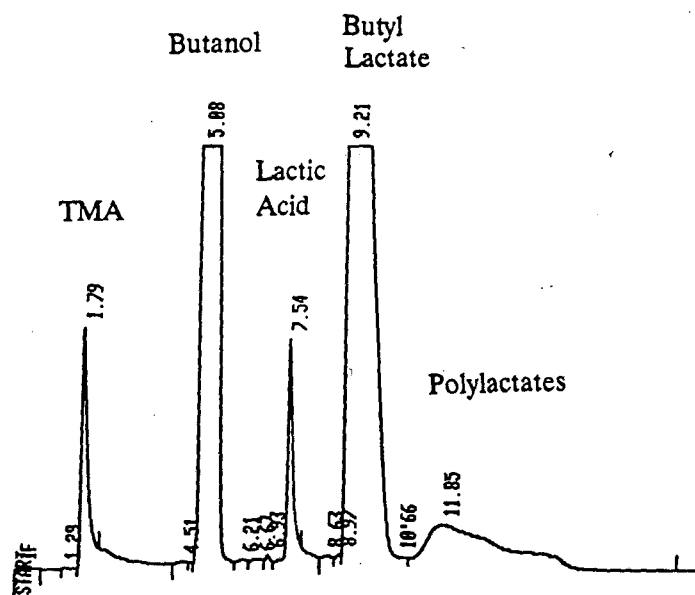
There remains the question of whether any other by-products are formed. A comparison of the gas chromatograms for the reactions of 1-butanol with trimethylammonium lactate and with lactic acid (Figure 6-4) reveals no major differences in the composition of the final products, aside from the presence of TMA in the former case. Certainly, non-volatile by-products could be formed irreversibly, and these would not be detected by the gas chromatograph. In addition, by-products could be formed in amounts which were not detectable under the experimental conditions.

Based on the results of the elemental analyses, the final reaction mixture from the esterification experiments contains approximately 10% of the nitrogen originally present in the initial solution. This nitrogen may be in the form of molecular TMA or trimethylammonium salts that are "trapped" in solution by kinetic or thermodynamic limitations. The nitrogen may also be in the form of by-products. Interestingly, most of the remaining TMA is removed overhead in the subsequent distillation step (see Section 6.3.4), as part of the fractions removed at 94°C or below. Therefore, it appears that a good deal of the nitrogen is in the form of TMA or trimethylammonium salts.

When trimethylammonium lactate is reacted with 1-butanol, the color of the final solution is a much darker yellow than when lactic acid itself is reacted with 1-butanol. This observation could indicate that some other species is present, at least in trace amounts. The color could result from reactions between sugars and/or TMA and/or lactic acid, as discussed above, in conjunction with the thermal cracking experiments. To resolve the question of whether or not by-products are formed irreversibly, and to determine what compound causes the observed deep yellow color, extensive analytical methods would need to be developed, and other experiments performed.



(a)



(b)

Figure 6-4. Chromatographs of Final Solutions
 (a) Esterification of Lactic Acid
 (b) Esterification of Trimethylammonium Lactate

6.3.2.2 Reaction Rate Experiments

Experiments in which the rate of reaction was measured were performed, following the procedure in Section 2.6. The experiments are not traditional kinetic studies, performed at constant temperature. Instead, the experiments were carried out at the boiling point of the mixture, so that TMA and the butanol/water azeotrope could be driven off at relatively high rates. The heating rate was kept approximately constant from one run to the next by maintaining a constant setting on the voltage regulator, and the temperature was allowed to rise with the boiling point of the mixture.

Initial experiments were conducted using trimethylammonium lactate solutions that had been pre-concentrated to varying degrees. Figures 6-5 through 6-7 present the rates of evolution of TMA and water, the rates of production of butyl lactate, and the temperature histories for three different degrees of pre-concentration. The rates of ester formation are compared in Figure 6-8. The initial solutions contained 0.2 moles lactic acid and 0.5 moles 1-butanol, but the amounts of water and TMA varied with the degree of pre-concentration. In the experiments shown in Figures 6-5 and 6-6, the trimethylammonium lactate solutions were concentrated so that 0.1 and 0.7 moles of water, respectively, remained in solution. The corresponding amounts of TMA are 0.13 and 0.17 moles, respectively. In the experiment shown in Figure 6-7, the trimethylammonium lactate solution was not concentrated at all (i.e. the initial concentration of 1.5 M was used). As a result, 5.7 moles water and 0.2 moles TMA are present.

The esterification process appears to consist of an induction step, during which water is driven off and very little ester formation occurs, and a second step, in which most of the ester production occurs. At the lowest water content (Figure 6-5), there is virtually no induction period. With 0.7 moles water present, the induction period is about 1.5 hours long, and with 5.7 moles water present, the induction period is about 7 hours long. During the induction period, the temperature of the solution remains approximately constant, as water

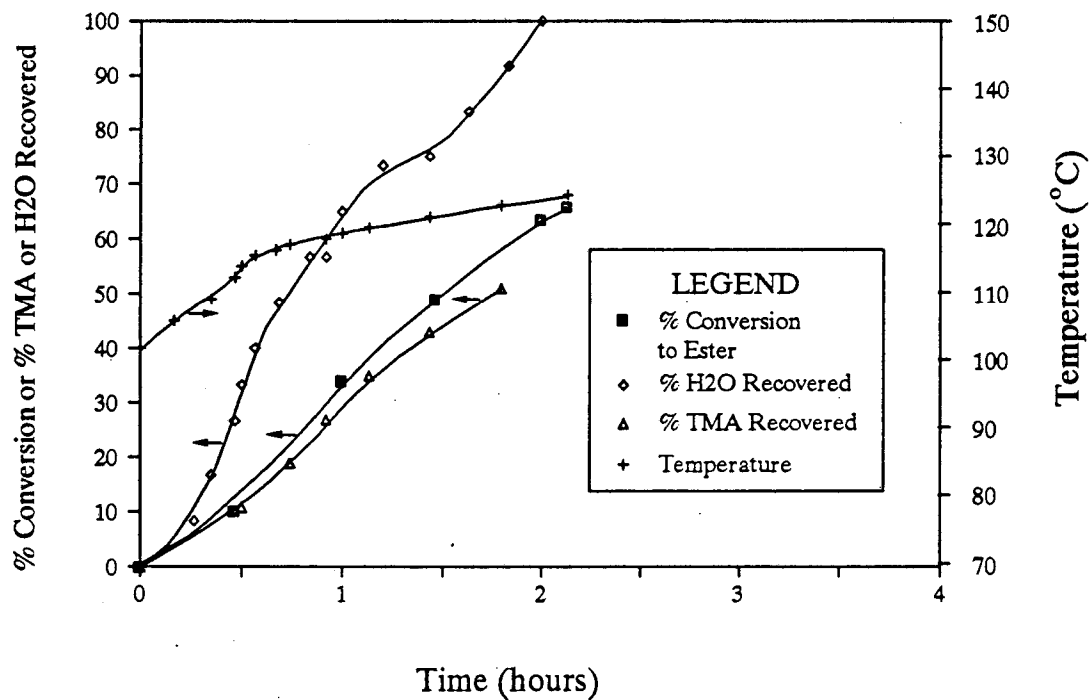


Figure 6-5. Results of Esterification Rate Experiment
 0.21 mol lactic acid, 0.13 mol TMA, 0.53 mol butanol
 and 0.1 mol water initially present, $P = 760$ mm Hg abs.

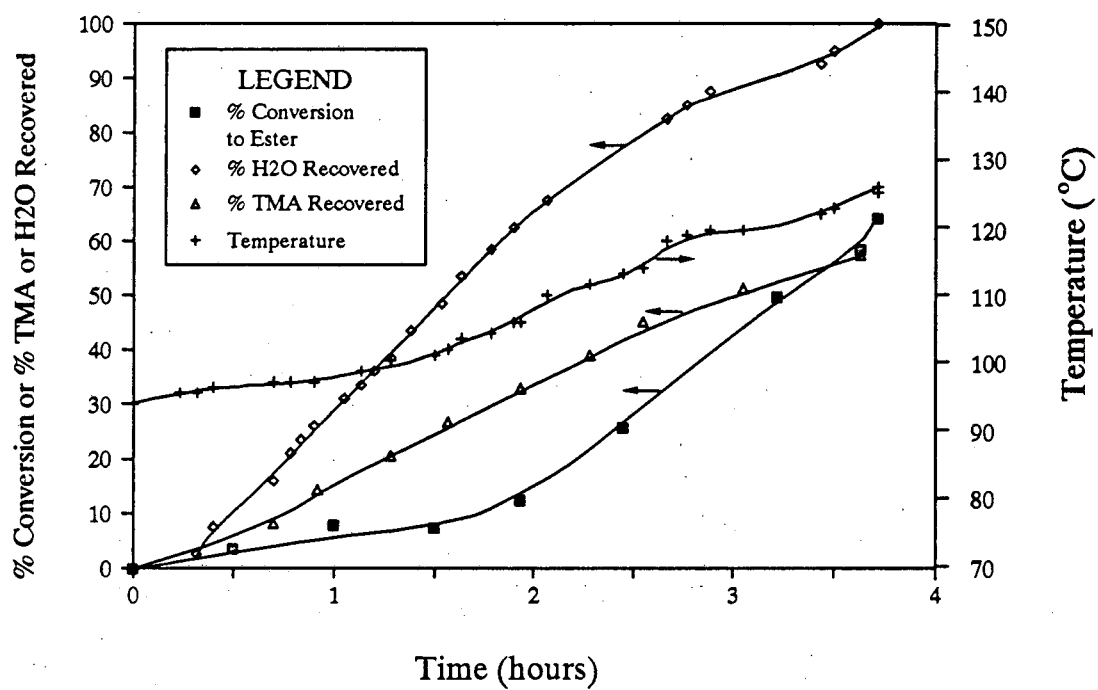


Figure 6-6. Results of Esterification Rate Experiment
 0.20 mol lactic acid, 0.17 mol TMA, 0.50 mol butanol
 and 0.7 mol water initially present, P = 760 mm Hg abs.

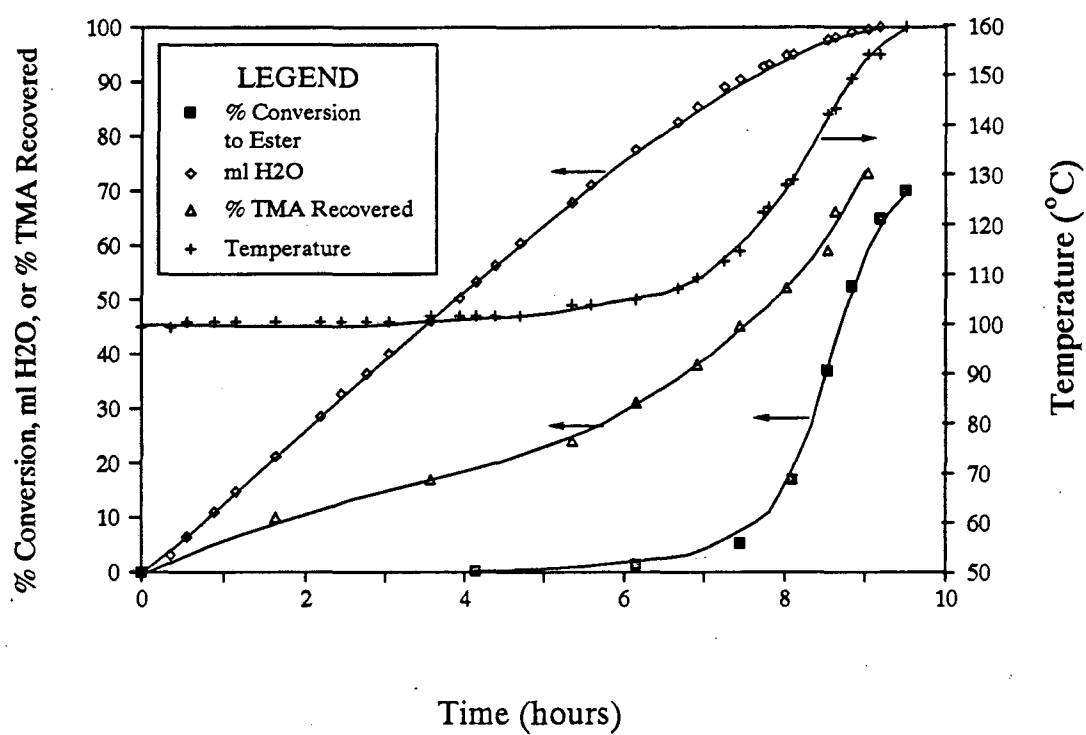


Figure 6-7. Results of Esterification Rate Experiment
 0.20 mol lactic acid, 0.20 mol TMA, 0.50 mol butanol
 and 5.7 mol water initially present, $P = 760$ mm Hg abs.

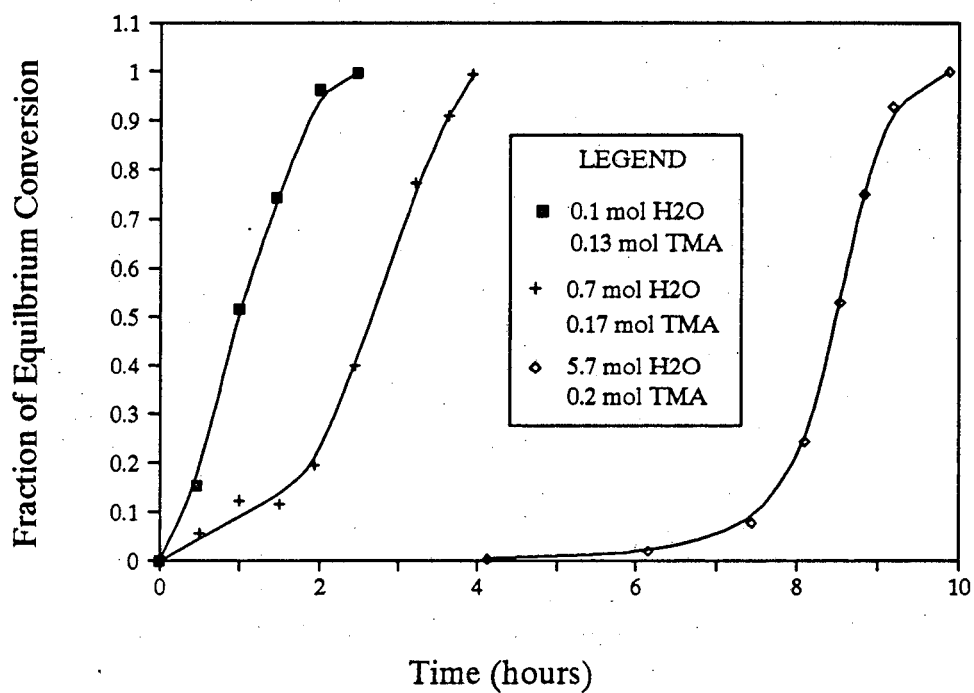
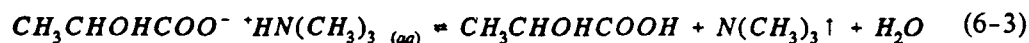


Figure 6-8. Effect of Degree of Preconcentration on Reaction Rate
0.2 mol lactic acid, 0.5 mol butanol and varying amounts of
TMA and water initially present, $P = 760$ mm Hg abs.

is evaporated. In general, the rate of evolution of TMA is smaller during the induction period, although in Figure 6-6, the rate is almost constant throughout the experiment.

The results of the above experiments indicate that it is desirable to pre-concentrate the trimethylammonium lactate before performing the esterification. Pre-concentration has no effect on the final conversion but increases the rate of esterification. If a 25 wt.% (3.9 M) TMA solution is used to regenerate the sorbent/extractant, the initial trimethylammonium lactate solution will be slightly less concentrated than the solution used in the experiment shown in Figure 6-6, but will contain a higher amount of TMA. By pre-concentrating to remove most of the water from solution, the reaction time could therefore be cut by a factor of at least two. The amount of time required for the pre-concentration step itself would, of course depend upon the heating rate. A final point is that it is not advisable to remove all the water from solution before the addition of 1-butanol, since this will produce the viscous, discolored solution generated in the simple thermal cracking experiments.

The slow initial rate of esterification may be related to the lower temperatures in the induction region, or to the higher water contents, or both. Presumably, the esterification of trimethylammonium lactate takes place in two steps, shown in Equations 6-3 and 6-4. In the first step, the trimethylammonium lactate is decomposed into lactic acid and TMA. In the second step, lactic acid reacts with the alcohol to form the ester and water.



Both reactions are driven toward the left in the presence of high concentrations of water. During the induction period, the amount of water in the system is reduced, so that both the cracking and the esterification reactions can proceed in the forward direction.

The fact that TMA is given off steadily throughout the experiments indicates that the cracking reaction, shown in Equation 6-3, may be the rate-limiting step, or one of several

rate-limiting steps. The rate of cracking of the trimethylammonium lactate, in the absence of 1-butanol, was therefore measured. Figure 6-9 presents the results of an experiment in which a solution of trimethylammonium lactate, containing 0.2 moles lactic acid, 0.14 moles TMA, and 0.65 moles water, was decomposed thermally. The amount of water in this solution is close to that present in the experiment shown in Figure 6-6. The solution was heated in a constant-temperature oil bath at about 140 °C, and the temperature of the solution ranged from 109 to 141 °C. This temperature range is representative of that observed in the analogous esterification experiment. The total reaction time for the cracking experiment is 1.3 hours, which is of the same order of magnitude as the reaction time required in the experiment shown in Figure 6-6. It therefore appears that the cracking reaction is important in determining the overall rate.

In a separate experiment, the rate of esterification of lactic acid, not in trimethylammonium form, was also examined. The initial solution contained 0.2 mol lactic acid, 0.5 mol 1-butanol and 3.7 mol water. This water concentration is roughly halfway between the water concentrations present in the experiments shown in Figures 6-6 and 6-7. The rate of evolution of water, the rate of formation of the ester, and the temperature history are shown in Figure 6-10. There is again an initial region in which the temperature remains constant and water is evolved at a constant rate. When the water is almost gone, the temperature rises and the esterification occurs at a faster rate. The total length of time for the esterification is about 10 hours, which is about the same as the time required for the experiment shown in Figure 6-7. It appears, then, that the rate of the reaction between lactic acid and 1-butanol, shown in Equation 6-4, also has a significant impact on the rate of reaction.

In Figure 6-10, significantly more ester is formed in the induction period than in the experiments with trimethylammonium lactate, even though the temperature in this region is essentially the same as that in the experiment shown in Figure 6-7. This observation supports

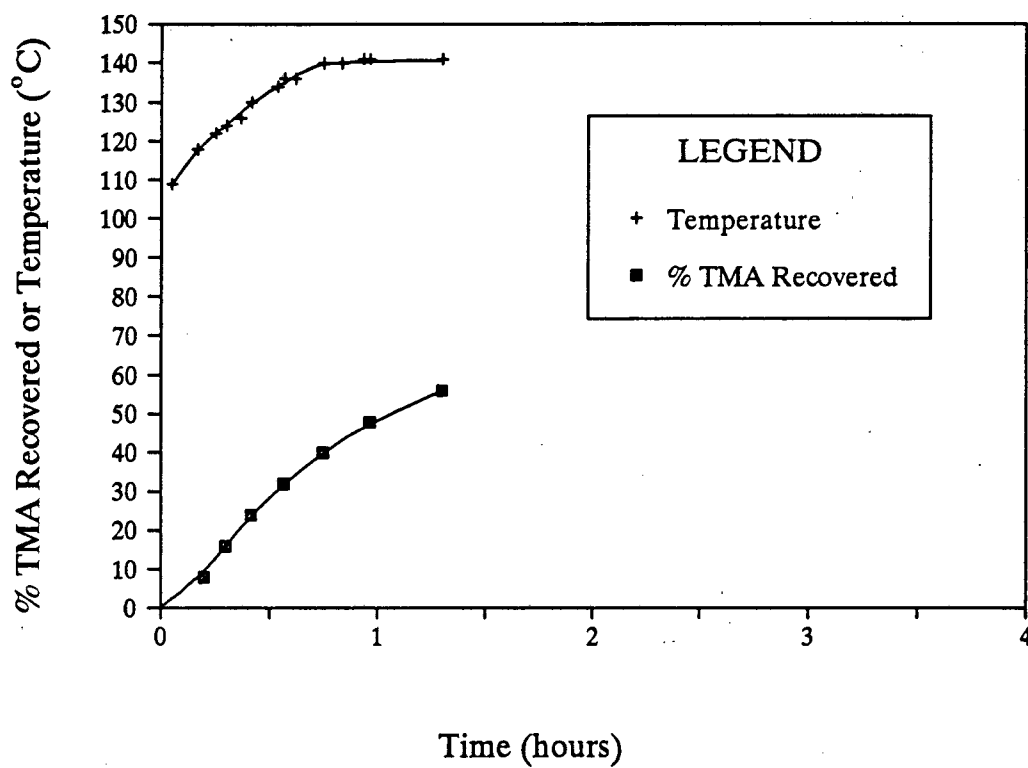


Figure 6-9. Cracking of Trimethylammonium Lactate
0.2 mol lactic acid, 0.14 mol TMA, 0.65 mol water
initially present, P = 760 mm Hg abs.

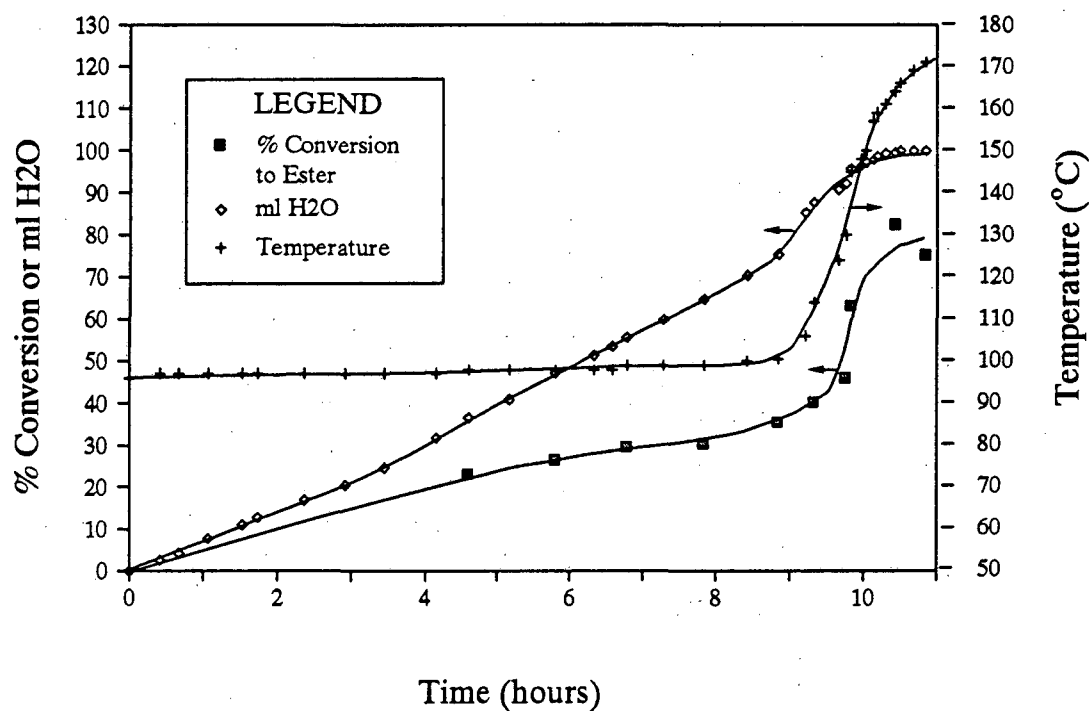


Figure 6-10. Results of Rate Experiment

Esterification of Lactic Acid

0.2 mol lactic acid, 3.7 mol water and 0.5 mol butanol

P = 760 mm Hg abs.

the idea that the cracking step may be the rate-limiting one, at least during the induction period. Once a higher temperature is reached, the rate of reaction of lactic acid with 1-butanol may also become significant in determining the overall rate of reaction.

Several potential catalysts were tested for their effects on the rate of reaction. The addition of a catalytic amount of sulfuric acid (5.3 mmol) to the reaction reduces the reaction time by a factor of almost 2, as shown in Figure 6-11. Since this amount of acid is sufficient to neutralize only about 3.5% of the TMA present, the mineral acid appears to act as a true catalyst, rather than simply displacing lactic acid from trimethylammonium lactate. The decrease in overall reaction time appears to be the result of a decrease in the induction period and a slight increase in the rate of esterification after the induction period, as reflected in the slopes in this region.

Silica gel and Amberlyst 15 (Rohm and Haas Co.), which is a cation exchange resin, also have slight catalytic effects, as shown in Figure 6-12. The time required for complete reaction is about 2.9 hours for the control, 2.6 hours in the presence of 2 g of Amberlyst 15, and 2 hours in the presence of 2 g silica gel. The major effects of the catalysts appear to be in the initial induction period. Outside this initial region, the reaction rates, as judged from the slopes of the curves, are almost the same. Basic and acidic alumina were also tested for catalytic activity. Neither was found to increase the rate of reaction significantly.

Finally, rates of esterification were compared for experiments performed using different ratios of butanol to lactate. In Figure 6-13, the rates of ester formation are presented for uncatalyzed reactions using butanol-to-lactate molar ratios of 2.5 and 10.0. The rate of reaction is significantly faster when 2.5 moles of 1-butanol are used per mole lactate. This result is approximately consistent with a second-order esterification reaction. At a 10.0 molar ratio, the calculated concentration of lactic acid is 0.94 mol/l, that of 1-butanol is 9.40 mol/l, and their product is 8.8 mol²/l². At a 2.5 molar ratio, the concentration of lactic acid is 2.65 mol/l, that of 1-butanol is 6.62 mol/l, and their product is 17.5 mol²/l². Thus, if it is

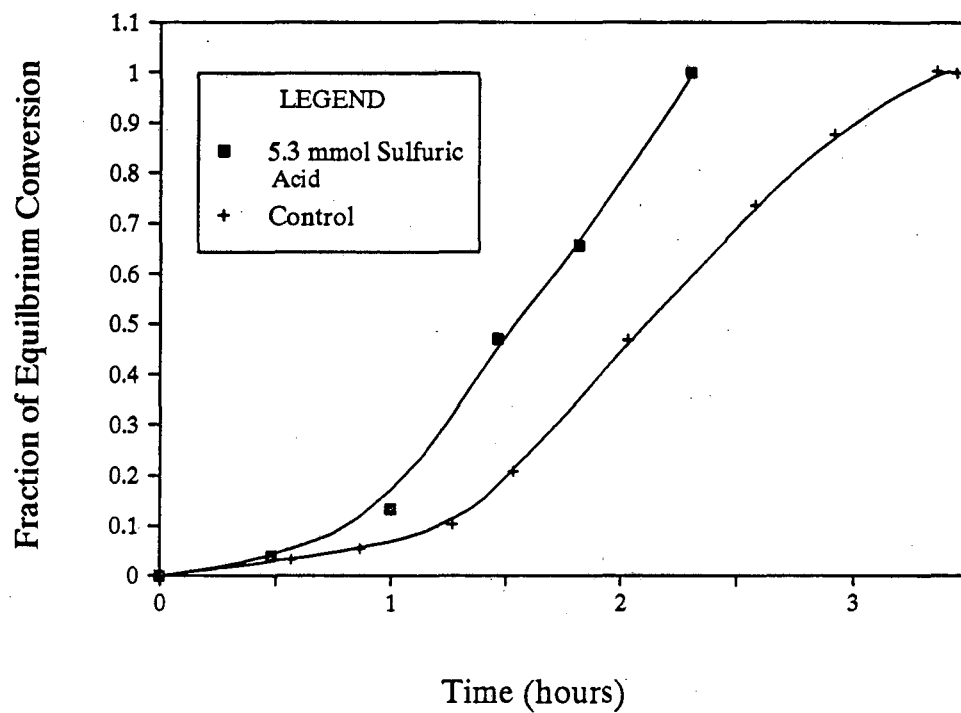


Figure 6-11. Effect of Sulfuric Acid Catalyst on Esterification Rate
0.2 mol lactic acid, 0.15 mol TMA, 0.5 mol butanol and
0.8 mol water initially present, $P = 760$ mm Hg abs.

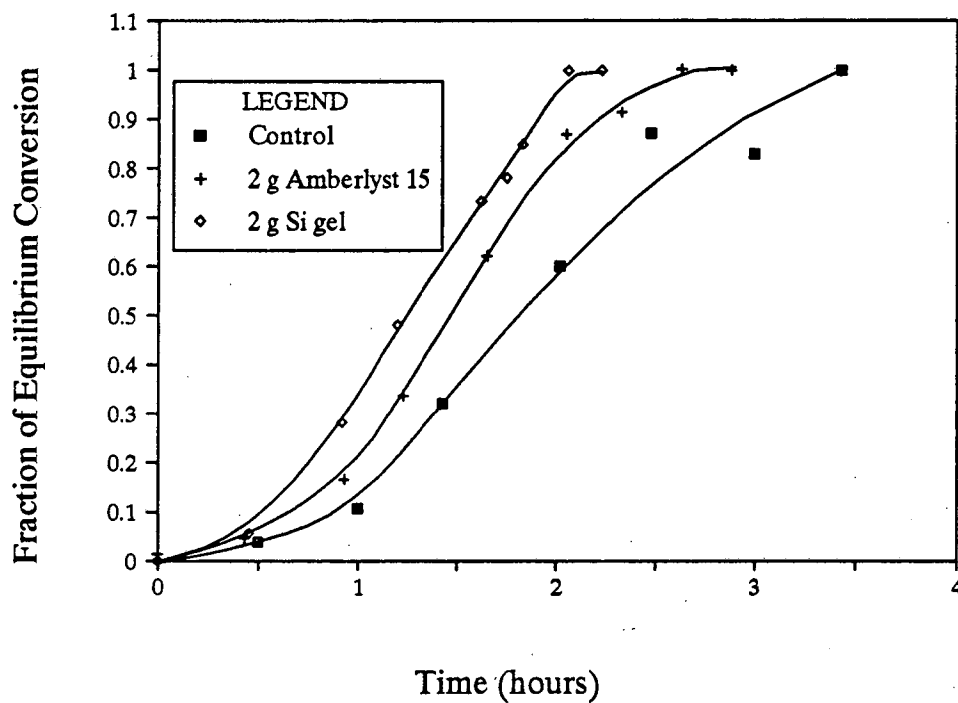


Figure 6-12. Effects of Amberlyst 15 and Silica Gel on Esterification Rate
0.2 mol lactic acid, 0.13 mol TMA, 0.5 mol butanol and
0.7 mol water initially present, $P = 760$ mm Hg abs.

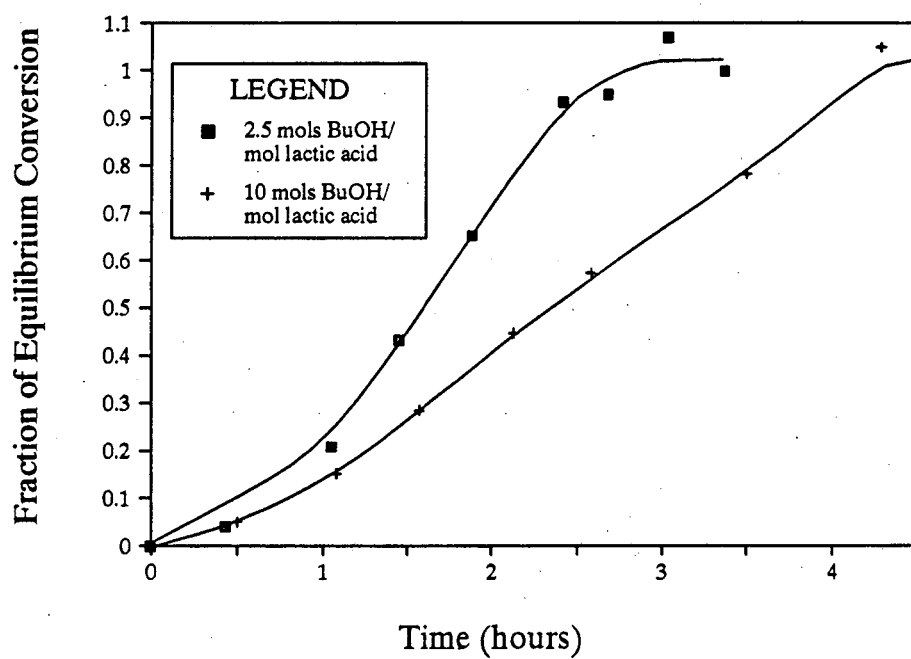


Figure 6-13. Effect of Butanol : Lactic Acid Ratio on Esterification Rate
0.2 mol lactic acid, 0.14 mol TMA, 0.7 mol water initially present
P = 760 mm Hg abs.

assumed that the esterification rate is first order in both lactic acid and 1-butanol, the initial rate observed with a butanol-to-lactate molar ratio of 2.5 should be twice that observed with a molar ratio of 10.0. If the slopes of the curves shown in Figure 6-12 are measured in the middle regions, after the induction period but before equilibrium is reached, the ratio of the slopes is equal to 1.74. This analysis is, of course, a gross simplification, since the effect of the cracking reaction has not been considered.

6.3.2.3 Summary and Conclusions

The esterification experiments show mixed results. Butyl lactate is formed at good yield. A significant amount of polylactate esters also appear to be formed, but these should be recyclable. A more serious concern is the discoloration of the final product, which indicates that some other by-product may be formed. There is no evidence that any by-product is formed in large amounts, however, and the levels formed may be acceptable in an industrial process.

The rate of reaction is quite slow, although pre-concentration steps and the use of weak catalysts, such as mineral acids, cation exchange resin, or silica gel, do increase the reaction rate. The fastest observed reaction time in these experiments was two hours. Thus, in order to implement the process industrially, high residence times would be necessary. If the reaction were to be carried out in a distillation column, high holdups would be necessary. This concerns will be addressed in further detail in Section 6.3.5. It should be possible to increase the reaction rate by running the reaction at a higher pressure. This may, however, lead to increased color formation.

6.3.3 Hydrolysis Step

The hydrolysis of butyl lactate was investigated in a series of experiments, described in Section 2.6. In the initial experiments, 3 moles water and 1 mole butyl lactate were

refluxed at their boiling point at atmospheric pressure. After four hours, very little reaction had occurred. Therefore, 1 ml concentrated sulfuric acid (0.036 equivalents) was added to the reaction flask. A 50% conversion was achieved within 30 minutes, and no further conversion was observed after two hours. It is therefore assumed that equilibrium was achieved. Two other runs were performed using the same ratio of water to butyl lactate, and the average equilibrium conversion was $(50.3 \pm 3.8) \%$ at the 95% confidence level. The average equilibrium constant for the esterification reaction was calculated from these data as 4.9 ± 1.1 . This equilibrium constant is within the range normally seen for esterification reactions (7). An experiment was also performed using 18 moles water, 1 mole butyl lactate and 1 ml concentrated sulfuric acid. A conversion of 0.80 was reached within 40 minutes, and no further conversion was observed after 1.5 hours. The calculated equilibrium constant for this esterification reaction was therefore 5.4.

The rate of reaction was measured in separate experiments at both reactant ratios. With the 3:1 ratio, the reaction time was 16 minutes or less, and with the 18:1 ratio, the reaction time was between 29 and 39 minutes. It is difficult to determine what causes the differences in rates from one phase ratio to the next. Since this is a two-phase reaction, the rate may be mass-transfer limited, in which case differences in interfacial areas from one phase ratio to the next may account for the observed differences in reaction rate. Nevertheless, it appears that the rate of reaction, with an acid catalyst, is sufficiently fast that industrial implementation is practicable. In particular, the reaction time is sufficiently fast that it should be possible to run the reaction in a distillation column. This point is discussed further in Section 6.3.5.

6.3.4 Distillation Steps

The batch esterification process performed in the laboratory involves two different distillation steps. The final reaction mixture from the esterification must be distilled to

recover excess 1-butanol and the butyl lactate product. In addition, the final reaction mixture from the hydrolysis step must be distilled to remove 1-butanol and unreacted butyl lactate from the lactic acid product. Both of these processes are discussed briefly in this section.

6.3.4.1 Distillation of Esterification Mixture

The final product from the esterification was distilled at 420 mm Hg abs., without a nitrogen atmosphere. The compositions and boiling ranges of the three fractions recovered are presented in Table 6-1. The first fraction formed two phases upon condensation. The compositions of both the top and bottom phases are given.

All fractions, including the butyl lactate product, were colorless. This is a major improvement over the thermal cracking process, where the colored components ultimately remained in the product. It is also expected that much improved purities could be achieved with proper distillation column design and operation.

Interestingly, trimethylamine is found in all fractions. To a certain extent, this could be the result of contamination of the distillate receiving flask. This is probably the case for the third fraction, which is primarily butyl lactate. However, a significant amount of TMA is found in the first and second fractions, which are primarily 1-butanol and/or water. As noted earlier, the fact that TMA is removed in this distillation, at temperatures less than 100 °C, indicates that a good portion of the TMA remaining in the final esterification mixture is not in the form of by-products. The presence of TMA probably is related to the fact that it is readily absorbable by alcohols (121). In the original esterification experiments, any TMA vapor released from the reaction flask passes over the Dean-Stark trap, which contains condensed 1-butanol and water. This liquid phase apparently absorbs TMA from the vapor stream and sends it back into the reactor.

Table 6-1. Distillation of Esterification Mixture

Fraction	Boiling Range (°C)	Wt. % 1-Butanol	Wt. % Butyl Lactate	Wt. % Water	Wt. % TMA
1 Top Layer	74.5 - 90	72	0	20	7.9
1 Bottom Layer	74.5 - 90	7.9	0	90	1.7
2	90 - 94	95.1	0	2.5	2.4
3	~153	9.1	89	-	0.16
Distillation Residue	Viscous and dark brown (not analyzed).				

The distillation residue was viscous and dark brown, with a caramel odor. Severe decomposition apparently occurs at the temperatures encountered in this distillation. As discussed in Sections 6.1 and 6.2, this is a common occurrence and one that is difficult to avoid except possibly under very high vacuum. It does, however, make recycle of the distillation residues difficult.

6.3.4.2 Distillation of Hydrolysis Mixture

Distillations of the final mixtures from the hydrolysis experiments were also performed. The catalyst was first neutralized with sodium hydroxide. The distillation was performed at 420 mm Hg abs. until most of the 1-butanol had been removed. The pressure was then lowered to 90 mm Hg, in an attempt to prevent discoloration of the residue.

Table 6-2 presents typical compositions of the overhead fractions. The final fraction was light yellow in color and showed peaks at high retention times on the gas chromatogram. This fraction may contain butyl lactoyllactate, which was isolated by Filachione and Costello (131), during distillation of an esterification mixture, as the fraction following butyl lactate.

Table 6-2: Distillation of Hydrolysis Mixture

Fraction	Boiling Range (°C)	Wt. % 1-Butanol	Wt. % Butyl Lactate	Wt. % Water
P = 420 mm Hg abs.				
1 Top Layer	74 - 77	73.8	7.5	3.3
1 Bottom Layer	74 - 77	7.8	0.3	92
2 Top Layer	77 - 79	72.7	8.8	2.6
2 Bottom Layer	77 - 79	7.9	0.4	92
P = 90 mm Hg abs.				
3	< 101	6.0	85.8	N/A
4	104 - 110	7.9	64.4	N/A
Distillation Residue	Viscous and dark brown (not analyzed).			

The distillation residue was brown and viscous, once again demonstrating that batch distillation in the presence of lactic acid is a difficult procedure.

An additional experiment was performed to test the heat stability of the lactic acid used in the current work. The 85% commercial syrup was heated at atmospheric pressure, and residual water was boiled from solution. The solution was allowed to reach temperatures of over 200 °C. After 2 hours at these temperatures, the lactic acid solution was yellow and caramel-like and had a distinctive caramel smell. It is not surprising, therefore, that distillations in which lactic acid is concentrated result in severe discoloration.

Decomposition of the lactic acid product could be prevented if a dilute solution of acid could be maintained during the final distillation step. This would be possible if complete hydrolysis of butyl lactate were achieved. The mixture to be distilled would then contain 1-butanol, water and lactic acid. 1-Butanol and some of the water could be taken overhead as the azeotrope, and the remaining product would be aqueous lactic acid. This experiment was performed in the laboratory. A solution containing 0.23 moles each of lactic acid and 1-butanol and 4.3 moles water was distilled at 390 mm Hg abs. All the 1-butanol and some of the water were removed. The final product, in the distillation flask, was a 2.4 N lactic acid solution with only a tinge of yellow color.

6.3.4.3 Summary

The distillation steps that would be carried out in a batch process are problematic. The distillation residue, which is the product in the case of the hydrolysis mixture, is invariably decomposed and discolored at the high temperatures encountered in the distillation.

6.3.5 Process Considerations

6.3.5.1 Choice of Alcohol

1-Butanol was used in this work because it allowed for easy removal of water from the system. The use of methanol would have been more difficult because it is more volatile than water and is fully miscible with water. Thus, there is no convenient method of driving water out of solution without also removing methanol. In an industrial process, however, it may be desirable to use some other alcohol. Methanol, for example, has generally been used to purify lactic acid industrially. The alcohol is continuously recovered overhead and recycled back to the process.

There are several advantages to a process using methanol. Because methanol is more volatile than water, the final step in the process, in which residual alcohol is removed from the hydrolyzate, is simplified. It might be preferable to use methanol rather than 1-butanol because the former has a lower latent heat of vaporization. On the other hand, the temperatures reached at atmospheric pressure probably will not be high enough for the esterification reaction to occur at a reasonable rate. Thus, if methanol is used, the system will almost certainly have to be pressurized.

6.3.5.2 Process Implementation

The problems inherent in a batch esterification process have been made clear through the experimental results. The major problem is that, during the distillation steps, concentrated lactic acid solutions are formed in the distillation pot, and at higher temperatures these solutions polymerize and discolor.

One alternative is to design the process such that the reaction and distillation steps occur simultaneously. One such process, shown in Figure 6-14, is based on a similar process discussed by Schopmeyer (120). That process purifies crude lactic acid through the methyl lactate. Other processes can be found in the literature (126, 127, 128, 129, 130). The alcohol is continuously recycled to the esterification reaction vessel. In this manner, a concentrated lactic acid solution is never allowed to accumulate in the bottom of a distillation column. Likewise, the hydrolysis step and the second distillation occur simultaneously. Discoloration and polymerization are minimized because an aqueous environment is always maintained in the hydrolysis tank. This method of implementation should eliminate the problems of decomposition associated with batch distillations. Relatively long residence times may be required if the rates of esterification are slow.

Another alternative is to use simultaneous reaction-distillation columns for both the esterification and hydrolysis steps, as shown in Figure 6-15. In this configuration, the

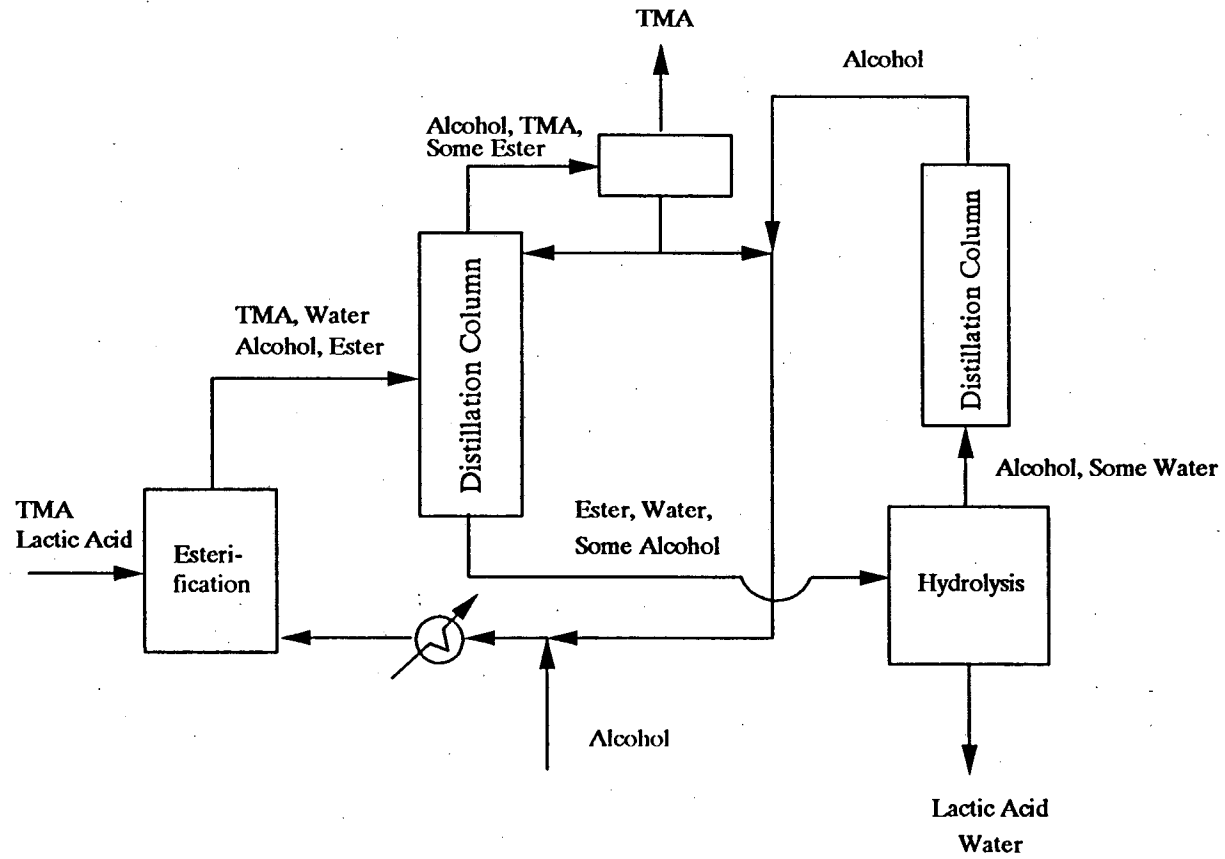


Figure 6-14. Esterification and Hydrolysis with Continuous Recycle

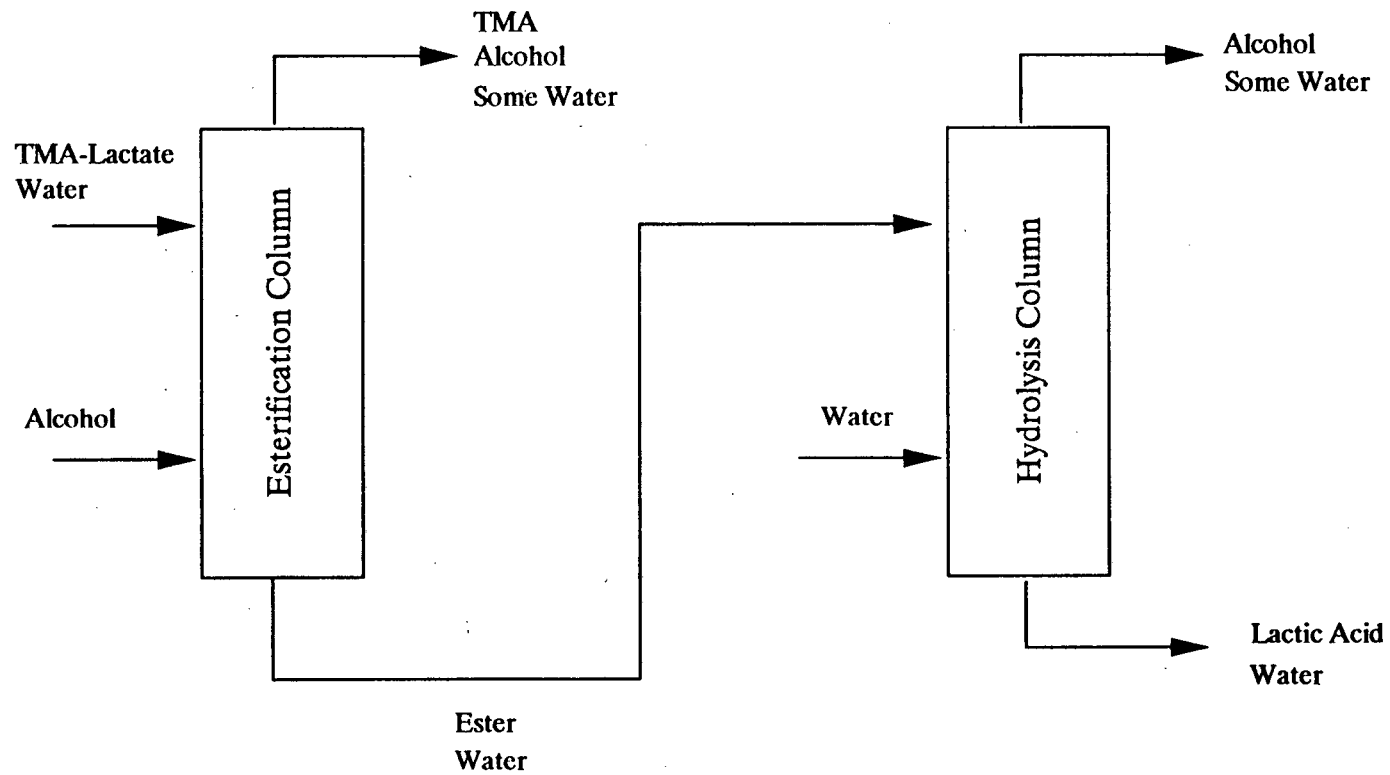


Figure 6-15. Esterification and Hydrolysis of Ester Using Two Simultaneous Reaction-Distillation Columns

products of the reactions are continuously removed, thus driving the reaction toward completion. Simultaneous reaction-distillation should work well for the hydrolysis reaction, since the reaction kinetics are relatively fast, and the relative volatilities of the various components are sufficiently different. Simultaneous distillation-reaction may not work well for the esterification process. Because this reaction proceeds very slowly, extremely large column holdups might be necessary to obtain complete conversion. If complete conversion is not achieved, lactic acid will be present in the bottoms of the first distillation column.

6.4 Conclusions

The esterification of trimethylammonium lactate may be preferable to thermal cracking, with or without solvent addition, because a much purer final product can be achieved. With both approaches, discoloration occurs at temperatures above 120 °C or so, but with the esterification process, the colored components are not taken overhead. Before the esterification could be implemented, however, a determination of the amount of product lost through by-product formation should be performed in order to determine if the process is economical.

A major drawback of the esterification process is the slow rate of reaction. The reaction rate could possibly be increased by performing the reaction at higher pressure, but this could lead to unacceptable levels of by-product formation. Pre-concentration of the trimethylammonium lactate also increases the rate of esterification, and small amounts of mineral acids and silica gel act as weak catalysts.

The preferred implementations for the esterification and hydrolysis involve simultaneous reaction and distillation, with recycle of reactants to the esterification/hydrolysis reaction vessels. With this approach, thermal decomposition of lactic acid in the bottoms of distillation columns is avoided. Simultaneous reaction-distillation in a distillation column is a potential method of implementing the esterification and hydrolysis processes. However, for

the esterification, the slow rate of reaction may necessitate undesirably large hold-ups in the distillation column.

CHAPTER 7. CONCLUSIONS

A three-step process has been proposed for the recovery of carboxylic acids from fermentation broths at $\text{pH} > \text{pK}_{\text{a}1}$. In the first step, the acid is recovered from the broth through complexation with a strongly basic sorbent or extractant. The sorbent/extractant is then regenerated by leaching with an aqueous solution of trimethylamine, which yields an aqueous trimethylammonium carboxylate solution. Finally, the trimethylammonium carboxylate is cracked, yielding acid product and TMA vapor for recycle.

Strongly basic sorbents have been shown experimentally to give good uptakes of carboxylic acids at $\text{pH} > \text{pK}_{\text{a}1}$. The most effective sorbents contain strongly basic amine groups. For example, Dowex MWA-1, a macroporous styrene-divinylbenzene resin with tertiary amine groups, and Amberlite IRA-35, a macroporous acrylic resin with tertiary amine groups, both sustain capacity to two or more pH units above the $\text{pK}_{\text{a}1}$ of the acid.

The performance of a particular sorbent at $\text{pH} > \text{pK}_{\text{a}}$ is a function of the acidity of the carboxylic acid being sorbed and of the basicity of the sorbent functional groups. This basicity is reflected in the initial slope of the sorption isotherm. For sorbents that are well described by Langmuir isotherms, the initial slope is given by the K value from the isotherm. It has been shown that the logarithm of the K value is roughly correlated with other measures of sorbent basicity, including the apparent pK_{a} , determined from mineral acid titrations, and the monomer pK_{a} , which can be calculated using group-contribution methods. The calculated monomer pK_{a} , the apparent pK_{a} and the sorption isotherm K value are useful for predicting sorbent performance at $\text{pH} > \text{pK}_{\text{a}}$.

With the exception of two quaternized resins, all of the sorbents studied are fully regenerable by leaching with an aqueous solution of trimethylamine. For most sorbents, 100% recovery of the acid is achieved when one equivalent of TMA is present for each equivalent of carboxylic acid. Amberlite IRA-35, which is a more strongly basic resin, requires

somewhat greater than a stoichiometric amount of TMA for complete regeneration.

Breakthrough studies with Dowex MWA-1 have shown that there are no major rate limitations in the adsorption process. The adsorption isotherm is highly favorable, and hence the breakthrough curve is self-sharpening. The process appears to be dominated by resistance by diffusion in the particle phase, although further studies are needed to develop a more complete model that can be used in scale-up calculations. The leaching step is also highly favorable, and a further degree of concentration is achieved through a focusing effect.

Strongly basic amine extractants also proved to be effective at recovering carboxylic acids at $\text{pH} > \text{pK}_a$. Amine extractants, such as Alamine 336 and Amberlite LA-2, function best in highly active diluents, such as chloroform and 1-octanol, which are capable of stabilizing the acid-amine complex. Secondary amines give better performance than tertiary amines in diluents that are capable of solvating the additional proton, e.g., alcohols and ketones. All of the extractants were fully regenerable by back-extraction into aqueous TMA. Neither phase-separation problems nor major rate limitations were observed.

There are several complications associated with using sorbents and extractants in real fermentation systems. Competitive uptake of other species may be a problem. In particular, the experimental work demonstrated that uptake of anions of strong acids, such as sulfate and phosphate, is a problem. Sulfate is taken up much more strongly than phosphate, and uptake of both anions is more severe with the sorbent, Dowex MWA-1, than with liquid extractants. With basic extractants, uptake of anions appears to be stronger in more active diluents. Fortunately, the levels of these anions in the broth are quite low, and it should be possible to remove them with a small pre-column placed before the main acid-recovery column.

Toxicity issues are another concern. In general, there are fewer toxic effects associated with the use of sorbents than with extractants. Liquid extractants can affect the microorganism through both the water-soluble and the immiscible portions. Effects of the latter type can be eliminated through the use of a membrane and/or an external extraction

loop. Techniques for minimizing the effects of the water-soluble portion have also been suggested. An important point is that, in most previous toxicity studies, no effort has been made to purify the extractants before use. Other studies should be performed with extractants which have been treated to remove soluble impurities.

The elevated temperatures encountered in a fermentation system will decrease the capacities of most strongly basic sorbents and extractants. However, this problem can be overcome by cooling the broth slightly and carrying out the sorption/extraction in an external loop.

Finally, the third step in the proposed process, the cracking of the trimethylammonium carboxylate, was examined in detail using lactic acid. Earlier studies by Poole and King [30] showed that with low-solubility acids, such as succinic and fumaric, the trimethylammonium salt can be cracked thermally, yielding acid crystals and TMA and water for recycle. With lactic acid, which is much more soluble and tends to self-esterify, simple thermal cracking performed in the batch mode results in a viscous mass still containing 0.27 moles TMA per mole acid. It may be possible, however, to perform the cracking with continuous addition of water to the system. Maintaining an aqueous environment may help to decrease polymerization and hence prevent the increase in viscosity, which may "trap" TMA in solution. Operating at elevated pressures should also help to increase the rate of cracking.

Simple thermal cracking with the addition of solvent was also examined. Addition of MiBK or butyl acetate to the system, followed by evaporation of the solvent, results in somewhat lower levels of TMA in the final product (0.09 - 0.13 moles of TMA per mole acid). Further removal of TMA may be possible at elevated pressures. An important complication is that final evaporation of the solvent results in polymerization and discoloration of the remaining lactic acid. Again, it is possible that polymerization could be prevented by maintaining an aqueous environment in the vessel, perhaps by using a solvent with a lower boiling point than water, or one that forms an azeotrope with water. Another disadvantage

of the thermal cracking approach, for lactic acid, is that the final product is taken from the bottom of a distillation column and hence will most likely contain substantial levels of impurities.

Another option is to esterify the trimethylammonium lactate by reaction with an alcohol. The ester could then be hydrolyzed back to the lactic acid product. The advantage of this approach is that the ester is taken off the top of a distillation column and hence can potentially be very pure. The reaction has been driven to 68% completion in a laboratory-scale experiment using 1-butanol at a molar ratio of 2.5 moles butanol per mole lactate. Other, higher-molecular-weight esters also appear to be formed, but it should be possible to recycle these back to the reactor. There is no evidence that other by-products are formed irreversibly, but extensive analytical methods would need to be developed in order to confirm this.

The esterification reaction appears to consist of two different phases. In the first, induction, phase, water is removed from the system and the reaction rate is slow. When most of the water has been removed, the esterification occurs at an increased rate. It is therefore desirable, from a reaction rate standpoint, to pre-concentrate the trimethylammonium lactate before performing the esterification.

The overall rate of esterification is relatively slow, with a reaction time on the order of several hours. The reaction presumably takes place in two steps. In the first, the trimethylammonium lactate is cracked, and in the second the freed lactic acid reacts with the alcohol. Both steps appear to be important in determining the overall rate of reaction, although at lower temperatures, the first step may be rate-controlling. Silica gel, concentrated mineral acids, and cation exchange resins were found to be weak catalysts for the reaction, reducing reaction time by up to a factor of two.

The hydrolysis reaction occurs much more rapidly than the esterification. In laboratory experiments using a mineral acid catalyst and a ratio of 3 moles water per mole

butyl lactate, equilibrium was achieved within 15 minutes. The equilibrium constant for the hydrolysis of butyl lactate was found to be 4.9-5.4.

Problems of discoloration, caramelization and polymerization occurred in the laboratory distillations of the esterification and hydrolysis mixtures. However, these problems could be overcome in a continuous process if lactic acid is not allowed to concentrate in the bottom of a distillation column. Methanol may be preferable to butanol in a continuous process, since it has a lower heat of vaporization and, in the final distillation step, can be distilled off, leaving behind aqueous lactic acid.

Industrially, it may be possible to carry out both the esterification and hydrolysis reactions in distillation columns. However, for the esterification, the hold-up times may be high, since the kinetics of the reaction are slow. Further studies at elevated pressures and with continuous processes are needed to determine the feasibility of the esterification approach.

REFERENCES

1. Jain, M.K., Datta, R., and Zeikus, J.G., "High-Value Organic Acids Fermentation - Emerging Processes and Products," in *Bioprocess Engineering: The First Generation*, Ghose, T.K. Ed., Ellis Horwood Limited, Chichester, 366-389 (1989).
2. *CRC Handbook of Chemistry and Physics*, 70th ed., Weast, R.C., Ed., CRC Press, Boca Raton, Florida, D165 (1989).
3. Vickroy, T.B., "Lactic Acid," in *Comprehensive Biotechnology*, Vol. 3, Blanch, H.W., Drew, S. and Wang, D.I.C., Eds., Pergamon Press, New York, Chapter 38, 761-776 (1985).
4. Glassner, D.A. and Datta, R., U.S. Patent 5,143,834 (September 1, 1992).
5. Kaneuchi, C., Seki, M. and Komagata, K., *Appl. Environ. Microbiol.*, **54**, 3053-3056 (1988).
6. Sato, M., Nakahara, T., and Yamada, K., *Agr. Biol. Chem.*, **36**, 1969-1974 (1972).
7. *Kirk-Othmer Encyclopedia of Chemical Technology*, 3rd ed., John Wiley & Sons, New York (1979). "Citric Acid," Vol. 6; "Hydroxycarboxylic Acids," Vol. 13; "Succinic Acid and Succinic Anhydride," Vol. 21; "Esterification," Vol. 9.
8. Davison, B.H. and Thompson, J.E., *Appl. Biochem. Biotechnol.*, **34/35**, 431-439 (1992).
9. Roffler, S.R., Randolph, T.W., Miller, D.A., Blanch, H.W., and Prausnitz, J.M., "Extractive Bioconversions with Nonaqueous Solvents," in *Extractive Bioconversions*, Mattiasson, B. and Holst, O., Eds., Marcel Dekker, New York, 133-171 (1991).
10. Strathmann, H., "Electrodialysis," in *Membrane Separations Systems - A Research & Development Needs Assessment*, U.S. Department of Energy, 8-1 to 8-53 (1990).
11. Bauer, B., Gerner, F.J. and Strathmann, H., *Desalination*, **68**, 279-292 (1988).
12. Mani, K.N., Chlanda, F.P. and Byszewski, C.H., *Desalination*, **68**, 149-166 (1988).
13. Czytko, M. and Ishii, K., "Continuous Glucose Fermentation for Lactic Acid Production Recovery of Acid by Electrodialysis," presented at the 5th DECHEMA Annual Meeting of Biotechnologists, Frankfurt am Main, Germany (1987).
14. Yao, P. and Toda, K., *J. Gen. Appl. Microbiol.*, **36**, 111-125 (1990).
15. Reschke, M. and Schügerl, K., *Chem. Eng. J.*, **28**, B11-B20 (1984).
16. Zhu, Y., and Sengupta, A.K., *Environ. Sci. Technol.*, **26**, 1990-1998 (1992).

17. Zhu, Y. and Sengupta, A.K., "Selective Sorption of Organic Carboxylates and Other Anions through Polymeric Ligand Exchange," Proceedings of 1st Separations Division Topical Conference on Separations Technologies: New Developments and Opportunities, AIChE Annual Meeting, Miami Beach, Florida, 513-517 (November 2-6, 1992).
18. Seevaratnam, S., Holst, O., Hjörleifsdottir, S., and Mattiasson, B., *Bioprocess Eng.*, **6**, 35-41 (1991).
19. Kulprathipanja, S. and Oroskar, R., U.S. Patent 5,068,418 (November 26, 1991).
20. Kulprathipanja, S., U.S. Patent 4,720,579 (January 19, 1988).
21. Kulprathipanja, S. and Strong, S.A., U.S. Patent 4,924,027 (May 8, 1990).
22. Garcia, A. and King, C.J., *Ind. Eng. Chem. Res.*, **28**, 204-212 (1989).
23. Kaufman, E.N., Cooper, S.P. and Davison, B.H., "Screening of Resins for Use in a Biparticle Fluidized Bed Bioreactor for the Continuous Fermentation and Separation of Lactic Acid," presented at the Fifteenth Symposium on Biotechnology for Fuels and Chemicals, Gatlinburg, Tennessee (1993).
24. Ernst, E.A. and McQuigg, D.W., "Adsorptive Purification of Carboxylic Acids," presented at the 1992 Annual Meeting, AIChE, Miami Beach, Florida (1992).
25. Starr, J.N. and King, C.J., *Ind. Eng. Chem. Res.*, **31**, 2572-2579 (1992).
26. Tamada, J.A. and King, C.J., *Ind. Eng. Chem. Res.*, **29**, 1333-1338 (1990).
27. Baniel, A.M., Blumberg, R. and Hadju, K., U.S. Patent 4,275,234 (June 23, 1981).
28. Busche, R.M., "Recovery of Fermentation Products: Least Cost or Highest Yield?," in *Separation Technology*, Li, N.N. and Strathmann, H., Eds., Engineering Foundation, New York, 75-121 (1987).
29. Yates, R.A., U.S. Patent 4,282,323 (August 4, 1981).
30. Poole, L.J. and King, C.J., *Ind. Eng. Chem. Res.*, **30**, 923-929 (1991).
31. Urbas, B., U.S. Patent 4,405,717 (September 20, 1983).
32. King, C.J. and Tung, L.A., U.S. Patent 4,132,456 (July 21, 1992).
33. "Chemical Prices," *Chemical Marketing Reporter*, 26-34 (April 19, 1993).
34. Lipinsky, E.S. and Sinclair, R.G., *Chem. Eng. Prog.*, **82**, 26-32 (1986).
35. Adelson, A., *The New York Times*, C5 (May 21, 1993).
36. Kertes, A.S. and King, C.J., *Biotechnol. Bioeng.*, **28**, 269-282 (1986).

37. Holten, C.H., *Lactic Acid: Properties and Chemistry of Lactic Acid and Its Derivatives*, Verlag Chemie, Weinheim/Bergstr., Chapter XI, 192-231 (1971).
38. Henkel Corporation, Blue Line Technical Bulletin, "Alamine 336," Tucson, AZ.
39. Ricker, N.L., Ph.D. Thesis, University of California, Berkeley, California (1978).
40. Tamada, J.A., Kertes, A.S. and King, C.J., *Ind. Eng. Chem. Res.*, **29**, 1319-1326 (1990).
41. Ricker, N.L., Michaels, J.N., and King, C.J., *J. Separ. Proc. Technol.*, **1**, 36-41 (1979).
42. Ritcey, G.M. and Ashbrook, A.W., *Solvent Extraction : Principles and Applications to Process Metallurgy*, Elsevier, New York, 230 - 289 (1984).
43. Rohm and Haas Company, "Rohm and Haas Ion Exchange Resins Laboratory Guide," Philadelphia (1988).
44. Henkel Corporation, Blue Line Technical Bulletin, "Aliquat 336," Tucson, AZ.
45. Marsh, S.F., *Solvent Extr. Ion Exch.*, **7**, 889-908 (1989).
46. Reilly Industries, Inc., "Reillex: A New Family of Crosslinked Polyvinylpyridines from Reilly," Indianapolis (1989).
47. Rohm & Haas Company, *Amberlite/Duolite Ion Exchange Resins: Technical Notes*, Philadelphia (1981).
48. Dow Chemical Company, *DOWEX Ion Exchange Resins Engineers' Handbook*, Midland, Michigan (1983).
49. Nace, E.D., "Comparison of Test Methods for Analysis of Strongly Basic Anion Exchange Resins," Rohm and Haas Company internal publication IWC-81-47, Philadelphia.
50. Frierman, M., M.S. Thesis, Dept. of Chemical Engineering, University of California, Berkeley, CA (1983).
51. Anderson, R.E., "Ion Exchange Separations," in *Handbook of Separation Techniques for Chemical Engineers*, Schweitzer, P.A., Ed., McGraw-Hill, New York, 1-387 to 1-444 (1988).
52. Dorfner, K., "Ion Exchangers," in *Ion Exchangers*, Dorfner, K., Ed., Walter de Gruyter, Berlin, Chapter 1 and Appendix I (1990).
53. Personal communication with Donald McQuigg, Reilly Industries, Inc., Indianapolis (April 1, 1991).
54. Perrin, D.D., Dempsey, G., and Serjeant, E.P., *pK_a Prediction of Organic Acids and Bases*, Chapman & Hall, London (1981).

55. Hodgkin, J.H. and Eibl, R., *React. Polym.*, **4**, 285-291 (1986).
56. Clifford, D. and Weber, W.J., Jr., *React. Polym.*, **1**, 77-89 (1983).
57. Personal communication with Donna Hardy, Bio-Rad Laboratories, Richmond, CA (August 24, 1990).
58. Personal communication with Phyllis Ferris, Dow Chemical Company, Midland, MI (October 3, 1990).
59. Wheaton, R.M. and Hatch, M.J., "Synthesis of Ion-Exchange Resins," in *Ion Exchange: A Series of Advances*, Vol. 2, Marinsky, J.A., Ed., Marcel Dekker, New York, 191-42 (1969).
60. Gustafson, R.L., Filius, H.F., and Kunin, R., *Ind. Eng. Chem. Fundam.*, **9**, 221-229 (1970).
61. Personal communication with J. Myers, Rohm & Haas Company, Philadelphia (July 10, 1992).
62. Helfferich, F., *Ion Exchange*, McGraw-Hill, New York (1962).
63. Kipling, J.J., *Adsorption from Solutions of Non-Electrolytes*, Academic Press, New York (1965).
64. Ruthven, D.M., *Principles of Adsorption & Adsorption Processes*, John Wiley & Sons, New York (1984).
65. Wankat, P.C., *Rate-Controlled Separations*, Elsevier Applied Science, New York, 257-258 and 338-340 (1990).
66. Marquardt, D.W., *J. Soc. Ind. Appl. Math.*, **2**, 431-441 (1963).
67. Kemp, D.S. and Vellaccio, F., *Organic Chemistry*, Worth Publishers, 374 (1980).
68. Chanda, M., O'Driscoll, K.F., and Rempel, G.L., *React. Polym.*, **4**, 39-48 (1985).
69. Harris, W.I., Stahlbush, J.R., Pike, W.C. and Stevens, R.R., *React. Polym.*, **17**, 21-27 (1992).
70. Kawabata, N., Yoshida, J-I, Tanigawa, Y., *Ind. Eng. Chem. Prod. Res. Dev.*, **20**, 386-390 (1981).
71. Helfferich, F., *J. Phys. Chem.*, **69**, 1178-1187 (1965).
72. Helfferich, F.G. and Hwang Y-L, *AIChE Symp. Ser.*, **81**, 17-27 (1985).
73. Bhandari, V.M., Juvekar, V.A. and Patwardhan, S.R., *Ind. Eng. Chem. Res.*, **31**, 1060-1080 (1992).

74. Sherwood, T.K., Pigford, R.L. and Wilke, C.R., *Mass Transfer*, McGraw-Hill, New York, 548-592 (1975).
75. Glueckauf, E. and Coates, J.E., *J. Chem. Soc.*, 1315 (1947).
76. Hall, K.R., Eagleton, L.C., Acrivos, A. and Vermeulen, T., *Ind. Eng. Chem. Fund.*, **5**, 212-223 (1966).
77. *Perry's Chemical Engineers' Handbook*, 6th ed., (Perry, R.H., Green, D.W. and Maloney, J.O., Eds.), McGraw-Hill, New York, Chapters 3 and 16 (1984).
78. Busbice, M.E. and Wankat, P.C., *J. Chromatogr.*, **114**, 369-381 (1975).
79. Tamada, J.A., Kertes, A.S. and King, C.J., *Ind. Eng. Chem.*, **29**, 1327-1333 (1990).
80. Yabannavar, V.M. and Wang, D.I.C., *Biotechnol. Bioeng.*, **37**, 1095-1100 (1991).
81. Yabannavar, V.M. and Wang, D.I.C., *Ann. NY. Acad. Sci.*, **506**, 523-535 (1987).
82. Yang, S-T, White, S.A. and Hsu, S-T, *Ind. Eng. Chem. Res.*, **30**, 1335-1342 (1991).
83. Kunin, R., "Liquid Ion Exchange Technology," in *Ion Exchange and Solvent Extraction: A Series of Advances*, Vol. 4, Marinsky, J.A. and Marcus, Y. (Eds.), Marcel Dekker, New York, 155-180 (1973).
84. Vieux, A.S., Rutagengwa, N., Rulinda, J.B., Balilkungeri, A., *Anal. Chim. Acta*, **68**, 415-424 (1974)
85. Manenok, G.S., Korobanova, V.I., Yudina, T.N., Soldatov, V.S., *Russ. J. Appl. Chem.*, **52**, 156-160 (1979).
86. Barrow, G.M. and Yerger, E.A., *J. Am. Chem. Soc.*, **76**, 5211-5216 (1954).
87. Yerger, E.A. and Barrow, G.M., *J. Am. Chem. Soc.*, **77**, 4474-4481 (1955).
88. Yerger, E.A. and Barrow, G.M., *J. Am. Chem. Soc.*, **77**, 6206-6207 (1955).
89. Schmidt, V.S., Mezhov, E.A., Rybakov, K.A., Rubisov, V.N., *Russ. J. Inorg. Chem. (Engl. Transl.)*, **23**, 1526-1527 (1978).
90. Schmidt, V.S., Mezhov, E.A., Rybakov, K.A., *Sov. Radiochem. (Engl. Transl.)*, **20**, 224-227 (1978).
91. Schmidt, V.S., Rybakov, K.A., Rubisov, V.N., *Russ. J. Anal. Chem.*, **38**, 896-900 (1983).
92. Grinstead, R.R. and Davis, J.C., *J. Phys. Chem.*, **72**, 1630-1638 (1968).
93. Eyal, A.M. and Baniel, A.M., *Solvent Extr. Ion Exch.*, **9**, 195-210 (1991).
94. Pearson, R.G. and Vogelsson, D.C., *J. Am. Chem. Soc.*, **80**, 1038-1043 (1958).

95. Izmailov, N.A. and Mozharova, T.V., *Russ. J. Phys. Chem.*, **34**, 814-818 (1960).
96. Schmidt, V.S. and Mezhov, E.A., *Russ. Chem. Rev.*, **34**, 584-599 (1965).
97. Tamada, J.A., Ph.D. Thesis, University of California, Berkeley, California, 1978.
98. Gusakova, G.V., Denisov, G.S., and Smolyanskii, A.L., *J. Gen. Chem. USSR (Engl. Transl.)*, **56**, 531-536 (1986).
99. Reschke, M. and Schügerl, K., *Chem. Eng. J.*, **28**, B25-B29 (1984).
100. Schügerl, K., "New Trends in the Extraction of Primary and Secondary Metabolites in Biotechnology," presented at the International Solvent Extraction Conference (ISEC), München, FRG (1986).
101. Wang, C.J., Bajpai, R.K., and Iannotti, E.L., *Appl. Biochem. Biotechnol.*, **28/29**, 589-603 (1991).
102. Cen, P. and Tsao, G.T., *Sep. Technol.*, **3**, 58-75 (1993).
103. Gailliot, F.P., Gleason, C., Wilson, J.J. and Zwarick, J., *Biotechnol. Prog.*, **6**, 370-375 (1990).
104. *American Type Culture Collection Catalogue of Bacteria and Bacteriophages*, 17th ed., Gherna, R., Pienta, P. and Cote, R. (Eds.), Rockville, Maryland, 114-119 and 290-328 (1989)
105. Bridson, E.Y., "Natural and Synthetic Culture Media for Bacteria," in *CRC Handbook Series in Nutrition and Food*, Section G, Vol. III, Rechcigl, M., Jr., Ed., CRC Press, Cleveland (1978).
106. Stanier, R.Y., Adelberg, E.A. and Ingraham, J.L., *The Microbial World*, 4th ed., Prentice-Hall, Englewood Cliffs, New Jersey, Chapter 2 (1976).
107. de Man, J.C., Rogosa, M. and Sharpe, M.E., *J. Appl. Bact.*, **23**, 130-135 (1960).
108. San-Martin, M., Pazos, C. and Coca, J., *J. Chem. Tech. Biotechnol.*, **54**, 1-6 (1992).
109. Reschke, M. and Schügerl, K., *Chem. Eng. J.*, **31**, B19-B26 (1985).
110. Letter from Brian Davison, Oak Ridge National Laboratory, Oak Ridge, Tennessee (September 28, 1992).
111. Holst, O. and Mattiasson, B., "Solid Sorbents Used in Extractive Bioconversion Processes," in *Extractive Bioconversions*, Mattiasson, B. and Holst, O., Eds., Marcel Dekker, New York (1991).
112. Althouse, J.W. and Tavlarides, L.L., *Ind. Eng. Chem.*, **31**, 1971-1981 (1992).
113. Srivastava, A., Roychoudhury, P.K. and Sahai, V., *Biotechnol. Bioeng.*, **39**, 607 (1992).

114. Lewis, V. P. and Yang, S., *Biotechnol. Prog.*, **8**, 104 (1992).
115. Yabannavar, V.M. and Wang, D.I.C., *Biotechnol. Bioeng.*, **37**, 716 (1991).
116. Cho, T. and Shuler, M.L., *Biotechnol. Prog.*, **2**, 53-60 (1986).
117. Laane, C., Boeren, S. and Vos, K., *Trends Biotechnol.*, **3**, 251 (1985).
118. Datta, R., *Biotechnol. Bioeng.*, **23**, 61 (1981).
119. Playne, M.J. and Smith, B.R., *Biotechnol. Bioeng.*, **25**, 1251 (1983).
120. Schopmeyer, H.H., "Lactic Acid," in *Industrial Fermentations*, Underkofler, L.A. and Hickey, R.J., Eds., Chemical Publishing Co., New York, 391-419 (1954).
121. *The Merck Index*, 10th ed., Windholz, M., Ed., Merck & Co., Inc., Rahway, New Jersey (1983).
122. Fleming, M., Parker, K.J. and Williams, J.C., *Proceedings of the International Society of Sugar Cane Technologists*, **13**, 1781-1800 (1968).
123. Ramaiah, N.A. and Kumar, M.B., *Proceedings of the International Society of Sugar Cane Technologists*, **13**, 1768-1780 (1968).
124. Nielsen, J.I. and Veibel, S., *Acta Polytechnica Scandinavica*, Copenhagen, Ch. 63, 25-57 (1967).
125. King, C.J., *Separation Processes*, 2nd. ed., McGraw Hill, New York, Ch.7, 309-359 (1980).
126. Filachione, E.M. and Fisher, C.H., *Ind. Eng. Chem.*, **38**, 228-232 (1946).
127. Wenker, H., U.S. Patent 2,334,524 (November 16, 1943).
128. Schopmeyer, H.H. and Arnold, C.R., U.S. Patent 2,350,370 (June 6, 1944).
129. Weisberg, S.M. and Stimpson, E.G., U.S. Patent 2,290,926 (July 28, 1942).
130. Keyes, D.B., *Ind. Eng. Chem.*, **24**, 1096-1103 (1932).
131. Filachione, E.M. and Costello, E.J., *Ind. Eng. Chem.*, **44**, 2189-2191 (1952).
132. Filachione, E.M., Costello, E.J. and Fisher, C.H., *J. Am. Chem. Soc.*, **73**, 5265-5267 (1951).

APPENDIX A: EXPERIMENTAL DATA

A.1 Sorption Isotherms

The results of the sorption isotherm experiments are shown in Table A.1. The experimentally measured quantities are listed below.

m	=	mass of sorbent (g)
W_o	=	mass of solution (g)
$C_{a,i}$	=	weight fraction acid in initial solution
$C_{a,f}$	=	weight fraction acid in final solution
$m(Q_a+Q_w)$	=	total solution uptake, after centrifugation (g)
$W_o\Delta C/m$	=	composite uptake of acid (g/g)
Q_a	=	individual uptake of acid (g/g)
Q_w	=	individual uptake of water (g/g)

Table A-1. Experimental Data for Sorption Isotherms

m	W_o	$C_{a,i}$	$C_{a,f}$	$m(Q_a+Q_w)$	$W_o\Delta C/m$	Q_a	Q_w
LACTIC ACID							
Amberlite IRA-910							
0.85554	11.08550	0.0090	0.0000	1.17802	0.1169	0.1169	1.2600
0.81920	10.94295	0.0183	0.0000	1.17033	0.2442	0.2442	1.1844
0.40567	10.44496	0.0095	0.0000	0.59742	0.2443	0.2444	1.2283
0.93017	11.41315	0.0270	0.0003	1.34502	0.3280	0.3284	1.1176
0.92699	11.09068	0.0315	0.0030	1.26452	0.3408	0.3449	1.0193
0.85664	11.13953	0.0451	0.0180	1.29572	0.3518	0.3790	1.1336
0.89835	11.63345	0.0542	0.0267	1.36534	0.3566	0.3972	1.1227
0.87968	11.29837	0.0631	0.0349	1.30591	0.3624	0.4142	1.0703
0.96935	11.31653	0.0756	0.0447	1.45381	0.3610	0.4280	1.0717
0.53325	10.73000	0.0795	0.0614	0.75160	0.3637	0.4503	0.9592
0.45591	18.44102	0.0822	0.0730	0.62994	0.3702	0.4710	0.9107
Amberlite IRA-35							
0.98941	10.03735	0.0815	0.0416	3.33473	0.4048	0.5450	2.8254
0.54809	10.11677	0.0815	0.0599	3.22571	0.3987	0.7512	5.1341
0.54156	19.90823	0.0815	0.0705	1.90240	0.4044	0.6520	2.8608
1.04010	10.13200	0.0598	0.0184	3.47388	0.4033	0.4647	2.8752
1.05830	10.05971	0.0500	0.0079	3.53059	0.4002	0.4265	2.9096
1.00220	9.98832	0.0450	0.0054	4.14718	0.3947	0.4170	3.7211
1.01960	9.96946	0.0401	0.0004	3.32208	0.3883	0.3895	2.8687
0.94403	9.98778	0.0349	0.0001	3.06448	0.3682	0.3685	2.8777
0.99230	9.98611	0.0300	0.0001	3.08501	0.3006	0.3010	2.8079
1.01859	9.93613	0.0252	0.0000	2.96661	0.2454	0.2455	2.6669
1.02984	10.02563	0.0200	0.0000	2.84501	0.1946	0.1946	2.5679
1.03807	9.89343	0.0150	0.0000	2.64782	0.1427	0.1427	2.4080

m	W_o	$C_{a,i}$	$C_{a,f}$	$m(Q_a+Q_w)$	$W_o\Delta C/m$	Q_a	Q_w

LACTIC ACID							
Dowex MWA-1							
1.02958	9.95988	0.0150	0.0001	1.61523	0.1438	0.1441	1.4248
0.95705	10.03706	0.0100	0.0001	1.33993	0.1040	0.1041	1.2959
1.06459	10.01322	0.0201	0.0002	1.80532	0.1875	0.1877	1.5080
1.05428	10.07679	0.0250	0.0003	1.94055	0.2359	0.2365	1.6042
1.04419	9.94983	0.0304	0.0008	2.01073	0.2821	0.2836	1.6420
1.05303	10.15536	0.0351	0.0022	2.16837	0.3173	0.3218	1.7374
1.06999	10.10901	0.0397	0.0028	2.18928	0.3486	0.3544	1.6917
0.97224	10.00345	0.0470	0.0130	2.01534	0.3498	0.3768	1.6961
1.03019	9.98007	0.0502	0.0138	2.15285	0.3526	0.3815	1.7083
1.04908	9.97253	0.0602	0.0231	2.22958	0.3527	0.4018	1.7235
0.97567	10.00881	0.0729	0.0378	2.03369	0.3601	0.4389	1.6455
0.48928	10.11939	0.0729	0.0558	1.06873	0.3537	0.4755	1.7087
0.28534	16.84679	0.0729	0.0676	0.75301	0.3159	0.4941	2.1449
0.30471	17.01514	0.0737	0.0674	1.06907	0.3518	0.5883	2.9202
0.54579	17.17610	0.0899	0.0791	1.19031	0.3399	0.5124	1.6685
0.48513	17.16036	0.1199	0.1106	1.23260	0.3290	0.6100	1.9308
0.99355	10.23064	0.1492	0.1143	2.16350	0.3594	0.6083	1.5693
Duolite A7							
0.99864	9.98439	0.0808	0.0455	2.30447	0.3529	0.4579	1.8497
0.47543	10.04724	0.0808	0.0635	1.25806	0.3656	0.5336	2.1125
0.49657	19.45657	0.0808	0.0712	1.20869	0.3761	0.5495	1.8846
1.00467	10.02418	0.0598	0.0268	2.25979	0.3293	0.3895	1.8597
1.00135	10.06009	0.0500	0.0188	2.20398	0.3135	0.3548	1.8462
0.99403	10.07674	0.0449	0.0149	2.16548	0.3041	0.3366	1.8419
1.02968	9.96765	0.0401	0.0104	2.23477	0.2875	0.3101	1.8603
1.00856	10.01539	0.0300	0.0049	1.95502	0.2496	0.2590	1.6794
1.01013	9.94444	0.0250	0.0032	1.99910	0.2151	0.2213	1.7577
0.98310	9.97290	0.0201	0.0014	1.77341	0.1896	0.1921	1.6118
0.99607	9.98705	0.0149	0.0006	1.65268	0.1435	0.1445	1.5147
1.02239	10.00130	0.0100	0.0005	1.51483	0.0933	0.0940	1.3877
0.92659	10.03943	0.0178	0.0010	1.72106	0.1828	0.1846	1.6728
0.90729	10.25647	0.0721	0.0410	1.74036	0.3516	0.4302	1.4880
1.01025	10.04197	0.0829	0.0474	2.34019	0.3529	0.4627	1.8538
1.00102	10.03798	0.0829	0.0478	2.35845	0.3520	0.4646	1.8915
0.99913	10.07900	0.0829	0.0482	2.33226	0.3500	0.4626	1.8717
1.00703	10.04989	0.0829	0.0477	2.36630	0.3513	0.4634	1.8864
1.00876	10.08991	0.0829	0.0478	2.30893	0.3511	0.4605	1.8284
1.00554	10.05945	0.0829	0.0478	2.32785	0.3511	0.4618	1.8532
1.00897	10.07108	0.0829	0.0478	2.37022	0.3504	0.4626	1.8865

m	W_o	$C_{a,i}$	$C_{a,f}$	$m(Q_a+Q_w)$	$W_o\Delta C/m$	Q_a	Q_w

LACTIC ACID							
Reillex 425							
0.92066	10.95590	0.0045	0.0020	1.11074	0.0297	0.0322	1.1743
0.93868	11.02493	0.0091	0.0047	1.28313	0.0521	0.0585	1.3084
0.92847	11.12634	0.0136	0.0075	1.19257	0.0728	0.0825	1.2020
0.96149	11.02409	0.0180	0.0105	1.28677	0.0855	0.0995	1.2388
0.92695	11.05238	0.0223	0.0138	1.34606	0.1023	0.1223	1.3298
0.96911	11.01107	0.0273	0.0170	1.34963	0.1171	0.1408	1.2518
0.96010	11.16365	0.0317	0.0206	1.31291	0.1293	0.1574	1.2101
1.01339	11.11236	0.0359	0.0235	1.47736	0.1361	0.1703	1.2875
0.96524	11.10053	0.0409	0.0278	1.43451	0.1505	0.1918	1.2944
0.94286	11.10803	0.0452	0.0319	1.41279	0.1561	0.2039	1.2945
0.94263	10.92938	0.0540	0.0391	1.44125	0.1730	0.2328	1.2962
0.87757	11.06385	0.0664	0.0508	1.41485	0.1969	0.2788	1.3335
0.48298	10.55701	0.0692	0.0600	0.92611	0.2002	0.3153	1.6022
0.67729	10.90861	0.0678	0.0554	1.09883	0.2001	0.2900	1.3324
0.21910	10.42214	0.0712	0.0671	0.42617	0.1942	0.3247	1.6204
0.45951	19.39518	0.0710	0.0664	0.78233	0.1926	0.3057	1.3969
0.26435	16.84820	0.0716	0.0687	0.49966	0.1860	0.3158	1.5743
0.46327	19.02263	0.0879	0.0824	0.81927	0.2271	0.3729	1.3956
0.50553	18.52329	0.1160	0.1097	1.65955	0.2322	0.5923	2.6905
0.48201	18.77417	0.1464	0.1404	0.93736	0.2322	0.5053	1.4394
0.46078	21.07901	0.1753	0.1704	0.94294	0.2240	0.5727	1.4737
SUCCINIC ACID							
Amberlite IRA-910							
0.22073	20.66535	0.0647	0.0591	0.37595	0.5257	0.6263	1.0769
0.30619	20.23869	0.0518	0.0439	0.53457	0.5216	0.5982	1.1476
0.35826	10.53310	0.0505	0.0335	0.54163	0.5007	0.5514	0.9604
0.72282	10.94857	0.0484	0.0182	1.01930	0.4574	0.4831	0.9271
0.95969	11.36034	0.0472	0.0110	1.32495	0.4281	0.4433	0.9373
0.73276	11.03521	0.0367	0.0093	1.00408	0.4132	0.4259	0.9443
0.62732	10.57033	0.0279	0.0054	0.86729	0.3797	0.3872	0.9953
0.22362	10.20629	0.0097	0.0025	0.33100	0.3297	0.3334	1.1468
0.76992	12.29697	0.0185	0.0004	1.00258	0.2893	0.2898	1.0124
0.23474	10.09736	0.0146	0.0055	0.37358	0.3897	0.3985	1.1930
0.62016	10.55604	0.0324	0.0084	0.87430	0.4086	0.4204	0.9894
0.90896	11.13465	0.0150	0.0000	1.18266	0.1838	0.1838	1.1174
0.88504	11.06466	0.0100	0.0000	1.11974	0.1250	0.1250	1.1402

m	W_o	$C_{a,i}$	$C_{a,f}$	$m(Q_a+Q_w)$	$W_o\Delta C/m$	Q_a	Q_w
SUCCINIC ACID							
Amberlite IRA-35							
0.19831	20.30949	0.0597	0.0540	0.50382	0.5838	0.7209	1.8196
0.54399	20.01757	0.0597	0.0452	1.59184	0.5336	0.6658	2.2604
0.94209	10.09255	0.0597	0.0196	2.89962	0.4296	0.4899	2.5879
0.58763	10.17377	0.0597	0.0313	1.85981	0.4917	0.5908	2.5742
0.96019	10.05111	0.0550	0.0144	2.86663	0.4250	0.4680	2.5175
1.00663	10.09745	0.0499	0.0101	2.95895	0.3992	0.4289	2.5105
1.04701	10.03935	0.0451	0.0065	2.99604	0.3701	0.3887	2.4728
0.95406	9.94083	0.0400	0.0053	2.72585	0.3616	0.3767	2.4804
1.00338	10.00937	0.0346	0.0024	2.78504	0.3212	0.3279	2.4478
0.96965	10.09819	0.0301	0.0015	2.70668	0.2978	0.3020	2.4894
1.00000	10.00000	0.0201	0.0000	2.61783	0.2010	0.2010	2.4169
1.01496	10.24315	0.0101	0.0000	2.34256	0.1019	0.1019	2.2061
Dowex MWA-1							
0.27019	20.39671	0.0759	0.0687	0.65485	0.5398	0.7063	1.7174
0.17813	18.83933	0.0618	0.0570	0.43023	0.5077	0.6453	1.7699
0.49668	15.35554	0.0604	0.0446	1.08912	0.4885	0.5863	1.6065
0.53862	10.19782	0.0604	0.0351	1.18288	0.4790	0.5561	1.6400
1.00893	15.25069	0.0604	0.0294	2.16487	0.4686	0.5317	1.6140
1.01179	10.01789	0.0597	0.0155	2.23129	0.4381	0.4722	1.7331
0.98272	10.09242	0.0498	0.0097	2.11021	0.4119	0.4327	1.7146
1.02334	10.01002	0.0400	0.0033	2.10479	0.3585	0.3654	1.6914
1.04449	10.16266	0.0352	0.0016	2.12827	0.3269	0.3302	1.7074
1.03423	10.10164	0.0300	0.00057	2.13092	0.2875	0.2887	1.7717
0.99369	10.04389	0.0200	0.00003	1.82683	0.2019	0.2019	1.6365
1.02028	9.91526	0.0099	0.00002	1.52402	0.0957	0.0958	1.3980
Dowex 66							
1.01533	9.98037	0.0101	0.0001	1.10048	0.0986	0.0987	0.9852
1.03904	10.01202	0.0206	0.0000	1.39506	0.1981	0.1982	1.1445
1.07625	9.94454	0.0307	0.0003	1.57727	0.2805	0.2810	1.1845
1.02927	9.97719	0.0367	0.0016	1.52660	0.3403	0.3427	1.1405
1.08085	9.98449	0.0406	0.0024	1.67646	0.3527	0.3564	1.1946
1.03011	10.02013	0.0505	0.0079	1.59526	0.4144	0.4266	1.1220
0.98936	10.04386	0.0615	0.0163	1.56543	0.4589	0.4847	1.0976
1.01228	15.12052	0.0615	0.0286	1.61411	0.4914	0.5370	1.0575
0.46985	10.13245	0.0615	0.0381	0.81334	0.5046	0.5706	1.1605
0.57221	14.97876	0.0615	0.0420	0.95437	0.5105	0.5805	1.0874
0.34885	19.59566	0.0615	0.0522	0.59834	0.5224	0.6119	1.1032

m	W_o	$C_{a,i}$	$C_{a,f}$	$m(Q_a+Q_w)$	$W_o\Delta C/m$	Q_a	Q_w
SUCCINIC ACID							
Bio-Rad AG3-X4							
0.99491	10.04774	0.0201	0.00019	1.40379	0.2011	0.2013	1.2096
0.99891	10.11105	0.0303	0.0015	1.39951	0.2911	0.2933	1.1078
1.00148	10.10506	0.0401	0.0062	1.44285	0.3423	0.3512	1.0896
1.00345	10.16510	0.0528	0.0148	1.63960	0.3850	0.4091	1.2248
1.00356	10.15142	0.0599	0.0200	1.53449	0.4035	0.4341	1.0950
1.00400	9.94841	0.0102	0.00003	1.09602	0.1005	0.1055	0.9911
1.00291	10.04199	0.0202	0.00017	1.24004	0.2008	0.2010	1.0354
0.96655	10.01148	0.0199	0.00028	1.11327	0.2036	0.2040	0.9478
1.02802	10.05579	0.0248	0.0006	1.25072	0.2369	0.2376	0.9490
1.01932	10.05076	0.0297	0.0018	1.38954	0.2750	0.2774	1.0858
1.01860	10.09308	0.0349	0.0042	1.50328	0.3042	0.3104	1.1654
1.02668	10.08517	0.0401	0.0055	1.45613	0.3395	0.3473	1.0710
1.03691	9.99572	0.0396	0.0065	1.50470	0.3192	0.3286	1.1225
1.01459	9.86631	0.0445	0.0098	1.33424	0.3367	0.3496	0.9655
1.00196	10.41248	0.0520	0.0132	1.64578	0.4039	0.4255	1.2171
1.02789	10.14297	0.0598	0.0197	1.51880	0.3960	0.4251	1.0525
Duolite A7							
0.57637	20.12822	0.0595	0.0464	1.48118	0.4575	0.5767	1.9931
1.05871	10.14207	0.0595	0.0190	2.33533	0.3880	0.4299	1.7759
0.56841	10.14566	0.0595	0.0350	1.31821	0.4373	0.5185	1.8006
1.01160	9.93549	0.0549	0.0164	2.17219	0.3781	0.4133	1.7339
1.04523	10.06304	0.0499	0.0127	2.21352	0.3581	0.3850	1.7327
1.03522	10.12609	0.0450	0.0100	2.14171	0.3424	0.3630	1.7058
1.01590	10.07867	0.0402	0.0075	2.09293	0.3246	0.3400	1.7202
1.00409	9.94651	0.0299	0.0029	1.99343	0.2673	0.2731	1.7122
1.03178	10.16658	0.0249	0.0017	1.96244	0.2288	0.2320	1.6700
0.99590	9.95771	0.0198	0.0007	1.79196	0.1910	0.1922	1.6071
0.97106	10.19676	0.0151	0.0004	1.65019	0.1540	0.1548	1.5446
1.02004	10.53278	0.0100	0.0004	1.59245	0.0992	0.0998	1.4613

m	W _o	C _{a,i}	C _{a,f}	m(Q _a +Q _w)	W _o ΔC/m	Q _a	Q _w

SUCCINIC ACID							
Reillex HPQ							
0.23528	19.70232	0.0647	0.0598	0.49992	0.4126	0.5397	1.5851
0.59015	13.25025	0.0529	0.0354	1.28872	0.3929	0.4703	1.7135
0.57571	13.26112	0.0532	0.0360	1.15216	0.3960	0.4680	1.5333
0.57207	13.26761	0.0532	0.0363	1.10566	0.3924	0.4625	1.4702
0.57551	13.27028	0.0532	0.0366	1.11513	0.3827	0.4536	1.4841
0.58573	13.36212	0.0532	0.0362	1.12343	0.3867	0.4562	1.4619
0.58942	13.45707	0.0532	0.0366	1.12870	0.3780	0.4481	1.4669
0.57515	13.23267	0.0532	0.0364	1.13552	0.3862	0.4581	1.5162
0.58166	13.24978	0.0531	0.0370	1.11875	0.3678	0.4390	1.4844
0.70055	10.88755	0.0226	0.0052	1.32047	0.2701	0.2799	1.6049
0.71210	10.95013	0.0179	0.0026	1.26691	0.2353	0.2399	1.5392
0.67751	10.81939	0.0135	0.0011	1.21251	0.1978	0.1997	1.5899
0.68363	10.77391	0.0090	0.0002	1.18144	0.1383	0.1386	1.5895
0.58658	10.96561	0.0273	0.0108	1.11300	0.3088	0.3293	1.5681
0.56490	11.02504	0.0461	0.0270	1.08773	0.3735	0.4255	1.5000
0.56625	10.95575	0.0367	0.0188	1.07485	0.3456	0.3813	1.5169
Reillex 425							
0.99701	11.53187	0.0047	0.0007	1.20162	0.0463	0.0471	1.1581
0.91648	10.90250	0.0091	0.0020	1.15477	0.0840	0.0865	1.1735
1.02948	11.49607	0.0134	0.0033	1.43342	0.1132	0.1177	1.2747
0.99204	11.51555	0.0181	0.0055	1.31884	0.1470	0.1543	1.1751
0.89114	10.72430	0.0227	0.0083	1.23182	0.1743	0.1857	1.1965
0.80293	11.08379	0.0276	0.0123	1.16983	0.2117	0.2297	1.2273
0.92403	11.22028	0.0362	0.0162	1.44051	0.2428	0.2680	1.2909
0.61454	10.95546	0.0332	0.0186	0.94784	0.2595	0.2882	1.2541
0.96535	11.26973	0.0407	0.0191	1.41615	0.2526	0.2807	1.1863
0.94483	11.27294	0.0450	0.0223	1.43695	0.2703	0.3042	1.2167
0.24507	20.52288	0.0490	0.0447	0.38835	0.3585	0.4293	1.1553
0.53345	10.68579	0.0469	0.0311	0.87041	0.3156	0.3663	1.2654
0.42233	15.49124	0.0481	0.0390	0.69892	0.3346	0.3992	1.2557
0.43379	20.55993	0.0485	0.0411	0.82343	0.3492	0.4272	1.4710
0.42063	10.56186	0.0566	0.0422	0.72136	0.3624	0.4348	1.2801
0.48906	20.68823	0.0577	0.0488	0.83284	0.3772	0.4604	1.2426
0.15636	20.85466	0.0652	0.0622	0.39563	0.3993	0.5566	1.9735

A.2 Sorbent pH Experiments

The results of the sorbent uptake-pH experiments are given in Table A.2.

Table A-2. Data from Sorbent Uptake-pH Experiments

Initial pH	Final pH	m	W_o	$C_{a,i}$	$C_{a,f}$	$m(Q_a+Q_w)$	$W_o\Delta C/m$	Q_a	Q_w

LACTIC ACID									
Amberlite IRA-910									
2.16	2.57	1.02499	11.00567	0.0398	0.0079	1.5368	0.3421	0.3540	1.1453
3.44	10.01	0.99584	11.03664	0.0397	0.0138	1.4083	0.2866	0.3062	1.1079
3.70	11.51	1.01330	10.98065	0.0398	0.0182	1.3775	0.2343	0.2590	1.1004
4.16	12.55	1.01808	11.06845	0.0398	0.0249	1.3305	0.1612	0.1938	1.1130
4.42	12.75	1.02523	11.08056	0.0398	0.0270	1.3703	0.1388	0.1749	1.1617
4.79	12.79	1.02257	11.02021	0.0396	0.0282	1.3256	0.1238	0.1603	1.1361
5.28	12.86	0.99455	10.97937	0.0399	0.0299	1.3054	0.1099	0.1491	1.1635
5.39	12.90	1.03325	10.95414	0.0398	0.0298	1.3199	0.1061	0.1441	1.1333
6.56	12.93	1.03310	11.02442	0.0398	0.0303	1.3363	0.1005	0.1398	1.1537
Amberlite IRA-35									
2.07	3.55	1.01340	11.00255	0.0399	0.0060	3.28032	0.3682	0.3876	2.8493
3.08	6.28	1.00489	11.09368	0.0401	0.0107	3.08907	0.3242	0.3572	2.7169
3.50	6.71	1.00814	10.98843	0.0401	0.0203	2.81381	0.2155	0.2722	2.5189
3.79	7.29	1.01585	11.05010	0.0400	0.0282	2.55100	0.1283	0.1991	2.3121
4.02	7.30	1.00605	11.13992	0.0399	0.0328	2.34582	0.0790	0.1554	2.1763
4.39	9.09	1.00848	11.02725	0.0399	0.0417	1.75043	-0.0202	0.0523	1.6834
6.11	9.53	1.00627	11.12512	0.0402	0.0433	1.78190	-0.0337	0.0429	1.7279
5.09	9.65	1.01500	11.20497	0.0400	0.0431	1.59779	-0.0344	0.0335	1.5407
4.77	5.91	0.99585	11.10715	0.0391	0.0136	3.31230	0.2843	0.3297	2.9964
2.81	8.88	1.00962	11.01063	0.0400	0.0390	1.93084	0.0112	0.0857	1.8267
3.15	9.00	1.01530	11.05303	0.0400	0.0406	2.00422	-0.0061	0.0739	1.9001
4.09	7.94	1.01778	11.04664	0.0401	0.0367	2.21544	0.0369	0.1168	2.0600
4.52	7.84	1.01307	10.97026	0.0401	0.0368	2.24419	0.0356	0.1171	2.0981
Dowex MWA-1									
2.2	2.67	1.00051	10.95633	0.0530	0.0135	2.11012	0.4324	0.4609	1.6481
3.9	4.70	1.00071	11.08576	0.0530	0.0190	2.04494	0.3762	0.4151	1.6284
4.1	5.07	0.9997	11.00459	0.0532	0.0233	2.06873	0.3287	0.3770	1.6924
4.4	5.46	0.99989	11.04408	0.0527	0.0264	1.99968	0.2909	0.3436	1.6563
4.8	6.04	1.00015	11.10465	0.0531	0.0331	2.04310	0.2219	0.2896	1.7532
5.2	6.52	0.99963	11.00599	0.0528	0.0377	1.88637	0.1663	0.2374	1.6497
5.8	7.39	1.00042	11.02941	0.0532	0.0452	1.54614	0.0883	0.1582	1.3873
7.66	8.00	1.00051	10.95633	0.0530	0.0504	2.11012	0.0285	0.1348	1.9743

Initial pH	Final pH	m	W_o	$C_{a,i}$	$C_{a,f}$	$m(Q_a+Q_w)$	$W_o\Delta C/m$	Q_a	Q_w
LACTIC ACID									
Duolite A7									
1.98	2.51	1.00022	11.03367	0.0400	0.0134	2.10332	0.2935	0.3217	1.78119
3.11	3.85	1.00929	11.11307	0.0397	0.0155	2.13085	0.2666	0.2993	1.81192
3.5	4.60	1.00463	11.07295	0.0399	0.0206	1.98620	0.2123	0.2531	1.72391
3.77	5.35	0.99554	11.03482	0.0399	0.0271	1.68146	0.1420	0.1877	1.50128
4.01	5.40	1.00125	11.02985	0.0400	0.0277	1.76723	0.1357	0.1846	1.58044
4.38	6.20	1.00245	10.98163	0.0401	0.0338	1.44675	0.0694	0.1181	1.32511
4.75	7.25	0.99944	10.97938	0.0399	0.0379	1.31609	0.0218	0.0718	1.24507
5.11	7.75	0.98396	10.94873	0.0401	0.0391	1.26323	0.0111	0.0613	1.22256
6.15	7.57	0.99064	11.03137	0.0398	0.0392	1.24316	0.0067	0.0559	1.19903
Reillex 425									
1.99	2.13	1.0028	11.03368	0.0395	0.0257	1.4684	0.1521	0.1897	1.2746
2.99	3.29	1.0138	11.00874	0.0396	0.0272	1.4525	0.1337	0.1727	1.2599
3.49	3.62	0.9953	11.07054	0.0397	0.0291	1.3969	0.1187	0.1595	1.2441
3.72	3.99	1.0153	11.01683	0.0395	0.0312	1.3401	0.0895	0.1307	1.1892
4.25	4.57	0.9947	11.15429	0.0398	0.0356	1.2547	0.0466	0.0915	1.1699
4.79	5.25	0.9820	11.02626	0.0395	0.0378	1.2034	0.0189	0.0652	1.1602
5.78	6.00	0.9917	11.16770	0.0396	0.0394	1.3107	0.0021	0.0542	1.2675
SUCCINIC ACID									
Amberlite IRA-910									
2.14	2.58	1.01783	10.98458	0.0531	0.0126	1.45393	0.4366	0.4547	0.9738
3.76	4.75	1.03361	11.02041	0.0530	0.0211	1.38673	0.3396	0.3680	0.9737
3.96	4.88	1.01248	11.06466	0.0534	0.0241	1.33583	0.3209	0.3527	0.9667
4.44	5.58	1.02526	10.96551	0.0532	0.0295	1.32964	0.2529	0.2912	1.0057
4.69	6.27	1.03585	10.98910	0.0529	0.0328	1.38134	0.2141	0.2578	1.0758
5.13	12.38	1.01529	10.95671	0.0531	0.0382	1.29665	0.1602	0.2091	1.0681
5.60	12.83	1.00697	10.98112	0.0531	0.0413	1.28587	0.1282	0.1810	1.0960
6.14	12.90	1.01839	11.04132	0.0529	0.0492	1.36908	0.0407	0.1068	1.2375
7.27	12.94	1.00643	10.95532	0.0530	0.0472	1.26563	0.0621	0.1215	1.1360
Amberlite IRA-35									
2.22	3.54	1.00109	11.07250	0.0528	0.0136	3.28280	0.4337	0.4782	2.8010
3.29	4.26	1.00516	11.15424	0.0530	0.0182	3.17178	0.3859	0.4434	2.7121
3.74	4.74	0.99753	11.02118	0.0532	0.0231	3.06744	0.3331	0.4040	2.6711
4.05	5.13	1.00875	11.02907	0.0531	0.0264	3.00545	0.2924	0.3709	2.6085
4.26	5.49	1.00821	11.07404	0.0530	0.0293	2.99757	0.2608	0.3478	2.6253
4.69	7.15	1.00682	10.95113	0.0528	0.0346	2.89056	0.1983	0.2975	2.5735
5.1	7.91	1.00650	10.97756	0.0530	0.0438	2.64927	0.1001	0.2155	2.4167
5.44	8.70	1.00678	11.07055	0.0529	0.0505	2.42707	0.0268	0.1484	2.2623
6.59	9.76	1.00895	11.06249	0.0528	0.0575	1.96554	-0.0520	0.0601	1.8880

Initial pH	Final pH	m	W_o	$C_{a,i}$	$C_{a,f}$	$m(Q_a+Q_w)$	$W_o\Delta C/m$	Q_a	Q_w

SUCCINIC ACID									
Dowex MWA-1									
~2.2	2.67	1.00051	10.95633	0.0530	0.0135	2.11012	0.4324	0.4609	1.6481
3.9	4.70	1.00071	11.08576	0.0530	0.0190	2.04494	0.3762	0.4151	1.6284
4.1	5.07	0.9997	11.00459	0.0532	0.0233	2.06873	0.3287	0.3770	1.6924
4.4	5.46	0.99989	11.04408	0.0527	0.0264	1.99968	0.2909	0.3436	1.6563
4.8	6.04	1.00015	11.10465	0.0531	0.0331	2.04310	0.2219	0.2896	1.7532
5.2	6.52	0.99963	11.00599	0.0528	0.0377	1.88637	0.1663	0.2374	1.6497
5.8	7.39	1.00042	11.02941	0.0532	0.0452	1.54614	0.0883	0.1582	1.3873
7.66	8.00	1.00051	10.95633	0.0530	0.0504	2.11012	0.0285	0.1348	1.9743
Bio-Rad AG3-X4									
3.78	4.58	1.00043	10.62161	0.0536	0.0221	1.57062	0.3340	0.3687	1.2012
4.03	4.85	1.00032	10.66245	0.0544	0.0247	1.40585	0.3168	0.3515	1.0539
4.54	5.59	1.00054	10.60354	0.0549	0.0305	1.49586	0.2588	0.3044	1.1906
4.83	6.07	1.00024	10.62072	0.0546	0.0343	1.46715	0.2156	0.2659	1.2009
5.31	6.54	1.00029	10.62642	0.0545	0.0378	1.47501	0.1774	0.2332	1.2414
5.71	8.10	1.00018	10.57642	0.0552	0.0476	1.11246	0.0805	0.1334	0.9789
6.90	11.19	1.00043	10.63348	0.0553	0.0519	1.18800	0.0359	0.0976	1.0899
Duolite A7									
2.12	2.82	0.99775	11.15077	0.0532	0.0192	2.07021	0.3796	0.4195	1.6554
3.2	3.93	0.99302	11.00130	0.0533	0.0223	2.00720	0.3438	0.3888	1.6325
3.72	4.72	0.99313	11.02162	0.0530	0.0292	2.02443	0.2638	0.3234	1.7151
3.97	5.01	1.00131	10.98645	0.0529	0.0324	1.88176	0.2247	0.2856	1.5937
4.28	5.17	1.01152	11.05351	0.0526	0.0331	1.88112	0.2128	0.2744	1.5853
5.13	6.15	1.00620	11.03571	0.0530	0.0455	1.60605	0.0827	0.1553	1.4409
4.7	5.58	1.00575	11.03571	0.0530	0.0386	1.71549	0.1577	0.2235	1.4821
5.48	6.55	1.00600	10.98776	0.0527	0.0486	1.39687	0.0443	0.1118	1.2767
6.53	7.61	0.99497	11.05247	0.0530	0.0537	1.22021	-0.0080	0.0579	1.1685
Reillex HPQ									
2.01	2.31	0.59015	13.25025	0.0529	0.0354	1.28872	0.3928	0.4701	1.7136
3.68	4.03	0.57843	13.16668	0.0530	0.0365	1.07814	0.3748	0.4428	1.4211
3.96	4.34	0.57770	13.19152	0.0531	0.0394	1.05162	0.3118	0.3836	1.4368
4.46	4.84	0.56449	13.20165	0.0530	0.0434	1.02804	0.2233	0.3023	1.5188
4.68	5.09	0.57263	13.17491	0.0530	0.0431	1.05136	0.2268	0.3060	1.5300
5.10	5.63	0.58628	13.24045	0.0530	0.0452	1.03688	0.1756	0.2556	1.5129
5.57	6.32	0.57538	13.33439	0.0530	0.0474	1.00244	0.1310	0.2136	1.5286
6.41	11.97	0.58477	13.46170	0.0529	0.0494	1.03032	0.0804	0.1675	1.5944
7.66	12.36	0.56654	13.26477	0.0527	0.0494	0.95862	0.0763	0.1599	1.5321
8.90	12.38	0.57327	13.25401	0.0532	0.0503	0.98817	0.0662	0.1530	1.5707

Initial pH	Final pH	m	W_o	$C_{a,i}$	$C_{a,f}$	$m(Q_a+Q_w)$	$W_o\Delta C/m$	Q_a	Q_w
SUCCINIC ACID									
Reillex 425									
5.70	5.93	1.07918	12.08957	0.0523	0.0534	1.20259	-0.0130	0.0465	1.0678
5.16	5.44	1.04351	12.04788	0.0522	0.0491	1.19829	0.0354	0.0918	1.0565
4.78	5.14	1.06095	12.12820	0.0525	0.0459	1.28257	0.0757	0.1311	1.0778
4.48	4.87	1.05832	12.23046	0.0524	0.0427	1.33629	0.1124	0.1663	1.0963
3.98	4.40	1.04158	12.04111	0.0521	0.0345	1.44294	0.2026	0.2505	1.1349
3.78	4.24	1.06569	12.09678	0.0524	0.0327	1.51824	0.2236	0.2703	1.1544
2.27	2.43	1.07247	12.12030	0.0523	0.0254	1.65406	0.3046	0.3437	1.1986

A.3 TMA Leaching Experiments

The results of the TMA leaching experiments are presented in Table A.3. The measured variables listed are self-explanatory.

Table A-3. Data from TMA Leaching Experiments

g Dry Sorbent	g Acid on Sorbent	TMA Solution		Mol TMA/ mol acid	Final Solution		% Recovery
		Wt. Fr.	g Used		g	Wt. Fr. Acid	
LACTIC ACID							
Amberlite IRA-910							
0.91104	0.39488	0.0521	12.33275	2.48	13.44563	0.0086	29.33
0.90507	0.38815	0.0060	12.49372	0.29	13.54664	0.0067	23.48
0.90897	0.38906	0.0121	12.25939	0.58	13.32090	0.0073	25.04
0.93610	0.39358	0.0170	12.30763	0.81	13.34726	0.0076	25.81
0.90612	0.39092	0.0223	12.25352	1.07	13.34240	0.0080	27.29
0.91205	0.39177	0.0279	12.50661	1.36	13.56701	0.0079	27.44
0.91988	0.39289	0.0336	12.31175	1.60	13.40248	0.0083	28.19
0.92344	0.39253	0.0000	12.41148	0.00	13.47023	0.0056	19.17
Amberlite IRA-35							
1.00883	0.52222	0.0526	12.23771	1.88	15.18362	0.0331	96.21
1.01485	0.52224	0.0455	12.30907	1.63	15.17286	0.0324	93.99
0.97513	0.50208	0.0385	12.41855	1.45	15.25381	0.0312	94.68
0.97686	0.50269	0.0320	12.50961	1.21	15.22337	0.0299	90.63
0.99942	0.51502	0.0255	12.60913	0.95	15.37420	0.0282	84.30
0.98772	0.50860	0.0193	12.58100	0.73	15.20273	0.0242	72.46
1.00311	0.51948	0.0129	12.43933	0.47	14.67494	0.0172	48.65
1.00418	0.51512	0.0066	12.49766	0.24	14.37226	0.0091	25.36
0.96629	0.50345	0.0000	12.97462	0.00	14.64524	0.0056	16.20

g Dry Sorbent	g Acid on Sorbent	TMA Solution		Mol TMA/ mol acid	Final Solution		% Recovery
		Wt. Fr.	g Used		g	Wt. Fr. Acid	

LACTIC ACID							
Dowex MWA-1							
0.99153	0.38613	0.0414	12.31182	2.01	14.36606	0.0266	98.94
0.98006	0.38393	0.0304	12.33534	1.49	14.34455	0.0263	98.21
0.99248	0.38673	0.0255	12.36358	1.24	14.39893	0.0263	97.77
0.97333	0.37877	0.0201	12.43060	1.01	14.45592	0.0256	97.89
0.98864	0.38516	0.0153	12.41113	0.75	14.37646	0.0199	74.40
0.98613	0.38542	0.0100	12.52855	0.50	14.37077	0.0140	52.07
0.98767	0.38482	0.0049	12.54930	0.24	14.31926	0.0075	27.78
0.93576	0.36515	0.0000	12.68475	0.00	14.33807	0.0040	15.87
Duolite A7							
0.97325	0.45099	0.0478	12.27581	1.98	14.52812	0.03146	101.34
0.98071	0.45375	0.0358	12.23934	1.47	14.51593	0.03159	101.06
0.96535	0.44850	0.0298	12.34819	1.25	14.62652	0.03093	100.87
0.96683	0.44721	0.0236	12.29251	0.99	14.52263	0.02895	94.02
0.97654	0.45250	0.0177	12.30097	0.73	14.46042	0.02194	70.12
0.98710	0.45455	0.0114	12.35698	0.47	14.39653	0.01631	51.64
0.97563	0.45054	0.0060	12.55470	0.25	14.54517	0.01254	40.49
0.97886	0.45286	0.0000	12.36018	0.00	14.36180	0.01079	34.22
Reillex 425							
0.89798	0.25696	0.030	12.34396	2.21	13.80954	0.01944	104.48
0.91043	0.26020	0.022	12.29379	1.61	13.77722	0.01948	103.15
0.90737	0.25972	0.019	12.54358	1.38	14.03196	0.01913	103.36
0.90247	0.25787	0.015	12.33700	1.07	13.79614	0.01905	101.90
0.91354	0.25863	0.011	12.30114	0.80	13.73350	0.01660	88.17
0.89810	0.25434	0.008	12.37743	0.56	13.77095	0.01469	79.55
0.91022	0.25650	0.004	12.28011	0.29	13.68100	0.01361	72.58
0.88566	0.25360	0.000	12.61118	0.00	13.95402	0.01125	61.89

g Dry Sorbent	g Acid on Sorbent	TMA Solution		Mol TMA/ mol acid	Final Solution		% Recovery
		Wt. Fr.	g Used		g	Wt. Fr. Acid	
SUCCINIC ACID							
Amberlite IRA-910							
0.42417	0.23692	0.0577	6.83519	3.33	7.32347	0.02015	62.28
0.42138	0.23828	0.0476	6.76787	2.70	7.32069	0.02026	62.25
0.42936	0.23306	0.0365	6.79566	2.13	7.35194	0.02014	63.53
0.42812	0.23897	0.0252	6.75401	1.42	7.30591	0.02038	62.31
0.42759	0.23649	0.0180	6.84840	1.04	7.37447	0.01800	56.13
0.42610	0.23165	0.0091	6.77814	0.53	7.40789	0.01377	44.04
0.44036	0.23692	0.0000	6.87864	0.00	7.34705	0.00826	25.62
Amberlite IRA-35							
0.99252	0.51198	0.0679	12.19783	3.23	15.41320	0.03383	101.86
0.96766	0.50568	0.0562	12.38450	2.75	15.51525	0.03246	99.59
0.98617	0.50588	0.0446	12.20794	2.15	15.11845	0.03103	94.04
0.98441	0.50870	0.0385	12.19654	1.84	15.32337	0.02930	88.27
0.95604	0.49598	0.0328	12.35059	1.63	15.37691	0.02641	81.88
0.97235	0.50390	0.0273	12.36347	1.34	15.34876	0.02305	70.21
0.98701	0.50783	0.0219	12.34203	1.06	15.28575	0.01876	56.47
0.96110	0.49844	0.0112	12.34792	0.55	15.15045	0.01443	43.86
0.96463	0.49990	0.0000	12.46584	0.00	15.41320	0.00698	21.24
Dowex MWA-1							
0.96565	0.46555	0.0546	12.32474	2.89	14.14264	0.0356	108.21
0.90007	0.48709	0.0417	12.32085	2.11	14.27018	0.0340	99.62
0.80839	0.43948	0.0364	12.47318	2.06	14.41299	0.0299	98.20
0.96089	0.46386	0.0345	12.28738	1.83	14.29013	0.0330	101.62
0.91663	0.49259	0.0307	12.24484	1.52	14.20175	0.0260	74.95
0.90624	0.48684	0.0209	12.24895	1.05	14.18856	0.0198	57.79
0.89896	0.48320	0.0103	12.30913	0.52	14.25536	0.0140	41.42
0.90044	0.48350	0.0000	12.27176	0.00	14.21941	0.0087	25.52
0.95503	0.46045	0.0000	12.15271	0.00	14.12750	0.0076	23.23

g Dry Sorbent	g Acid on Sorbent	TMA Solution		Mol TMA/ mol acid	Final Solution		% Recovery
		Wt. Fr.	g Used		g	Wt. Fr. Acid	
SUCCINIC ACID							
Bio-Rad AG3-X4							
0.98820	0.41961	0.0548	12.71874	3.31842	14.04683	0.02755	92.24
0.98500	0.41868	0.0456	12.81501	2.78839	14.15565	0.02653	89.69
0.98717	0.41858	0.0363	12.95826	2.24508	14.26094	0.02563	87.31
0.96500	0.41497	0.0307	12.75760	1.88558	14.22651	0.02483	85.13
0.97069	0.41537	0.0263	12.74625	1.61233	14.06126	0.02261	76.52
0.95902	0.41167	0.0232	12.88729	1.45097	14.27226	0.01875	65.01
0.96630	0.41094	0.0159	12.81096	0.99026	14.01670	0.01473	50.25
0.96977	0.41193	0.0077	12.72355	0.47515	13.89099	0.01257	42.38
0.98021	0.41516	0.0076	12.77970	0.46738	13.87455	0.01165	38.93
0.95842	0.40593	0.0000	12.72996	0.00000	13.94455	0.00644	22.12
Duolite A7							
0.97068	0.42209	0.0338	12.28854	1.97	14.40578	0.02840	96.93
0.95760	0.41659	0.0249	12.39473	1.48	14.62246	0.02190	76.87
0.95211	0.41456	0.0207	12.36060	1.23	14.85086	0.01968	70.51
0.97335	0.41845	0.0168	12.32048	0.99	14.70492	0.01715	60.26
0.95704	0.41610	0.0124	12.36047	0.74	14.51214	0.01517	52.90
0.95283	0.41975	0.0089	12.45747	0.53	14.31197	0.01252	42.67
0.95595	0.41074	0.0045	12.52554	0.27	14.33189	0.00983	34.30
0.96331	0.41613	0.0000	12.92709	0.00	14.66875	0.00680	23.98
Reillex HPQ							
0.54755	0.25627	0.0270	13.20150	2.78	14.05200	0.0136	74.83
0.54801	0.25347	0.0221	13.19389	2.30	14.01014	0.0139	76.80
0.54295	0.24627	0.0176	13.45547	1.92	14.27054	0.0133	76.94
0.55952	0.25523	0.0131	13.49095	1.38	14.31920	0.0126	70.81
0.56128	0.25149	0.0087	13.68088	0.95	14.51298	0.0107	61.90
0.54737	0.25073	0.0045	13.55076	0.49	14.38796	0.0087	50.02
0.54752	0.24034	0.0000	13.55812	0.00	14.37662	0.0069	41.29
Reillex 425							
0.96675	0.32072	0.029	13.46783	2.47	15.00819	0.0226	105.87
0.94925	0.31444	0.024	13.29700	1.99	14.81364	0.0215	101.33
0.98819	0.32292	0.018	13.42042	1.46	14.92421	0.0203	94.02
0.98175	0.32107	0.012	13.56120	0.97	15.00406	0.0171	80.11
0.97055	0.31468	0.009	13.65366	0.78	15.06714	0.0147	70.23
0.97039	0.28966	0.000	13.62869	0.00	14.69492	0.0087	43.92

A.4 Fixed-Bed Experiments

The results of the fixed-bed experiments are listed in Table A.4. The measured variables listed are self-explanatory.

Table A-4. Data from Fixed-Bed Experiments

Run #1

Wt. MWA-1 (g): 3.45745
Flow rate (ml/min): 1.52

BREAKTHROUGH CURVE

5.25 wt.% succinic acid

Vol. (ml)	Ave. Vol. (ml)	Wt. % Acid
4.6	2.3	0.00
12.2	8.4	0.00
19.0	15.6	0.01
26.8	22.9	0.34
34.2	30.5	1.37
41.6	37.9	2.51
49.0	45.3	3.51
56.4	52.7	4.20
63.8	60.1	4.65
71.2	67.5	4.93
78.6	74.9	5.10
86.6	82.6	5.23
94.7	90.65	5.23
102.8	98.75	5.23
110.9	106.85	5.28
119.0	114.95	
127.1	123.05	5.28
135.2	131.15	
143.3	139.25	
151.4	147.35	
159.5	155.45	
167.6	163.55	5.28
175.7	171.65	5.28

Void Volume (ml): 7.22
Calculated Capacity (g/g): 0.513
Total Acid Loaded (g): 1.777

TMA LEACHING

5.25 wt.% TMA

Vol. (ml)	Ave. Vol. (ml)	Wt. % Acid
180.6	178.13	5.45
186.6	183.55	7.24
193.9	190.20	6.72
200.8	197.30	5.25
208.1	204.40	3.76
215.4	211.73	2.45
223.2	219.30	1.03
231.0	227.10	0.32
238.3	234.65	0.09
245.6	241.95	0.02

Void Volume (ml)	7.4
Acid Recovered (g)	1.742
% Recovery	98.05

SECOND BREAKTHROUGH CURVE

294.3	292.13	0.00
298.9	296.58	0.00
304.7	301.80	0.00
309.6	307.14	0.00
313.6	311.57	0.01
321.3	317.42	0.60
329.0	325.12	2.12
336.7	332.82	3.27
344.4	340.52	4.02
352.1	348.22	4.57
359.8	355.92	4.91
368.1	363.92	5.09
375.8	371.92	5.21
383.5	379.62	5.20
391.2	387.32	5.26
398.9	395.02	5.30

Void Volume (ml)	7.22
Calculated Capacity (g/g)	0.516
Total Acid Loaded (g)	1.783

Run #2

Wt. MWA-1 (g): 4.70886
Flow rate (ml/min): 1.17

BREAKTHROUGH CURVE

5.25 wt.% succinic acid

Vol. (ml)	Ave. Vol. (ml)	Wt.% Acid
7.2	3.6	0.0
14.4	10.8	0.0
21.6	18.0	0.0
28.8	25.2	0.0
36.0	32.4	0.005
40.8	38.4	0.094
43.5	42.15	0.094
47.4	45.45	0.27
54.9	51.15	1.94
62.4	58.65	3.5
69.9	66.15	4.33
77.4	73.65	4.78
84.9	81.15	5.03
92.4	88.65	5.15
99.9	96.15	5.18
107.4	103.65	5.24
114.9	111.15	5.24
122.4	118.65	
129.9	126.15	5.27
137.4	133.65	

Void Volume (ml) 9.83
Calculated Capacity (g/g) 0.526
Total Acid Loaded (g) 2.478

TMA LEACHING
5.25 wt.% TMA

Vol. (ml)	Ave. Vol. (ml)	Wt.% Acid	Wt.% TMA
144.1	140.75	5.27	0.00
151.6	147.85	7.79	2.97
159.1	155.35	7.91	4.20
166.6	162.85	6.37	5.14
174.1	170.35	5.08	4.90
181.6	177.85	3.92	4.98
189.1	185.35	2.59	5.14
196.6	192.85	1.00	5.10
204.1	200.35	0.25	4.86
211.6	207.85	0.06	
219.1	215.35	0.02	

Sum of Wt.%*Vol./100 (g)	2.977
Void Volume (ml)	9.83
Acid Recovered (g)	2.461
% Recovery	99.31

Run #3

Wt. MWA-1 (g): 4.70515
 Flow rate (ml/min): 3.1

BREAKTHROUGH CURVE

5.25 wt.% succinic acid

Vol. (ml)	Ave. Vol. (ml)	Wt.% Acid
4.65	2.325	0.0
9.3	6.975	0.0
13.95	11.625	0.0
18.6	16.275	0.0
23.25	20.925	0.006
27.9	25.575	0.037
32.55	30.225	0.255
37.2	34.875	0.811
41.85	39.525	1.45
46.5	44.175	2.02
51.15	48.825	2.52
55.8	53.475	2.95
60.45	58.125	3.32
65.1	62.775	3.62
69.75	67.425	3.91
74.4	72.075	4.14
79.05	76.725	4.33
83.7	81.375	4.5
88.35	86.025	4.65
93.0	90.675	4.78
97.65	95.325	4.86
102.3	99.975	4.95
106.95	104.625	5.02

Void Volume (ml) 9.833
 Calculated Capacity (g/g) 0.463 *
 Total Acid Loaded (g) 2.181

* not at equilibrium with feed

TMA LEACHING
5.25 wt.% TMA

Vol. (ml)	Ave. Vol. (ml)	Wt.% Acid	Wt.% TMA	pH
111.45	109.2	4.86	0.00	2.72
115.95	113.7	6.07	1.23	3.77
120.45	118.2	6.99	3.11	4.41
124.95	122.7	6.77	3.75	4.77
129.45	127.2	6.17	4.18	5.06
133.95	131.7	5.49	4.33	5.37
138.45	136.2	4.88	4.43	5.83
142.95	140.7	4.33	4.51	8.42
147.45	145.2	3.81	4.33	9.32
151.95	149.7	3.27	4.34	9.65
156.45	154.2	2.71		9.93
160.95	158.7	2.11		10.16
165.45	163.2	1.59		10.36
169.95	167.7	1.14	4.73	10.53
174.45	172.2	0.78	4.80	10.72
178.95	176.7	0.54		10.88
183.45	181.2	0.41		11.00
187.95	185.7	0.23		11.21
192.45	190.2		4.66	11.39
196.95	194.7		4.83	11.64
201.45	199.2			11.78
205.95	203.7			11.87
210.45	208.2		4.88	11.94
Void Volume (ml)				9.833
Acid Recovered (g)				2.303
% Recovery				105.59

Run #4

Wt. MWA-1 (g): 5.59327
 Flow rate (ml/min): 1.54

BREAKTHROUGH CURVE
 5.25 wt.% succinic acid

Vol. (ml)	Ave. Vol. (ml)	Wt.% Acid
7.6	3.8	0.0
14.9	11.25	0.0
22.2	18.55	0.0
29.5	25.85	0.0
34.9	32.2	0.0
41.4	38.15	0.0
49.1	45.25	0.004
56.8	52.95	0.496
64.5	60.65	1.96
72.2	68.35	3.22
79.9	76.05	4.07
87.6	83.75	4.62
95.3	91.45	4.95
103.0	99.15	5.12
110.7	106.85	5.22
118.4	114.55	5.25
126.1	122.25	5.25
133.8	129.95	
141.5	137.65	5.26
149.2	145.35	
156.9	153.05	
164.6	160.75	5.28

Void Volume (ml) 11.68
 Calculated Capacity (g/g) 0.521
 Total Acid Loaded (g) 2.915

Run #5

Wt. MWA-1 (g): 4.70128
 Flow rate (ml/min): 1.4

BREAKTHROUGH CURVE
 2.53 wt.% succinic acid

Vol. (ml)	Ave. Vol. (ml)	Wt.% Acid
7.0	3.5	0.0
12.4	9.7	0.0
16.09	14.245	0.0
18.89	17.49	0.0
21.29	20.09	0.0
24.15	22.72	0.0
28.85	26.5	0.0
36.07	32.46	0.0
43.35	39.71	0.0
50.93	47.14	0.0
58.51	54.72	0.0
66.09	62.3	0.015
73.67	69.88	0.09
81.25	77.46	0.366
88.83	85.04	0.807
96.41	92.62	1.25
103.99	100.2	1.63
111.57	107.78	1.92
119.15	115.36	2.13
126.73	122.94	2.28
133.13	129.93	2.38
139.18	136.155	2.44
144.58	141.88	2.47
149.98	147.28	2.5
156.03	153.005	2.52
162.38	159.205	2.52
169.6	165.99	2.52
177.18	173.39	2.53
184.76	180.97	2.53

Void Volume (ml) 9.817
 Calculated Capacity (g/g) 0.469
 Total Acid Loaded (g) 2.204

Contact column with 5.25 wt.% succinic acid to fully load resins with 2.445 g acid. Then perform TMA leaching.

TMA LEACHING
10.3 wt.% TMA

Vol. (ml)	Ave. Vol. (ml)	Wt.% Acid	Wt.% TMA
192.51	164.955	5.71	0.32
200.26	196.385	10.34	5.18
208.01	204.135	10.20	7.30
215.76	211.885	7.42	7.50
222.61	219.185	4.19	7.22
230.36	226.485	1.07	7.73
238.11	234.235	0.19	8.07
245.86	241.985	0.03	8.32
253.61	249.735	0.00	8.11
261.36	257.485		8.28
269.11	265.235		8.32
276.86	272.985		8.41
284.61	280.735		8.35
292.36	288.485		8.50
300.11	296.235		8.58
307.86	303.985		8.61
315.61	311.735		
323.36	319.485		8.63

Void Volume (ml)	9.817
Acid Recovered (g)	2.480
% Recovery	101.43

Run #5

Wt. MWA-1 (g): 4.70008
 Flow rate (ml/min): 1.5

BREAKTHROUGH CURVE

4.01 wt.% lactic acid

Vol. (ml)	Ave. Vol. (ml)	Wt.% Acid
7.7	3.85	0.0
15.8	11.75	0.0
23.5	19.65	0.0
31.2	27.35	0.0
38.9	35.05	0.01
46.6	42.75	0.27
54.3	50.45	1.59
62.0	58.15	2.92
69.7	65.85	3.62
77.4	73.55	3.93
85.1	81.25	4.03
92.8	88.95	4.1

Void Volume (ml) 9.81
 Calculated Capacity (g) 0.375
 Total Acid Loaded (g) 1.764

TMA LEACHING

2.59 wt.% TMA

100.9	96.85	4.12
109.0	104.95	4.61
116.4	112.7	4.45
123.8	120.1	3.95
131.2	127.5	3.57
138.6	134.9	3.29
146.0	142.3	2.77
153.4	149.7	1.91
160.8	157.1	0.59
168.2	164.5	0.14
175.6	171.9	0.10
183.0	179.3	0.03

Void Volume (ml) 9.81
 Acid Recovered (g) 1.853
 % Recovery 105.0

A.5 Back-Extraction of Lactic Acid from Aliquat 336 in Toluene

The results of the experiment in which lactic acid was back-extracted from 0.31 M Aliquat 336 in toluene are given in Table A.5. The experimentally measure quantities are self-explanatory.

Table A-5. Results of Back-Extracting Lactic Acid from 0.3 M Aliquat 336 in Toluene

Loading Phase: Contact 15.0 ml 0.308 M Aliquat 336 with 15.0 ml 0.45 M aqueous lactic acid.

Back-Extraction Phase: Contact 10.0 ml extract with 10.0 ml 0.51 M TMA.

Initial mol/L Acid	Final mol/L Acid	Final pH	mols Acid Loaded	mol/L Acid in Back- Extract	% Recovery
0.445	0.373	5.12	0.00108	0.014	13.0
0.445	0.377	5.12	0.00102	0.013	12.7

A.6 Extractant pH Experiments

The results of the extractant uptake-pH experiments are given in Table A.6. The experimentally measured quantities are listed below.

- $[\overline{\text{HA}}]_{\text{tot}}$ = concentration of acid (all forms) in aqueous phase, mol/L
 $[\underline{\text{HA}}]_{\text{tot}}$ = concentration of acid (all forms) in organic phase, mol/L
 Z = loading of extractant

Table A-6. Data from Extraction Experiments

Initial pH	Final pH	$[\overline{\text{HA}}]_{\text{tot}}$	$[\underline{\text{HA}}]_{\text{tot}}$	Z calculated from $[\overline{\text{HA}}]_{\text{tot}}$	Z calculated from $[\underline{\text{HA}}]_{\text{tot}}$
LACTIC ACID					
0.297 M Alamine 336 in Chloroform					
Contact 15.0 ml organic phase with 15.0 ml 0.45 M lactic acid					
2.02	2.57	0.305	0.152	1.027	1.002
2.53	3.21	0.296	0.156	1.000	0.991
2.98	3.76	0.286	0.173	0.963	0.932
3.55	4.75	0.247	0.207	0.832	0.818
3.75	5.35	0.193	0.262	0.650	0.634
4.19	6.00	0.107	0.342	0.360	0.362
5.10	7.02	0.015	0.433	0.051	0.056
4.63	6.38	0.045	0.407	0.152	0.144
4.40	6.06	0.089	0.360	0.300	0.304
2.02	2.46	0.305	0.152	1.027	1.002
2.63	3.24	0.299	0.152	1.006	0.974
2.98	3.61	0.294	0.161	0.989	0.961
4.13	6.20	0.108	0.165	0.364	0.341
5.15	6.95	0.018	0.349	0.061	0.052
0.299 M Alamine 336 in MiBK					
Contact 15.0 ml organic phase with 15.0 ml 0.45 M lactic acid					
2.48	3.25	0.286	0.165	0.957	0.954
3.53	4.36	0.196	0.265	0.656	0.619
3.77	4.75	0.153	0.306	0.512	0.480
4.21	5.16	0.082	0.372	0.274	0.261
4.56	5.59	0.038	0.408	0.127	0.139
4.41	5.47	0.051	0.397	0.171	0.179
5.42	6.48	0.002	0.442	0.007	0.026

Initial pH	Final pH	$\frac{[A^-]}{[HA]}$ [HA] _{tot}	[HA] _{tot}	Z calculated from [HA] _{tot}	Z calculated from [HA] _{tot}
---------------	-------------	---	---------------------	--	--

LACTIC ACID

0.299 M Alamine 336 in MiBK

Contact 15.0 ml organic phase with 15.0 ml 0.45 M lactic acid

1.92	2.46	0.302	0.149	1.010	1.005
3.46	4.47	0.243	0.212	0.813	0.796
2.46	3.08	0.289	0.152	0.967	0.998
3.08	3.93	0.276	0.177	0.923	0.912
3.82	5.36	0.171	0.296	0.572	0.515
4.17	5.84	0.099	0.364	0.331	0.289
4.61	6.36	0.015	0.418	0.050	0.108
5.41	7.39	0.010	0.456	0.033	-0.019
5.57	7.58	0.005	0.461	0.017	-0.036
4.59	6.38	0.051	0.408	0.171	0.141
4.59	6.36	0.05	0.409	0.167	0.139

0.299 M Amberlite LA-2 in Chloroform

Contact 15.0 ml organic phase with 15.0 ml 0.45 M lactic acid

2.67	2.41		0.146		
2.97	3.38	0.302	0.152	1.010	0.997
3.50	3.73	0.308	0.161	1.030	0.966
3.75	4.76	0.257	0.199	0.860	0.838
4.15	5.50	0.181	0.272	0.605	0.596
4.60	6.04	0.117	0.334	0.391	0.386
5.68	6.43	0.059	0.390	0.197	0.199
4.61	7.33	0.006	0.438	0.020	0.040

0.299 M Amberlite LA-2 in MiBK

Contact 15.0 ml organic phase with 15.0 ml 0.45 M lactic acid

1.90	2.57	0.326	0.128	1.090	1.077
2.59	3.40	0.318	0.139	1.064	1.041
3.01	4.05	0.288	0.167	0.963	0.947
3.45	4.49	0.250	0.206	0.836	0.817
3.72	4.88	0.185	0.270	0.619	0.603
4.16	5.33	0.109	0.334	0.365	0.389
5.62	6.90	0.008	0.427	0.027	0.078
4.61	6.02	0.045	0.401	0.151	0.164

Initial pH	Final pH	$\overline{[HA]}_{tot}$	$[HA]_{tot}$	Z calculated from $[HA]_{tot}$	Z calculated from $[HA]_{tot}$
---------------	-------------	-------------------------	--------------	-----------------------------------	-----------------------------------

LACTIC ACID

0.299 M Alamine 336 in 1-Octanol

Contact 15.0 ml organic phase with 15.0 ml 0.45 M lactic acid

1.90	2.44	0.306	0.132	1.023	1.063
3.01	3.96	0.282	0.156	0.943	0.983
3.45	4.94	0.258	0.193	0.863	0.860
3.72	5.88	0.190	0.264	0.635	0.622
4.16	6.67	0.105	0.347	0.351	0.345
5.62	8.35	0.004	0.452	0.013	-0.007
4.61	7.61	0.042	0.410	0.140	0.133

SUCCINIC ACID

0.298 M Alamine 336 in Chloroform

Contact 15.0 ml organic phase with 15.0 ml 0.45 M succinic acid

2.12	2.73	0.289	0.166	0.970	0.952
2.81	3.48	0.286	0.169	0.960	0.944
3.20	3.99	0.281	0.176	0.943	0.919
3.69	4.70	0.260	0.197	0.872	0.848
3.98	5.06	0.232	0.229	0.779	0.743
4.50	5.44	0.167	0.291	0.560	0.532
4.79	5.55	0.136	0.321	0.456	0.433
5.40	5.92	0.051	0.405	0.171	0.152
6.00	6.39	0.012	0.437	0.040	0.044

0.298 M Alamine 336 in MiBK

Contact 15.0 ml organic phase with 15.0 ml 0.45 M succinic acid

2.12	2.84	0.323	0.131	1.082	1.070
2.81	3.60	0.305	0.148	1.022	1.012
3.20	3.97	0.286	0.168	0.960	0.947
3.69	4.46	0.227	0.231	0.762	0.736
3.98	4.71	0.189	0.279	0.634	0.574
4.50	5.07	0.114	0.347	0.383	0.345
4.79	5.19	0.081	0.380	0.272	0.235
5.40	5.61	0.023	0.435	0.077	0.050
6.00	6.13	0.005	0.455	0.017	-0.017

Initial pH	Final pH	$\overline{[HA]}_{tot}$	$[HA]_{tot}$	Z calculated from $[HA]_{tot}$	Z calculated from $[HA]_{tot}$
---------------	-------------	-------------------------	--------------	-----------------------------------	-----------------------------------

SUCCINIC ACID

0.294 M Alamine 336 in 1-Octanol

Contact 15.0 ml organic phase with 15.0 ml 0.45 M succinic acid

2.20	2.60	0.267	0.184	0.908	0.904
2.83	3.36	0.268	0.187	0.912	0.896
3.19	3.68	0.246	0.212	0.837	0.810
3.61	4.23	0.236	0.220	0.803	0.782
3.96	4.50	0.190	0.268	0.646	0.618
4.50	5.13		0.316		0.454
4.74	5.37	0.126	0.340	0.429	0.376
5.37	5.93	0.059	0.410	0.201	0.137
6.05	6.43	0.016	0.453	0.054	-0.011
6.98	7.11	0.000	0.465	0.000	-0.052

0.299 M Amberlite LA-2 in Chloroform

Contact 15.0 ml organic phase with 15.0 ml 0.45 M succinic acid

2.19	2.61	0.300	0.150	1.003	1.004
3.59	4.37	0.282	0.168	0.943	0.943
3.96	4.88	0.258	0.196	0.863	0.848
3.22	3.86	0.293	0.153	0.980	0.992
4.52	5.33	0.188		0.629	
2.86	3.48	0.297	0.155	0.993	0.988
4.78	5.57	0.143	0.314	0.478	0.454
5.38	5.91	0.058	0.396	0.194	0.182
5.98	6.26	0.014	0.436	0.047	0.046

0.299 M Amberlite LA-2 in MiBK

Contact 15.0 ml organic phase with 15.0 ml 0.45 M succinic acid

2.19	2.74	0.330	0.108	1.104	1.143
3.59	4.31	0.271	0.170	0.906	0.935
3.96	4.73	0.233	0.212	0.779	0.798
3.22	3.91	0.301	0.141	1.007	1.034
4.52	5.23	0.152	0.281	0.508	0.566
2.86	3.53	0.313	0.118	1.047	1.109
4.78	5.40	0.120	0.324	0.401	0.422
5.38	5.8	0.041	0.399	0.137	0.170
5.98	6.19	0.0005	0.438	0.002	0.041

Initial pH	Final pH	$[HA]_{tot}$	$[HA]_{tot}$	Z calculated from $[HA]_{tot}$	Z calculated from $[HA]_{tot}$

SUCCINIC ACID					
0.299 M Alamine 336 in 1-Octanol					
Contact 15.0 ml organic phase with 15.0 ml 0.45 M succinic acid					
2.20	2.41	0.242	0.216	0.809	0.784
2.83	3.27	0.226	0.208	0.756	0.809
3.19	3.59	0.218	0.230	0.729	0.736
3.61	4.02	0.190	0.257	0.635	0.644
3.96	4.40	0.171	0.279	0.572	0.571
4.50	4.97	0.125	0.337	0.418	0.377
4.74	5.39	0.128	0.336	0.428	0.380
5.37	6.43	0.076	0.395	0.254	0.185
6.05	7.09	0.021	0.447	0.070	0.011
6.98	7.66	0.0003	0.464	0.001	-0.046

A.7 Back-Extraction of Lactic Acid from Amberlite LA-2 in 1-Octanol

The results of the back-extraction experiment are given in Table A.7.

Table A-7. Data from Back-Extraction of Lactic Acid from Amberlite LA-2 in 1-Octanol

Add 10.0 ml extract (Amberlite LA-2/1-octanol containing 0.142 M lactic acid) to 10.0 ml aqueous TMA of varying concentrations.

[TMA]	mol TMA/ mol acid	$[HA]_{tot}$	$[HA]_{tot}$	Fractional Recovery	
				From $[HA]_{tot}$	From $[HA]_{tot}$
0.29	2.04	0.141	0.000	0.994	1.000
0.25	1.76	0.142	0.000	1.002	1.000
0.22	1.55	0.141	0.000	0.991	1.000
0.18	1.27	0.144	0.000	1.015	1.000
0.15	1.06	0.135	0.002	0.951	0.987
0.12	0.85	0.106	0.036	0.744	0.758
0.08	0.56	0.072	0.071	0.505	0.523
0.04	0.28	0.036	0.107	0.254	0.282
0.00	0.00	0.004	0.143	0.025	0.047

A.8 Uptakes of Sulfuric and Phosphoric Acids by Dowex MWA-1

The results of the Dowex MWA-1/sulfuric acid and Dowex MWA-1/phosphoric acid uptake experiments are shown in Table A.8.

Table A-8. Uptake Data for Sulfuric and Phosphoric Acids on Dowex MWA-1

m	W_o	$C_{a,i}$	$C_{a,f}$	$W_o\Delta C/m$
Sulfuric Acid				
1.00596	9.89346	0.00046	0.00001	0.00444
0.37600	10.39982	0.00091	0.00001	0.02501
0.29542	10.29332	0.00132	0.00001	0.04574
0.23744	10.01313	0.00180	0.00001	0.07552
0.31296	10.21735	0.00226	0.00001	0.07347
0.15748	18.89258	0.00226	0.00065	0.19303
0.81762	10.78413	0.01491	0.00016	0.19457
1.18837	10.72514	0.02970	0.00345	0.23691
0.88653	10.11852	0.02970	0.00726	0.25612
0.49130	10.16439	0.02970	0.01620	0.27930
Phosphoric Acid				
1.00596	9.89346	0.00046	0.00001	0.00444
0.37600	10.39982	0.00091	0.00001	0.02501
0.29542	10.29332	0.00132	0.00001	0.04574
0.23744	10.01313	0.00180	0.00001	0.07552
0.31296	10.21735	0.00226	0.00001	0.07347
0.15748	18.89258	0.00226	0.00065	0.19303
0.81762	10.78413	0.01491	0.00016	0.19457
1.18837	10.72514	0.02970	0.00345	0.23691
0.88653	10.11852	0.02970	0.00726	0.25612
0.49130	10.16439	0.02970	0.01620	0.27930

**A.9 Breakthrough Curves for Lactic Acid on Dowex MWA-1
in Presence of Sulfate and Phosphate**

The results of the breakthrough experiments for lactic acid on Dowex MWA-1 in the presence of sulfate and phosphate are given in Table A.9. The measured variables listed are self-explanatory.

**Table A-9. Breakthrough Data for Lactic Acid on Dowex MWA-1
in the Presence of Sulfate and Phosphate**

Run #1

Wt. MWA-1 (g): 4.7
Flow rate (ml/min): 1.5

4.05 wt. % Lactic Acid
0.06 wt. % Sulfate

Average Volume (ml)	Wt.% Lactic Acid
4.05	0.00
11.9	0.00
19.5	0.00
27.1	0.02
34.7	0.05
42.3	0.30
49.9	1.41
57.5	2.55
65.1	3.38
72.7	3.66
80.3	3.87
87.9	4.11
95.5	4.04
103.1	
110.7	4.05

Run #2

Wt. MWA-1 (g): 4.72079
Flow rate (ml/min): 1.5

4.02 wt. % Lactic Acid
0.25 wt. % Phosphate

Average Volume (ml)	Wt.% Lactic Acid

3.9	0.00
11.5	0.00
18.9	0.17
26.3	0.27
33.7	0.39
41.1	0.75
48.5	1.62
55.9	2.43
63.3	3.05
70.7	3.56
78.1	3.84
85.5	3.99
92.9	4.06
100.3	4.08
107.7	4.10
115.1	4.10
122.5	4.09
129.9	4.10
137.3	4.09
144.7	4.08
189.1	4.06

Run #3

Wt. MWA-1 (g): 4.7311
 Flow rate (ml/min): 1.5

4.00 wt. % Lactic Acid
 0.60 wt. % Sulfate

Average Vol. (ml)	Wt.% Lactic Acid	Wt.% Sulfate
3.95	0.00	0.00
11.6	0.15	0.01
19	0.64	0.01
26.4	0.85	0.00
33.8	1.05	0.00
41.2	1.35	0.00
48.6	1.98	0.00
56	3.30	0.00
63.4	4.11	0.00
70.8	4.48	0.00
78.2	4.21	0.00
85.6	4.82	0.00
93	4.86	0.00
100.4	4.86	0.01
107.8		0.01
115.2		0.02
122.6		0.03
130		0.05
137.4		0.08
144.8		0.11
152.2		0.17
159.6		0.23

Void Volume (ml) 10.48
 Total Sulfate Loaded (g) 0.86

TMA LEACHING
2.59 wt.% TMA

Average Vol. (ml)	Wt.% Lactic Acid	Wt.% Sulfate
167.7	4.36	0.23
176.2	2.89	2.25
184.4	1.40	3.69
192.6	0.67	2.81
200.8	0.30	2.08
209.0	0.09	0.77
217.2	0.02	0.14
225.4	0.07	0.00
233.6	0.00	0.00
241.8	0.00	0.00
250.0	0.00	0.00
258.2	0.00	0.00
Void Volume (ml)		10.48
Total Sulfate Recovered (g)		0.96
% Recovery		112

Run #4

Wt. MWA-1 (g): 4.7057
Flow rate (ml/min): 1.5

4.13 wt. % Lactic Acid
0.64 wt. % Sulfate

Average Volume (ml)	pH	Wt.% Lactic Acid	Wt.% Sulfate
3.85		0.00	0.00
11.1		0.10	0.00
17.9	9.21	0.41	0.00
24.7		0.84	0.00
31.85	8.74	1.00	0.00
39.35		1.13	0.00
46.85	4.26	1.51	0.00
54.35		2.47	0.00
61.85	3.42	3.27	0.00
69.35		3.84	0.00
76.85	3.24	4.19	0.00
84.35		4.39	0.002

Average Volume (ml)	pH	Wt.% Lactic Acid	Wt.% Sulfate
91.85	3.14	4.52	0.02
99.35		4.58	0.03
106.85	3.09	4.56	0.04
114.35		4.61	0.05
121.85	3.1	4.57	0.06
129.35		4.57	0.07
136.85	3.1	4.55	0.08
144.35		4.56	0.09
151.85	3.16	4.54	0.11
159.35		4.53	0.13
166.85	3.16	4.50	0.15
174.35		4.48	0.16
181.85	3.14	4.47	0.18
189.35		4.46	0.20
196.85	3.14	4.43	0.22
204.35		4.40	0.24
211.85	3.12	4.39	0.28
219.35		4.37	0.32
228.35	3.09	4.30	0.36

Bed Volume (ml) 10.43
Acid Loaded (g) 1.21

5.36 wt.% TMA

237.6	3.11	4.42	0.51
245.4	3.9	4.71	2.35
253.0	4.94	3.68	3.48
260.6	6.36	2.34	3.44
268.2	8.3	1.26	3.05
275.8	9.95	0.57	1.87
283.4	10.67	0.20	0.59
291.0	11.22	0.08	0.13
298.6	11.59	0.04	0.03
306.2	11.78	0.03	0.009
313.8	11.85	0.02	
321.4	11.88	0.02	
329.0	11.91	0.01	0.001
336.6	11.92	0.00	

Bed Volume (ml) 10.43
Phosphate Recovered (g) 1.14
% Recovery 94.3

A.10 Leaching of Sulfate and Phosphate from Dowex MWA-1

The results of the experiment in which sulfate and phosphate were leached from Dowex MWA-1 are given in Table A.10.

Table A-10. Data from Leaching of Sulfate and Phosphate from Dowex MWA-1

m	W_o	$C_{a,i}$	$C_{a,f}$	$m(Q_a+Q_w)$	$W_o\Delta C/m$	Q_a	

Sulfuric Acid -- Loading							
1.02379	20.32063	0.0299	0.0159	2.06282	0.28	0.31	
1.00935	20.28727	0.0299	0.0160	2.04127	0.28	0.31	
1.03142	20.32728	0.0299	0.0158	2.17387	0.28	0.31	
Phosphoric Acid -- Loading							
1.00514	20.57608	0.0604	0.0365	2.27574	0.49	0.57	
1.03654	20.63492	0.0604	0.0360	2.35761	0.49	0.57	
1.00903	20.55593	0.0604	0.0366	2.31402	0.48	0.57	

Mass Wet Sorbent	g Acid	g TMA Soln.	Wt.% TMA	mol TMA/ mol Acid	Wt. Final Soln.	Wt. Fr. Acid	% Recovery

Sulfuric Acid -- Leaching							
3.00733	0.31	19.71807	0.0252	2.66	21.72509	0.0141	99
2.95202	0.30	19.74802	0.0252	2.71	21.80669	0.0147	105
3.01570	0.30	19.75164	0.0252	2.73	21.82672	0.0152	110
Phosphoric Acid -- Leaching							
3.11691	0.55	24.69362	0.0252	1.89	26.86290	0.0206	101
3.21957	0.56	24.65013	0.0252	1.85	26.76363	0.0196	94
3.17590	0.55	24.68523	0.0252	1.88	26.60447	0.0214	105

A.11 Selectivity Experiments

The results of the selectivity experiments are given in Table A.11. The measured variables listed are self-explanatory.

Table A-11. Data from Selectivity Experiments

Phosphate/Lactic Acid

ml Aqueous Soln.	Initial Wt.% Lactic	Initial Wt.% PO ₄	ml Organic Phase	Final Aq. Wt.% Lactic	Lactic in Org. (mol/L)	Final Aq. Wt.% PO ₄	α

0.3 M Amberlite LA-2/MiBK							
100	3.96	0.58	3.5	3.83	0.39	0.63	0
100	3.96	0.58	7	3.71	0.39	0.59	0
100	3.96	0.58	10	3.60	0.39	0.61	0
100	2.00	0.54	3.5	1.93	0.23	0.61	0
100	2.00	0.54	7	1.84	0.26	0.59	0
100	2.00	0.54	10	1.76	0.27	0.60	0
0.3 M Amberlite LA-2/1-Octanol							
100	3.96	0.58	3.5	3.88	0.24	0.62	0
100	3.96	0.58	7	3.75	0.33	0.63	0
100	3.96	0.58	10	3.69	0.29	0.60	0
100	2.00	0.54	3.5	1.91	0.29	0.61	0
100	2.00	0.54	7	1.84	0.27	0.61	0
100	2.00	0.54	10	1.80	0.22	0.61	0
0.3 M Alamine 336/MiBK							
100	3.93	0.56	10	3.50	0.48	0.56	0.0
90	3.93	0.56	15	3.38	0.37	0.52	0.5
70	3.93	0.56	15	3.21	0.38	0.54	0.2
100	2.01	0.54	10	1.73	0.31	0.57	0.0
90	2.01	0.54	15	1.62	0.26	0.54	0.0
70	2.01	0.54	15	1.52	0.25	0.54	0.0
0.3 M Alamine 336/1-Octanol							
100	3.93	0.56	10	3.63	0.33	0.56	0.0
90	3.93	0.56	15	3.51	0.28	0.51	0.9
70	3.93	0.56	15	3.37	0.29	0.49	1.2
100	2.01	0.54	10	1.76	0.27	0.57	0.0
90	2.01	0.54	15	1.62	0.26	0.55	0.0
70	2.01	0.54	15	1.52	0.25	0.53	0.1

g Sorbent	g Soln.	Initial Wt.% Lactic	Initial Wt.% PO ₄	Final Wt.% Lactic	Final Wt.% PO ₄	α
Dowex MWA-1						
0.51	101.28	4.01	0.58	3.93	0.50	8.0
1.00	101.30	4.01	0.58	3.85	0.39	12.2
1.22	101.33	4.01	0.58	3.79	0.36	10.7
0.52	100.74	2.03	0.54	1.97	0.48	3.8
1.02	100.77	2.03	0.54	1.89	0.38	5.8
1.25	100.44	2.03	0.54	1.85	0.34	6.0
1.40	100.74	2.03	0.54	1.82	0.33	5.5

Sulfate/Lactic Acid

In these studies, concentrations of lactic acid in the organic phase marked with * were determined by analyzing a TMA leachate.

ml Aqueous Soln.	Initial Wt.% Lactic	Initial Wt.% SO ₄	ml Organic Phase	Final Aq. Wt.% Lactic	Lactic in Org. (mol/L)	Final Aq. Wt.% SO ₄	α
0.3 M Amberlite LA-2/MiBK							
100	4.00	0.29	7	3.85	0.30*	0.22	6.5
100	4.00	0.29	10	3.81	0.30*	0.20	6.4
100	2.00	0.29	7	1.95	0.20*	0.22	5.0
100	2.00	0.29	10	1.92	0.20*	0.19	5.7
0.3 M Amberlite LA-2/1-Octanol							
100	4.00	0.29	3.5	4.15	0.14*	0.26	10.7
100	4.00	0.29	7	4.11	0.16*	0.22	13.1
100	4.00	0.29	10	4.05	0.17*	0.19	14.2
100	2.00	0.29	3.5	2.07	0.09*	0.26	8.8
100	2.00	0.29	7	2.04	0.09*	0.22	11.1
100	2.00	0.29	10	2.00	0.11*	0.19	11.1
0.3 M Alamine 336/MiBK							
100	4.03	0.28	10	3.76	0.30	0.19	6.6
90	4.03	0.28	15	3.60	0.28	0.16	7.0
70	4.03	0.28	15	3.46	0.29	0.14	8.7
100	2.02	0.28	10	1.85	0.19	0.19	5.0
90	2.02	0.28	15	1.75	0.18	0.16	5.3
70	2.02	0.28	15	1.64	0.20	0.14	6.1

ml Aqueous Soln.	Initial Wt.% Lactic	Initial Wt.% SO ₄	ml Organic Phase	Final Aq. Wt.% Lactic	Lactic in Org. (mol/L)	Final Aq. Wt.% SO ₄	α
0.3 M Alamine 336/1-Octanol							
100	4.03	0.28	10	3.90	0.15	0.18	16.3
90	4.03	0.28	15	3.78	0.17	0.12	22.3
70	4.03	0.28	15	3.71	0.16	0.09	35.4
100	2.02	0.28	10	1.93	0.10	0.18	11.7
90	2.02	0.28	15	1.86	0.11	0.12	16.3
70	2.02	0.28	15	1.80	0.12	0.09	23.9

g Sorbent	g Soln.	Initial Wt.% Lactic	Initial Wt.% SO ₄	Final Wt.% Lactic	Final Wt.% SO ₄	α
Dowex MWA-1						
0.50	101.00	3.96	0.29	4.03	0.20	106
1.03	100.82	3.96	0.29	3.98	0.10	203
1.20	101.55	3.96	0.29	3.97	0.08	223
1.40	100.61	3.96	0.29	3.95	0.05	317
0.50	100.88	2.00	0.29	2.30	0.20	45
1.00	100.30	2.00	0.29	2.02	0.11	116
1.20	100.65	2.00	0.29	2.00	0.08	132

A.12 Dowex MWA-1 Isotherm at 37 °C

Uptake data for lactic acid on Dowex MWA-1 at 37 °C are given in Table A.12.

Table A-12. Uptake Data for Lactic Acid on Dowex MWA-1 at 37 °C

m	W _o	C _{a,i}	C _{a,f}	W _o ΔC/m
1.02132	9.97139	0.01000	0.00007	0.09695
1.03547	9.98385	0.01500	0.00012	0.14347
1.01895	10.01899	0.01980	0.00024	0.19233
1.01030	10.11329	0.02490	0.00055	0.24375
1.01367	10.13574	0.03000	0.00137	0.28627
1.03203	9.90285	0.03470	0.00265	0.30754
1.00313	10.00274	0.04070	0.00716	0.33445

A.13 Thermal Cracking of Trimethylammonium Lactate

Data from the thermal cracking experiments, with and without solvent addition, are given in

Table A.13.

Table A-13. Rate Data for Thermal Cracking of Trimethylammonium Lactate

Experiment #1

Initial Solution: 0.076 mol lactic acid
0.077 mol TMA
3.5 mol water

Time (hr)	Temp. (°C)	ml Water	% TMA Recovered
0.28	68.0	0.0	
0.45	79.0	0.0	
0.53	82.0	0.0	
0.78	83.0	0.0	
0.95	84.0	0.0	
1.53	83.0	2.0	
1.87	83.5	4.5	
2.03	83.5	5.0	
2.28	83.5	7.2	
2.53	84.0	9.1	
2.88	84.0	11.2	
3.12	84.0	13.0	
3.53	85.0	17.4	
3.80	87.0	22.0	
3.97	86.0		
4.30			6.49
4.33	86.0	30.0	
4.53	87.0	34.2	
4.73	88.0	38.8	
5.03	90.0	45.0	
5.28	93.0	50.0	
5.30			12.99
5.52			19.48
5.53	99.0	57.0	
5.63			25.97
5.70	100.0		
5.78			32.47
5.80	104.0	59.2	
5.97			38.96
6.12	110.0		
6.33			45.45
6.55	113.0	60.2	
7.02	120.0		51.95
8.03	120.0		61.82

Experiment #2 - with addition of MiBK

Initial Solution: 0.076 mol lactic acid
 0.023 mol TMA
 < 0.01 mol water

Time (hr)	Temp. (°C)	ml Soln. Off	% TMA Recovered	
0.00		0.0		Add 30 ml & boil off
0.25	68	0.0		
0.53	86	0.0		
0.87	92	0.0		
0.92		0.0	10.96	
1.00	96	0.0		
1.12	97	7.2		
1.25	97	14.0		
1.42	99	22.5		
1.50		25.2		Add 30 ml & boil off
1.75	97	25.9		
1.85	100	28.0	21.83	
1.92	101	32.0		
2.08	104	45.5		Add 40 ml & boil off
2.50	93			
2.67	96	52.5		
2.87	98	66.1		
3.12	105	85.5	32.70	
3.62				Add 60 ml & reflux
4.87	100			
5.25			43.57	
6.03				Boil off MiBK
6.87			54.43	
7.13		102.5		
7.70		140.5		Boil off complete

Experiment #3 - with addition of butyl acetate

Initial Solution: 0.076 mol lactic acid
 0.03 mol TMA
 < 0.01 mol water

Time (hr)	Temp. (°C)	% TMA Recovered	
0.40	90	11.70	Add 40.0 ml and reflux
0.78	90	20.03	
1.08	90	28.37	
1.62	94	36.70	
1.70	94	45.03	
2.78	94	53.37	
5.07	94	61.70	
6.15	97		Boil off
6.48	120		
6.77	120		

A.14 Esterification of Trimethylammonium Lactate

Data from the esterification experiments are given in Table A.14. The measured variables listed are self-explanatory.

Table A-14. Rate Data for Esterification of Trimethylammonium Lactate

Run #1

Initial Solution: 0.21 mol lactic acid
0.13 mol TMA
0.53 mol butanol
0.1 mol water

Time (hr)	ml H ₂ O	Temp. (°C)	% Conversion	% TMA Recovered
0.00	0.0	110	0.00	0.00
0.17	0.0	115		
0.27	0.5			
0.35	1.0	119		
0.47	1.6	123	10.13	
0.50	2.0	125		10.76
0.57	2.4	127		
0.67		128		
0.68	2.9			
0.73		129		18.80
0.83	3.4			
0.92	3.4	130		26.84
1.00	3.9	131	34.04	
1.13		132		34.87
1.2	4.4			
1.43	4.5	134		42.91
1.47			49.00	
1.63	5.0			
1.80		136		50.95
1.83	5.5			
2.00	6.0		63.47	
2.30		138	65.87	

Run #2

Initial Solution: 0.20 mol lactic acid
 0.17 mol TMA
 0.5 mol butanol
 0.7 mol water

Time (hr)	ml H ₂ O	Temp. (°C)	% Conversion	% TMA Recovered
0.00	0.0	100	0.00	0.00
0.23	0.0	102		
0.32	0.5	102		
0.40	1.5	103		
0.50			3.58	
0.70	3.2	104		8.23
0.78	4.2	104		
0.83	4.7			
0.90	5.2	104		
0.92				14.37
1.00			7.92	
1.05	6.2			
1.13	6.7	106		
1.20	7.2			
1.28	7.7	108		20.52
1.38	8.7			
1.50		109	7.45	
1.53	9.7			
1.57		110		26.67
1.63	10.7	112		
1.78	11.7	113		
1.90	12.5	115		
1.93		115	12.54	32.82
2.07	13.5	120		
2.28		122		38.96
2.45		124	25.74	
2.55		125		45.11
2.67	16.5	130		
2.77	17.0	131		
2.88	17.5	132		
3.05		132		51.26
3.22 ⁶			49.74	
3.43	18.5	135		
3.50	19.0	136		
3.63			58.51	57.40
3.72	20.0	139		
3.98		140	64.27	

Run #3

Initial Solution: 0.20 mol lactic acid
 0.20 mol TMA
 0.50 mol butanol
 5.7 mol water

Time (hr)	ml H ₂ O	Temp. (°C)	% Conversion	% TMA Recovered
0	0.0	95.0	0.00	0.0
0.35	3.5	95.0		
0.55	7.0	96.0		
0.88	12.0	96.0		
1.15	16.0	96.0		
1.63	23.0	96.0		9.99
2.18	31.0	96.0		
2.45	35.5	96.0		
2.77	39.5	96.0		
3.05	43.5	96.0		
3.57	50.0	97.0		17.02
3.93	54.5	97.0		
4.13	57.8	97.0	0.20	
4.38	61.0	97.0		
4.70	65.5	97.0		
5.35	73.5	99.0		24.04
5.58	77.0	99.0		
6.15	84.0	100.0	1.38	31.07
6.67	89.5	102.0		
6.92	92.5	104.0		38.09
7.25	96.5	107.0		
7.45	98.0	109.0	5.35	45.12
7.73	100.5	116.0		
7.80	101.0	117.0		
8.02	102.8	121.0		52.14
8.10	103.0	122.0	17.00	
8.53	105.9	134.0	37.04	59.17
8.63	106.4	135.0		66.19
8.83	107.4	140.5	52.45	
9.03	107.9	145.0		73.22
9.18	108.4	145.0	64.94	
9.95		150.0	69.98	

Run #4

Initial Solution: 0.20 mol lactic acid
 0.14 mol TMA
 0.65 mol water

Time (hr)	Temp. (°C)	% TMA Recovered
--------------	---------------	--------------------

0.00		
0.05	109.00	
0.17	118.00	
0.20		8.00
0.25	122.00	
0.30	124.00	16.00
0.37	126.00	
0.42	130.00	24.00
0.53	134.00	
0.57	136.00	32.00
0.62	136.00	
0.75	140.00	40.00
0.83	140.00	
0.93	141.00	
0.97	141.00	48.00
1.30	141.00	56.00

Run #5

Initial Solution: 0.20 mol lactic acid
 0.50 mol butanol
 3.7 mol water

Time (hr)	Temp. (°C)	% Conversion	
0	0.0	96.0	
0.42	1.8	97.0	
0.67	3.0	97.0	
1.07	5.5	97.0	
1.53	7.8	97.0	
1.73	9.0	97.0	
2.37	12.0	97.0	
2.92	14.5	97.0	
3.45	17.5	97.0	
4.15	22.5	97.0	
4.60	26.0	98.0	23.12
5.17	29.0	98.0	
5.80	33.5	98.0	26.60
6.33	36.5	98.0	
6.58	38.0	98.0	
6.78	39.5	99.0	29.66
7.28	42.5	99.0	
7.83	46.0	99.0	30.44
8.42	50.0	100.0	
8.83	53.5	100.5	35.60
9.22	60.5	106.0	
9.33	62.3	114.0	40.23
9.67	64.5	124.0	
9.77	65.5	130.0	46.09
9.83	68.0	145.0	63.26
9.97	68.5	148.0	
10.03	69.0	150.0	
10.13	69.5	157.0	
10.18	70.0	159.0	
10.30	70.5	161.0	
10.43	70.7	164.0	82.51
10.50	71.0	166.0	
10.68	71.0	169.0	
10.85	71.0	171.0	75.33

Run #6

Initial Solution: 0.20 mol lactic acid
 0.15 mol TMA
 0.49 mol butanol
 0.8 mol water
 5.3 mmol sulfuric acid

Time (hr)	ml H ₂ O	Temp. (°C)	% Conversion	% TMA Recovered
0.00	0.0	102	0.00	0.00
0.08		104		
0.20				
0.23	0.5	104		
0.27	1.0	105		
0.33	3.0	105		9.32
0.42	4.0	107		
0.48	5.0	108	2.35	16.26
0.62	7.0	109		
0.65	7.5			23.19
0.73	8.0	111		
0.83	9.5	116		30.12
1.00	11.0	121	8.01	37.06
1.15	12.0	129		43.99
1.28	12.5	131		50.92
1.47	13.0	132	28.16	57.86
1.65	13.5	134		64.79
1.82		137	39.28	
1.92		138		71.72
2.23	14.0	142		78.66
2.30	14.0	143	59.81	

Run #7

Initial Solution: 0.20 mol lactic acid
 0.15 mol TMA
 0.50 mol butanol
 0.8 mol water

Time (hr)	ml H ₂ O	Temp. (°C)	% Conversion	% TMA Recovered
0.00	0.0	102	0.00	0.00
0.17		102		
0.57	4.1	106	2.47	9.32
0.63	5.6	106		16.26
0.75	6.6			
0.83	7.8	109		23.19
0.87	8.3	110	4.07	
1.02	9.3	111		30.12
1.17	10.3	113		
1.27	10.5	116	7.68	
1.38	11.0	118		37.06
1.53	12.5	121	15.38	43.99
1.70	13.5	128		
1.88	14.0	129		50.92
2.03	14.5	130	34.74	57.86
2.35	15.5	134		64.79
2.58		135	54.52	71.72
2.83	16.0	137		
2.92		138	64.84	78.66
3.20	16.5	140		
3.33		140		
3.35	16.7		74.19	85.59
3.43		142	73.96	

Run #8

Initial Solution: 0.20 mol lactic acid
 0.13 mol TMA
 0.50 mol butanol
 0.7 mol water

Time (hr)	ml H ₂ O	Temp. (°C)	% Conversion	% TMA Recovered
0	0.0	103.0	0.0	0
0.22		105.0		
0.37	1.0	108.0		
0.50	2.0	109.0	2.90	
0.63	3.0	111.5		
0.75	4.0	112.0		10.53
0.85	4.5	113.0		
1.00	5.0	114.0	7.92	
1.07	6.0	116.0		18.53
1.12	6.6	118.0		
1.20	7.1	121.0		
1.43	7.6	124.0	23.57	26.53
1.50	8.0			
1.73	8.5	131.0		
1.83	9.5	132.0		34.53
2.02	10.0	134.0	44.06	
2.18	11.0			
2.27		137.0		42.53
2.48	11.5	138.0	63.95	
2.65	11.7	139.0		50.53
2.83	12.0	139.0		
3.00	12.5	140.0	60.87	
3.17	12.7	141.0		
3.43	13.0	142.0	70.55	58.53

Run #9

Initial Solution: 0.20 mol lactic acid
 0.13 mol TMA
 0.50 mol butanol
 0.7 mol water
 2.0 g Amberlyst 15

Time (hr)	ml H ₂ O	Temp. (°C)	% Conversion	% TMA Recovered
0	0.0	104.0	0.95	0
0.25	2.0	107.0		
0.35	3.0	108.0		10.53
0.43	4.0	111.0	3.10	
0.57	5.0	113.0		18.76
0.75	7.0	116.0		26.76
0.93	8.5	125.0	11.27	
0.98				34.76
1.03	9.0	126.0		
1.15	10.0	128.0		42.76
1.23	10.5	129.0	22.85	
1.32	11.0	130.0		
1.37		132.0		50.76
1.48		134.0		
1.57	11.3	134.5		58.76
1.65	11.5	135.0	42.14	
1.82	12.0	137.0		66.76
1.93	12.5	137.5		
2.05	13.0	138.0	58.94	74.76
2.33	13.5	140.0	62.06	
2.38		141.0		82.76
2.50		141.0		
2.63	13.7	142.0	67.91	
2.88	14.0	142.0	67.79	

Run #10

Initial Solution: 0.20 mol lactic acid
 0.13 mol TMA
 0.50 mol butanol
 0.7 mol water
 2.0 g silica gel

Time (hr)	ml H ₂ O	Temp. (°C)	% Conversion	% TMA Recovered
0	0.0	102	0.00	0
0.33	2.0	111		
0.45	3.0	111	3.52	15.04
0.92	6.5	129	17.36	38.23
1.03		134		
1.12	7.0	137		49.65
1.20		138	29.62	
1.37	7.0	140		61.08
1.62	7.3	144	45.23	
1.75		144	48.10	
1.83	7.8	140	52.35	72.51
1.96		143		
2.06	8.8	148	61.57	
2.16		148	61.60	

Run #11

Initial Solution: 0.20 mol lactic acid
 0.14 mol TMA
 2.0 mol butanol
 0.7 mol water

Time (hr)	ml H ₂ O	Temp. (°C)	% Conversion	% TMA Recovered
0	0.0	105.0	0.00	0
0.22	1.5			
0.38	3.0	109.0		
0.45	3.8	110.5		10.57
0.50			3.25	
0.68	5.0	112.0		
0.90	6.0	114.0		20.57
1.08	7.5	116.0	9.69	
1.12				30.57
1.57	10.5	120.0	18.16	40.57
1.78	11.4	121.0		50.57
2.13	12.0	122.0	28.56	
2.25	12.2	122.0		60.57
2.43	12.5	122.0		
2.58			36.65	
2.73	13.0			70.57
3.50	13.2	122.0	49.94	80.57
3.93	13.5	122.0		
4.28			66.99	
4.50			63.89	

APPENDIX B: FITTING OF SORPTION ISOTHERMS

As described in Section 3.3.3, several isotherm models were fitted to the experimental data. Least-squares estimates of the parameters were determined by nonlinear regression using the STATGRAPHICS NONLIN procedure.

B.1 Langmuir Isotherms

The uptake data for all acid/sorbent systems were fitted with simple Langmuir isotherms. As discussed in Chapter 3, the sorption data for lactic acid are, in general, well described by simple Langmuir curves. The one exception is the multifunctional Duolite A7, which, as shown in Figure B-1, is poorly described by a simple Langmuir isotherm. Because of this poor fit and the known multifunctionality of this sorbent, a dual-site Langmuir curve was also fitted to the data. The resulting fit (presented in Figure 3-10) is good.

The uptakes of succinic acid by all sorbents except Reillex 425 (see Figure 3-15) are poorly fit by Langmuir isotherms, as shown in Figures B-2 through B-7. For the Duolite A7/succinic acid system, a dual-site Langmuir isotherm (Figure 3-17) describes the data well. The uptakes of succinic acid by the five remaining sorbents were examined in greater detail.

B.2 Model Choices for Succinic Acid Isotherms

Fruendlich and dual-site Langmuir isotherms were fitted to the data for succinic acid and Bio-Rad AG3-X4, Dowex MWA-1, Amberlite IRA-35, Amberlite IRA-910 and Reillex HPQ. These two models were compared with the Langmuir model through a visual examination of the resulting graphs, through examination of the residuals (i.e., experimental values minus fitted values) as a function of acid concentration, and through a comparison of the residual standard deviations. As an example, consider the case of succinic acid and Amberlite IRA-35. From Figure B-5 it is clear that the Langmuir isotherm does not give a

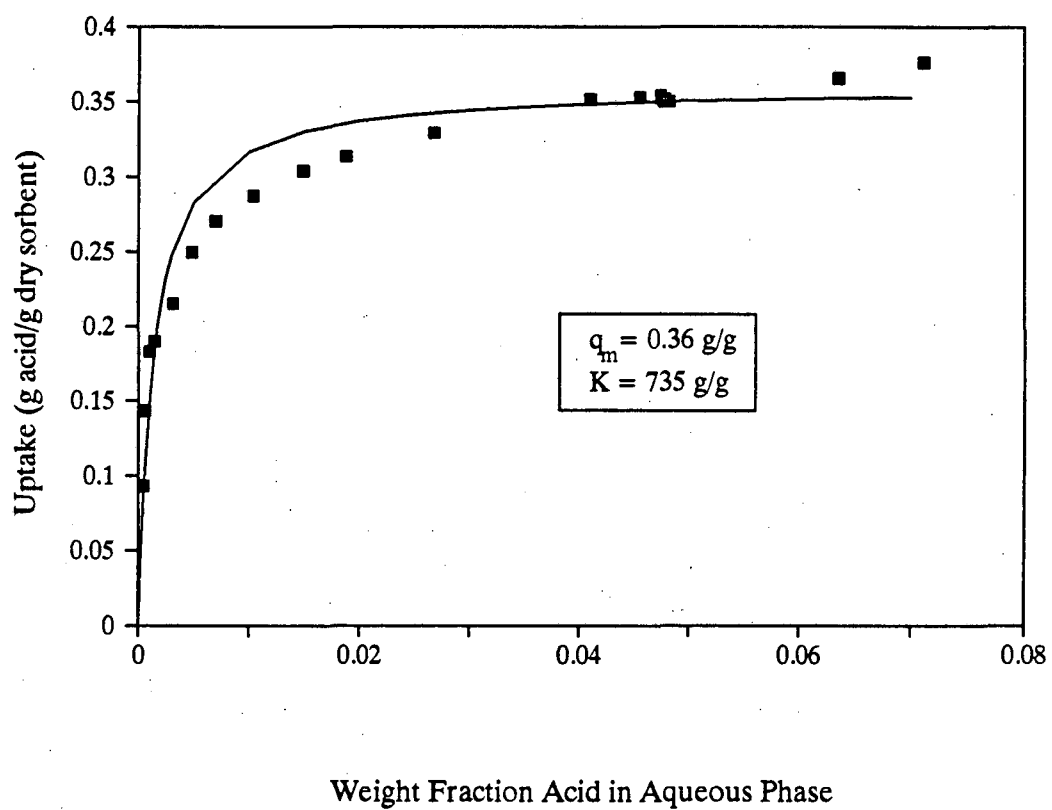


Figure B-1. Uptake of Lactic Acid by Duolite A7
Fitted with Langmuir Isotherm

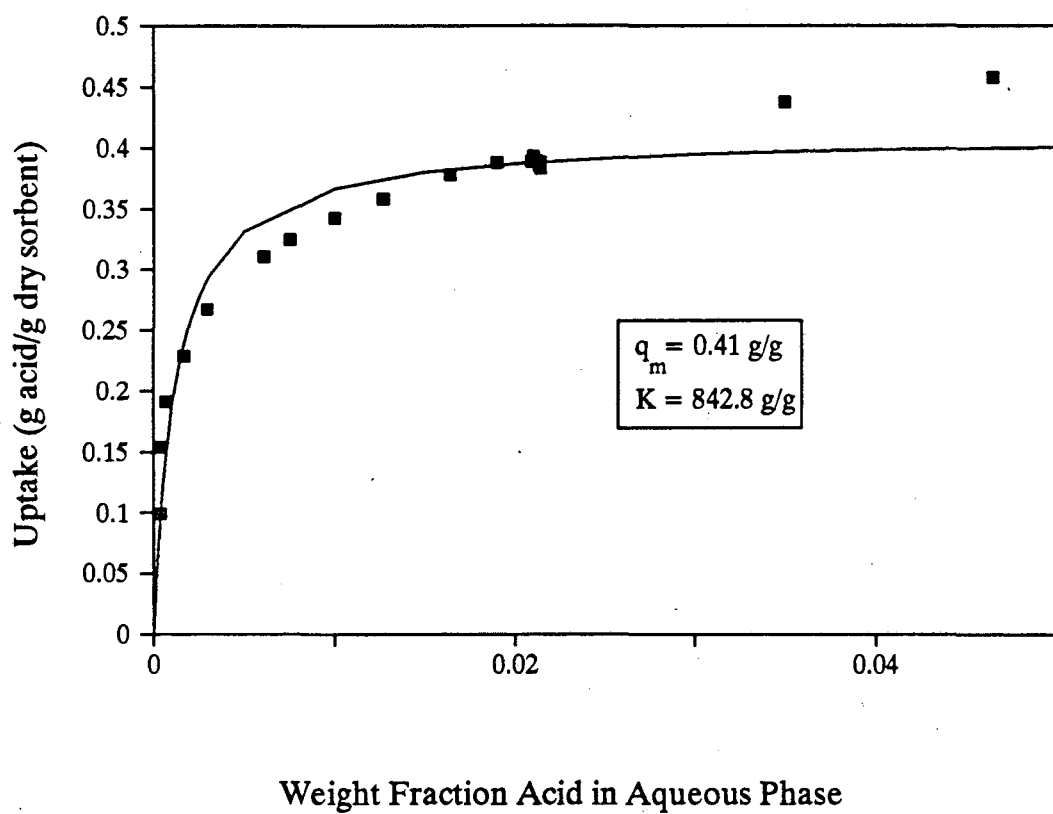


Figure B-2. Uptake of Succinic Acid by Duolite A7
Fitted with Langmuir Isotherm

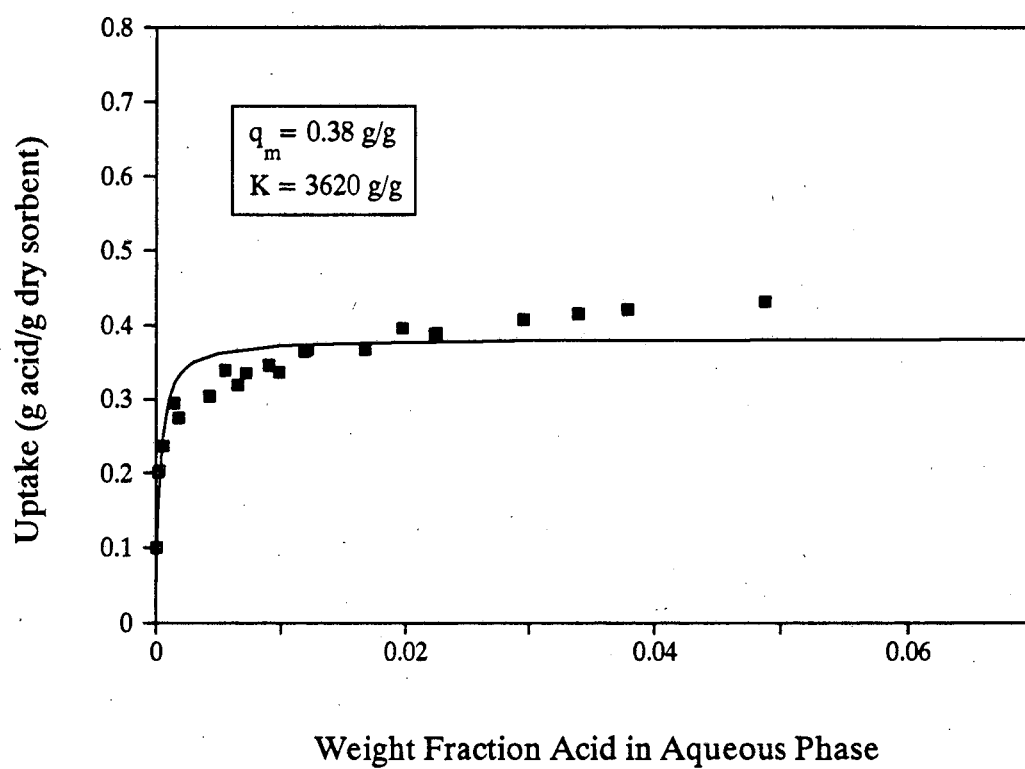


Figure B-3. Uptake of Succinic Acid by Bio-Rad AG3-X4
Fitted with Langmuir Isotherm

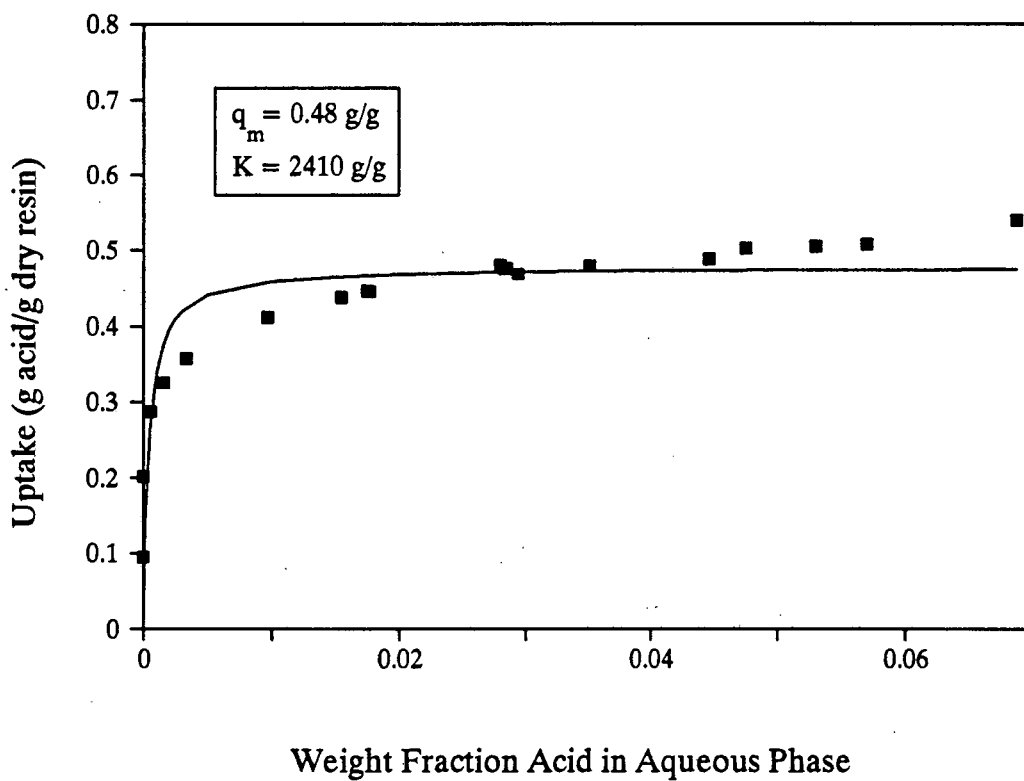


Figure B-4. Uptake of Succinic Acid by Dowex MWA-1
Fitted with Langmuir Isotherm

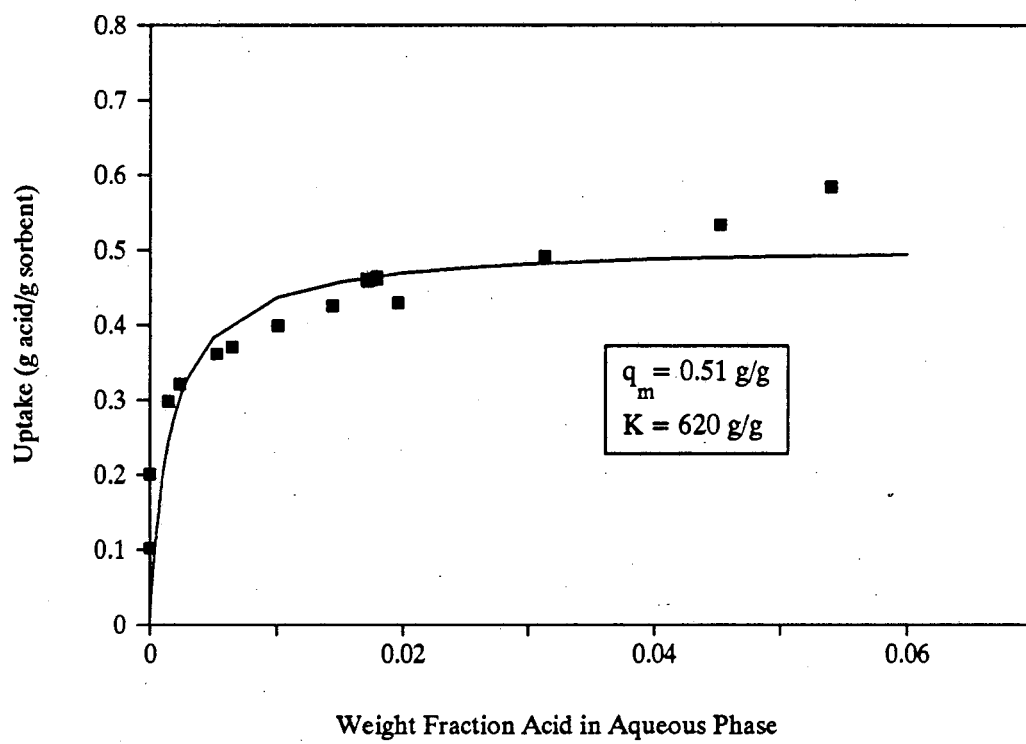


Figure B-5. Uptake of Succinic Acid by Amberlite IRA-35
Fitted with Langmuir Isotherm

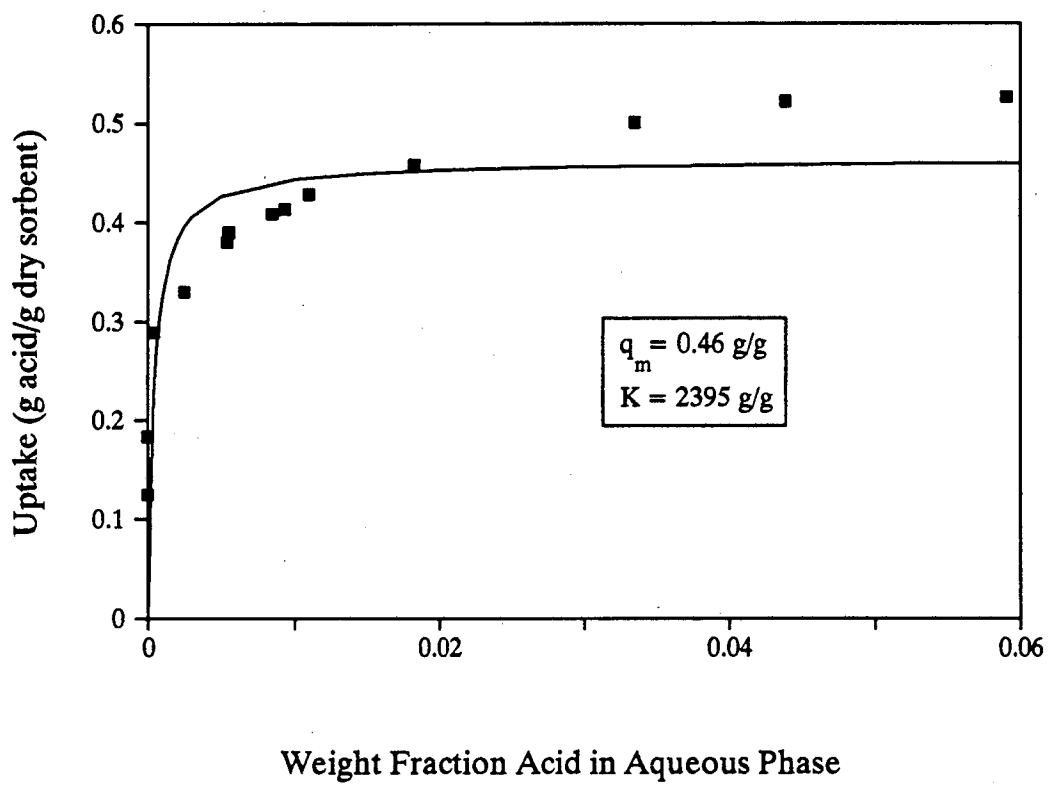


Figure B-6. Uptake of Succinic Acid by Amberlite IRA-910
Fitted with Langmuir Isotherm

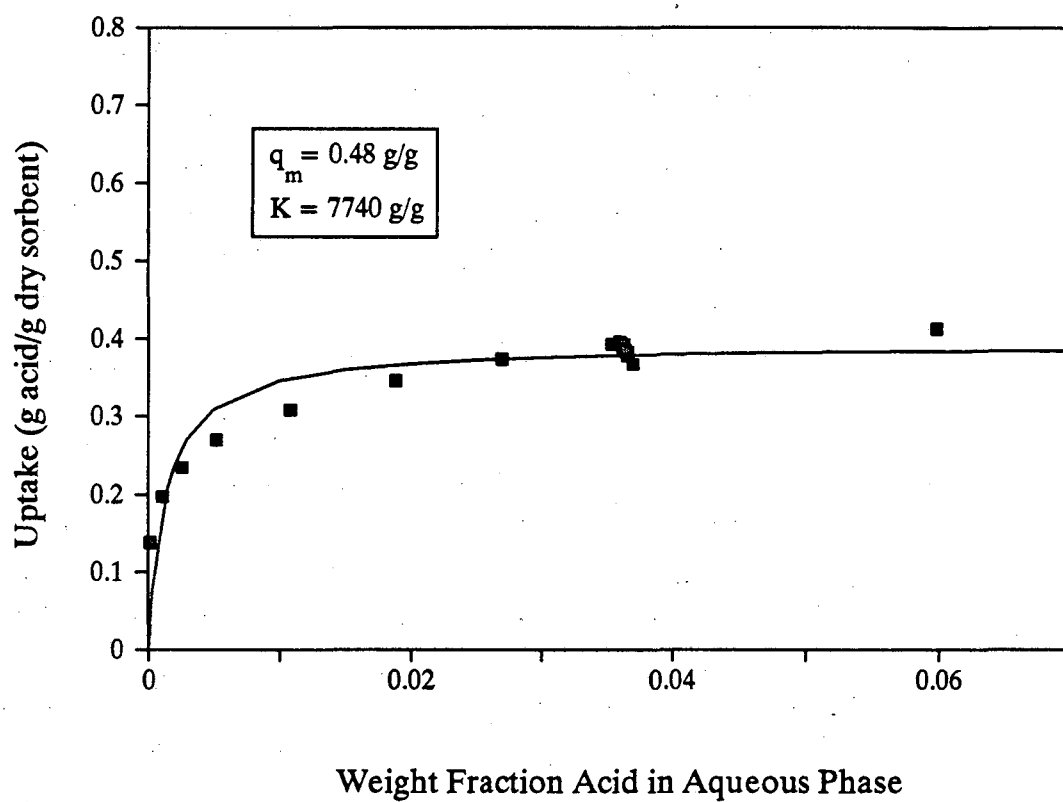


Figure B-7. Uptake of Succinic Acid by Reillex HPQ
Fitted with Langmuir Isotherm

good fit to the data. Figure B-8 shows a plot of the residuals from this fit versus the weight fraction acid in solution. The residuals are not randomly scattered, but instead have a definite parabolic shape, indicating a systematic misfit of the model to the data. At the low and high ends of the concentration range studied, the model underpredicts the uptake, whereas at moderate concentrations it overpredicts the uptake. The standard deviation of the residuals for this model fit is 0.057.

Figure 3-21 shows the Freundlich isotherm that was fitted to the same data, and Figure B-9 is the corresponding residual plot. The isotherm appears to give a good fit to the data. Furthermore, the residuals are somewhat more randomly scattered and are, in general, much smaller. The residual standard deviation is 0.023, reflecting the better fit of this model to the data. Note that both the Freundlich and Langmuir isotherms contain the same number of parameters. Thus, it makes sense to compare residual standard deviations in this manner.

Figure B-10 is a fitted isotherm of the dual-site Langmuir form, and Figure B-11 is the corresponding residual plot. The residual plot is very similar to that for the Freundlich isotherm. The residuals are again smaller than those for the simple Langmuir model and show a less well-defined pattern. The residual standard deviation is 0.022. This value is lower than that for the Freundlich isotherm, as it should be, since the dual-site Langmuir model has two additional parameters. However, the fit of the model to the data is not improved greatly by the use of four parameters, and, as a result, the residual standard deviation is only slightly lower. Since both the Freundlich and the dual-site Langmuir models give approximately the same fits, and since there is no apparent physical basis for using a dual-site model (i.e. the resin is not multifunctional), the Freundlich isotherm was used to model the data.

Models for the other four sorbents were chosen using similar lines of reasoning. For all five sorbents, the Freundlich isotherm was the model of choice.

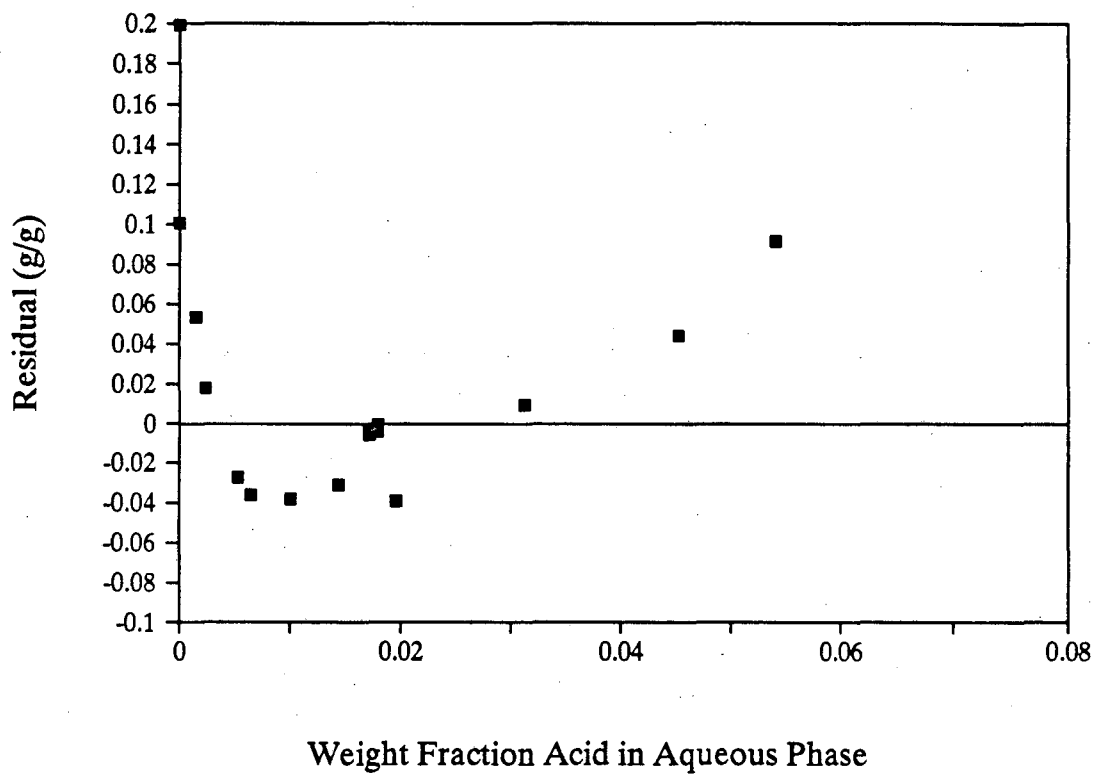


Figure B-8. Residuals from Fit of Langmuir Isotherm to Succinic Acid/Amberlite IRA-35 Data

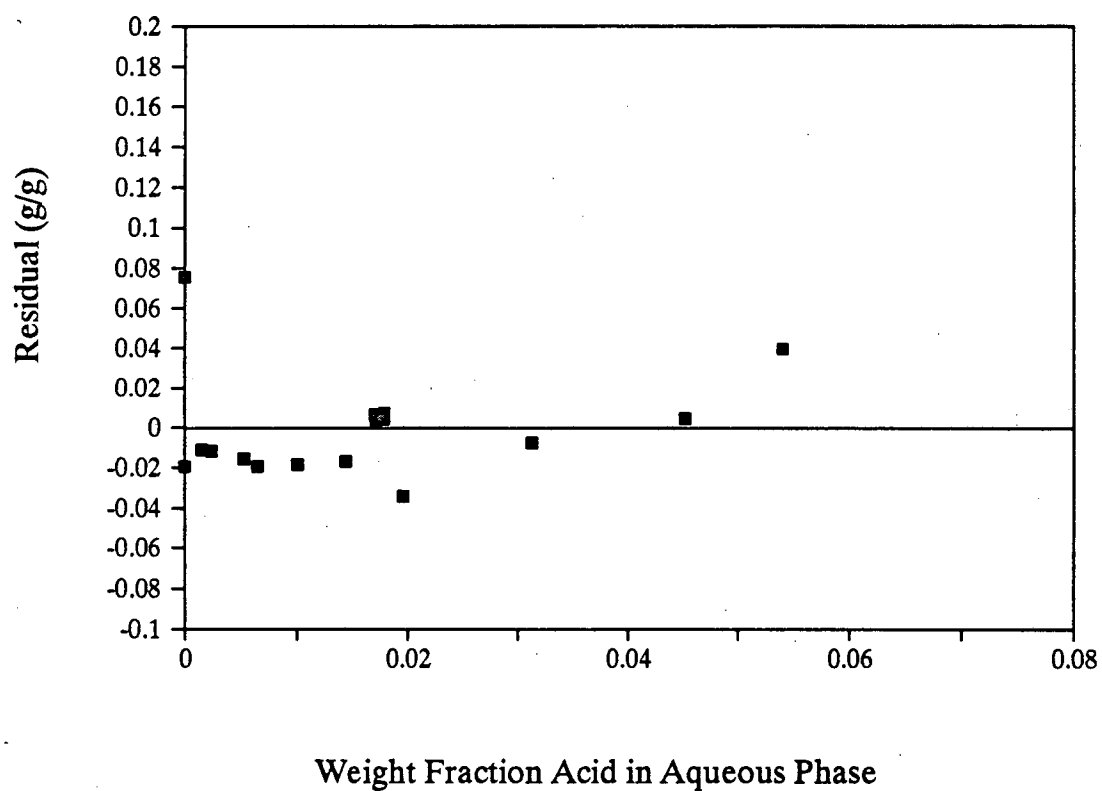


Figure B-9. Residuals from Fit of Freundlich Isotherm to Succinic Acid/Amberlite IRA-35 Data

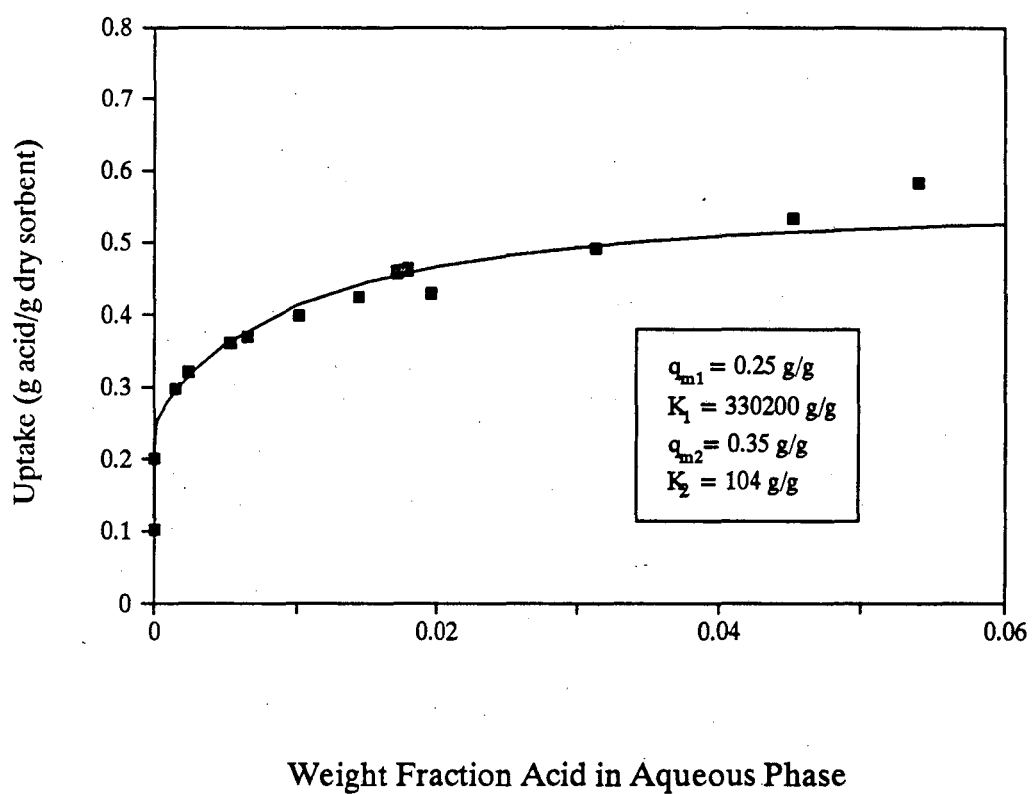


Figure B-10. Uptake of Succinic Acid by Amberlite IRA-35
Fitted with Dual-Site Langmuir Isotherm

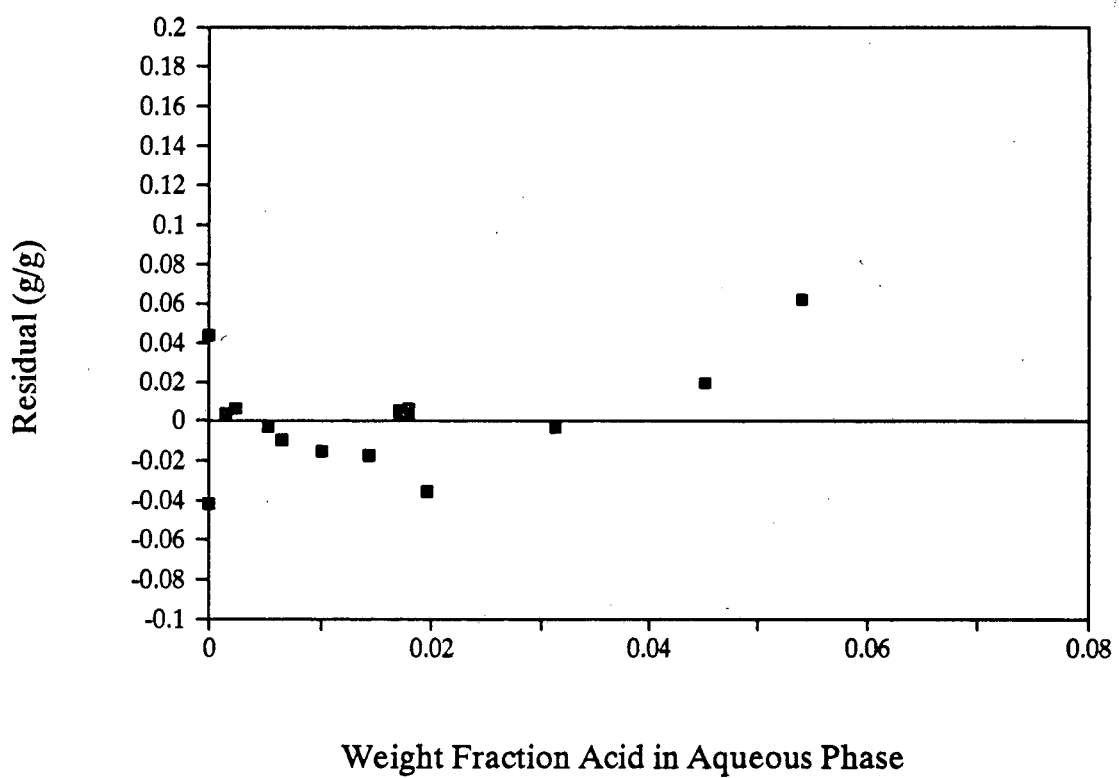


Figure B-11. Residuals from Fit of Dual-Site Langmuir Isotherm to Succinic Acid/Amberlite IRA-35 Data

B.3 Use of Competitive Langmuir Model with Low-pH Isotherms

Finally, in Section 3.4.2.2, the uptake-pH curves for succinic acid and Bio-Rad AG3-X4, Dowex MWA-1, and Amberlite IRA-35 were fitted using competitive Langmuir isotherms that accounted for uptake of both un-ionized acid and bisuccinate ions. An attempt was made to apply the same competitive Langmuir models to the low-pH isotherms. From the equilibrium total acid concentrations (measured experimentally) and the dissociation constants for the acid, the solution pH and the distribution of succinic acid species were calculated. At the lowest total acid concentrations, small amounts of bisuccinate were present. The percent total acid in un-ionized form is 97.3 % at a total acid concentration of 1.0 wt. % and 92 % at a total acid concentration of 0.1 wt.%. The predicted uptakes were then calculated from the concentrations of un-ionized acid and bisuccinate using the competitive Langmuir isotherms from Section 3.4.2.2.

The resulting theoretical curves are shown in Figures B-12 through B-14. For Bio-Rad AG3-X4 (Figure B-12), the competitive Langmuir curve gives a somewhat better fit to the data than the simple Langmuir isotherm, but the fit is not as good as that achieved with a Freundlich isotherm. For Dowex MWA-1 and Amberlite IRA-35, the fits are even poorer than with a simple Langmuir isotherm. Therefore, although uptake of bisuccinate effectively explains the results of uptake experiments at $\text{pH} > \text{pK}_a$, it is not clear that bisuccinate uptake is a major factor at lower pH values.

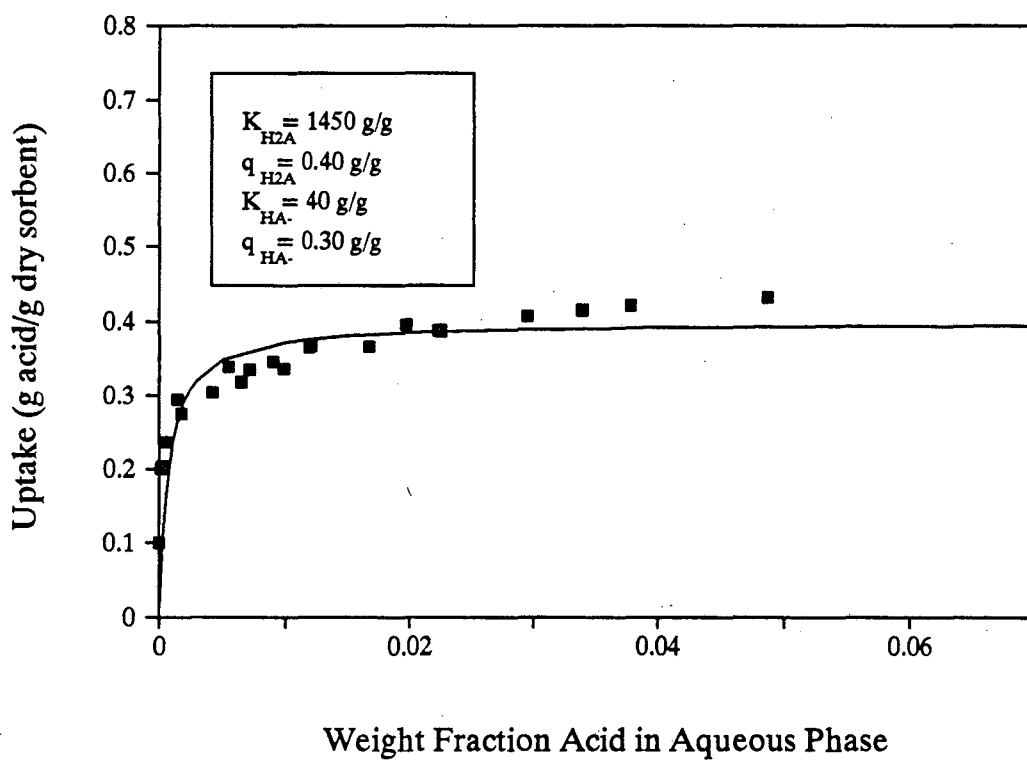


Figure B-12. Uptake of Succinic Acid by Bio-Rad AG3-X4 Fitted with Competitive Langmuir Model

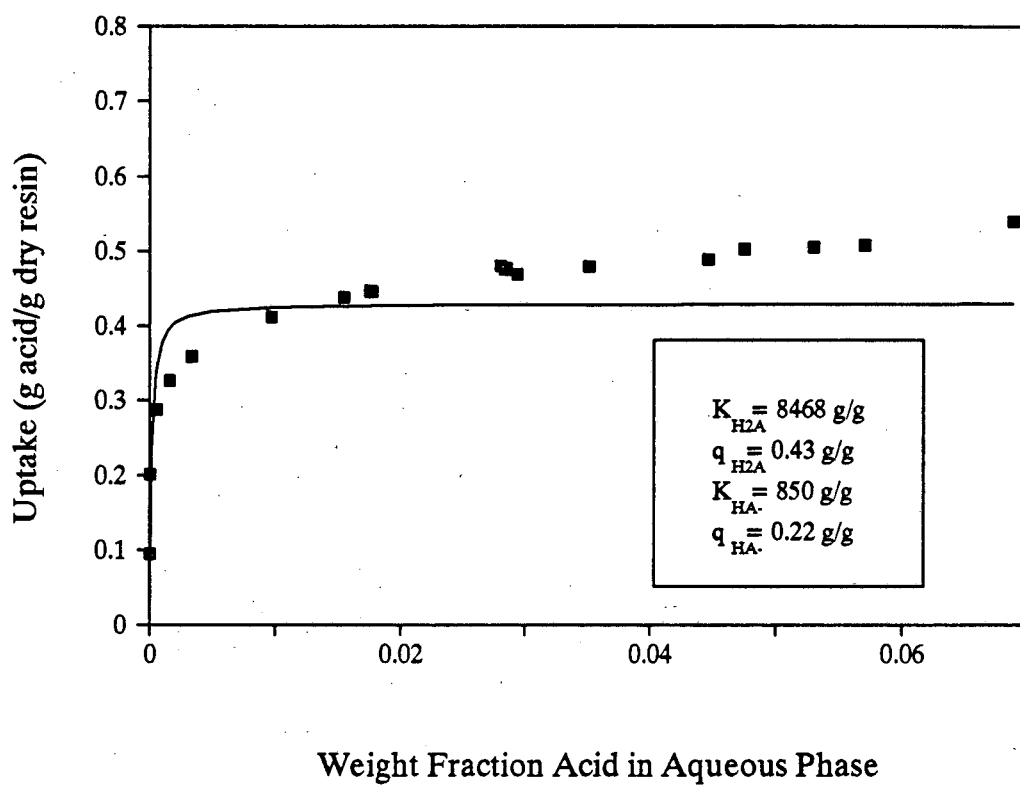


Figure B-13. Uptake of Succinic Acid by Dowex MWA-1
Fitted with Competitive Langmuir Model

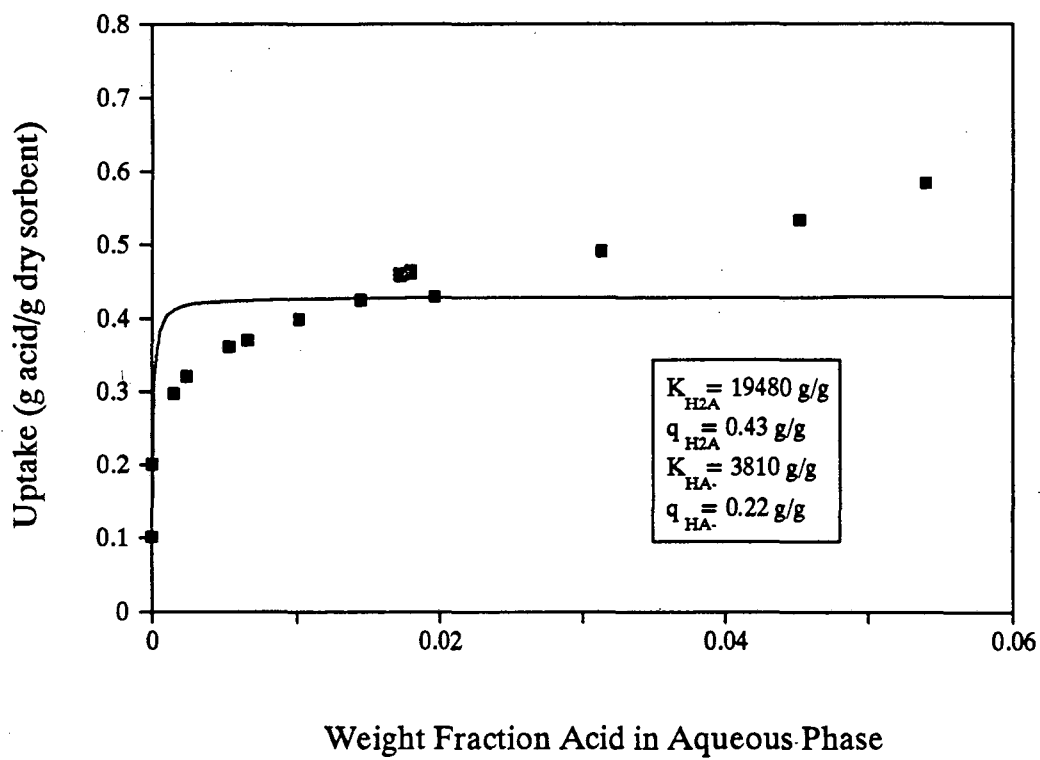


Figure B-14. Uptake of Succinic Acid by Amberlite IRA-35
Fitted with Competitive Langmuir Model

APPENDIX C: NOMENCLATURE

General

K_a	dissociation constant for acid
K_w	dissociation constant for water
$K_{a,b}$	dissociation constant for trimethylammonium
brackets	denote concentration, in mol/L except where noted
overbars	denote organic-phase (solid sorbent or organic extractant)

Chapter 3Apparent pK_a Determination:

$\overline{[B^-]}$	concentration of unprotonated basic sorbent sites, equivalents per unit volume of ion exchanger
$\overline{[BH^+]}$	concentration of protonated basic sorbent sites, equivalents per unit volume of ion exchanger
$\overline{[H^+]}$	concentration of hydrogen ions inside sorbent, equivalents per unit volume of ion exchanger
$\overline{[X]}$	concentration of ionogenic groups in resin (= $\overline{[B^-]} + \overline{[BH^+]}$) equivalents per unit volume of ion exchanger
α'	degree of dissociation of ionogenic groups
$[Cl^-]$	concentration of chloride ions in solution, moles per unit volume

Monomer pK_a Calculations:

ΔG°	change in free energy for ionization of an acid functional group
R	gas constant
T	temperature
pK_a°	pK_a of parent compound in Taft equation
ρ^*	constant for particular ionization reaction in Taft equation
σ^*	substituent effect in Taft equation

LFER:

k_i^I, k_i^{II}	equilibrium or rate constants in LFER
-------------------	---------------------------------------

Sorbent Experiments:

C_{HA}	weight fraction un-ionized lactic acid in solution
C_{A^-}	weight fraction lactate in solution
C_{H_2A}	weight fraction un-ionized succinic acid in solution
C_{HA^-}	weight fraction bisuccinate in solution
$C_{A^{2-}}$	weight fraction succinate in solution
C_a	weight fraction total acid (all forms) in solution
	subscript i indicates initial solution, subscript f indicates final solution
W_o	initial mass of solution, g
m	mass of sorbent used, g
Q_w	individual uptake of water, g water/g dry resin
Q_a	individual uptake of acid, g acid/g dry resin

Isotherm Models:

q	selective uptake of acid by sorbent, g acid/g sorbent
K	affinity constant for simple Langmuir isotherm, g solution/g acid
q_m	capacity parameter for simple Langmuir isotherm, g acid/g dry sorbent
K_1, K_2	affinity constants for two types of sites in dual-site Langmuir model, g solution/g acid
q_{m1}, q_{m2}	capacity parameters for two types of sites in dual-site Langmuir model, g acid/g dry sorbent
a	coefficient in Freundlich isotherm
n	exponent in Freundlich isotherm
K_{H_2A}, K_{HA^-}	affinity constants for H_2A and HA^- in competitive Langmuir model, g solution/g acid
q_{m, H_2A}, q_{m, HA^-}	capacity parameters for H_2A and HA^- in competitive Langmuir model, g acid/g dry sorbent
$K_{ave.}$	weighted-average K-value for dual-site Langmuir model, g solution/g acid

Uptake-pH Models:

$[BOH]$	concentration of hydroxyl ions bound to quaternary sites on resin, expressed in terms of the equivalent g succinic acid/g dry sorbent that could occupy the sites
$[BAB]$	concentration of succinate ions bound to quaternary sites on resin, g acid/g dry sorbent
$[BAH]$	concentration of bisuccinate ions bound to quaternary sites on resin, g acid/g dry sorbent

K_3	modified equilibrium constant for reaction $2 \overline{BOH} + H_2A = \overline{BAB} + 2H_2O$, in (g solution)(g sorbent)/(g acid) ²
K_4	modified equilibrium constant for reaction $\overline{BOH} + H_2A = \overline{BAH} + H_2O$, in g solution/g acid
q_{max}	capacity parameter in quaternized resin model, g acid/g sorbent

Leaching Experiments:

q_{init}	individual uptake of acid in loading phase of leaching experiment, g acid/g dry sorbent
α	fraction of acid in un-ionized form (see Equation 3-35)
ASR	aqueous/sorbent phase ratio, l/g
MW	molecular weight of acid, g/gmol
[TMA]	concentration of unprotonated TMA in aqueous phase, mol/l
[TMAH ⁺]	concentration of protonated TMA in aqueous phase, mol/l
[TMA] _{tot}	concentration of TMA (all forms) in aqueous phase, mol/l (= [TMA] + [TMAH ⁺])
β	fraction of TMA in protonated form

Fixed-Bed Experiments:

ϵ	interstitial void fraction of bed
ρ_B	bulk density of sorbent, cm ³ /g dry sorbent
ρ	density of solution, g/cm ³
v	average fluid velocity, cm ³ /min
x	distance in axial direction, cm
t	time, min

$C_{a,o}$	weight fraction total acid in feed
q_o	sorbent-phase concentration in equilibrium with $C_{a,o}$, g acid/g dry sorbent
k_p	particle-phase mass transfer coefficient in linear- driving-force model, min^{-1}
a	interfacial area per unit volume of bed, cm^2/cm^3
q^*	resin-phase concentration in equilibrium with solution phase, g acid/g solution
$t_{1/2}$	time at which $C_a = C_{a,o}/2$
D_{eff}	effective diffusivity, calculated from $k_p a$ via Equation 3-48, cm^2/min
d_p	diameter of sorbent particle, cm
D_{pore}	pore diffusivity in pore-diffusion model, cm^2/min

Chapter 4

$[\text{HA}]$	concentration of un-ionized monocarboxylic acid in aqueous phase, mol/L
$[\text{A}^-]$	concentration of carboxylate ion in aqueous phase, mol/L
$[\text{HA}]_{\text{tot}}$	concentration of total monocarboxylic acid (all forms) in aqueous phase, mol/L (= $[\text{HA}] + [\text{A}^-]$). Subscript i denotes initial solution.
$[\text{H}_2\text{A}]$	concentration of un-ionized dicarboxylic acid in aqueous phase, mol/L
$[\text{HA}^-]$	concentration of bicarboxylate ion in aqueous phase, mol/L
$[\text{A}^{2-}]$	concentration of carboxylate ion in aqueous phase, mol/L
$[\text{H}_2\text{A}]_{\text{tot}}$	concentration of total dicarboxylic acid (all forms) in aqueous phase, mol/L (= $[\text{H}_2\text{A}] + [\text{HA}^-] + [\text{A}^{2-}]$). Subscript i denotes initial solution.
$[(\text{HA})_p \text{B}_q]$	concentration of complex containing p acid molecules and q amine molecules, mol/l

β_{pq}	true equilibrium constant for reaction $pHA + q\bar{B} = \overline{(HA)_p B_q}$
K_{pq}	apparent equilibrium constant for above reaction
$\overline{[HA]}$	concentration of uncomplexed acid in organic phase, mol/L
$\overline{[HA]}_{tot}$	concentration of total acid (all forms) in organic phase, mol/L ($= \overline{[HA]} + \Sigma p \overline{[(HA)_p B_q]}$)
$\overline{[B]}$	concentration of uncomplexed amine extractant in organic phase, mol/L.
$\overline{[B]}_{tot}$	concentration of total amine extractant (all forms) in organic phase, mol/L ($= \Sigma q \overline{[(HA)_p B_q]} + \overline{[B]}$)
P	partition coefficient ($= \overline{[HA]}/[HA]$)
Z	loading of amine extractant ($= \overline{[HA]}_{tot} / \overline{[B]}_{tot}$)
WS	aqueous-to-organic phase ratio (l/l)
Φ	volume fraction diluent in organic phase

Chapter 5

C_{SO_4}	concentration of sulfate in aqueous phase
\overline{C}_{SO_4}	concentration of sulfate in organic phase
C_a	concentration of lactic acid in aqueous phase
\overline{C}_a	concentration of lactic acid in organic phase
α	separation factor, $= \frac{\overline{C}_{SO_4} / C_{SO_4}}{\overline{C}_a / C_a}$ for sulfate/lactic acid

LAWRENCE BERKELEY LABORATORY
UNIVERSITY OF CALIFORNIA
TECHNICAL INFORMATION DEPARTMENT
BERKELEY, CALIFORNIA 94720